The primate brain: Evolutionary history & genetics

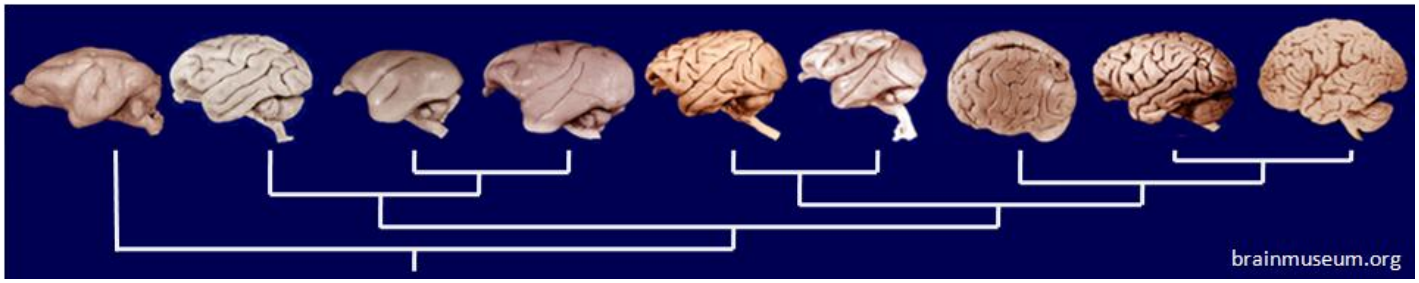

Stephen H. Montgomery

Darwin College, University of Cambridge

2011

This dissertation is submitted for the degree of Doctor of Philosophy

Declaration

This dissertation is the result of my own work and includes nothing which is the outcome of work done in collaboration except where specifically indicated in the text and acknowledgments.

This dissertation does not exceed the 60,000 word limit excluding figure legends, referencing and appendices.

Stephen H. Montgomery, BA
Cambridge, 2011

The primate brain: Evolutionary history & genetics

Summary

The expansion of the brain is a major hallmark of primate evolution. However, the fossil record of temporal changes in primate brain size is incomplete and often difficult to interpret. As such, whether brain expansion was limited to a few lineages or was a ubiquitous trend across the primate phylogeny, and how frequently brain size has decreased, are not clear. Using phylogenetic methods and published datasets of brain size I have reconstructed the evolutionary trajectories of brain and body size in primates. The results show that, from a small-bodied and small-brained ancestor, both absolute and relative brain size have shown strong temporal trends to increase and have done so multiple times independently across primate lineages. However, despite a general trend to expand, brain size does decrease in some lineages. Major episodes of brain mass reduction occurred in the Callitrichidae and Cheirogaleidae and are associated with episodes of body size dwarfism. Relative brain size decreased less frequently and can generally be attributed to increased body mass rather than decreased brain mass.

I subsequently explored whether the parallel evolution of increased brain size is due to parallelism at the molecular level by studying the molecular evolution of candidate genes across a broad selection of species representing all major clades of anthropoids. These genes were selected as their proposed roles in neurogenesis are associated with cell fate switches highlighted by The Radial Unit Hypothesis, which offers a developmental model of how mammalian brain size evolves. Using molecular tests for positive selection, I show that many of these genes have been under pervasive positive selection across anthropoids. Furthermore, it is demonstrated that the molecular evolution of several key genes is associated with neonatal brain size, suggesting a role in prenatal development that is consistent with a direct effect on neuronal proliferation, and with other structures which provide insights into the role of these genes in brain evolution.

This study demonstrates that brain expansion has occurred in parallel across primates and that the genetic basis of brain size evolution may be conserved. It highlights the potential use of adopting comparative methods, and the benefits of utilising primate diversity, when studying the genetic basis of brain evolution.

Acknowledgements

I am very grateful to my supervisor Dr. Nick Mundy whose guidance and tolerance of tangents has made my PhD enjoyable to do and hopefully relatively successful. I thank Drs. Isabella Capellini, Chris Venditti and Prof. Rob Barton for many helpful and stimulating discussions and for contributing to some of the ideas presented in chapters 3 and 5 (any bad ideas are mine of course). Thanks also to my advisors, Dr. Chris Jiggins and Prof. Barry Keverne, and Dr. Adrian Friday for their constructive criticism and advice at key stages of the project. Drs. Brenda Bradley and Marie Pointer were invaluable sources of advice (practical and otherwise) and together with Dr. Neil Walsh, Dr. Tim O'Connor, Oscar Brusa and Philipp Kappell made life in the lab more enjoyable than it would otherwise have been. A big thank you to Linda Wheatley for sorting out more things than I am probably aware of. The Zoology department is a friendly and helpful place and I have greatly enjoyed my time here. As well as those mentioned above the company of Dr. Marta Costa, Rich Merrill, Rich Wallbank, Vera Warmuth, late arrivals Nick Grumpton and Kelly Richards and many others helped make the more tedious days more tolerable. Thanks also to Drs. George Speller and Simon Baxter for enticing me into the Zootallurgy Cricket team; captaining the side was surely my greatest.

This project could not have been completed without the help of those who donate tissue samples. We are grateful Andrew Kitchner and Drew Bain (National Museums Scotland), Mike Bruford (Zoological Society London) Leona Chemnick (Center for Reproduction of Endangered Species, San Diego Zoo), Jackie Hooley (Twycross Zoo), Kellie Wyatt (Bristol Zoo) and Christian Roos (Gene Bank of Primates, German Primate Center) for providing samples.

I am greatly indebted to Charlotte BB Skelly who has kept me (mostly) sane and (overly) well fed throughout my PhD. Her patience, support and unwavering faith in my ability to muddle through has been a great help. Thanks to my brother Michael for his passionate interest in monkey brains and for his continual demand for proof that I am not a dumbass. Finally I've dedicated this thesis to Dr. Mum and Prof. Dad who have supported me through 21 years of education. They've always stressed the importance of hard work and a good education, hopefully this is proof I was listening at least some of the time.

I thank the BBSRC for a 4-year studentship and the Leverhulme Trust for additional funding.

Dedication

For Mum and Dad, two great apes.

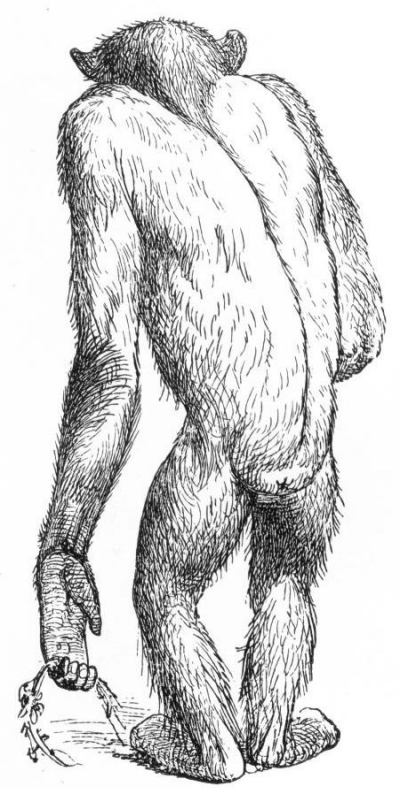

“I take a jealous pride in my Simian ancestry.
I like to think that I was once a magnificent hairy fellow living in the trees,
and that my frame has come down through geological time
via sea jelly and worms and Amphioxus, Fish, Amphibians, Reptiles, and Apes.
Who would exchange these for the pallid couple in the Garden of Eden?"

Wilhelm N. P. Barbellion, *The Journal of a Disappointed Man*, 1919

Contents

Abbreviations

AIC	Akaike information criteria
BM	Brownian motion
BMR	Basal metabolic rate
bp	Base pair
CI	Confidence interval
DNA	Deoxyribonucleic acid
ECV	Endocranial volume
GLS	Generalised least squares
Lh	Likelihood
LRT	Likelihood ratio test
MCMC	Markov-Chain Monte Carlo
ML	Maximum likelihood
ML	Maximum likelihood
my	Million years
NWM	New World monkeys
OSVZ	Outer sub-ventricular zone
OU	Ornstein-Uhlenbeck
OWM	Old World monkeys
PCR	Polymerase chain reactions
PGLS	Phylogenetic generalised least squares
RNA	Ribonucleic acid
SNP	Single nucleotide polymorphism
SZ	Sub-ventricular zone
VZ	Ventricular zone
ω	dN/dS ratio (nonsynonymous rate/synonymous rate)

Chapter 1

Introduction

"from so simple a beginning endless ~~forms~~ brains most beautiful and most wonderful have been, and are being, evolved."

Charles Darwin, *On the Origin of Species*, 1859

1. Introduction

1.1 Primate diversity

The interest in primate brain evolution is as old as Darwinian theory itself (Darwin, 1859, 1871; Huxley, 1863; Wallace, 1889). Primates are the order to which our own species belongs and much of the motivation behind studying primate evolution has been to cast light on the evolutionary origins of modern humans. The diversity of non-human primates is therefore often underappreciated and neglected by scientists and the public alike. There are over 350 living species of primates (Groves, 2001) which range in size from 30g (*Microcebus myoxinus*) to over 150kg (*Gorilla beringei*/*Gorilla gorilla*) (Jones *et al*., 2009) and extinct species showed an even greater diversity in size (Fleagle, 1999). All aspects of primate ecology vary widely; diet, locomotion, daily and seasonal activity patterns, reproductive and social ecology all show a complex distribution and evolutionary history across primates (Napier & Napier, 1995; Fleagle, 1999). Given the extent of this ecological variation it is little wonder that primate brains vary remarkably in size both in terms of absolute mass, from less than 2g to just under 1.5kg (Isler *et al*., 2008), and relative to body mass, from the mammalian average to the largest relative brain size to have ever evolved (Jersion, 1973; Martin, 1990). Understanding how this diversity evolved, what the evolutionary significance of variation in brain size and structure is, and how and why brain evolution along the human lineage departs from the general primate pattern is a major goal of modern evolutionary biology (Carroll, 2003; Goodman *et al.*, 2005; Barton, 2006a; Pollen & Hoffman, 2008; Vallender, 2008).

1.2 The fossil record & evolutionary history of primate brains

Living primates last shared a common ancestor 80-90 million years ago and today are most closely related to the Dermoptera and Scandentia (Perelman *et al*., 2011). Living primates (euprimates) are the only surviving clade of a larger radiation of primates including members of the paraphyletic group the Plesiadapiformes (Bloch *et al*., 2007) which radiated during the Late Cretaceous and Palaeocene (Fleagle, 1999; Bloch *et al*., 2007). Among the earliest Plesiadapiform primates thought to be basal to the subsequent radiation were species belonging to the genus *Purgatorius* which were small, insectivorous species (van Valen & Sloan, 1965;

Fleagle, 1999; Bloch *et al*., 2007). The Plesiadapiformes, in particular the Plesiadapids, were a successful and diverse clade during the Paleocene to Late Eocene which varied in body size as much as living strepsirrhines (Fleagle, 1999) and occupied a non-leaping arboreal niche (Silcox *et al*., 2009). The fossil record of early primate brain evolution is unsurprisingly incomplete. However, a handful of well preserved specimens offer some clues as to the evolutionary origins of the primate brain. Silcox *et al*. (2009) described the virtual endocast of an Early Eocene Plesiadapiform belonging to the order Paromomyoidea, *Ignacius graybullianus*. *I. graybullianus* weighed approximately 150g and had a small relative brain size and cerebrum compared to living primates, but had large olfactory bulbs and lacked orbital convergence (Silcox *et al.*, 2009). Similar conclusions are drawn from the endocast of *Plesiadapis cookei*, a Plesiadapoid (Gingerch & Gunnell, 2005) and *Microsyops annectens*, a Microsyopid (Silcox *et al*., 2010). Although each species has some derived traits the general features of these endocasts imply that early primates had small brains, were more dependent on olfactory cues and lacked the visual specialisations found amongst living species. Hence the expansion and specialisation of the primate brain may have occurred after the origin of euprimates (Silcox *et al*., 2009).

The precise timing and extent of the initial expansion of brain size in euprimates and whether brain expansion was limited to or concentrated on particular branches or lineages is hard to test using the limited information provided by the fossil record. Clues as to the adaptive origins of euprimates have been sought by an examination of shared features among living primates. These include grasping extremities, reduction or loss of claws, optic convergence and enhanced vision at the expense of the olfactory sense, and enlarged brains (Cartmill, 1992). This suite of adaptations may be related to life in a fine-branch arboreal niche (Cartmill, 1992; Bloch & Boyer, 2002) perhaps as a visually orientated predator of insects (Cartmill, 1992; Martin, 1990) or as a nectar feeder, evolving in response to the origin of angiosperms (Sussman, 1991). Such reconstructions depend on the assumption that these traits were present in the last common ancestor of euprimates. The earliest euprimates found in the fossil record (*Altiatlasius, Altanius*; Bloch *et al.*, 2007) were small bodied c.50-100g (Fleagle, 1999) but remains are not sufficiently preserved to extract information on the origins of primate brain expansion. The earliest euprimates for which endocranial volume can be estimated belong to extinct clades of Adapoidea, Omomyoidea and tarsiforms (Jersion, 1973; Gurche, 1982). They show some

expansion in relative brain size compared to Plesiadapiformes, but still fall towards the lower end of the range seen in modern euprimates (Jerison, 1973; Martin, 1990). The data available for early anthropoid primates (e.g. the New World monkey *Chilecebus*; *Aegyptopithecus* a genus of early catarrhines; the Old World monkey *Victoriapithecus*; and early apes such as *Proconsul*) suggest brain expansion may have had a complex history, with some expansion during the radiation of anthropoid clades but with further increases along lineages leading to extant species (Jerison, 1973; Walker *et al*., 1983; Martin, 1990; Benefit & McCrossin, 1997; Sears *et al*., 2008). Perhaps the only lineage with a near continuous fossil record for endocranial volume is that leading to our own species (Wood & Collard, 1999; Carroll, 2003; Ash & Gallup, 2007) which is somewhat ironic given human evolution is under taught in schools and for many one of the more contentious periods in the history of life (Berkman *et al*., 2008). Generally however the fossil record provides a broken and scattered picture of primate brain evolution and leaves many key questions unanswered.

1.3 The costs of brain expansion

The brain is a metabolically expensive tissue; even at rest it consumes a disproportionately high amount of energy relative to its mass (Mink *et al*., 1981). In humans, despite only accounting for 2% of body mass the brain consumes 20% of the body's energy budget (Ketty, 1957). This disproportionate cost has been explained by invoking a conserved, fixed energy budget per neuron across mammalian species such that the large energetic cost of the human brain is linked to the expansion in neuron number (Herculano-Houzel, 2011a). The energetic cost associated with large brains has long been seen as a constraint on brain expansion (Martin, 1981; Martin & MacLaren, 1985). It has been suggested that these energetic costs are accommodated by increased metabolic turnover (indexed by the basal metabolic rate; BMR) (Martin, 1996). This hypothesis is supported by some phylogenetic analyses across mammals, although only a modest amount of variation in brain size is explained by variation in BMR (Isler & Van Schaik, 2006). Other analyses did not support the relationship, especially with neonatal brain size (Pagel & Harvey, 1988) which may be the more relevant trait if the costs of brain development are incurred by the mother (Martin & MacLaren, 1985). However, a more recent analysis found that once gestation length and maternal body size are controlled for, relative

neonatal brain size is associated with BMR, suggesting BMR may constrain neonatal brain size by affecting the rate of foetal brain growth, but not postnatal brain growth (Barton & Capellini, 2011).

An alternative way of accommodating the costs of increased brain size may be to "trade off" these costs against other energy hungry tissues (the "expensive tissue hypothesis"; Aiello & Wheeler, 1995). In primates it was suggested that there is a trade off between the size of the digestive system and brain size, with selection for increased brain size requiring shifts to higher quality, easy-to-digest diets (Aiello & Wheeler, 1995). Further evidence for a link between diet quality and the energetic costs of brain size come from studies of wild primates which suggest species which live in less productive, or more seasonally variable, habitats have restricted brain sizes (Taylor & van Schaik, 2006; van Woerden *et al*., 2010). A dietary shift associated with the evolution of cooking may also have been important during human evolution (Carmody & Wrangham, 2009). The relationship between gut size, diet quality and brain size does not appear to be a mammal wide phenomenon (Jones & MacLarnon, 2004) but it has been proposed that the broader concept of "tissue trade-offs" may be of general importance with different trade-offs occurring in different groups (Barton, 2006a).

Developmental trade-offs may also occur between life history traits. Neonatal brain size has been shown to correlate with gestation length (Pagel & Harvey, 1988) and Martin (1996) suggested gestation length and BMR correlate with adult brain size. More recent analyses show that placental mammals with larger brains have longer pre and postnatal growth phases and require prolonged maternal investment which is mediated prenatally by the length of gestation and maternal BMR, and postnatally by length of lactation (Barton & Capellini, 2011). Gestation length is itself influenced by placental morphology with greater interdigitation being associated with shorter gestation times, but there is no effect on brain or body size suggesting placental morphology specifically affects foetal growth rates (Capellini *et al*., 2010). In contrast brain size in marsupial mammals appears to be largely determined by a specific prolongation of lactation (Weisbecker & Goswami, 2010).

1.4 The cognitive significance of brain size

Given the costs and trade-offs involved in producing highly encephalised offspring, the evolution of large brains is assumed to have a fitness benefit. The evolutionary significance of brain size has long been debated (Jerison, 1973; Deacon, 1990; Martin, 1990; Striedter, 2005; Healy & Rowe, 2007; Sherwood *et al*., 2008) but it is assumed that animals with bigger brains are more intelligent (Gibson *et al.*, 2001; but see also Chittka & Niven, 2009). Much of the discussion around the adaptive significance of brain size has been clouded by the desire for humans to come out on top of whatever measure of brain size is considered (Deacon, 1990; Roth & Dicke, 2005). The human brain is remarkably large (Deacon, 1997) but is surpassed both in mass and neuron number by some species of cetaceans and elephants (Roth & Dicke, 2005). However these are of course large bodied animals and as brain and body mass are linearly correlated much attention is given to measures of brain size that control for body size (Jerison, 1973; Roth & Dicke, 2005). Happily, when this is done humans tend to have the largest relative brain size and the fossil record of brain size during human evolution suggests a history of progressive expansion (Jerison, 1973).

There is indeed some evidence supporting the suggestion that relative brain size is an adaptive trait**.** For example variation in relative brain size is associated with differences in diet and arboreality suggesting brain size is under selection in relation to the cognitive demands associated with the physical environment (Clutton-Brock & Harvey, 1980; Harvey *et al*., 1980). Larger brain size is associated with social learning and innovation rate in primates, which may reflect some underlying cognitive ability to cope with a variable social or physical environment (Reader & Laland, 2002; Lefebvre *et al*., 2004). Larger brains are also associated with increased survival in novel environments and increased longevity (Sol *et al*., 2008; González-Lagos *et al*., 2010) suggesting large brains may provide some general survival advantage (the "cognitive buffer" hypothesis; Sol, 2009; but see also Barton & Capellini, 2011).

Recent attention has shifted to measures of general cognitive ability across primates using meta-analyses of published studies on cognition (Deaner *et al*., 2006; Reader *et al*., 2011). This has shown that some primates consistently perform better than others across a range of cognitive paradigms including social, physical and ecological traits which suggests different cognitive abilities have coevolved (Deaner *et al*., 2006; Reader *et al*., 2011). Initially it was shown that

these measures of general cognitive ability correlate with absolute brain size but not any measure of relative brain size (Deaner *et al*., 2006), this contradicts the previous emphasis on relative brain size (Jerison, 1973) but is consistent with some previous analyses (Gibson *et al.*, 2001) and is not entirely unexpected if brain mass accurately represents the number of "computational units" in the nervous system (Byrne, 1995; Gibson *et al*., 2001). However, variation between meta-analyses produces some conflicting results with both measures of absolute size and relative size being significantly associated with cognitive ability when considered independently (Schultz & Dunbar, 2010; Deaner *et al*., 2011) or as variables in multiple regressions (Schultz & Dunbar, 2010), though the statistical validity of using relative and absolute size in the same model is perhaps questionable.

Regardless of whether relative or absolute brain size is the more pertinent trait, evidence suggests brain size as a gross trait does have some evolutionary significance. However, whether selection acts on the brain as a whole or specifically selects for particular regions with particular functions is a key question with relevance both for the evolutionary ecology and evolutionary development of brain size (Barton, 2006a).

1.5 The evolutionary ecology of primate brain architecture

Finlay and Darlington (Finlay & Darlington 1995; Finlay *et al.*, 2001) have argued that different regions of the brain evolve in a coordinated way due to developmental constraints associated with the timing of neurogenesis in different brain regions. They therefore suggest adaptive evolution of particular regions of the brain is rare (Finlay & Darlington, 1995). However it has since been shown that coordinated evolution between brain components reflects functional connections between them, and that the mammalian brain has in fact evolved in a mosaic manner at both a coarse (Barton & Harvey, 2000) and fine scale (Barton *et al.*, 2003; Whiting & Barton, 2003; Barton, 2007). The mosaic evolution of the mammalian brain is associated with ecological adaptation through specialisation of brain architecture, and convergence in brain architecture between unrelated species that occupy similar ecological niches, implying region-specific responses to selection is common (de Winter & Oxnard, 2001).

Of particular interest has been the notable expansion in the volume of the neocortex and associated structures during primate evolution (Barton & Harvey, 2000). However,

understanding what these selection pressures were, and which regions of the brain responded to them during primate evolution is complicated by the integrated nature of the functional systems of the brain (Barton, 2006a; Healy & Rowe, 2007). Two aspects of primate evolution, sensory (in particular visual) specialisation and social behaviour, have received the most attention. Primates are visually orientated mammals with increased orbital convergence and broad stereopsis (Heesy, 2009). Visual specialisation has also left its mark on the primate brain. Primates with relatively large brains also have expanded visual areas, relative to the rest of the brain, with a particular expansion in the the parvocellular system which has roles in processing information on fine detail and colour (Barton *et al*., 1995; Barton, 1998). In addition the relative size of the visual centres is associated with both ecological and social variables (Barton, 1998). Although the size of olfactory bulbs and visual centres are negatively correlated in primates, perhaps suggesting a trade-off between senses (Barton *et al*., 1995), regions of the brain associated with olfaction also show correlations with ecological factors (main olfactory bulbs) and social ecology (accessory olfactory bulbs) (Barton, 2006b).

Numerous comparative studies have demonstrated a positive association between the relative expansion of the neocortex and measures of social complexity (e.g. Sawaguchi, 1992; Dunbar, 1992; Barton, 1996; Dunbar & Schultz, 2007) leading to the "social brain hypothesis" (Dunbar, 1998) which suggests that the information-processing capacity of the primate brain constrains group size, and that selection for increased social cognition has contributed to cortical expansion. Interestingly, adaptation of the visual system and the neocortex appear to be related suggesting social cognition may have a visual component (Barton, 1996, 1998; Joffe & Dunbar, 1997). In catarrhines this may be related to increased production and visual processing of facial expressions (Dobson & Sherwood, 2011). However, social group size and pair bonding, two commonly used measures of social complexity, are not associated with either increased relative brain size or neocortex size in strepsirrhine primates (Barton, 1996; MacLean *et al*., 2009) and relative neocortex size is also associated with ecological traits such as diet and activity pattern (Barton, 1996; MacLean *et al*., 2009). Hence whilst social cognition may be an important aspect of primate ecology (Cheney *et al.*, 1986; Kudo & Dunbar, 2001; Barrett & Henzi, 2005) and may have been an important factor during the expansion of the primate neocortex and whole brain

size (Sawaguchi, 1992; Dunbar, 1992; Barton, 1996) it is unlikely that primate brain evolution has a simple ecological basis.

Neocortex size is also unlikely to be the only target of selection. Barton and colleagues have argued for a significant role of the cerebellum, which has roles in sensory-motor behaviour, and cortico-cerebellar co-evolution during primate brain evolution (Whiting & Barton, 2003; Barton, 2006a). Furthermore there is evidence that the ecological pressures and anatomical evolutionary response to this selection may differ between the sexes (Lindenfors *et al*., 2007). In addition volumetric differences are not the only way in which brains can evolve (Deacon, 1990; Preuss, 2001; Sherwood *et al*., 2008). Variation in micro-anatomical structure (Schenker *et al*., 2008; Casanova *et al*., 2009; Semendeferi *et al*., 2010), synaptic plasticity or neuronal connectivity (Deacon, 1990; Sherwood *et al*., 2008), neural scaling and density (Herculano-Houzel *et al*., 2008), synapse proteome complexity (Emes *et al*., 2008) and brain metabolism (Fu *et al*., 2011) all have the potential to affect brain function but unfortunately available data is generally insufficient for full comparative analysis. Volumetric changes may, however, be representative of underlying changes in structure. Further insights into the nature of primate brain evolution can be gleaned from comparative studies of brain development.

1.6 Evolution and the development of primate brains

In volumetric terms the region of the primate brain which has experienced the greatest increase in size is the neocortex (Barton & Harvey, 2000). Although other regions of the brain have also expanded during primate evolution (Whiting & Barton, 2003) and volumetric changes in different brain regions may not reflect underlying changes in neuron number (Herculano-Houzel, 2010) the neocortex has generally been the focus of evolutionary biologists who seek to explain how and why primate brains evolve. The molecular and developmental aspects of this thesis concentrate on changes that may contribute to the evolution of neocortex size and I therefore mainly discuss models of cortical development here. In particular I focus on the development and evolution of neuron number.

Primate neocortical neurogenesis is restricted to prenatal development (Rakic, 1988; Rakic, 2002; Bhardwaj et al., 2006). Postnatal brain growth is largely driven by gliagenesis (Low & Cheng, 2006), axon growth (Sauvageot & Stiles, 2002) and myelination (Sowell *et al.*, 2001)

rather than by production of new neurons. Pre and postnatal brain growth have independent influences on adult brain size; indeed, the two are uncorrelated (Barton & Capellini, 2011) suggesting they have an independent genetic basis (Harvey & Krebs, 1990; Barton & Capellini, 2011). Across living primates whole brain and cortex volume linearly correlate with total and cortical neuron number respectively (Herculano-Houzel *et al*., 2006; Azevedo *et al.*, 2009; Gabi *et al*., 2010; Herculano-Houzel & Kaas, 2011). There are no significant differences in neuron size, density or the ratio of neuronal/non-neuronal cells (Herculano-Houzel *et al*., 2006; Gabi *et al*., 2010) and human data fit the primate wide relationship (Azevedo *et al.*, 2009). The increase in primate brain volume is therefore predominantly due to an increase in neuron and non-neuron cell number (Azevedo *et al.*, 2009).

The increased volume of the cortex is largely due to an expansion in the surface area and concomitant folding (Jerison, 1973; Prothero & Sundsten, 1984; Hofman, 1989). In contrast, brain expansion in primates and across mammals is accompanied by a disproportionately small increase in cortical thickness (Hofman, 1989). The Radial Unit Hypothesis (Rakic, 1988, 1995, 2007) provides a developmental explanation for how this pattern of increasing surface area without major increases in thickness can arise concomitantly with changes in neuron number. The Radial Unit Hypothesis states that the cortex is constructed of stacks of radially arranged neurons, called ontogenetic columns, each of which has its origins from the same region of the ventricular zone (VZ), the part of the developing brain where cortical neurons originate (Rakic, 1988). The number of these ontogenetic columns determines the surface area of the cortex, whereas the number of neurons in each column determines the thickness (Rakic, 1988, 1995). The neurons in each column are derived from the same apical progenitor cell; these cells undergo a period of symmetric, proliferative division producing an exponentially increasing progenitor pool, before switching to asymmetric, neurogenic divisions (Götz & Huttner, 2005). Increasing the duration of the proliferative divisions of apical progenitor cells will therefore produce a lateral expansion of the cortex through increased numbers of ontogenetic columns, whereas increasing the duration of neurogenic division will result in radial expansion through increased neurons/column (Rakic, 1998, 1995; Cavines *et al*., 1995). A predominance of the role of the former would explain the dominant role of increases in surface area during brain expansion.

One criticism of the hypothesis that the expansion of the cortex is primarily due to a lateral expansion of radial units is that this should cause an increase in the surface area of the cortex but also of the lateral ventricle, which is not observed (Kriegstein *et al.*, 2006). A role for the proliferation of neurogenic progenitor cells after the cessation of symmetric division of apical progenitors has therefore been invoked (Kriegstein *et al*., 2006; Pontious *et al.*, 2008; Fietz *et al*., 2010). At the onset of neurogenesis apical progenitors divide asymmetrically to produce a neuron and a radial glial cell. These radial glial cells undergo a number of asymmetrical divisions to produce another radial glial cell and either a neuron or a basal (or intermediate) progenitor cell which migrates to the sub-ventricular zone (SVZ) and divides symmetrically to produce two neurons (Götz & Huttner, 2005). A shift towards the production of basal progenitors over single neurons could therefore double the number of neurons produced (Kriegstein *et al*., 2006; Pontious *et al.*, 2008). The Radial Unit Hypothesis predicts these extra neurons would contribute to radial growth (i.e. an increase in radial unit thickness). An alternative hypothesis, the Intermediate Progenitor Hypothesis, predicts these will contribute to two ontogenetic units and therefore to lateral expansion (Pontious *et al*., 2008).

It has recently been shown that gyrencephalic (highly folded) brains are characterised by neural progenitor cell proliferation in the VZ and, unlike species with lissencephalic (smooth) brains, in the outer subventricular zone (OSVZ). This additional region of proliferation in gyrencephalic species is hypothesised to make a significant contribution to cortical expansion (Fietz *et al.*, 2010; Hansen *et al.*, 2010). Proliferating cells in the OSVZ show characteristic features of radial glial cells and repeatedly divide asymmetrically, self-renewing and producing a neuron with each division (Fietz *et al.*, 2010). The repeated division of these OSVZ progenitors could therefore affect neuron number, and could have a much larger effect than the apical-progenitor to basal-progenitor lineage (Fietz *et al.*, 2010). It is thought that increased neuronal production via OSVZ-progenitors would lead to cone-shaped radial units, with wider pial (external) surfaces than ventricular surfaces, as OSVZ-progenitors maintain contact with the pial surface and may act as founder cells of radial subunits (Fietz & Huttner, 2010). Fietz and Huttner (2010) have therefore suggested the increase in basal-over-apical ratio of radial units in gyrencephalic cortices reflects either an increase in the number of OSVZ-progenitors produced

per apical progenitor and/or increase in the number of neurons produced per single OSVZ-progenitor. In both cases the mitotic division of the progenitor cells is asymmetric.

The control of neuron number during development therefore relies on a number of key cell fate switches. Changes in the timing of these switches are likely to affect the number of neurons produced and therefore the development of brain size. In addition apoptosis of neural progenitors is thought to have a major influence on the development of brain size (Rakic, 1988, 1995, 2007; Blaschke *et al*., 1996; Haydar *et al*., 1999; Roth & D'sa, 2001). Evidence for a functional role for differential neural progenitor survival in the development of cortical volume comes from manipulation studies in mice. Disruption of several key apoptotic genes result in an increased cortical volume in developing mice (Kuida *et al*., 1996; 1998; Depaepe *et al*., 2005) suggesting evolutionary changes in the rate of apoptosis could bring about changes in brain size ("less is more", Rakic, 2005).

1.7 How can genetics contribute to understanding brain evolution?

Although mammalian models of development suggest hypotheses of how primate brains may evolve these are often difficult to test. Data from comparative studies of development in primates are typically limited to a few "model" species: *Callithrix*, *Macaca* and humans. Phylogenetic studies of development in a broader range of species are not possible - not only is the cost prohibitive but it is also ethically questionable. Evolutionary and quantitative genetics have the potential to provide answers to some key questions surrounding brain evolution using non-invasive techniques:

- What is the nature of brain:body allometry?
- What are the relative contributions of constraint and selection to mosaic brain evolution?
- What are the key developmental pathways targeted by selection during brain evolution?
- Is there a conserved genetic basis to brain evolution?
- To what extent did human evolution diverge from the general primate pattern?
- What, if anything, is "unique" about human genetic evolution? Does this provide insights into what is "unique" about human brain evolution?

Both quantitative and molecular genetic studies have greatly enhanced our understanding of the proximate mechanisms behind brain evolution as well as hinting at some of the possible functional changes under selection. However, comparative genetics has yet to reach its potential largely due to the tendency to analyse molecular evolution in isolation from phenotypic evolution leading to uncertainty over the functional relevance of genes with interesting patterns of evolution (Gilbert *et al*., 2005; Kelley & Swanson, 2008; Pollen & Hoffman, 2008) and a certain degree of anthropocentrism (Goodman *et al*., 2005; Vallender, 2008).

1.8 Quantitative genetics of primate brains

Quantitative genetic analysis has been extensively applied to brain size for many decades (Sholl, 1948) and technological advances have continued to open new avenues of research (e.g. Rogers *et al.*, 2007; Fears *et al.*, 2009; Panizzon *et al.*, 2009). Brain size has been shown to be a highly heritable trait in studies of lab mice with narrow-sense heritability scores (h^2) of 0.6-0.7 (Fuller & Geils, 1972; Roderick *et al*., 1976; Atchley *et al.*, 1984). Human brain size shows similarly high heritability of numerous structural phenotypes (h^2 = 0.5-0.9; see Peper *et al.*, 2007). These data are complimented by studies of the size of the whole brain or components of the brain in colonies of free ranging primates including *Papio hamadryas* (Mahaney *et al.*, 1993; Rogers *et al.*, 2007, 2010; Kochunov *et al*., 2009), *Chlorocebus aethiops sabaeus* (Fears *et al*., 2009), *Macaca mulatta* (Cheverud *et al*., 1990) and *Saimiri sciureus* (Lyons *et al*., 2002). These all reveal a high heritability for both total brain volume as well as in individual brain components such as the cerebrum and cerebellum. They also reveal a complex picture of genetic correlations between structures within the brain.

Fears *et al*. (2009) found that after including total brain volume as a covariate the volume of the cerebrum, cerebellum, hippocampus and corpus callosum all have a significant genetic component suggesting each phenotype is highly heritable independent of the genetic component of total brain size. They therefore suggest two categories of genetic variant contribute to the genetic architecture of brain structure, one which acts on general brain size and another which acts in a region specific manner (Fears *et al*., 2009). Similarly Rogers *et al*. (2010) found evidence that there is no significant genetic correlation between cerebral surface area and the degree of gyrification (or folding) of the cortex. They did however find a surprising negative

genetic correlation between cerebral volume and gyrification in both baboons and humans. This would suggest that genetic changes that increase cerebral volume actually decrease gyrification (Rogers *et al*., 2010). Primate brain expansion is accompanied by an increase in gyrification (Jerison, 1973; Zilles *et al*., 1989) so the authors suggest that when selection acted on genetic variants that brought about an evolutionary increase in size a second independent selection pressure must have acted to bring about an increase in cortical folding (Rogers *et al*., 2010). The surface area and thickness of the cortex have also been shown to have an independent genetic basis (Panizzon *et al*., 2009; Winkler *et al*., 2010). Hence different regions of the brain and different aspects of the development of a particular structure may be largely genetically independent.

A major topic of research has been the quantitative genetics of brain:body allometry (Lande, 1979). Experimental selection studies in laboratory mice have shown that selection on brain mass results in a correlated increase in body size, and selection on body size results in a correlated increase in brain size (Fuller & Geils, 1972; Roderick *et al*., 1976; Atchley *et al*., 1984). What the nature of this correlation is, and how it evolves, is of major importance to understanding the constraints and developmental pathways that shape brain evolution. Lande (1979) proposed a quantitative genetics model where allometry evolves from selection on more than one trait. He suggested that the shallow intra-specific brain:body slopes are due to selection on body size whilst the steeper inter-specific slopes are caused by selection on brain size over longer periods of time. Lande (1979) went on to argue that the evolution of increased encephalization in primates, and in particular humans, may have been facilitated by a reduction in the genetic correlation between brain and body size such that selection could act on brain size without antagonistic selection associated with increasing body size. Atchley and colleagues (Atchley *et al*., 1984; Riska & Atchley, 1985) have suggested that the genetic correlation between adult brain and body size reflects a developmental association that occurs early in ontogeny, in particular during early periods of cell multiplication rather than later periods of cell enlargement. They suggest this correlated development of brain and body growth may arise if both traits are responding to one or more somatic stimuli or hormones (Atchley *et al*., 1984; Riska & Atchley, 1985). However as discussed above different brain components may be genetically independent so beyond whole brain size what traits are changing during these

selection experiments and whether the increase in brain size is due to increased cell size or neuron number (Herculano-Houzel *et al*., 2006) are unanswered questions.

An important additional consideration is whether allometric relationships are conserved during evolution. Cross species analyses of quantitative traits suggest that the heritability of a trait and the genetic covariance between traits can themselves evolve (Lofsvold, 1986; Kohn & Atchley, 1988). Such adaptive evolution of allometry may have a major influence on the potential for divergent evolutionary trajectories by altering developmental constraints (Klingenberg, 2010). In this respect it is notable that in some strains of laboratory mice brain and body weight are not genetically correlated (Belknap *et al*., 1992). We also do not know to what extent results from rodents can be applied to primates. It has been suggested that brain:body allometry has evolved differences in primates compared to rodents (Lande, 1979) but the exact extent and nature of primate brain:body allometry is unclear.

Quantitative genetic analysis of brain size and structure therefore reveal a complicated picture of genetic covariance between brain and body size and within the brain itself. It is clear however that many aspects of brain development are not genetically correlated suggesting independent selection pressures acted in concert to shape the evolution of the primate brain.

1.9 Evolutionary genetics of primate brains

Molecular genetic studies of primate brain evolution have proceeded along two complementary paths (Varki & Altheide, 2007; Bradley, 2008). An increasingly dominant approach has been to adopt genome-wide, hypothesis-free analyses to search genomes or transcriptomes for interesting evolutionary patterns (e.g. Dorus *et al*., 2004). The second approach involves more focused studies of candidate genes motivated by some prior hypothesis (e.g. Zhang, 2003). Both approaches have advantages and disadvantages and both have substantially contributed to our understanding of the proximate mechanisms involved in primate brain evolution (Varki & Altheide, 2007; Varki & Nelson, 2007; Marques-Bonet *et al*., 2009). Genomic approaches have the probable advantage of being hypothesis-free and are capable of deciphering general patterns; however, they are limited in taxonomic breadth to a handful of species, are generally anthropocentric in their aims and approach, and often leave the gene-phenotype divide unbridged. Candidate gene studies are often rooted in hypotheses drawn from

developmental biology so are better positioned to bridge that gap. As only one or a few loci are under investigation they more often include a wider range of species which offers greater power of detecting genuine signatures of selection and shifts in selection pressure. However, studies of candidate genes rely on prior reasoning for selecting those genes, which may be lacking or incorrect, and quantifying the contribution and relevance of single loci to brain evolution is a major challenge. Here I summarise the main findings from both approaches to date.

1.9.1 Comparative genomics & transcriptomics

Genomic studies have pursued several lines of enquiry: the evolution of protein coding genes, the evolution of conserved non-coding regions and the evolution of gene expression. They were largely facilitated by the completion of a human genome (International Human Genome Sequencing Consortium, 2001; Venter *et al*., 2001), a chimpanzee (*Pan troglodytes*) genome (Chimpanzee Sequencing and Analysis Consortium, 2005) and a macaque (*Macaca mulatta*) genome (Rhesus Macaque Genome Sequencing and Analysis Consortium, 2007). Generally these studies seek to identify evolutionary changes along the human lineage compared to the chimpanzee lineage using the macaque as an out-group with the assumption that these changes relate to the human phenotypic evolution and "human uniqueness".

The earliest human-chimpanzee comparisons found low levels of divergence at the molecular level, suggesting the evolutionary origins of our species lay in a small number of genetic changes which affect gene expression (King & Wilson, 1975). This hypothesis was supported by early studies of gene expression profiles in adult humans and chimpanzees (Enard *et al*., 2002; Cáceres *et al*., 2003). Although gene expression profiles for brain tissue are more conserved than heart and liver tissue the ratio of change on the human branch to that on the chimpanzee branch was found to be highest for brain tissue (Enard *et al*., 2002; Cáceres *et al*., 2003; Uddin *et al*., 2004; Khaitovich *et al*., 2005a). Genes significantly up regulated in humans were found to be enriched for interesting functional categories such as synaptic transmission, synaptic plasticity and vesicle release (Cáceres *et al*., 2003) and aerobic energy metabolism (Uddin *et al*., 2004; Babbitt *et al*., 2010; Fu *et al*., 2011). Models of expression divergence expected under neutral evolution were subsequently employed to show that the pattern of expression divergence on the human lineage bears the signature of positive selection (Khaitovich

et al., 2005b; Khaitovich *et al*., 2006a; Chaix *et al*., 2008). Whilst the observed effect may be due to as few as 10% of genes the signal is robust and brain-specific (Preuss *et al*., 2004; Khaitovich *et al*., 2005b; Khaitovich *et al*., 2006b).

These broad scale comparisons of adult brain tissue have been advanced in two ways. First, the focus has shifted to analyses of different components of brain tissue (Khaitovich *et al.*, 2004; Giger *et al*., 2010). Khaitovich *et al*. (2004) analysed divergence in gene expression in four regions of the cerebral cortex, the cerebellum and the caudate nucleus. They found that the overall gene expression patterns between regions of the brain are largely conserved between humans and chimpanzee, with a relatively small and constant subset of genes in each region being significantly different between species (Khaitovich *et al.*, 2004). The conservation of co-expressed genes and gene networks was confirmed in an independent study (Oldham *et al*., 2006). Interestingly, Khaitovich *et al.* (2004) also provided evidence that genes with divergent gene expression levels were not randomly distributed across the genome and were associated with regions of the human genome with high levels of segmental duplication, although the selection pressures shaping these structural changes is unclear (Varki *et al*., 2008). Given the predominant focus on gene expression evolution in the cortex it is notable that a greater percentage of genes show human-chimpanzee differences in the cerebellum than other regions (Khaitovich *et al*., 2004). Recently gene expression in different cell types has also been explored. Giger *et al*. (2010) analysed the divergence in gene expression in neuronal and endothelial cells from prefrontal cortex (Brodmann area 9 and 46). They found higher levels of between-species divergence relative to within-species variation for genes expressed in neurons than endothelial cells, suggesting gene expression in these two cell classes has experienced contrasting selection pressures.

A second advance has been the study of ontogenetic changes in gene expression between species. Subtle changes in the levels and timing of gene expression have the potential to cause major phenotypic effects and it is likely that differences in gene expression during development may have had a larger role in brain evolution than differences in gene expression in adult brains (Preuss *et al*., 2004; Khaitovich *et al*., 2006b). Somel *et al.* (2009) analysed levels of expression of c. 8,000 genes across the postnatal lifespan of humans, chimpanzees and macaques. They found that ontogenetic changes in gene expression were generally conserved across species but

the human lineage was significantly enriched for genes with a "neotenic" shift (i.e. changes in gene expression were delayed) (Somel *et al.*, 2009). Again, a relatively small proportion of genes are involved but this result nonetheless provides molecular evidence for the hypothesis that neoteny played a role in human evolution (Montagu, 1955).

Ontogenetic studies such as this have the potential to identify interesting patterns of evolution; unfortunately as yet no study has examined ontogenetic changes in prenatal gene expression which may have had a major influence on brain development. A couple of studies suggest further examination of changes during foetal development may be a fruitful line of enquiry. Uddin *et al.* (2008) found that genes with high levels of expression in the human foetal brain and signatures of positive selection on the human lineage are enriched for genes involved in cell adhesion and neural connectivity, whereas genes with high levels of expression in adult brains and signatures of positive selection in humans are enriched for genes involved in energy metabolism. This suggests different selection pressures have shaped the evolution of genes involved in pre and postnatal development. Lambert *et al*. (2011) analysed gene expression differences between different cortical regions of the human foetal brain and subsequently explored the levels of divergence in non-coding sequence in neighbouring genes. They found evidence that suggests genes expressed differentially between cortical regions are linked to fast-evolving non-coding sequence not only on the human lineage, but also on other mammalian lineages suggesting selection may have acted on genes controlling prenatal cortical specialisation (Lambert *et al*., 2011).

Changes in gene expression must be caused by mutations in *cis* or *trans* regulatory elements and it has been suggested that the genetic basis of "human uniqueness" will lie in these regions (Carroll, 2003; Sholits & Noonan, 2009). Several studies have analysed the rate of evolution of promoter regions in 5'-flanking regions of protein coding genes. These suggest that many promoter regions have evolved rapidly during human and non-human primate evolution (Haygood *et al*., 2007; Taylor *et al*., 2006). Regions close to genes involved in neural and nutritional functions were highlighted as being potential targets of positive selection (Haygood *et al*., 2007). However, difficulty in dissecting the relative roles of selection and neutral processes may confound interpretations of the adaptive significance of these high evolutionary rates (Taylor *et al*., 2006; Hoffman & Birney, 2010). In addition, functional analysis of human and

chimpanzee promoters suggest differences in promoter activity do not closely relate to differences in gene expression (Heissig *et al*., 2005). It has also been shown that both non-coding and protein coding RNAs have divergent gene expression in humans and chimpanzees (Babbitt *et al*., 2010) suggesting the need to study regulatory elements which are not associated with coding genes.

A parallel line of enquiry has been to identify regions of non-coding sequence that are conserved across primates or mammals and to examine these for accelerated rates of evolution during human evolution (Bush & Lahn, 2005; Prabhakar *et al*., 2006; Pollard *et al*., 2006). This approach has highlighted individual loci or classes of genes during human evolution. Prabhakar *et al*. (2006) for example find the strongest evidence for human-specific acceleration in non-coding regions near to genes involved in neuronal cell adhesion. However they also show that the same class of genes are accelerated during chimpanzee lineages, although the exact loci involved are different (Prabhakar *et al*., 2006). In contrast Pollard *et al*. (2006) found that human specific accelerations of non-coding sequence are enriched for regions near genes involved in DNA binding and transcriptional regulation with 24% adjacent to neurodevelopmental genes. They highlight a particular locus (*HAR1*) as the fastest evolving conserved non-coding region along the human lineage. *HAR1* is part of an RNA gene expressed in the developing cortex in association with reelin, which is involved in forming the layered structure of the cortex (Pollard *et al*., 2006). Generally, rapidly evolving non-coding sequences appear to be enriched for functional roles in neurogenesis (Haygood *et al*., 2010). However, there is often little overlap between regions highlighted in different studies (Bush & Lahn, 2008; Haygood *et al*., 2010) and, as with studies of promoter regions, disentangling neutral and adaptive processes has proved difficult. The accelerated rate of evolution of *HAR1* for example has been explained by the region being a hotspot for biased gene conversion rather than positive selection (Galtier & Duret, 2007).

An alternative source of genetic change is the loss of conserved non-coding regions. McLean *et al*. (2011) recently identified 510 conserved non-coding regions which were deleted along the human lineage after divergence from the chimpanzee lineage; of these over 80% are also absent from the draft Neanderthal genome. These lie upstream or downstream of genes enriched for steroid hormone receptor signalling and neural function and include several notable

candidate genes such as *CDK5RAP2*, *MAOA*, *MCPH1* and *FOXP2* (see below) (McLean *et al*., 2011). Functional evidence from two genes, the androgen receptor (*AR*) and a tumour suppressor gene expressed in the developing brain (*GADD45G*), support the hypothesis that some of these deletions may have had phenotypic effects (McLean *et al*., 2011). Interestingly they also show an enrichment of deleted conserved regions near genes involved in synapse and postsynaptic membrane function in chimpanzees (McLean *et al*., 2011) which complements the findings of Prabhakar *et al*. (2006). No information is given about whether any of the same genes are highlighted in both human and chimpanzees.

Although a dominant argument has been that changes in gene regulation underpin human phenotypic evolution (King & Wilson, 1975; Carroll, 2003; Sholits & Noonan, 2009; Haygood *et al*., 2010) structural changes in protein coding genes can also contribute to phenotypic evolution (Hoekstra & Coyne, 2007; Lynch & Wagner, 2008; Stern & Orgogozo, 2008). The first large scale study of protein coding gene evolution during human evolution found that genes involved in the nervous system development had accelerated rates of evolution along the human lineage compared to the chimpanzee, macaque and rodent lineages (Dorus *et al*., 2004). This study considered only a few hundred genes and subsequent reanalysis with larger numbers of genes have refuted this original finding and clearly show that the majority of brain expressed genes are under purifying selection and that the human lineage does not have an over abundance of rapidly evolving brain genes (Nielsen *et al*., 2005; Shi *et al*., 2006; Wang *et al*., 2007). In fact it was suggested that more protein-coding genes evolved under positive selection in chimpanzees than humans (Bakewell *et al*., 2007) although a more recent analysis suggests similar numbers of protein-coding genes were targeted by selection during human, chimpanzee and gorilla evolution (Scally *et al*., in review). Genome-wide scans for positively selected genes do however highlight potential candidate genes for further investigation (Dorus *et al.*, 2004; Yu *et al*., 2006; XueBin *et al*., 2007; Uddin *et al*., 2008) although consistency between studies is often low. Interestingly, several genes have been identified as being targeted by positive selection in both chimpanzees and humans (Bakewell *et al*., 2007); this could be due to parallel selection pressures in the two lineages but could also reflect the presence of more pervasive selection across primates. The addition of new genomes may resolve this issue. For example, a reanalysis of selection pressure on primate coding genes following the sequencing of two Orang-utan genomes (*Pongo albeii*

and *Pongo pygmaeus*) highlighted genes involved in visual perception and glycolipid metabolism (Locke *et al*., 2011). The addition of the gorilla genome has also highlighted genes involved in brain development and sensory perception as having accelerated rates of evolution in African Great Apes, with significant levels of parallelism between species (Scally *et al*., in review).

Currently the limited number of primate genomes makes a full assessment of which genes evolved under positive selection across primates and which genes if any have human-specific accelerations in evolutionary rate impossible. Whilst this is likely to change in the near future, with ambitious plans to sequence the genomes of up to 146 primate species (Genome 10K Community of Scientists, 2009), wider comparative analysis of candidate genes are necessary to test the conclusions drawn from genome scans.

1.9.2 Candidate genes

By focusing on specific loci the candidate gene approach has the potential for wider phylogenetic and functional analysis. Candidate genes have come from several sources; they may be highlighted as having high rates of evolution or signatures of selection by genome scans either across species or within human populations, or they may be associated with human neurodevelopmental disorders or identified as having a role in brain development in mice mutants or gene knockout studies. Key candidate genes proposed to have a role in primate brain evolution can be lumped into general categories; genes involved in neural proliferation, genes involved in cell death, genes involved in energy metabolism and genes involved in behavioural disorders.

Perhaps the most intensively studied group of candidate genes are the microcephaly genes (Ponting & Jackson, 2005; Thornton & Woods, 2009). Autosomal recessive primary microcephaly is a congenital disorder characterised by reduced growth of the cerebral cortex in the absence of environmental, metabolic or cytogenetic aetiologies (Bond & Woods 2006; Cox *et al*., 2006). In humans it is inherited as a recessive Mendelian trait involving at least eight loci (Thornton & Woods, 2009), of which six have now been identified at the molecular level: *ASPM*, *MCPH1*, *CDK5RAP2*, *CENPJ*, *STIL* and *WDR62* (Jackson *et al.*, 1998; Bond *et al.*, 2002; Bond *et al.*, 2005; Thornton & Woods, 2009; Kumar *et al.*, 2009; Nicholas *et al*., 2010). These genes

are all expressed in the foetal brain (Bond *et al*., 2002, 2005; Jackson *et al*., 2002; Kouprina *et al.*, 2005; Kumar *et al*., 2009) and have functions in neurogenesis (see chapter 5).

Initial studies of the molecular evolution of the first four microcephaly genes to be identified (*ASPM*, *MCPH1*, *CDK5RAP2* and *CENPJ*) found evidence for accelerated rates of evolution (Zhang, 2003; Evans *et al.*, 2004a; Evans *et al.*, 2004b; Wang & Su, 2004; Kouprina *et al*., 2004; Evans *et al.*, 2006). Initially it was thought selection was limited to the human branch (Zhang, 2003) but high rates of evolution were subsequently shown on several internal ape lineages (Evans *et al.*, 2004a; Evans *et al.*, 2004b; Wang & Su, 2004) and non-human terminal branches (Kouprina *et al*., 2004). More recently it was proposed that episodic positive selection has acted on *ASPM* across primates in association with increased relative forebrain size (Ali & Meier, 2008). Generally however, despite having interesting patterns of evolution direct evidence linking selection on microcephaly genes to brain evolution is lacking (Ponting & Jackson, 2005) and it remains possible that the phenotypic relevance of this selection is unrelated to brain evolution (Ponting, 2006).

The role of microcephaly genes in brain evolution became more controversial following the suggestion that two microcephaly genes, *ASPM* and *MCPH1*, experienced positive selection in recent human history (Evans *et al*., 2005; Mekel-Bobrov *et al*., 2005). These results proved controversial as the putatively advantageous haplotypes were found to be unequally distributed between human populations which, for some, implied an equally non-homogeneous distribution of cognitive abilities (see Balter, 2006). The findings of these studies have been challenged on two fronts. First the evidence for selection itself has been disputed- it has been argued that demographic effects can explain the distribution of haplotypes (Curat *et al*., 2006; Yu *et al*., 2007). It is also of interest that scans for recent positive selection in the human genome have not highlighted *ASPM* or *MCPH1* but have detected selection on two other microcephaly genes, *CENPJ* and *CDK5RAP2* (Voight *et al*., 2006). A second criticism has been the lack of evidence linking these loci to variation in human brain size or structure. A number of studies have consistently shown a lack of any association between single nucleotide polymorphisms (SNPs) of *ASPM, MCPH1* or *CDK5RAP2* and various brain-related phenotypes (Woods *et al*., 2006; Dobston-Stone *et al*., 2007; Mekel-Bobrov *et al*., 2007; Rushton *et al*., 2007; Timpson *et al*., 2007; Bates *et al*., 2008). This has had the result that studies of *MCPH1* and *ASPM* have become

a showcase example of over interpretation of DNA sequence analysis resulting in unsupported adaptive stories (Nielsen, 2009). However, two recent studies suggest that variation in microcephaly genes do contribute to variation in human brain size (Wang *et al*., 2008; Rimol *et al*., 2009) reaffirming these genes as good candidates for contributing to the genetic basis of brain evolution in humans and other primates. Other genes with accelerated rates of evolution that may contribute to evolutionary changes during neurogenesis include *ADCYAP1* and *SHH. ADCYAP1* encodes the protein PACAP, which has a role in cortical neurogenesis, and has signatures of positive selection on the human terminal branch but is otherwise highly conserved across primates (Wang *et al*., 2005). *SHH* encodes a signalling molecule involved in developmental patterning in the nervous system. It has been suggested the *SHH* has an accelerated rate of evolution and potentially altered post-translational modifications in primates (Dorus *et al*., 2006).

Neuron number may evolve by changing the number of neurons produced during development or by changing the number that survive. Apoptosis amongst neural progenitors is thought to have a major influence on the development of brain size (Blaschke *et al*., 1996; Haydar *et al*., 1999; Roth & D'sa, 2001). Vallender and Lahn (2006) suggest that genes involved in the caspase-dependent apoptotic pathway have significantly higher evolutionary rates in primates and highlight the *APAF1-CASP9-CASP3* signalling cascade in particular. These genes cause macrocephaly when disrupted in mice (Haydar *et al*., 1999; Roth & D'sa, 2001) and it is plausible that selection for reduced apoptotic activity could bring about increases in brain size (Rakic, 2005). *Cernunnos-XLF* has also been proposed as a target of positive selection during primate evolution (Pavlicek & Jurka, 2006). *Cernunnos-XLF* is a nonhomologous end-joining factor involved in double strand break repair mutations, can cause microcephaly when disrupted and has a high rate of evolution along the terminal human branch (Pavlicek & Jurka, 2006).

One of the more consistent results from both expression studies and genome scans is the apparent rapid evolution of genes involved in aerobic energy metabolism (Dorus *et al.*, 2004; Uddin *et al*., 2004, 2008; Babbitt *et al*., 2010; Fu *et al*., 2011; Locke *et al*., 2011) which is of particular interest given the energetic costs of large brains (see above). Candidate gene studies support the contention that many genes involved in energetic metabolism have been targeted by selection. For example, the gene encoding the enzyme glutamate dehydrogenase, which has a

key role in recycling the excitatory neurotransmitter glutamate, was duplicated during the origin of apes (Burki & Kaessmann, 2004). The duplicated copy has evolved a brain-specific expression profile and evolved under positive selection (Burki & Kaessmann, 2004). Genes involved in the electron transport chain also show evidence of accelerated rates of evolution (Grossman *et al*., 2004; Doan *et al.*, 2005; Uddin *et al*., 2008). It has been proposed that the functional consequence of this selection is related to the high energetic demands of the cortex (Grossman *et al*., 2004). Interestingly, genes involved in aerobic metabolism also have high rates of evolution along the lineage leading to elephants which have convergently evolved large brain masses (Goodman *et al*., 2009) providing independent support for a link between large brains and molecular adaptations to meet their energetic cost.

Several other candidate genes have been linked to evolutionary changes which may relate to human behaviour or cognition (Andrés *et al*., 2004; Crespi *et al*., 2007; Weiss *et al.*, 2007). The most intriguing of these is the role of *FOXP2* in language (Enard *et al*., 2002). *FOXP2* is associated with a severe speech and language disorder (Lai *et al*., 2001) and, although strongly conserved across mammals, has accumulated two non-synonymous mutations in the coding region and bears a signature of positive selection during human evolution (Enard *et al*., 2002). The signature of selection extends beyond the coding region suggesting selection for linked non-coding sequence, perhaps regulatory elements, may have been important (Ptak *et al*., 2009). In this respect it is notable that *FOXP2* lies close to a human-specific deletion of a conserved non-coding region (McLean *et al*., 2011). However, the two amino acid substitutions do have functional effects. FOXP2 regulates different transcriptional elements in humans compared to chimpanzees, and these newly acquired targets are differentially expressed between the two species (Konopka *et al*., 2009). Using a novel 'humanised' mouse model Enard and colleagues have demonstrated that the human *FOXP2* gene alters neuron morphology, dendrite length and plasticity in cortico-basal ganglia circuits which suggests the derived human mutations may have contributed to increased fine-tuning of motor control in conjunction with the evolution of language (Enard *et al*., 2010; Reimers-Kipping *et al*., 2011; Enard, 2011). The combination of evidence from molecular and functional analyses therefore strongly implicates *FOXP2* as having a role in vocal learning during human evolution (Enard, 2011).

A final source of candidate genes which may contribute to either brain development or behaviour are imprinted loci. Genomic imprinting is a phenomenon in which a gene's expression is dependent on parental origin (Hall, 1997). Imprinted loci can show skewed expression of either the maternal or the paternal allele, and the pattern of expression may also be stage- and tissue-specific (Davies *et al.*, 2005). Although traditionally thought to be limited to less than 1% of the expressed genome (Luedi *et al.*, 2007) imprinting may have had important roles in mammalian evolution. One proposed role is in primate brain development and evolution (Keverne *et al.*, 1996a, 1996b; Keverne, 1997). Parental genomes were first shown to be non-equivalent in functional terms by studies of chimeric mouse embryos which were either parthenogenetic (Pg, duplicated maternal genome) or androgenetic (Ag, duplicated paternal genome) (Surani *et al*., 1986; Solter, 1988). Striking phenotypic differences were observed between the two experimental groups with Ag cells making a greater contribution to the mesoderm than Pg cells, which contributed significantly more to brain tissue. Keverne *et al.* (1996) performed a similar experiment focusing solely on brain development. Within the brain the genomes were again seen to be non-equivalent, with Pg cells enhancing the growth of the cortex and striatum, whilst Ag cells accumulated in the pre-optic area and hypothalamus. This result strongly suggests that the parental genomes differ in their functional effects during brain development due to the cumulative effects of imprinted genes. Keverne *et al.* therefore proposed that imprinted genes could provide a control mechanism for the mosaic development of the mammalian forebrain and may have facilitated the rapid increase in primate brain size.

Other lines of evidence suggest the role of imprinted loci in brain development may be generally important in mammals. A large proportion of imprinted genes are expressed in the central nervous system and many have roles in cell survival and differentiation (Davies *et al.*, 2005; Wilkinson *et al*., 2007). Of particular interest are neurodevelopmental and behavioural disorders which result from the disruption of imprinting status of particular gene clusters in humans (Wilkinson *et al*., 2007). Two examples are Prader-Willi syndrome and Angelman syndrome, both of which are caused by mutations or deletions at chromosome 15q11-13 (Flint, 1992). Within this region are several loci which appear to be specifically imprinted in the brain (Nicholls *et al.*, 1998) with functions which could potentially affect brain size and development (Goos & Silverman, 2001). Imprinted loci have also been implicated in some cases of autism,

schizophrenia, Williams syndrome and a number of other neurological disorders (Falls *et al.*, 1999; Davies *et al.*, 2005). Williams syndrome is a particularly interesting case as subjects display characteristics of microcephaly (Jernigan *et al.*, 1993).

If imprinted genes are involved in controlling differential deposition of cells during brain development it is possible that they would be targets of selection during episodes of adaptive evolution in the size of different brain regions. Despite a high level of interest in genomic imprinting and in the genetic basis of primate brain evolution, this hypothesis remains largely untested. Only two previous studies have identified accelerated evolution of imprinted genes during human evolution, in *PEG3* (Dorus *et al.*, 2004) and *KLF14* (Parker-Katiraee *et al.*, 2007), but in both cases the authors could not rule out a relaxation of selective pressure as the cause. Recent studies making use of high throughput sequencing techniques also suggest the number of imprinted loci expressed in the brain may be much higher than previously thought (Gregg *et al*., 2010). Unravelling the adaptive significance of genomic imprinting in the brain may be a challenging but fruitful endeavour.

Genomic, transcriptomic and candidate gene studies have all contributed to our understanding of what sorts of genetic changes have occurred during human and non-human primate evolution. However, they do suffer from a number of problems. With a handful of exceptions the link between the evolution of the gene under consideration and brain evolution is speculative, typically only a few primates are considered and an anthropocentric view of brain evolution permeates the field. Generally, little information is available on the history of brain size and structure during non-human primate evolution (see above) making molecular genetics studies difficult to interpret. Several authors have noted the need to integrate phenotypic information into genetic studies to move beyond generating hypotheses to testing hypotheses (Carroll, 2003; Goodman *et al.*, 2005; Barton, 2006b; Pollen & Hoffman, 2008; Vallender, 2008). One way of doing so is to develop mouse models to study the effects of different gene variants on development (Enard *et al*., 2009). Although such an approach has the potential to produce novel insights into the genetic and developmental basis of brain evolution a mouse is not a primate and confounding variables such as the influence of the genetic background on a gene's function may mask interesting patterns or question interesting results (Gilbert *et al*., 2005; Vallender *et al*., 2008). A complementary approach which has the potential to allow evolutionary

analyses and hypothesis testing across many species comes from adopting the comparative method (Pagel & Harvey, 1991) to study genetics and gene-phenotype links (Carroll, 2003; Gilbert *et al*., 2005; Goodman *et al*., 2005; Kelley & Swanson, 2008; Vallender, 2008; Vallender *et al*., 2008; Pollen & Hoffman, 2008).

1.10 Aims & approach of this thesis

The aim of this thesis is to attempt to address the gap between molecular and phenotypic studies of brain evolution. The approach taken follows two paths. The first attempts to provide a phenotypic framework to "fill in the gaps" of the fossil record of primate brain evolution. This should allow patterns of selection on candidate genes to be interpreted in terms of the presumed phenotypic result of this selection, changes in brain size. The second path adopts comparative methodology to study the phenotypic relevance of candidate gene evolution. In particular I emphasise the need to collect data from a broad range of species to permit a full assessment of the distribution of different selection pressures across primates and to use the diversity of primate brain sizes to derive and test explicit hypothesis. Along the way I discuss the meaning of various results in relation to brain:body allometry, selection pressures and constraints on brain evolution, parallelism and convergence, the controversial brain of *Homo floresiensis* (Brown *et al*., 2004), the "uniqueness" of *Homo sapiens* and the genetic basis of adaptation.

1:11 Thesis outline

Chapter two introduces the general methodology used throughout the thesis.

Chapter three includes analyses of the evolutionary history of brain size across primates which demonstrate that strong evolutionary trends shape primate brain evolution and suggest brain and body mass respond to contrasting selection pressures.

Chapter four focuses on brain evolution in two groups of primates which buck the trend of increasing brain mass. I explore the changes in life history surrounding reductions in body size and discuss the relationship between brain and body mass reduction in callitrichids and cheirogaleids.

Chapter five analyses the molecular evolution of five genes associated with human microcephaly. I show all five evolved under pervasive positive selection and test the hypothesis that these genes contribute to evolutionary changes of neuron number though lateral expansion of neural progenitors using comparative methods.

Chapter six examines the evolution of another candidate gene with a potential role in the evolution of cortical thickness. I argue that *NIN* was targeted by positive selection to bring about changes in the duration of neurogenic radial glial cell proliferation.

Chapter seven summarises the results of the thesis and sets them in context with other studies. I draw some general conclusions about how primate brains evolved from a genetic and developmental perspective and suggest some ways to move our understanding of primate neurogenetics forward.

Chapter 2

Materials & methods

"It is good to rub and polish our brain against that of others."

attributed to Michel de Montaigne, *Essais I*, 1580

2. Materials & methods

This chapter contains general information on phenotypic datasets and phylogenies used throughout the thesis, as well as details and discussion of laboratory, bioinformatic and comparative methods used. Specific details of how these methods were employed are given in each chapter.

2.1 Phenotypic data

The phenotypic analyses and gene-phenotype association tests were performed using previously published phenotypic datasets. Data for body mass, brain mass and volumes of specific brain regions were obtained from previously published data (Bauchot & Stephan, 1969; Stephan *et al.*, 1981; Zilles & Rehkemper, 1988). Data on neonatal brain and body size (22 taxa) were obtained from Capellini *et al.* (2011). Additional data for extant species and sex-specific endocranial volumes and body masses were taken from Isler *et al.* (2008). Through a literature search I obtained data for fossils where cranial remains were sufficiently intact to make reliable estimates of cranial capacity (23 taxa). Cranial capacity estimates were converted to brain mass using the equation given in Martin (1990):

$$Log(cranial\ capacity) = [1.018 \times Log(brain\ mass)] - 0.025$$

Where body and brain mass estimates were not available from the same individual the body mass estimate for that species given in Fleagle (1999) was used. Data on the number of neural and non-neural cells in primate brains were taken from Herculano-Houzel *et al.* (2007, 2008), Gabi *et al*. (2010) and Azevedo *et al*. (2009). Data on white and grey matter volume in the cerebellum and neocortex comes from Bush and Allman (2003). Data on testis mass for 30 genera were taken from Harcourt *et al.* (1995). Life history variables used in chapter 4 including neonatal and adult body mass, gestation length, litter size, weaning age, inter-birth interval, age at sexual maturity and maximum longevity were obtained from the PanTHERIA dataset (Jones *et al.*, 2009). All phenotypic data is given in Appendix I.

In most cases the phenotypic data is based on a small number of individuals and the degree of intraspecific variation is unknown. However where interspecific variation greatly

exceeds intraspecific variation, as is expected to be the case for brain size, results of comparative analyses are not biased by intraspecific variation (see Nunn & Barton, 2001). It is also likely that error introduced by sampling small numbers of individuals will lead to an underestimate of correlation coefficients between two traits (Nunn & Barton, 2001; Ives *et al*., 2007).

2.2 Phylogeny

It is important to incorporate both topology and branch length information during phylogenetic analyses as species are part of a hierarchically structured phylogeny and are therefore not statistically independent, and differences in time since divergence from the common ancestors determines differential potential for evolutionary change (Felsenstein, 1985; Pagel, 1999; Nunn & Barton, 2001; Finarelli & Flynn, 2006). For genus level analyses I used a composite phylogeny of primates produced from published trees. The topology is taken from Goodman *et al.* (2005) for haplorhine primates and Horvath *et al.* (2008) for strepsirhines. Proportional branch lengths were obtained from recent studies of primate divergence dates (Opazo *et al.*, 2006; Page & Goodman, 2001; Poux & Douzery, 2004; Purvis, 1995) scaled to agree with dates of divergence for the deeper primate nodes estimated by Steiper and Young (2006). The tree obtained therefore has branch length information and is ultra-metric. There are two trichotomies: one between the Cebidae, Pitheciidae and Atelidae, the other at the base of Cebidae. As the topology of this composite phylogeny is well studied and the branch lengths are based on the best available divergence date estimates in all subsequent analyses it is assumed the phylogeny is known without error. Where fossil data were included I followed Finarelli and Flynn (2006) in minimising phylogenetic assumptions and placed extinct taxa as polytomies at the node nearest to their estimated position in the primate phylogeny. Branch lengths for fossil species were calculated as the time from this node to the end of the geological period in which they are last found. Both phylogenetic relationships and temporal presence in the fossil record were taken from Fleagle (1999). Where the programs described below require a fully bifurcating tree, trichotomies were randomly resolved and the new, intervening branch given a branch length of zero.

Where multiple species within the same genus are included in an analysis the consensus tree from the 10K Trees Website (Arnold *et al*., 2010) was used with additional branching

information for species not included in Arnold *et al*. coming from Bininda-Emonds *et al*. (2007). The topologies of these two trees are largely consistent both with each other and the intra-generic tree described above.

2.3 Comparative methods

2.3.1 The comparative approach

Phylogenetic comparative methods and ancestral state reconstruction play important roles in evolutionary biology (Pagel, 1999; Martins, 2000). They enable historical evolutionary processes, and the function and evolution of specific traits, to be inferred from patterns of diversity in extant species (Harvey & Pagel, 1991; Cunningham *et al.,* 1998; Pagel, 1999). Ancestral state reconstructions across phylogenies allow insights into the temporal evolution of specific traits, data on which may otherwise be missing, whilst comparative analysis of correlated evolution between traits or between a trait and some aspect of the environment and can be used to infer adaptive processes (Pagel, 1999; Martins, 2000). Both approaches have been criticised in the past as the validity of results are dependent on the assumptions made by the model of evolution that underpins the method (see Martins, 2000; Freckleton & Harvey, 2006). Popular methods of implementing phylogenetic comparative analysis, including Independent Contrasts (Felsenstein, 1985) and Generalised Least Squares (Pagel, 1997), adopt Brownian motion (BM) to model trait evolution. BM is a 'neutral' model of random drift. BM may not be suitable if the trait is evolving under persistent selection through time, when different lineages are subject to the same selective regime or when stabilising selection and stasis have shaped a trait's evolution (Felsenstein, 1985; Butler & King, 2004). This is particularly so for ancestral state reconstructions where the quality of inferences made are wholly dependent on the accuracy of the ancestral state estimates. Several previous studies have used weighted square change parsimony and maximum likelihood (ML) to reconstruct ancestral character states and infer the adaptive origins of phenotypes (Soligo & Martin, 2006; Finarelli & Flynn, 2006, 2007; Masters *et al.,* 2007) and to study important genotype-phenotype associations (Ali & Meier, 2008). These methods have been criticised as they fail to provide reliable estimates when there are directional evolutionary changes and may also be adversely affected when ancestral states fall outside the range of extant species (Oakley & Cunningham, 2000; Garland *et al.*, 2005).

However, recent advances in methodology allow characteristics of a trait's mode of evolution which deviate from BM to be accounted for, permitting more accurate ancestral state reconstructions and comparative analysis. The two most successful strategies for doing so take different approaches. The first involves estimating parameters that describe the rate and mode of a trait's evolution and using these to transform the phylogeny by scaling branch length to improve the fit of the tree and data to the BM model (Pagel, 1997). This approach allows for a "model" of evolution to be built which is optimised for the trait under consideration, and has the advantage of requiring no *a priori* information about how that trait evolves. The second strategy adopts a niche-filling or Ornstein-Uhlenbeck (OU) model (Hansen, 1997; Butler & King, 2004). The OU model incorporates selection and assumes species' traits are evolving towards selective optima representing a hypothesised number of discrete 'niches' (Butler & King, 2004). This approach is of particular use for studying adaptive radiations (Butler & King, 2004; Freckleton & Harvey, 2006) and can be used to test hypotheses about the number of selective optima driving the evolution of a clade of related species. However, as the number of optima must be defined *a priori* some hypothesis of how or why the trait evolves is required to avoid data dredging. For phenotypic traits which respond to a large number of variables in a complex way, such as brain size, there is often no easily defined hypothesis. I therefore focus on methods incorporating a BM model and in particular on BayesTraits (Pagel, 1997, 1999; Pagel *et al.*, 2004; Organ *et al.*, 2007) which takes the phylogenetic scaling approach to account for deviation from BM. However, I do acknowledge the potential use of niche-filling models and recent advances in the methodology which incorporate a randomly evolving predictor variable(s), as opposed to discrete 'niches' (Butler & King, 2004), to determine selective optima (Hansen *et al.*, 2008) may be of particular use.

2.3.2 Phylogenetically controlled regressions

A key tool in the comparative toolbox is the phylogenetically controlled regression (Pagel, 1999; Martins, 2000) which permits the testing of adaptive hypotheses and the study of co-evolution and allometry whilst taking into account the non-independence of related species. The phylogenetically controlled regressions performed in this thesis were carried out in BayesTraits (Pagel, 1997, 1999; Pagel *et al.*, 2004; Organ *et al.*, 2007) which implements

Phylogenetic Generalised Least Squares models (PGLS). With PGLS the phylogeny is converted into a variance-covariance matrix, where the diagonal of the matrix gives information on the path length from root to tips (the 'variance') and the off-diagonal values of the matrix provide information on the shared evolutionary history of any pair of species, that is the time from the root to the last common ancestry (the 'covariance') (Pagel, 1997, 1999; Freckleton *et al.*, 2002; Capellini *et al.*, 2011). In a PGLS regression, the variance-covariance matrix is included into the error term of the regression model, and the resulting estimated regression parameters (i.e. slopes and intercepts) are 'phylogenetically controlled' (Pagel, 1997, 1999; Freckleton *et al.*, 2002; Capellini *et al.*, 2011).

The advantage of implementing PGLS in BayesTraits comes from being able to estimate a series of parameters which improve the fit of the data and tree to the model of evolution when there is significant deviation from Brownian motion. These parameters are lambda, which reveals to what extent the phylogeny predicts the pattern of covariance between species for a trait (the phylogenetic signal); kappa, which stretches and compresses branch lengths and tests for stasis in longer branches; and delta which scales path lengths and tests for adaptive radiations or a greater importance of temporally early change. These are first estimated and where a parameter is significantly different from the default value of 1, as determined using a likelihood ratio test (LRT) in Maximum Likelihood (Pagel, 1999) or Bayes Factors in Bayesian MCMC (Kass & Raftery, 1995; Gilks *et al.*, 1996), can then be estimated in the final regression analysis. While lambda can be estimated alone, kappa and delta are better estimated as additional parameters in the model that also included lambda. In this thesis PGLS is used to calculate measure of various phenotypes relative to body size, and to test for significant associations between two or more traits.

2.3.3 Ancestral state reconstructions: Weighted Square-Change Parsimony

Ancestral state reconstructions provide a window on the evolution of traits poorly represented in the fossil record (Harvey & Pagel, 1991; Cunningham *et al.*, 1998). However given the error associated with such analyses (Cunningham *et al.*, 1998; Oakley & Cunningham, 2000; Garland *et al.*, 2005) it is beneficial to estimate ancestral states using a range of methods to test the robustness of the results under different assumptions and to attempt to find the most

reliable set of ancestral states. To reconstruct ancestral brain and body sizes in primates I employ three methods. The first adopts a parsimony approach implemented in Mesquite (Maddison & Maddison, 2008). Weighted squared-change parsimony infers ancestral states by minimising the square-change along branches (Maddison, 1991; Schluter *et al.*, 1997). Parsimony approaches are not considered to be robust to violations of assumptions of constant rate of evolution or equal probability of change in either direction (Pagel, 1999; Oakley & Cunningham, 2000; Webster & Purvis, 2001; Pedersen *et al.*, 2006).

2.3.4 Ancestral state reconstructions: Maximum-Likelihood

The second approach is a Maximum Likelihood (ML) method implemented in ANCML (Schluter *et al.*, 1997). ML reconstruction in ANCML is based on a BM model to estimate transitions at any node along the phylogeny. The advantages of this method are that the probability of change at any point in the tree is not dependent on a prior state change or on changes on other branches (Cunningham *et al.*, 1998). Like parsimony approaches however, the model assumes a constant rate of evolution and may perform poorly if the trait shows an evolutionary trend (Cunningham *et al.*, 1998; Oakley & Cunningham, 2000; Webster & Purvis, 2001; see below). ANCML provides standard errors for each nodal value reconstruction. However, these are considered to be underestimated and difficult to compare across methods (Garland *et al.*, 1999).

2.3.5 Ancestral state reconstructions: Bayes Traits

Finally, ancestral state reconstructions were performed in Bayesian framework with MCMC in BayesTraits (Pagel, 1999; Pagel *et al.*, 2004) following the method described in Organ *et al.* (2007). BayesTraits implements more complex models and can scale branch lengths in the phylogeny to account for deviation from BM (Pagel, 1997). The ancestral state reconstruction is therefore performed in two steps. First, one identifies the best fitting evolutionary model (see below) to the species data, then in the second step this model is used to infer unknown ancestral states at internal nodes along the tree.

The constant variance random walk (BM) model has only one parameter, alpha, which describes the instantaneous variance of evolution (Pagel 1997, 1999); this model represents the

default model with all branch length scaling parameters, kappa, lambda and delta, set as one (described above; Pagel, 1997, 1999). The rate parameters can be estimated in ML or Bayesian MCMC. The branch length scaling parameters can be estimated simultaneously and because these parameters can improve the fit to the data and thus help identify the best evolutionary model for the data. Whether or not these scaling parameters significantly differ from the default value is determined using a Likelihood Ratio Test (LRT) in ML or Bayes Factors in MCMC.

The Likelihood Ratio Statistic is computed as:

-2(Log[Lh(null model)] – Log[Lh(alternative model)])

For nested models the p-value is determined using a chi-square distribution where the degrees of freedom are the difference in estimated parameters between the two models.

The Bayes Factor is computed as:

-2(Log[Harmonic Mean ofLh(null model)] – Log[Harmonic Mean of Lh(alternative model)]).

A Bayes Factor greater than 2 is taken as positive evidence for a difference between the two models with the best fitting model having the highest log(harmonic mean), a Bayes factor greater than 5 represents 'strong' evidence and greater than 10 is 'very strong' evidence (Kass & Raftery, 1995). Where the rate parameters were significantly different to one they are incorporated in the estimation for the best fitting model. Therefore, contrary to parsimony and the Weighted-Square Change Parsimony and ML approach taken in ANCML, this method has the advantage of finding the best model of trait evolution before estimating ancestral states.

Once the best model is established it is then possible to test if a directional-change random walk model improves the fit to the data relative to the best non-directional random walk model, obtained as described above. While the non-directional random walk model has one parameter – alpha, the variance of evolution - the directional random-walk model has an additional parameter (beta) that captures the directional change using a regression between trait values and the total path length (Pagel 1997, 1999). This analysis can only be done with a tree that incorporates fossil species as the directional model requires root-to-tip path length variation in order to estimate directionality unless the scaling parameters are used; in ultrametric trees of extant species all species have the same total path length. The harmonic mean of the likelihoods of the directional and non-directional random walk models can be compared with Bayes Factors (Kass & Raftery, 1995; Gilks *et al.*, 1996) to determine which model fits the data best (see

above). Once the final model with estimates of lambda, kappa, delta and beta (where they are significantly different to the null model) is obtained this model can be used to reconstruct ancestral states. As it is optimised to take into account particular features of the mode of evolution of a trait it is expected to produce more reliable ancestral state reconstructions (Pagel, 1997, 1999; Organ *et al.*, 2007).

Results of the BayesTaits analyses obtained using 2 or 10 million runs were qualitatively similar, therefore I performed all analyses with 2 million Markov chain Monte Carlo (MCMC) runs after a burn-in of 500,000, sampling every 100 runs, and repeated multiple times to test the stability of the harmonic means. All analyses were performed using uniform priors (prior range: -100 to +100). Rate deviation was adjusted to obtain an acceptance of the proposed model parameters (above) between 20% and 40%. Ancestral state reconstructions were then estimated using the best evolutionary model for the data; data deviation was adjusted to obtain an acceptance rate for each node's estimate between 20-40%.

2.4 Laboratory methods

This thesis takes a candidate gene approach, identifying genes with key roles in brain development, which have large phenotypic effects when disrupted and which have previously been shown to have high rates of evolution. The goal of the laboratory work was to amplify regions of candidate genes across a large range of species to allow proper comparative analyses to explicitly test whether selection on these genes is associated with brain size.

The majority of genomic DNA samples had previously been extracted from tissue samples using Qiagen kits; where DNA was newly extracted it was done so using standard protocols and Qiagen QIAmp DNA mini kits. For each candidate gene sequence data from previous studies and primate genomes were collected from the online databases GenBank and Ensembl. From these sequences primers were designed in conserved regions using Primer3Plus (Untergasser *et al*., 2007). Polymerase chain reactions (PCR) were prepared in a 25µl total volume containing: 2.5 U Taq polymerase (BIOTAQ DNA polymerase, BIOLINE, London, UK), 1 x reaction buffer, 1.5mM $MgCl_2$, 0.4mM each dNTP, 0.4µM each primer and c. 50ng DNA. PCRs were performed in DNA Engine (MJ Research) or G-Storm (GSI) cyclers under the

following conditions: 94ºC for 2 min; 40 x (94 ºC for 30 s, 55-62ºC for 45 s, 72ºC for 45-120 s); and 72ºC for 7 min.

In some cases when the targeted region was larger than 2kb PCRs were prepared in a 20 µl total volume containing: 0.2µl Phusion high-fidelity DNA polymerase (Finnzymes, BioLabs Inc., New England), 1 x Phusion GC buffer, 1mM $MgCl_2$, 0.2mM dNTP, 0.5µM of each primer and c. 50ng DNA. These PCRs were performed under the following conditions: 98ºC for 60s; 60 x (98ºC for 10s, 58-62ºC for 30s, 72ºC for 200s); and 72ºC for 10 min.

PCR products were purified using Qiagen QIAquick PCR purification kits. Cycle sequencing on both strands was carried out using BIG DYE v. 3.1 (PE Biosystems) under standard conditions with 6.5µl of template, 0.5µl 10mM primer, 2µl 5X buffer and 1µl BIG DYE. Cycle sequencing was performed under the following conditions: 24 x (96ºC for 10s, 57ºC for 5s, 60ºC for 2 min). Following the sequencing reaction DNA was precipitated by adding 40µl of 80% ethanol for 20 min at 4ºC, spinning at 37,000 rpm for 30min, tipping off the liquid and adding 200µl of 70% ethanol, spinning for a further 15 min then tipping off the liquid before spinning upside down on a dry towel for 12s at 1000rpm. Precipitated DNA was sent to the Oxford Sequencing Centre, Dept. Zoology for Sanger sequencing. Sequences were edited in SEQMAN v. 5.05 (DNASTAR Inc.) and aligned and checked in CLUSTALW in MEGA 4.0 (Tamura *et al*., 2007). Exons of each candidate gene were concatenated and analysed together.

2.5 Analysis of molecular evolution

2.5.1 Protein coding gene evolution & *dN/dS*

A common measure used to infer selection pressures acting on coding regions of genes is the ratio of rates of non-synonymous to synonymous fixed base changes. Estimation of *dN/dS* ratios (ω) was carried out using a codon-based maximum likelihood method (codeml in PAML version 4; Yang, 2007). Several analyses were performed to test the hypothesis that the candidate loci have experienced positive selection across primates, in particular in relation to brain size evolution. Nested models are compared using the likelihood ratio statistic (see above) to critical values of the Chi-square distribution and degrees of freedom as the difference in the number of parameters estimated by each model.

2.5.2 Site models

To detect positive selection across primates I implemented the site models. These allow the ω to vary among sites but not across lineages (Nielson & Yang, 1998; Yang *et al.*, 2000). The site model tests for positive selection can be carried out using two pairs of models. The first pair compare Model M1a and Model M2a (Wong *et al.*, 2004; Yang *et al.*, 2005). Model M1a (NearlyNeutral) allows sites to fall into two categories with ω <1 (purifying selection) and ω = 1 (neutral evolution), whilst model M2a (PositiveSelection) allows sites to fall into three categories with ω <1, ω = 1 and ω >1 (positive selection) (Yang *et al.*, 2005). The second pair compares Model 8a and Model 8 (Swanson *et al.*, 2003; Wong *et al.*, 2004). These models use the beta distribution to describe the numbers of sites across different categories of ω. M8 has 11 site classes (10 from the beta distribution plus 1 additional class), where one of these classes may have an ω >1. In Model 8a this latter class is restricted to have an ω = 1. The critical Likelihood Ratios boundaries of significance for this test are are 2.71 at 5% and 5.41 at 1%. The results obtained throughout this thesis for the M8-M8a and M1a-M2a comparisons were highly similar, unless otherwise stated I therefore only present results for the M1a-M2a test as these have slightly lower false positive rates and are more conservative than the M8-M8a test (Wong *et al*., 2004). Site models and Branch-Site models (see below) both implement a Bayes Empirical Bayes method to identify specific codons under positive selection by calculating the posterior probability for site classes (Yang *et al.*, 2005).

2.5.3 Branch models

Branch models allow ω to vary across branches in the phylogeny but not across sites. The extreme form of this is the 'free-ratio' model, where the ω of each branch is estimated separately. When compared to the null model 0, where all sites and branches share one ω, it can act as a test for heterogeneity in rates across lineages. Where a branch is hypothesised *a priori* to have experienced positive selection, the branch models can be used as a test for positive selection by comparing a model where the ω of that branch is estimated separately from the rest of the tree to a model where the ω of that branch is fixed to 1 (Yang, 1998; Yang *et al.*, 1998). Branch models can also be used to compare whether or not ω varies between clades or pre-defined lineages. In

addition they can be used to calculate the root-to-tip ω for the lineage leading from the last common ancestor of a clade to each terminal species.

2.5.4 Branch-Site models

An additional method of testing for positive selection which is restricted to one or a few branches, consistent with the action of episodic selection and phenotypic change, implements the Branch-Site models which allow ω to vary across sites and between two categories of branches determined *a priori* (Yang & Nielsen, 2002; Zhang *et al.*, 2005; Yang *et al.*, 2005; Anisimova & Yang, 2007). Here an experimental model, in which a proportion of sites in branches labelled as the foreground branches is allowed to have an ω >1, is compared to a null model, in which the ω of this class of sites is fixed to 1 (neutral evolution), using a LRT. This test has been used to investigate associations between the action of positive selection on candidate genes and phenotypic evolution where the foreground branches are determined based on the pattern of evolution displayed by the phenotype of interest (Yang & Nielsen, 2002; Zhang *et al.*, 2005). The use of these models should be limited to cases where positive selection has not acted across the whole phylogeny (i.e. non-significant site model tests) and where the foreground branches can be labelled *a priori* (Yang & Nielsen, 2002; Anisimova & Yang, 2007). It is also likely that their use only makes biological sense when the phenotype of interest evolves in a punctuated or episodic manner, assuming the mode of phenotypic evolution reflects the mode of selection at the molecular level.

2.5.5 Caveats with *dN/dS*

Despite their widespread use analyses of selection using *dN/dS* have been criticised by some. Hughes (2006) has critiqued the logic behind applying codon based models on the basis that *dN* may frequently exceed *dS* by chance, that tests are usually applied without any *a priori* hypothesis about why the gene should be targeted by positive selection, that there is difficulty in distinguishing relaxed constraint from positive selection, and with the assertion that most adaptive change will likely occur through single, rather than successive, amino-acid replacements. Other issues highlighted have been the possibility of biased codon usage affecting the synonymous rate and therefore the *dN/dS* (Yang & Bielawski, 2000) and temporal effects on

dN/dS between closely related species (Rocha *et al.*, 2006; Wolf *et al.*, 2009). Codon-based models also assume all amino acid changes are equally advantageous during positive selection, ignoring differing chemical properties of amino acids (Yang & Bielawski, 2000). The Branch-Site models in particular have been criticised for having high false positive rates (Nozawa *et al.*, 2010) although this is contested and counter-simulations suggest the tests are conservative (Yang & dos Reis, 2011). Despite these potential sources of error considered use of codon-based models of selection remains an important tool in studying molecular evolution across species (Yang, 2006)

2.6 Methods of detecting evolutionary associations between genes and phenotypes

Finding causal links between molecular and phenotypic evolution, particularly adaptive evolution, is a major goal of contemporary research (Hoekstra & Coyne, 2007; Stern & Orgogozo, 2008). This is a challenging goal, especially in large vertebrates such as primates where our ability to test the hypothesised functional link between signatures of positive selection and phenotypic evolution may be severely limited. Two different but complementary approaches offer potential ways to do so. The first approach is to test the functional consequence of divergent gene sequences using transgenic techniques to introduce the sequence of interest into a model organism (Enard *et al.*, 2009; Pulvers *et al.*, 2010). This approach has the significant advantage of potentially revealing the phenotypic consequences of adaptive mutations or divergent selection but in some cases these effects may potentially be masked due to the different genetic backgrounds of the species of interest and the model. The second approach adopts the comparative method to study molecular evolution by explicitly testing for associations between molecular evolution of candidate genes and phenotypic evolution (Lanfear *et al.*, 2010). Recently phylogenetic models which include phenotypic and molecular components have been developed (O'Connor & Mundy, 2009; Lartillot & Poujol, 2011; Mayrose & Otto, 2011) which have the potential to offer new ways of hypothesis testing and generation both at a genome and candidate gene level. However, these models are in their infancy.

A growing number of candidate gene analyses have sought to explicitly test hypothesised gene-phenotype links by adopting comparative methods, such as Independent Contrasts and PGLS, to test for an association between *dN/dS* and the phenotype of interest whilst controlling

for phylogeny. This is the approach taken in this thesis. Previous analyses which have tested for correlations in this way have typically used the *dN/dS* of the terminal branches (e.g. Dorus *et al.*, 2004; Nadeau *et al.*, 2007). However whilst a species' phenotype reflects the whole phenotypic evolution, the *dN/dS* of the terminal branch does not reflect the whole genotypic evolution. I therefore used the branch models to estimate the average *dN/dS* ratio from the last common ancestor of all the species in each dataset to each terminal species tip. The root-to-tip *dN/dS* is more inclusive of the evolutionary history of a locus and is a property of the species tip, rather than the terminal branch, and is therefore more suitable for regressions against phenotypic data from extant species. In addition, by analysing the rate of evolution since the last common ancestor of the species in our dataset all branches are the same length and therefore not subject to temporal effects on *dN/dS* (Rocha *et al.*, 2006; Wolf *et al*., 2009). One assumption of PGLS analysis is that the residuals of the model are normally distributed. As the residuals of regressions using *dN/dS* ratios were not normally distributed, I used $Log_{10}(dN/dS)$ to improve normality. Residuals of regression analysis with log-transformed *dN/dS* did not violate assumptions of normality and constant variance.

These values were then set as species data and used in a PGLS regression with phenotypic measures in BayesTraits as explained above (Pagel, 1999; Pagel *et al.*, 2004; Organ *et al*., 2006). The significance of the regression coefficient was determined using a one-tailed t-test as I specifically hypothesise associations between *dN/dS* and the phenotype in the direction that the phenotype is evolving as higher *dN/dS* values should be associated with greater phenotypic changes where that gene contributes the genetic basis of that phenotype. The opposite result would suggest an increase in *purifying* selection has acted on a locus as the phenotype evolved and, whilst interesting, would suggest that the locus does not contribute to the genetic basis of *change* in that phenotype and could not explain why the locus has evolved adaptively. Both recently suggested requirements for justifying the use of one-tailed tests are therefore met: I explain why I hypothesised an association in a particular direction *and* why the opposite pattern can be treated the same as a non-significant trend in the expected direction (Ruxton & Neuhäuser, 2010). As the size of our dataset for this analysis is limited by the availability of neonatal brain size data, and the imperfect overlap between phenotype and gene sequence datasets, it is highly likely that the small sample size will result in low power to reject the null

hypothesis. To minimise the chances of Type I errors, I restricted the analyses to a small number of critical tests, and I conducted a series of control analyses. In addition a Jack-knife approach was taken to test the robustness of the associations found and to identify any outliers which have a dominant effect on the slope of the regression. Where more than one phenotype is considered, comparisons of non-nested models were performed using Akaike Information Criterion (AIC: calculated as (2 x no. parameters) + (-2 x Log[Likelihood])) to identify the best supported model, where a lower value indicates a better fitting model, and a difference between models greater than two suggests a substantial difference (Burnham & Anderson, 2002).

In addition to the standard *dN/dS* ratios, I used multiple regressions to investigate the association between phenotype and *dN* while controlling for *dS*. Both approaches examine variation in *dN* and *dS* relative to one another, but they make different assumptions about the nature of the underlying relationship. For example, a significant *dN/dS*-phenotype relationship suggests an association between phenotypic evolution and selection acting on a locus and may be obtained when both change together in a tightly correlated fashion but with one changing at a faster rate than the other (so that the ratio correlates with the absolute value of the changes), whereas in this case a multiple regression would show no significant correlation. Hence, differences in the results obtained may be informative about the nature of the gene-phenotype correlation.

As mentioned above, an alternative method of investigating associations between genes and phenotypes is to use the Branch-Site models to test for the significance of the association between large phenotypic changes and positive selection having acted on relevant genes. This can be done by reconstructing ancestral states, selecting branches along which the phenotype shows high rates of evolution and setting these as the foreground branches in Branch-Site models (Yang, 2005; Anisimova & Yang, 2007). This method relies on obtaining reliable ancestral state reconstructions and assumes positive selection does not act across the whole phylogeny. I explore the potential use of these models for making gene-phenotype associations for continuous traits.

This page was intentionally left blank.

Chapter 3

Trajectories of primate brain evolution

"The idea of progressive evolution is a product of the uneasy marriage between Darwinism and the *scala naturae* theories of the mid 19th century."

Terrence Deacon, *Rethinking Mammalian Brain Evolution*, Amer. Zool. 30, 1990

3. Trajectories of primate brain evolution

3.0 Summary

Brain size is a key adaptive trait. It is often assumed that brain size showed a general evolutionary trend to increase in primates, yet recent fossil discoveries have documented brain size decreases in some lineages, raising the question of how general a trend there was for brains to increase over evolutionary time. In this chapter I present the first systematic phylogenetic analysis designed to answer this question. I performed ancestral state reconstructions of three traits (absolute brain mass, absolute body mass, relative brain mass) using data from 37 extant and 23 extinct primate species and three approaches to ancestral state reconstruction. The results show that whilst both absolute and relative brain mass generally increased over evolutionary time, body mass did not. I confirm that brain expansion began early in primate evolution and show that parallel increases occurred in all major clades. Despite a general trend to expand, brain size does decrease in some lineages. Major episodes of brain mass reduction occurred in the Callitrichidae and Cheirogaleidae and are associated with episodes of body size dwarfism. Relative brain size decreased less frequently and can largely be attributed to increased body mass rather than decreased brain mass. Applying the results to the contentious case of *Homo floresiensis*, I find a number of scenarios under which the proposed evolution of the *H. floresiensis* brain appears to be plausible, dependent on body mass and phylogenetic position. Further analyses of the phylogenetic position of *H. floresiensis* and better body mass estimates are required to confirm the plausibility of the evolution of its small brain mass. Importantly, the results offer insights into how selection has brought about increases in brain size and provide a phenotypic framework with which we can interpret the results from analyses of the molecular evolution of genes involved in brain development.

3.1 Introduction

Extant primate brains, which vary from 1.8g (*Microcebus murinus*) to 1330g (*Homo sapiens*), fall within the range of non-primate mammalian brain masses (Roth & Dicke, 2005). However, after correcting for allometric scaling with body mass primates have relatively large brains compared to most other mammals (Barton, 2006a). A trend towards brain expansion is assumed to have occurred throughout mammalian, and in particular primate, evolution (Jerison, 1973, but see Deacon, 1990; Shultz & Dunbar, 2010) and this has been interpreted as an indication of directional selection on cognitive abilities, due, for example, to arms races in social cognition (Dunbar & Schultz, 2007; Pérez-Barberia *et al.*, 2007).

Recent studies, however, indicate that brain size, measured either in volume or mass, may have decreased in some vertebrate lineages (Niven, 2005; Safi *et al.*, 2005). Decreases in both absolute and relative brain size appear to have occurred in a number of taxa including birds (Boerner & Krüger, 2008), bats (Safi *et al.*, 2005), bovids (Köhler & Moyá-Solá, 2004), elephants (Roth, 1992) and hippopotami (Simmons, 1999; Weston & Lister, 2009). Dwarfism following island isolation ('the island rule') can account for some of these decreases (Niven, 2007; Weston & Lister, 2009) but not all. For at least some of these cases it is likely that a reduction in brain size has occurred to meet the demands of the species' changing ecological needs rather than being due to geographical isolation *per se* (Safi *et al.*, 2005; Boerner & Krüger, 2008).

Although many studies have investigated the possible selective advantages and disadvantages of increased brain size in primates (Aiello & Wheeler, 1995; Barton, 1998, 2006a; Dunbar, 1998; Brown, 2001; Reader & Laland, 2002), few consider how frequently brain size has reduced or to what extent these selective pressures fluctuate through time. Periods of primate evolution which show decreases in brain size are of great interest as they may yield insights into the selective pressures and developmental constraints acting on brain size. Bauchot and Stephan (1969) noted the evolution of reduced brain size in the dwarf Old World monkey *Miopithecus talapoin* and Martin (1990) suggested relative brain size in great apes may have undergone a reduction based on the cranial capacity of the extinct hominoid *Proconsul africanus*. Taylor and van Schaik (2007) reported a reduced cranial capacity in *Pongo pygmaeus morio* compared to other orangutan populations and hypothesise this reduction is selected for as a result of scarcity

of food. Finally, Henneberg (1998) showed that during the late Pleistocene human absolute brain size has decreased by 10%, accompanied by a parallel decrease in body size.

The importance of understanding the evolution of reduced brain size in primates has recently been brought into sharp focus with the discovery of a small-brained hominin, *Homo floresiensis*, which overlapped both geographically and temporally with modern humans (Brown *et al.*, 2004; Roberts *et al.*, 2009). This has challenged our understanding of human evolution and created much debate over whether *H. floresiensis* was a distinct species or a pathological example of modern humans (Jacob *et al.*, 2006; Hershkovitz *et al.*, 2007; Delaval & Doxsey, 2008). Studies describing the endocast and post-cranial features of the type specimen (LB1) have resulted in mixed conclusions (Weber *et al.*, 2005; Falk *et al.*, 2005; Falk *et al.*, 2007; Larson *et al.*, 2008; Tocheri *et al.*, 2007; Gordon *et al.*, 2008; Falk *et al.*, 2009; Jungers *et al.*, 2009). Analyses using known cases of dwarfism to model brain and body size reduction in *H. floresiensis* from an ancestral *Homo erectus* population suggested insular dwarfism cannot explain the smaller brain and body size (Martin *et al.*, 2006a; Martin *et al.*, 2006b; but see Weston & Lister, 2009). However recent studies have found that both the degree and temporal rate of reduction in body size observed in *H. floresiensis*, assuming ancestry with *H. erectus*, fall within the range of body size reductions in other island primate species (Bromham & Cardillo, 2007; Welch, 2009). An alternative phylogenetic hypothesis for *H. floresiensis* has recently been proposed and indicates that this species may not have evolved by insular dwarfism of a known *Homo* species (Argue *et al.*, 2009). Instead Argue *et al.* (2009) propose two equally parsimonious cladograms in which *H. floresiensis* is a distinct early species of *Homo*, which emerged after *H. rudolfensis* and either before or after *H. habilis*. The debate about the place of *H. floresiensis* in the primate tree and the possible evolutionary significance of its small size and encephalization could be illuminated by placing the specimens in the context of a broader phylogenetic analysis.

Reconstructing ancestral brain and body sizes provides a means of testing the generality of the trend of increasing brain and body size through primate evolution. It also provides estimates of brain and body sizes at key points along the primate phylogeny allowing inferences to be made about the ecology of the ancestors of key clades, based on what is known about the relationship between body size, ecology and life history traits in living primates (Jungers, 1985;

Fleagle, 1999). Furthermore the results could provide a phenotypic framework with which to interpret results from evolutionary genetics studies of genes involved in brain development. However, before making any inferences based on estimated ancestral states it is vital to perform a thorough comparison of reconstruction methods in order to obtain the most robust estimates. Previous studies have used parsimony and maximum likelihood (ML) methods to reconstruct ancestral character states and infer the adaptive origins of phenotypes (e.g. Soligo & Martin, 2006; Finarelli & Flynn; 2006, 2007; Masters *et al.*, 2007). However, basing conclusions on these methods may be problematic as they fail to provide reliable estimates when there are directional evolutionary changes and can also be adversely affected when ancestral states fall outside the range of extant species (Oakley & Cunningham, 2000; Garland *et al.*, 1999), as is expected to be the case for primate brain evolution (Jerison, 1973). Incorporating data from fossils can improve ancestral reconstruction estimates as they may more completely describe the range and temporal distribution of the character's history, and thus help improve the estimated nodal values both in the presence of directional trends and when ancestral values are markedly different from extant species values (Polly, 2001; Finarelli & Flynn, 2006). More recently, a method to model directional change and find the best-fitting models of evolution *prior* to ancestral state reconstruction in a Bayesian framework has been developed (e.g. Pagel *et al.*, 2004; Organ *et al.*, 2007).

Here I investigate the evolution of brain and body mass in Primates and assess whether brain mass and body mass show evidence of directional trends, whether brain size has increased in parallel across primates or is primarily restricted to particular clades or periods, and quantify the frequency of brain size reductions. Given the strong allometric relationship between brain and body mass (Jerrison, 1973; Barton, 2006a), relative brain size is most commonly used in comparative studies (Healy & Rowe, 2007) that aim to test the evolutionary significance of an increased brain mass above that predicted from a species' body mass (e.g. Dunbar & Schultz, 2007; MacLean *et al.*, 2009). However absolute brain mass is of evolutionary relevance too (Striedter, 2005; Marino, 2006); it may be related to cognitive ability (Deaner *et al.*, 2007) and it is correlated with neuron number (Herculano-Houzel *et al.*, 2007) which in turn is likely to have important implications for cognitive performance (Roth & Dicke, 2005). Furthermore, analysis of absolute brain and body size is necessary in order to interpret the nature of evolutionary

changes in relative brain size because relative brain size is an artificial, composite trait whose developmental basis lies in changes in either brain or body mass which may be largely independent (Shea, 1983). I therefore investigated the evolutionary history of both relative and absolute brain size.

Three approaches to reconstructing the evolutionary history of these traits were used: weighted squared-change parsimony, maximum likelihood (ML) and a Bayesian Markov-chain Monte Carlo (MCMC) method implemented in BayesTraits (Maddison, 1991; Schluter *et al.*, 1997; Pagel *et al*., 2004; Organ *et al.*, 2007) (see chapter 2), and performed each analysis with and without the inclusion of fossil data, following previous studies showing that ancestral state reconstruction are improved by including fossil data particularly when traits evolved under a directional trend (Polly, 2001; Finarelli & Flynn, 2006). I assessed the sensitivity of each method to the inclusion of fossil data, and also compared estimates between methods. The aim of the model comparison is to test whether any method produces consistent estimates with and without the inclusion of fossils, as this might suggest a more robust method which is less affected by aspects of the trait's evolution which decrease the accuracy of ancestral state reconstructions, such as directional trends or ancestral values which lie outside of the range of extant species. Second, to explicitly model and assess statistically whether there was a directional increase in brain and body mass, I compared ancestral state reconstructions when a directional constant-variance random walk model of evolution was assumed vs. a non-directional constant-variance random walk model as implemented in BayesTraits (Pagel *et al.*, 2004; Organ *et al.*, 2007), using the phylogeny with fossil species included. I then examined the pattern of change in brain and body size through the tree under the most supported model.

I discuss the implications of my results for hypotheses on the adaptive origins of modern primates, and identify branches along which brain mass has increased greatly or at a high rate, or along which brain mass has decreased in either absolute or relative terms. Finally I use my results to evaluate alternative scenarios about the origin of *H. floresiensis*, specifically from three different populations of *H. erectus* and from *H. habilis*. This analysis aims to evaluate whether descent of *H. floresiensis* from a putative ancestral population involves a decrease in brain and body mass that is beyond those observed in other primate lineages.

3.2 Methods summary

Previously published data were collected for 37 extant primate genera including 14 catarrhines, 12 platyrrhines, one tarsier and 10 strepsirhines, and 23 extinct species (see chapter 2). The dataset includes 7 extinct hominins, which I use to examine whether ancestral values were overly influenced by the large disparity between the brain mass of *Homo sapiens* and the other apes. To calculate relative brain mass I performed a phylogenetically-controlled regression between log(brain mass) and log(body mass) in BayesTraits (Pagel *et al.*, 2004; Pagel & Meade, 2006). The PGLS regression analysis was performed with MCMC. I first identified the regression model that best described the relationship between brain and body mass by testing whether additional branch-length scaling parameters (lambda, kappa, delta) to the default BM model improved the fit to the data. This was done in a Bayesian framework (Kass & Raftery, 1995; Gilks *et al.*, 1996; Organ *et al*., 2007). Where a parameter was significantly different from the default value of 1 it was then estimated in the final regression analysis. The regression was highly significant (t_{59} = 14.53, R^2 = 0.858, $p < 0.001$), the branch-length scaling parameters lambda and delta were not significantly different from the default value of one (lambda: lambda=0.979, LR = 2.04, p = 0.153; delta: delta= 1.091, LR = 0.03, p = 0.857). Conversely, kappa was estimated to be 0.474, significantly different to one (LR = 8.132, p = 0.004). Relative brain mass on body mass for each species (extant or extinct) was calculated as residual values using the regression equation: log(brain mass) = 2.18 + 0.684[log(body mass)]. These residuals were used to test for an evolutionary trend to increase relative brain mass and to reconstruct ancestral states.

Relative brain size was analysed using two alternative approaches. With the first approach, termed ‘residuals second’, I inferred ancestral brain and body sizes at each node and then derived relative brain size as the residual brain size on body size using the ancestral state estimates at the nodes and the phylogenetically controlled GLS equation. This approach has the advantage of first finding the best fitting model for brain and body mass, but does not explicitly model the correlated evolution of brain and body mass, and cannot be used for testing directionality in the evolution of encephalization (relative brain mass) if brain and body size evolved under different models. With the second approach, ‘residuals first’, I explicitly modelled the evolution of encephalization as relative brain size, by first calculating the residuals of brain

on body mass in the extant species with the phylogenetically controlled fit line, and then used these residuals as data to perform an ancestral state reconstruction of relative brain size. This approach has the advantage of modelling encephalization but it cannot incorporate two distinct models for brain and body mass should they evolve under different models and residuals are not deemed 'real' data (Freckleton, 2009). These two approaches, however, produced very similar relative brain size values, as the residuals at each node returned by the two methods were highly correlated ($r_s = 0.979$, $p < 0.001$) and I therefore present only the results of the 'residuals second' method.

The genus level phylogeny used is described in chapter 2 and shown in Figure 3.1. In addition I used the two most parsimonious hominin topologies obtained by Argue *et al.* (2009) to analyse the evolution of *H. floresiensis*. Here branch lengths were determined based on the earliest and latest known fossils for each species (Fleagle 1999; Wood & Collard, 1999; Vekua *et al.*, 2002; Roberts *et al.*, 2009), with divergence dates of internal nodes coming from the first appearance of any species within the lineages which evolved from that node. Where the time of origin for a lineage could not be determined in this way I minimise phylogenetic assumptions by placing the node in the centre of the branch.

Ancestral state reconstructions of absolute brain and body mass and relative brain mass at each node of the phylogeny were estimated using three methods: weighted squared-change parsimony in Mesquite (Maddison & Maddison, 2008), ML in ANCML (Schluter *et al.*, 1997), and Bayesian MCMC (Kass & Raftery, 1995; Gilks *et al.*, 1996) in BayesTraits following Organ *et al.*'s (2007) method, all of which incorporate phylogenetic information and are described in chapter 2. In addition I implemented the test for directional trends using BayesTraits.

Table 3.1 shows the rate parameter estimates from the Bayesian MCMC analysis in BayesTraits using the constant-variance random walk model to identify the best model before the ancestral state reconstruction. The Bayesian MCMC posterior distributions of lambda were not significantly different from the default value of one for any of the three traits. I tested whether the posterior distributions of kappa and delta differed from the default value of one by comparing the harmonic mean of the model in which the parameter was estimated to the harmonic mean of the model where it was set as one. The default value of one was used in the final analysis when the Bayes Factor was less than two (see chapter 2). For absolute body size neither kappa (Bayes

Factor = 0.740) nor delta (Bayes Factor = 0.063) differed from one. For absolute brain size both kappa (Bayes Factor = 3.00) and delta (Bayes Factor = 2.00) differed from one. Finally for relative brain size both kappa (Bayes Factor = 5.753) and Delta (Bayes Factor = 6.192) differed from one. The posterior distribution of kappa and delta were therefore estimated in the best-fitting model for absolute and relative brain size used to compare the non-directional and directional models and in the reconstruction analysis. As kappa and delta are better estimated with lambda, I also estimated lambda in the final analysis of absolute and relative brain size.

Table 3.1 Estimation of rate parameters*

Trait	Kappa	Delta	Lambda
Body mass	0.936 (±0.009)	0.636 (±0.009)	0.980 (±0.002)
Brain mass	0.704 (±0.013)	0.740 (±0.017)	0.978 (±0.004)
Relative brain size	0.660 (±0.012)	0.497 (±0.016)	0.915 (±0.009)

* Results of Bayesian analysis shown as the mean with 95% confidence intervals

To test for the sensitivity of each method to the inclusion of fossil species, I followed Webster and Purvis (2002) and checked the strength of the association between estimates at each node made with and without fossil data using correlation analysis in GenStat (VSN[i], UK). For the Bayesian analysis I calculated the mean of the posterior distribution of the ancestral states at each node of the tree. Because some sets of estimates made with different methods were not normally distributed, I used Spearman's rank correlation for all tests to allow correlation coefficients (r_s) to be fully comparable throughout the analysis.

The change in brain and body mass along each branch was calculated by taking the difference between consecutive nodes. As the estimates for each node using absolute values of log brain and body mass are log values, subtracting consecutive node values gives a proportional change in mass. I therefore also converted log values into absolute numbers before calculating differences to get the absolute change in mass. Estimates of ancestral relative brain mass are

based on residual values from a regression analysis of two log values. I therefore simply subtracted successive nodes to calculate change in relative brain mass. Finally, to control for differential potential for divergence due to longer time since the last splitting event I repeated the analysis and calculated the rate of change by dividing the change along a branch by the branch length, for each measure of brain mass.

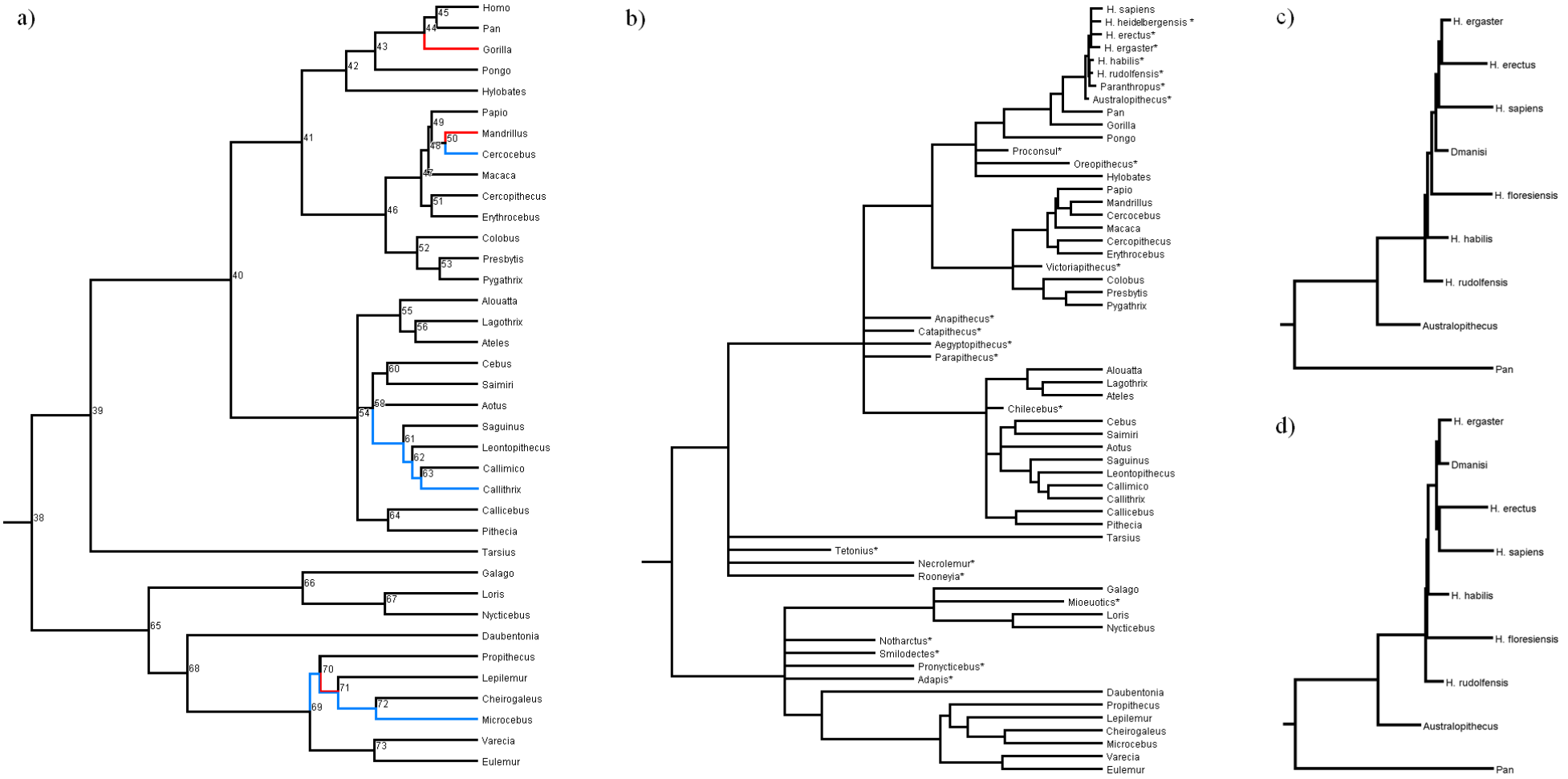

Figure 3.1 Phylogeny of primates with extinct primates

a) Phylogeny of extant primate genus, branches are drawn proportional to time. The node labels can be used to interpret Table 3.4. Red branches indicate a decrease in relative brain size, the blue branches indicate a decrease in absolute brain mass. b) Phylogeny used for main reconstruction analysis. Extinct primates are denoted with an asterisk (*); c) & d) Phylogenies of hominins used for the *H. floresiensis* analysis based on the two most parsimonious topologies from Argue *et al.* (2009); the rest of the phylogeny was left as shown in a). c) corresponds to Argue *et al.*'s Tree 1 and d) to Tree 2. Branches are drawn proportional to time. This figure was prepared in Mesquite (Maddison & Maddison, 2008).

3.3 Results & discussion

3.3.1 Ancestral reconstructions: congruence & inconsistencies between estimates

Ancestral values for all nodes of the tree with and without the inclusion of fossil data were highly correlated for absolute brain mass (parsimony, Spearman's correlation coefficient (r_s) = 0.932; ML, r_s = 0.932; Bayesian MCMC, r_s = 0.993, all $p < 0.001$) and body mass (parsimony, r_s = 0.939; ML, r_s = 0.941; Bayesian MCMC, r_s = 0.960, all $p < 0.001$). ML and parsimony methods produce almost identical results for estimates made with (r_s =1.000, $p < 0.001$) and without fossils (r_s =1.000, $p < 0.001$). I therefore only present the results of further comparisons between ML and Bayesian MCMC. The lower r_s values in the parsimony and ML analyses are caused by increased disparity between the estimates at deeper nodes. In particular, estimates of log(brain mass) using fossils are 10-15% lower for the root (Figure 3.1, node 38), the ancestral haplorhine (node 39), the ancestral anthropoid (node 40) and the ancestral New World monkey (node 54) than estimates made without inclusion of the fossil data (Figure 3.2a), suggesting the accuracy of the estimates decreases at the deeper nodes when fossil data are not used. The standard errors in ML analysis support this conclusion, being larger for deeper nodes. Conversely, the results of the Bayesian MCMC analysis do not show this disparity and deep nodes fall on the same line as shallower nodes (Figure 3.2 a & b**)** although confidence intervals of the root estimate are still higher than those of all other nodes.

The results from the Bayesian analyses agree more strongly with ML when fossil data are included than when they are excluded for both brain mass (with fossils: r_s = 0.995, $p < 0.001$; without fossils: r_s = 0.923, $p < 0.001$; Figure 3.2 c & d) and body mass (r_s = 0.981, $p < 0.001$ with fossils; r_s = 0.926, $p < 0.001$ without fossils). The greatest disparity between estimates made without fossils between parsimony/likelihood analysis and Bayesian MCMC analysis are found at the root (node 38), the ancestral haplorhine (node 39), the ancestral anthropoid (node 40), the ancestral strepsirhine (node 65) and the ancestral lemur (node 68). When fossil data are included, disparity between the MCMC and ML remains for nodes 38 and 39, with the estimates from the Bayesian analysis being lower than those made by the other methods.

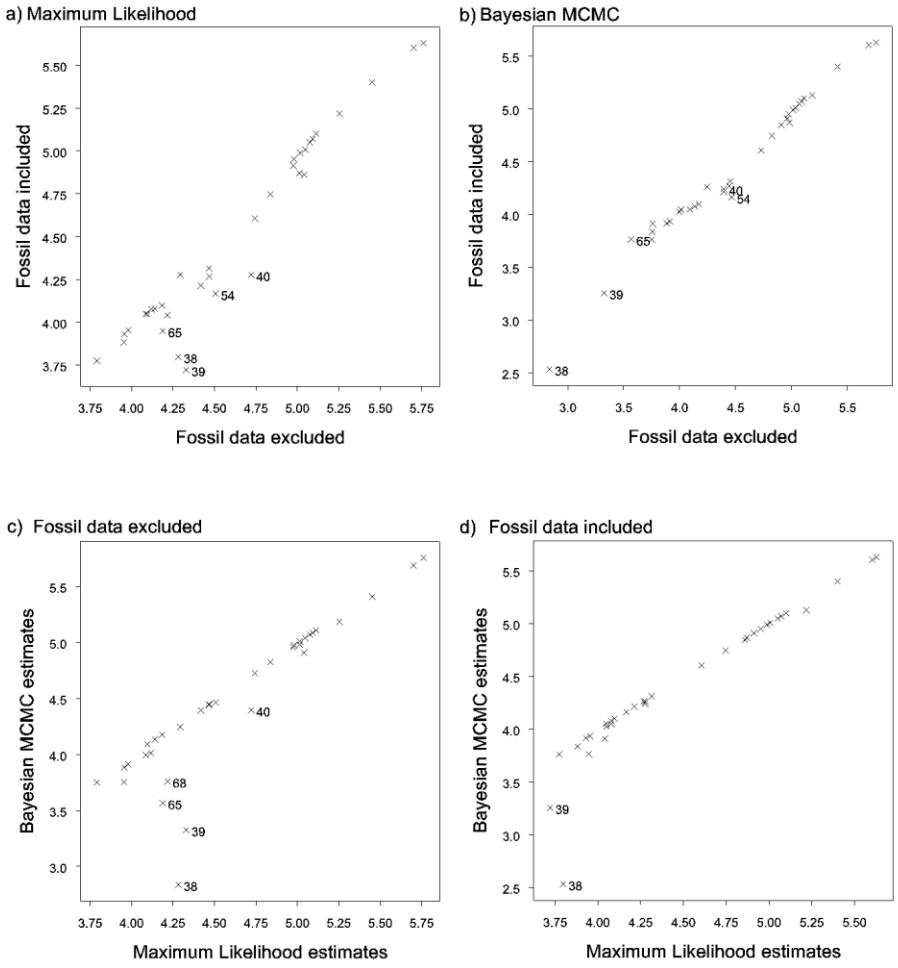

Figure 3.2 Correlations between estimates of absolute brain mass in log(mg)
a) with and without fossil data using ML; b) with and without fossil data using Bayesian MCMC; c) without fossil data between ML and Bayesian MCMC results; d) with fossil data between ML and bayesian MCMC results. Numbers indicate nodes in Figure 3.1.

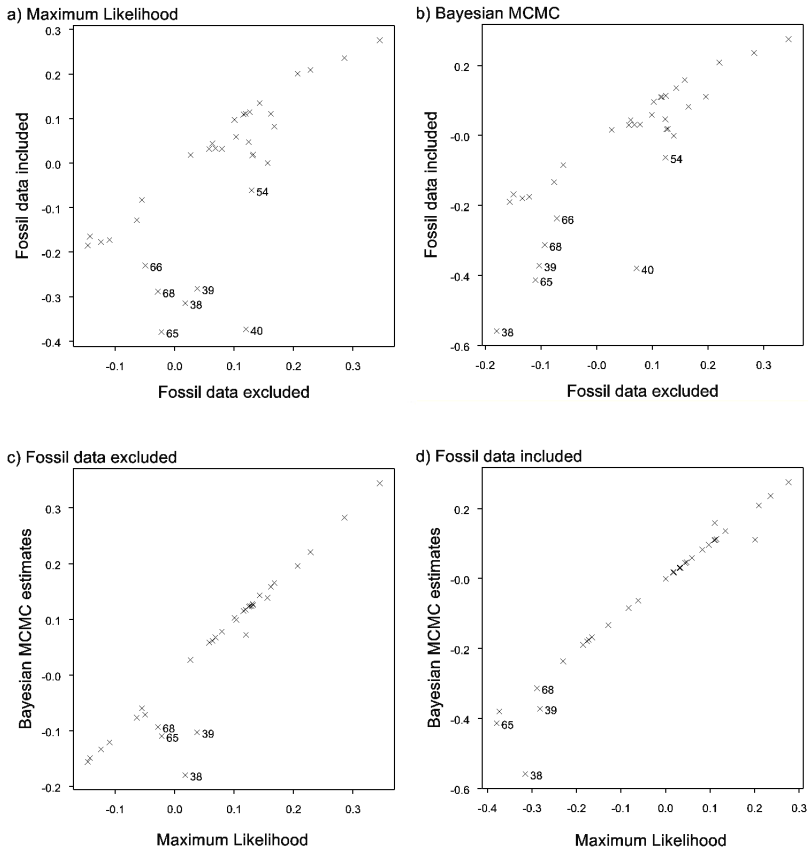

Figure 3.3 Correlations between estimates of relative brain mass
a) with and without fossil data using ML; b) with and without fossil data using Bayesian MCMC; c) without fossil data between ML and Bayesian MCMC results; d) with fossil data between ML and bayesian MCMC results. Numbers indicate nodes in Figure 3.1.

The level of congruence between ancestral state estimates made with and without fossil data was much lower for relative brain mass than for absolute brain mass. Spearman's rank correlations for all three methods were highly significant although r_s values were much lower for ML (r_s = 0.743, p< 0.001) and parsimony (r_s = 0.743, p< 0.001) than for the Bayesian analysis (r_s = 0.835, p< 0.001). All three approaches performed poorly when estimating ancestral states of deep nodes, as indicated by the large disparities between estimates made with and without fossils (Figure 3.3, a & b). Estimates of ancestral relative brain mass using parsimony and ML were highly consistent both with and without fossil data (for both analyses: r_s = 1.000, p< 0.001). The results from Bayesian MCMC analysis were again more similar to those estimated by the two other methods when fossil data were included (r_s = 0.994 with fossils, r_s = 0.968 without; Figure 3.3, c & d).

It is interesting to note that for all three approaches the estimated brain mass of the last common ancestor of humans and chimpanzees is larger when fossil data are not included. For example, the average estimate of brain mass for the *Homo-Pan* ancestor using MCMC analysis was 569.4g (95% CI: 567.7 - 572.2g) without fossils, whilst when fossils were included the average estimate was 425.6g (95% CI: 424.2 – 426.8g). This suggests the mass of the human brain can exert a large influence over ancestral state reconstructions in the great ape clade.

To summarise, parsimony and ML produced ancestral state estimates that were more discrepant between analyses with and without fossils when compared to estimates obtained with Organ *et al.*'s (2007) method in a Bayesian framework. Moreover, the estimates of the Bayesian analysis were more consistent with those produced by ML and parsimony when fossil data were included. These results thus suggest that Organ *et al.*'s (2007) method is more robust and therefore preferable for reconstructing ancestral states with my dataset. Although I cannot say whether this approach will generally perform most reliably when reconstructing ancestral states in taxa where little or no fossil data are available, the results suggest that this might be the case. It would therefore be interesting to test whether Organ *et al.*'s (2007) method for reconstructing ancestral states does perform better than parsimony and ML in the absence of fossil data using simulations and datasets where the ancestral states are known (e.g. Oakley & Cunningham, 2000).

One possible reason for lower consistency in estimates with and without fossils, particularly for ML and parsimony, might be the presence of directional trends (Oakley & Cunningham, 2000; Webster & Purvis, 2002). Although this problem can in part be mitigated by incorporating fossil data that provide temporal information and variation not observed among living species and improve the accuracy of ancestral state reconstructions with these two methods (Polly, 2001; Finarelli & Flynn, 2006), neither parsimony nor ML can explicitly model directional trends, unlike the methods implemented in BayesTraits. I next addressed this issue and tested whether body size, brain size and encephalization evolved under directional trends in primates.

3.3.2 Evolutionary trends in body and brain mass evolution

I tested for evolutionary trends by comparing a directional random-walk model to the non-directional random-walk model in BayesTraits. The implementation of the directional model requires variation in root-to-tip branch length (Pagel, 1997, 1999; Organ *et al.*, 2007) which in an otherwise ultrametric tree is provided by the inclusion of fossil data. To explicitly test for directionality in encephalization rather than simply inferring this from the evolutionary histories of brain and body mass, I used the residuals of brain size on body size of the species (computed as explained above with the 'residuals first' approach) as species data of relative brain size in this analysis. The 'residuals second' approach could not be used in this context since it is based on residuals computed at internal nodes of the phylogeny.

I found no evidence for a directional trend in the evolution of absolute body mass; as the directional model did not provide a better fit to the data when compared to the non-directional model (Table 3.2; Figure 3.4). Therefore, in agreement with other authors (Soligo & Martin, 2006; Soligo, 2006), I conclude that there is no evidence for Cope's Rule (Alroy, 1998; Polly, 1998), which states body size tends to increase through time, in primates. In contrast there is strong evidence for a trend of increasing absolute and relative brain size (Table 3.2; Figure 3.4) suggesting that the expansion of the primate brain has been of major evolutionary significance across the modern primate phylogeny and throughout primate evolution.

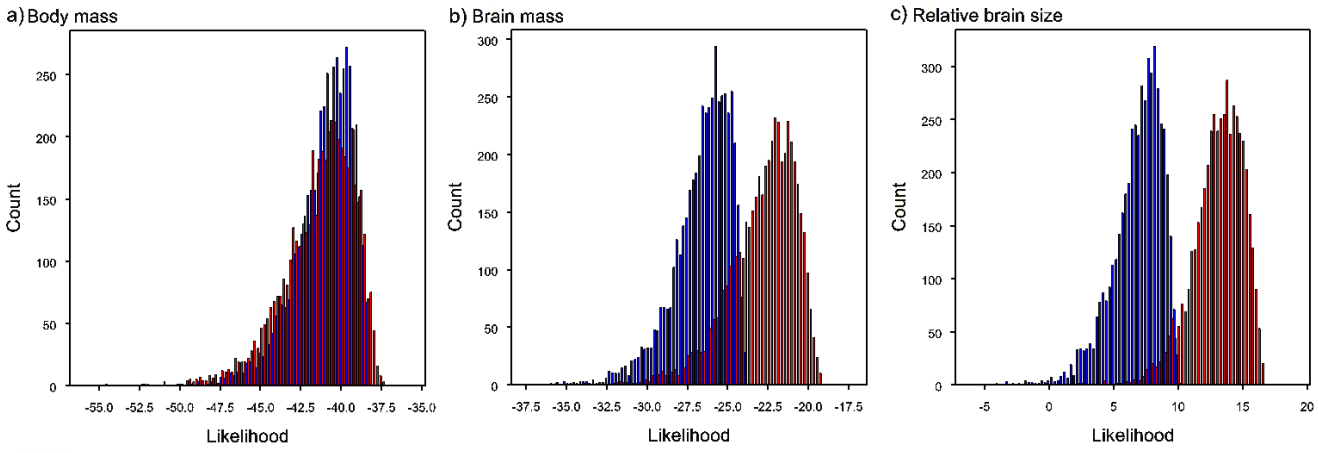

Figure 3.4 Posterior distributions of log-likelihoods for the non-directional and directional models; a) body mass; **b) brain mass**; **c) relative brain size.** The log-likelihood of the directional model is shown in red, the non-directional model in blue. The posterior distributions of ancestral state estimates were obtained using uniform priors, 2 million iterations and a sampling interval of 100 (see chapter 2). The harmonic means and Bayes Factors of the posterior distributions are given in Table 3.2.

Table 3.2 Tests for evolutionary trends [1]

Phenotype	**Harmonic mean Log(Lh): Constant-variance model**	**Harmonic mean Log(Lh): Directional model**	**Bayes Factor**
Absolute body size	-44.688	-45.275	-1.174
Absolute brain size	-30.282	-27.087	6.390
Relative brain size	1.647	8.576	13.857

[1] The model with the highest log-likelihood is the best-fitting model.

To assess how the presence of a directional trend affects the accuracy of estimates made with a non-directional model I performed correlations between the results obtained from the directional and non-directional models. Correlations between the estimates made for absolute brain mass under the directional and non-directional models suggest no nodes are estimated less accurately than others under the non-directional constant-variance model ($r_s = 0.995$, $p < 0.001$). However, the directional model tends to give lower estimates for all nodes (Figure 3.5 a). For relative brain mass the r_s between estimates under directional vs. non-directional model is lower ($r_s = 0.943$, $p < 0.001$) and, whilst nodes are generally estimated as having lower values under the directional model (Figure 3.5 b), the ancestral state reconstructions for the deepest nodes tend to differ more drastically.

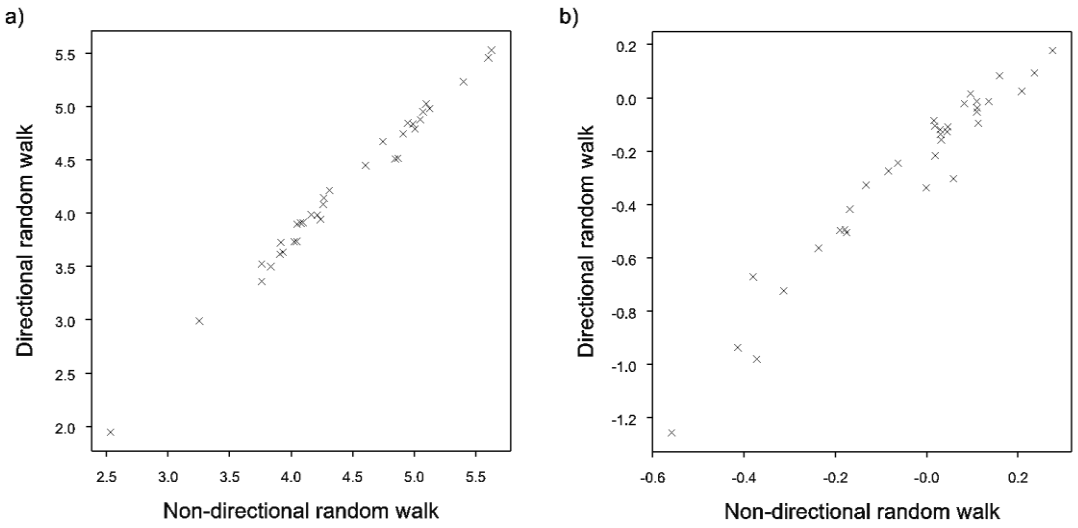

Figure 3.5 Correlations between estimates made using directional constant variance random walk and non-directional constant variance random walk models in BayesTraits; a) absolute brain mass and **b) relative brain mass.**

Taken together these results suggest that the ancestral state reconstruction procedure implemented in Bayesian framework following Organ *et al.* (2007) might be more reliable in comparison to parsimony and ML methods, as it first identifies the best predictive model based on known data, and then uses such a model to infer unknown ancestral states. In addition it can explicitly model directionality, and therefore I could identify a directional trend to increase in both absolute and relative brain mass – but not body mass - in primates. For the purposes of this thesis, I conclude that the most reliable estimates are thus obtained with Bayesian analyses, under a non-directional random walk model for body mass and directional random walk for absolute brain mass (Table 3.3).

3.3.3 Brain:body allometry

These results provide confirmation for the suggestion that strong evolutionary trends have governed the evolution of primate brain size (Jerison, 1973). In contrast body mass evolution has not tended to increase in primates implying brain and body mass have been subject to separate selection pressures and have been able to respond to these selection pressures. This result has relevance for interpreting brain:body allometry, and in turn may suggest some features of the nature of the genetic structure of brain evolution in primates.

Most notably these results are in close agreement with those of Lande (1979). Lande (1979) derived a quantitative genetic model which describes how evolutionary allometry can arise through natural selection on multiple traits. Lande then used this, in conjunction with data from artificial selection experiments on brain weight, and the correlated increase in body mass, to show that there is a strong additive genetic correlation between brain and body weight in mice. With this he subsequently demonstrated that the shallow slopes of brain:body scaling among closely related mammalian species are largely due to selection on body mass, whilst the steeper slope obtain for intergeneric data is explained by selection on both brain and body mass, suggesting that at a macroevolutionary scale natural selection is able to act on genetic changes which alter the covariation between the two traits.

Lande went on to discuss evidence that the genetic correlation between brain and body weight decreases with increasing relative brain mass and showed that the genetic correlation between brain and body weight in primates is approximately a third of that estimated from

selection experiments in mice. This implies that changes in primate brain mass were only weakly coupled to changes in body mass (Lande, 1979). This becomes important when directional selection acts on brain mass. If primates shared the high genetic correlations found in mice selection on brain mass would lead to giantism and/or antagonistic selection on body mass constraining the evolution of large brains. Hence the evolution of the degree of encephalization seen in humans, for example, could only be facilitated by a reduction in brain:body genetic correlation.

The results presented here support this conclusion by demonstrating brain and body mass experienced different selective regimes with directional selection on brain size occurring without a correlated directional expansion of body mass as hypothesised by Lande (1979). This implies that during primate evolution selection has preferentially acted on genetic variation which alters brain mass but has low pleiotropic effects on body mass. However, despite this there is still a strong correlation between the change in brain and body mass along each branch across the phylogeny (t_{68} = 11.170, $p < 0.001$, R^2 = 0.642; Figure 3.6) implying adaptive co-evolution of brain and body size and/or a reduced genetic correlation.

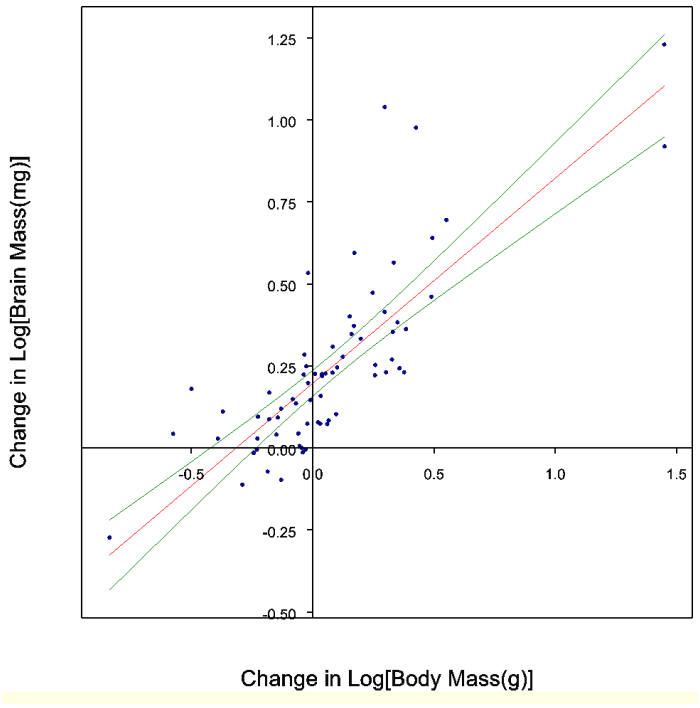

Figure 3.6 Correlated changes in brain and body mass. Green lines show 95% confidence intervals.

Table 3.3 Ancestral state estimates using most supported models

Node (see Figure 3.1)	Log[Body mass (g)]	Log[Brain mass (mg)]	Relative brain mass
38	1 (±0.0001)	2.08 (±0.0215)	-1.26
39	2 (±0.0021)	3.02 (±0.0047)	-0.97
40	3 (±0.0016)	3.94 (±0.0025)	-0.67
41	3 (±0.0023)	4.51 (±0.0032)	-0.34
42	4 (±0.0017)	4.98 (±0.0024)	-0.04
43	4 (±0.0022)	5.23 (±0.0028)	0.03
44	4 (±0.0018)	5.46 (±0.0025)	0.09
45	4 (±0.0016)	5.53 (±0.0023)	0.17
46	3 (±0.0017)	4.51 (±0.0031)	-0.30
47	3 (±0.0015)	4.79 (±0.0024)	-0.10
48	4 (±0.0015)	4.88 (±0.0023)	-0.05
49	4 (±0.0015)	4.95 (±0.0023)	-0.01
50	4 (±0.0015)	5.02 (±0.0022)	0.01
51	3 (±0.0016)	4.84 (±0.0024)	-0.02
52	3 (±0.0019)	4.74 (±0.0026)	-0.12
53	4 (±0.0017)	4.85 (±0.0024)	-0.09
54	2 (±0.0013)	3.98 (±0.0022)	-0.24
55	3 (±0.0020)	4.45 (±0.0026)	-0.11
56	3 (±0.0020)	4.67 (±0.0026)	0.09
58	2 (±0.0016)	3.98 (±0.0023)	-0.21
60	3 (±0.0020)	4.21 (±0.0027)	-0.02
61	2 (±0.0018)	3.91 (±0.0026)	-0.15
62	2 (±0.0018)	3.91 (±0.0025)	-0.14
63	2 (±0.0018)	3.90 (±0.0024)	-0.12
64	3 (±0.0022)	4.14 (±0.0027)	-0.10
65	3 (±0.0018)	3.39 (±0.0036)	-0.94
66	2 (±0.0029)	3.50 (±0.0034)	-0.56
67	2 (±0.0028)	3.72 (±0.0031)	-0.32
68	3 (±0.0026)	3.62 (±0.0044)	-0.72
69	3 (±0.0023)	3.74 (±0.0036)	-0.51
70	2 (±0.0023)	3.73 (±0.0034)	-0.49
71	2 (±0.0023)	3.64 (±0.0032)	-0.50
72	2 (±0.0023)	3.52 (±0.0030)	-0.41
73	3 (±0.0025)	4.08 (±0.0033)	-0.27

3.3.4 Primate origins

Having obtained the most reliable estimates of ancestral states at each node in the tree for each phenotype it is then possible to use these to make evolutionary inferences. For example the most supported estimate of the body mass at the root of the primate tree using Bayesian analysis is largely consistent with some previous qualitative estimates. Martin (1990) suggested the ancestral primate probably weighed less than 500g, while Fleagle (1999) used early primate fossils to conclude that the ancestral primate was probably as small as 20g. This is similar to my estimated body mass at the root of the phylogeny obtained with the inclusion of fossil species (48.98g, 95% CI: 48.97g - 50.00g; Figure 3.7). The estimate made without the fossils is similarly low (37.71g, CI: 37.60g- 37.76g). Both estimates of body mass at the root lie within the range of the proposed extinct sister-group to modern primates, the plesiadapiforms, which ranged from 7g (the *Micromomyidae* family) to 3000g (the *Carpolestidae* family), and is consistent with the estimated body masses of two putative early modern primates *Altanius* (10g) and *Altiatlasius* (50-100g) (Fleagle, 1999; Bloch *et al.*, 2007). In contrast, a much higher estimate of ancestral primate body mass [1171g (95% CIs: 236-3610g)] was recently obtained using a parsimony method and extant species data only (Soligo & Martin, 2006). However, the results discussed above show that parsimony leads to overestimates of body size in the absence of fossil data, questioning Soligo & Martin's conclusion.

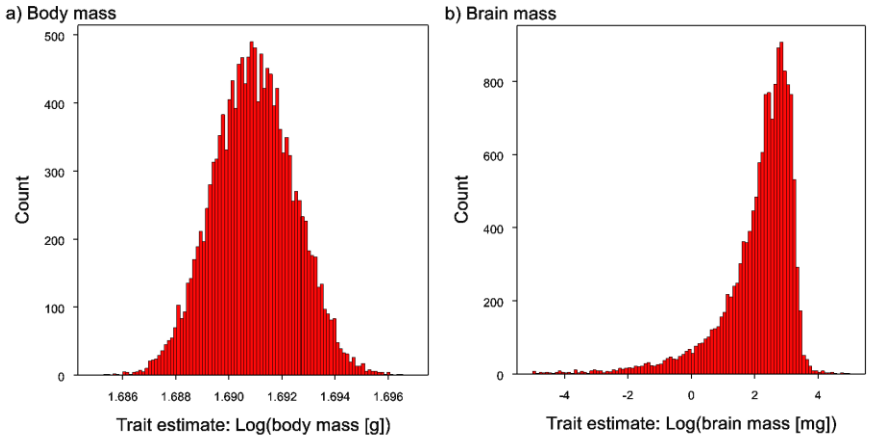

Figure 3.7 Posterior distributions of trait estimates for the LCA of living primates for a) body mass; **b) brain mass**. Histograms are plotted from a posterior distribution of ancestral state estimates obtained using uniform priors (prior range: -100 to +100) acceptance rates were within 20-40% (see methods). To ensure the chain fully explored the parameter space, I extended the MCMC run to 25 million iterations with a sampling interval of 1500.

Body mass variation is associated with a number of behavioural, ecological and life history traits (Jungers, 1985; Barton, 1992; Peters, 1983; Schmidt-Nielsen, 1984; Charnov & Berrigan, 1993; Ross, 1997; Fleagle, 1999; Dial *et al.*, 2008) which are frequently used to infer characteristics of extinct species. Small body mass in extant primates (less than 500g) is usually associated with nocturnality, an insectivorous trophic niche (Kay, 1984) and a leaping mode of locomotion (Fleagle, 1999). The probable small body mass of the ancestral primate has been interpreted as evidence that it occupied a fine-branch niche and was adapted for grasping small insect prey (Cartmill, 1972; Martin 1990). On the basis of correlates of body mass and ecological and life history traits of living primates (Jungers, 1985; Fleagle, 1999), the estimated mass at the root would suggest the ancestral primate was a leaping insectivore, which might have had a lifespan of 4-6 years. This proposed ecology suggests that visual specialisation to meet the demands of a fine-branch, insect grasping niche may have had a significant role in the early expansion of the primate brain (Martin, 1990; Barton, 1998), a hypothesis consistent with recent evidence revealing an association between visual expansion and brain size in fossil endocasts of early primates (Silcox *et al.*, 2009).

The reconstructions suggest the ancestral primate had a small brain (120.23mg, 95% CI: 114.42mg - 126.33mg) which, relative to body mass, was much smaller than in any living primate. This result is consistent with a study of a virtual endocast of *Ignacius graybullianus*, an Early Eocene Plesiadapiform (Paromomyidae), which indicated that early primates exhibited only small advances in brain mass over ancestral groups and that the majority of increases in brain size occurred after the origin of modern primates (Silcox *et al.*, 2009). Finally I note that the best estimate of brain mass for the last common ancestor of *Homo* and *Pan* (338.75mg, 95% CI: 321.37mg – 340.64mg; which equates to a cranial capacity of 355.16cm^3, 95% CI: 336.61cm^3 – 357.17cm^3) is similar to estimates for the two earliest hominids known from the fossil record, the 7.7 million year old *Sahelanthropus tchadensis* (360-370cm^3; Zollikofer *et al.*, 2005) and the 4.4 million year old *Ardipithecus ramidus* (280-350cm^3; Suwa *et al.*, 2009). These two fossil species were not included in my analysis due to uncertainty in their phylogenetic position which has only recently been resolved (Suwa *et al.*, 2009).

3.3.5 Increases in brain mass in particular lineages

I next examined the amount of change along different branches of the tree, both as total change and as rate of change. I first calculated the means of the posterior distribution of the ancestral states for each node, using the same posterior predictive model developed for brain and body mass, and then computed the change in absolute brain and body mass, and relative brain mass (using the 'residuals second' approach described above) along each branch by comparing the values (either observed (Appendix 1) or estimated (Table 3.3)) at consecutive nodes. The estimates show that both absolute and relative brain size have increased in all major clades of primates (Figure 3.8; examples shown in Figure 3.9 a & b).

Changes in absolute brain mass along each branch of the phylogeny can be considered in two ways: a proportional increase (log(mass descendent)-log(mass ancestor)) and an absolute increase in mass (described above). The average proportional change in absolute brain mass along a branch is 0.243, with changes greater than 0.344 being in the upper quartile, which includes branches from all the major clades of the phylogeny. Notably, three of the top four proportional increases are along the deepest branches (ancestral primate to ancestral strepsirrhine (node 38-node 65; see Figure 3.1), 1.310; ancestral primate to ancestral haplorhine (node 38-node 39), 0.942; ancestral haplorhine to ancestral anthropoid (node 39-node 40), 0.929), suggesting selective pressures favouring the expansion of the brain were strong early in primate evolution. Interestingly the proportional increase along the terminal human branch is only the 7th largest change (0.594). However in terms of absolute change the terminal human branch shows the largest change, almost four times greater than the second biggest change.

The average proportional change in relative brain mass is 0.201 (i.e. 20.1% increase), with changes above 0.278 falling in the upper quartile, which again includes branches from all major primate groups. The five branches which show the largest increase in relative brain mass are the terminal *Tarsius* branch (0.917), the terminal *Daubentonia* branch (0.837), the terminal *Galago* branch (0.514), the terminal human branch (0.479) and the branch between the ancestral anthropoid and ancestral platyrrhine (node 40-node 54; 0.431). Because *Daubentonia* and *Tarsius* are no more gregarious than their close relatives (Smuts *et al.*, 1987), this suggests that social complexity is unlikely to have been the sole factor in primate brain mass evolution (c.f. Dunbar & Shultz, 2007) and that other selective pressures have also been important. For example

the large brain of *Daubentonia* is partly due to olfactory specialisation (Stephan *et al.,* 1981; Kaufman *et al.,* 2005) which is consistent with the hypothesis that selection acting on sensory systems had a significant role in brain size evolution (Barton *et al.,* 1995; Barton, 2006b).

I next examined evolutionary changes along branches controlling for branch length. The average rates were an increase of 0.025/million years (i.e. a 2.5% increase in log(mass)/million years) for a proportional change in brain mass, 5640mg/million years for an absolute change in brain mass, and 0.020/million years for a change in relative brain mass confirming that most change in relative brain mass was due to brain rather than body mass. The branch with the highest rate of change in absolute brain mass is the terminal human branch (140,000 mg/million years). However for rate of proportional change in absolute brain mass the human branch comes only 4th, below the branches between the last common ancestor of macaques and other *Papionini*, and the last common ancestor of baboons, mangabeys and mandrills (node 48-node 49), the ancestral primate and ancestral haplorhine (node 38-node 39) and the branch between the last common ancestor of Cebinae, Aotinae and Callitrichidae, and the ancestral Cebinae (node 58-node 60). The rate of change in relative brain mass along the human branch (0.068/million years) is also exceeded by the branch between the last common ancestor of *Alouatta*, *Ateles* and *Lagothrix* with the last common ancestor of *Ateles* and *Lagothrix* (node 55-node 56; 0.73), the branch connecting the last common ancestor of Cebinae, Aotinae and Callitrichidae, and the ancestral Cebinae (node 58-node 60; 0.074/million years) and the branch connecting the last common ancestor of the Papionini with the last common ancestor of *Papio*, *Mandrillus* and *Cercocebus* (node 48- node 49; 0.084). I therefore conclude that only in terms of absolute mass and the rate of change in absolute mass has the increase in brain size been exceptional along the terminal branch leading to humans. Once scaling effects with body mass have been accounted for the rate of increase in relative brain mass remains high but is not exceptional. It is also notable that the estimated brain size of the last common ancestor of modern primates is smaller relative to body size than any living primate species and that the expansion of the primate brain began early, with the deepest branches (e.g. node 38-node 39; node 38-node 65; node 39-node 40) ranking in the upper quartile in terms of both increases in absolute and relative brain mass (Table 3.4).

Figure 3.8 Phenograms for changes in a) body mass; **b) brain mass; c) relative brain size**
The topology of the tree is as shown in Figure 3.1. Branch lengths are drawn according to the difference in log(mass) between consecutive nodes for brain and body mass, or the difference in residual brain mass for relative brain size such that at any point in the phenogram the phenotypic state can be read off the x-axis. Branches in red show increases in size, branches in blue show decreases.

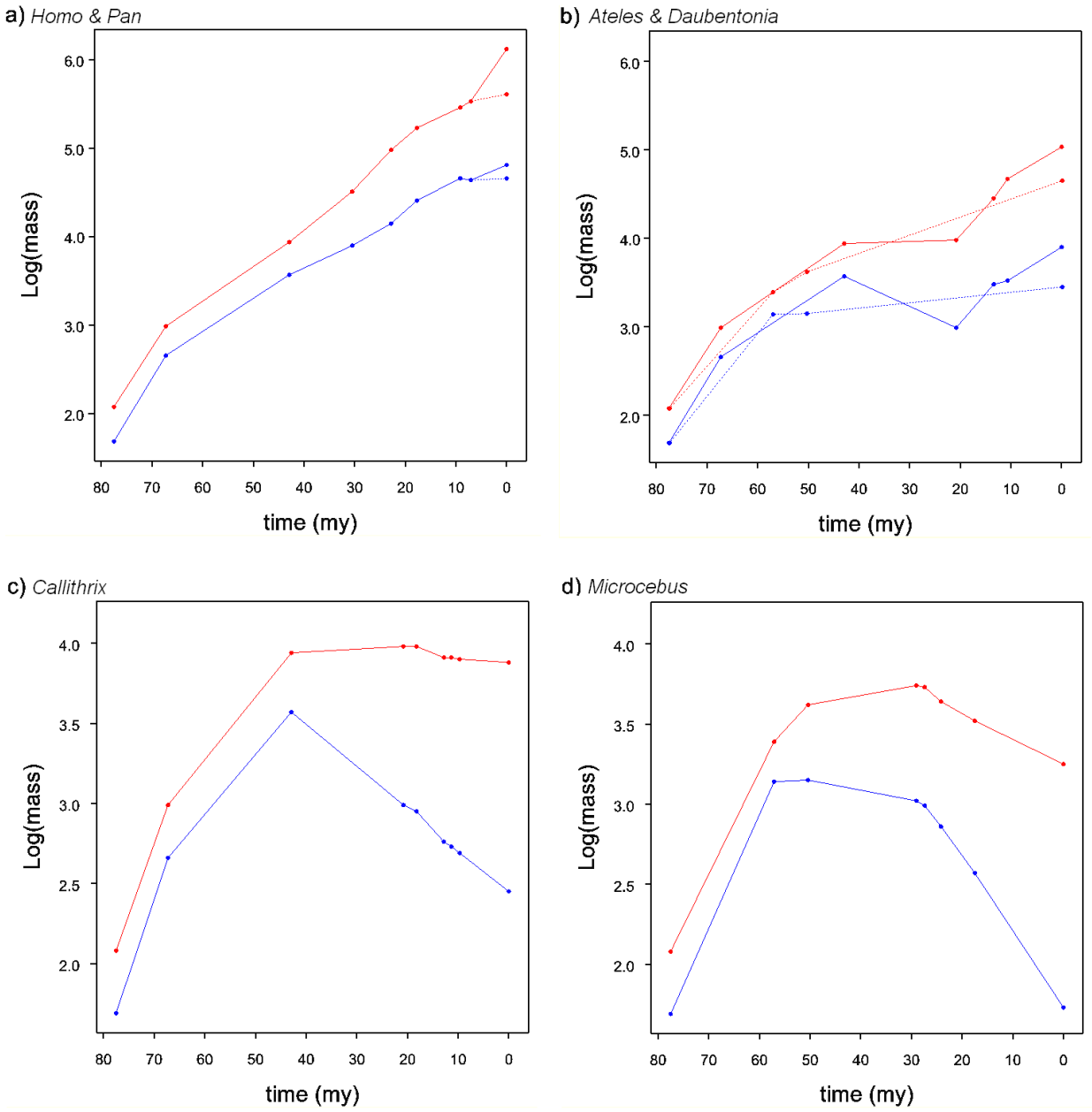

Figure 3.9 Examples of parallel evolutionary trajectories of brain and body mass
Evolution of brain (red) and body (blue) mass from the ancestral primate to **a)** ***Homo*** (solid line) and ***Pan*** (dashed line) and **b)** ***Ateles*** (solid line) and ***Daubentonia*** (dashed line) showing parallel increase in brain and body mass; **c)** ***Callithrix,*** and **d)** ***Microcebus*** demonstrating secondary reduction in both brain and body mass: note the reduction in brain mass is lower than the reduction in body mass leading to an increase in relative brain size (Table 3.4).

Table 3.4 Change in absolute brain and body mass and relative brain mass along each branch

Branch	Change in absolute brain mass				Change in body mass				Change in relative brain mass	
	Proportional change	Rate (/million years)	Absolute change (mg)	Rate (mg/million years)	Proportional change	Rate (/million years)	Absolute change (g)	Rate (g/million years)	Change	Rate (/million years)
40..41	0.565 (±0.0033)	0.039	23400	1610	0.334 (±0.0026)	0.023	4270	294	0.330	0.023
41..42	0.473 (±0.0032)	0.061	63300	8220	0.247 (±0.0024)	0.032	6080	790	0.305	0.040
42..43	0.253 (±0.0029)	0.050	75700	14800	0.259 (±0.0021)	0.051	11400	2240	0.067	0.013
43..44	0.222 (±0.0031)	0.026	114000	13400	0.257 (±0.0024)	0.030	20600	2410	0.061	0.007
44..45	0.074 (±0.0027)	0.036	53300	25739	-0.022 (±0.0015)	-0.011	-2300	-1110	0.084	0.040
45..*Homo*	0.594 (±0.0023)	0.084	991000	140000	0.172 (±0.0016)	0.024	21200	3000	0.479	0.068
45..*Pan*	0.078 (±0.0023)	0.011	66200	9360	0.022 (±0.0016)	0.003	2240	317	0.066	0.009
44..*Gorilla*	0.243 (±0.0025)	0.027	215000	23400	0.358 (±0.0018)	0.039	59000	6440	-0.005	-0.001
43..*Pongo*	0.383 (±0.0028)	0.022	242000	13700	0.359 (±0.0022)	0.020	31600	1780	0.155	0.009
42..*Hylobates*	0.029 (±0.0024)	0.001	6550	287	-0.391 (±0.0018)	-0.017	-8340	-366	0.298	0.013
41..46	0.006 (±0.0015)	0.001	454	82.8	-0.054 (±0.0026)	-0.010	-935	-170	0.045	0.008
46..47	0.278 (±0.0037)	0.045	29200	4700	0.124 (±0.0019)	0.020	2310	371	0.200	0.032
47..48	0.084 (±0.0024)	0.063	13300	98.9	0.066 (±0.0012)	0.049	1530	1150	0.042	0.031
48..*Macaca*	0.093 (±0.0023)	0.011	17900	2120	-0.144 (±0.0015)	-0.017	-3070	-364	0.182	0.022
48..49	0.074 (±0.0022)	0.150	13900	28300	0.031 (±0.0008)	0.064	814	1660	0.041	0.084
49..*Papio*	0.354 (±0.0023)	0.045	112000	14100	0.330 (±0.0015)	0.042	13300	1680	0.130	0.016
49..50	0.073 (±0.0025)	0.031	16200	6950	0.060 (±0.0014)	0.026	1750	749	0.028	0.012
50..*Mandrillus*	0.231 (±0.0022)	0.041	73800	13200	0.377 (±0.0015)	0.067	18600	3330	-0.022	-0.004
50..*Cercocebus*	-0.005 (±0.0022)	-0.001	-1190	-212	-0.230 (±0.0015)	-0.041	-5530	-986	0.158	0.028
47..51	0.044 (±0.0022)	0.024	6580	3590	-0.059 (±0.0014)	-0.032	-1180	-644	0.078	0.043
51..*Cercopithecus*	0.029 (±0.0025)	0.024	4770	601	-0.228 (±0.0024)	-0.029	-3330	-420	0.185	0.023
51..*Erythrocebus*	0..198 (±0.0024)	0.004	39600	4990	-0.019 (±0.0016)	-0.002	-352	-44.4	0.211	0.027
46..52	0.230 (±0.0024)	0.025	22800	4140	0.082 (±0.0020)	0.015	1450	264	0.174	0.032
52..*Colobus*	0.149 (±0.0037)	0.042	22600	2160	-0.083 (±0.0019)	-0.008	-1471	-140	0.206	0.020
52..53	0.230 (±0.0026)	0.014	14800	3670	0.097 (±0.0018)	0.024	2130	530	0.036	0.009
53..*Presbytis*	0.149 (±0.0028)	0.026	49300	7620	0.303 (±0.0017)	0.047	10720	1660	0.024	0.004
53..*Pygathrix*	0.103 (±0.0024)	0.036	6880	106	-0.150 (±0.0017)	-0.023	-3100	-479	0.143	0.022
40..54	0.231 (±0.0024	0.006	900	40.8	-0.576 (±0.0020)	-0.026	-2710	-123	0.431	0.020
54..55	0.041 (±0.0029)	0.002	18300	2470	0.489 (±0.0021)	0.066	2040	276	0.127	0.017
55..*Alouatta*	0.270 (±0.0026	0.020	24100	1800	0.327 (±0.0020)	0.024	3380	252	0.047	0.004
55..56	0.225 (±0.0026)	0.082	19000	6930	0.038 (±0.0017)	0.014	276	101	0.199	0.073
56..*Lagothrix*	0.333 (±0.0026)	0.031	54100	5080	0.198 (±0.0020)	0.019	1910	179	0.198	0.019
56..*Ateles*	0.362 (±0.0026)	0.034	61100	5730	0.385 (±0.0020)	0.036	4710	441	0.099	0.009
54..64	0.159 (±0.0028)	0.030	4250	794.7	0.033 (±0.0021)	0.006	76.9	14.4	0.136	0.025
64..*Callicebus*	0.136 (±0.0027)	0.009	5100	330	-0.069 (±0.0022)	-0.004	-155	-10.1	0.183	0.012

Table 3.4 cont'd. Change in absolute brain and body mass and relative brain mass along each branch

Branch	Change in absolute brain mass				Change in body mass				Change in relative brain mass	
	Proportional change	Rate (/million years)	Absolute change (mg)	Rate (/million years)	Proportional change	Rate (/million years)	Absolute change (mg)	Rate (/million years)	Change	Rate (/million years)
64..*Pithecia*	0.401 (±0.0027)	0.026	21100	1370	0.153 (±0.0022)	0.010	445	28.8	0.297	0.019
54..58	0.000 (±0.0015)	-0.000	-5.87	-2.26	-0.045 (±0.0015)	-0.017	-95.9	-36.9	0.030	0.012
58..*Aotus*	0.249 (±0.0025)	0.014	7460	410	-0.027 (±0.0016)	-0.001	-149	-8.16	0.267	0.015
58..60	0.227 (±0.0031)	0.087	6630	2550	0.053 (±0.0016)	0.020	114	43.8	0.191	0.074
60..*Cebus*	0.640 (±0.0027)	0.041	54700	3510	0.0493 (±0.0020)	0.032	2100	135	0.303	0.019
60..*Saimiri*	0.269 (±0.0027)	0.011	7730	495	-0.179 (±0.0020)	-0.011	-336	-21.6	0.291	0.019
58..61	-0.072 (±0.0030)	-0.013	-1470	-272	-0.186 (±0.0020)	-0.034	-308	57.0	0.263	0.049
61..*Saguinus*	0.088 (±0.0026)	0.007	1830	143	-0.180 (±0.0018)	-0.014	-195	-15.2	0.211	0.016
61..62	-0.004 (±0.0024)	-0.003	-72.4	-49.9	-0.028 (±0.0013)	-0.020	-36.3	-25.0	0.015	0.011
62..*Leontopithecus*	0.219 (±0.0025)	0.019	5300	467	0.039 (±0.0018)	0.003	51.3	4.52	0.192	0.017
62..63	-0.013 (±0.0025)	-0.008	-241	-145	-0.041 (±0.0013)	-0.025	-48.8	-29.4	0.015	0.009
63..*Callimico*	0.146 (±0.0024)	0.015	3140	324	-0.009 (±0.0018)	-0.001	-9.97	-1.03	0.152	0.016
63..*Callithrix*	-0.015 (±0.0024)	-0.002	-260	-26.8	-0.243 (±0.0018)	-0.025	-210	-21.7	0.152	0.016
39..40	0.919 (±0.0024)	0.038	7700	316	0.900 (±0.0027)	0.037	3560	146	0.303	0.012
39..*Tarsius*	0.533 (±0.0047)	0.008	2550	38.0	-0.570 (±0.0021)	-0.008	-5.67	-0.084	0.917	0.014
38..39	0.942 (±0.0220)	0.091	927	90.0	0.976 (±0.0021)	0.095	109	10.6	0.282	0.027
38..65	1.310 (±0.0218)	0.064	2330	114	1.449 (±0.0018)	0.071	1330	65.3	0.319	0.016
65..66	0.111 (±0.0050)	0.004	713	26.6	-0.377 (±0.0033)	-0.014	-791	-29.5	0.374	0.014
66..*Galago*	0.180 (±0.0034)	0.006	1630	53.9	-0.494 (±0.0029)	-0.017	-402	-13.3	0.514	0.017
66..67	0.224 (±0.0036)	0.016	2140	149	-0.033 (±0.0032)	-0.003	-48.1	-3.36	0.241	0.017
67..*Loris*	0.095 (±0.0031)	0.006	1290	81.2	-0.222 (±0.0028)	-0.014	-218	-13.7	0.249	0.016
67..*Nycticebus*	0.372 (±0.0031)	0.023	7190	451	0.173 (±0.0028)	0.011	259	16.3	0.256	0.016
65..68	0.226 (±0.0057)	0.034	1680	250	0.006 (±0.0028)	0.001	32.2	4.79	0.219	0.033
68..*Daubentonia*	1.039 (±0.0044)	0.021	41000	814	0.301 (±0.0026)	0.006	1390	27.5	0.837	0.017
68..69	0.120 (±0.0041)	0.006	1320	61.7	-0.119 (±0.0035)	-0.006	-363	-17.1	0.211	0.010
69..70	-0.005 (±0.0026)	-0.003	-56.3	-34.1	-0.034 (±0.0033)	-0.018	-69.9	-42.4	0.016	0.010
70..*Propithecus*	0.695 (±0.0034)	0.025	21300	778.0	0.548 (±0.0023)	0.020	2500	91.4	0.318	0.012
70..71	-0.097 (±0.0029)	-0.030	-1080	-333	-0.128 (±0.0032)	-0.040	-253	-78.3	-0.008	-0.002
71..*Lepilemur*	0.246 (±0.0032)	0.010	3280	136	0.096 (±0.0023)	0.004	190	2.89	0.176	0.007
71..72	-0.112 (±0.0032)	-0.017	-980	-148	-0.292 (±0.0033)	-0.044	-353	-53.1	0.086	0.013
72..*Cheirogaleus*	0.309 (±0.0030)	0.018	3460	198	0.082 (±0.0023)	0.005	78.5	4.48	0.252	0.014
72..*Microcebus*	-0.273 (±0.0030)	-0.016	-1560	-88.9	-0.841 (±0.0023)	-0.048	-318	-18.1	0.300	0.017
69..73	0.347 (±0.0036)	0.031	6670	595	0.155 (±0.0033)	0.014	466	41.6	0.238	0.021
73..*Varecia*	0.415 (±0.0033)	0.023	19400	1090	0.294 (±0.0025)	0.017	1490	83.4	0.212	0.012
73..*Eulemur*	0.284 (±0.0033)	0.016	11200	627	-0.037 (±0.0025)	-0.002	-114	-6.37	0.307	0.017

3.3.6 Decreases in brain mass and evolutionary scenarios for *H. floresiensis*

Despite both absolute and relative brain mass showing strong and significant evolutionary trends to increase, several branches go against this trend (Figure 3.8; examples shown in Figure 3.9 c & d; Table 3.4). Absolute brain mass decreases on ~14% of branches (10/70); independent decreases are observed in Old World monkeys (the terminal *Cercocebus* branch); in New World monkeys - several branches in the callitrichids, supporting the conclusion that this family has evolved by a process of phyletic dwarfism (Ford, 1980); and in strepsirhines - several branches in the lemur clade. Branches on which there is an overall decrease in absolute brain mass account for ~6% of the total evolutionary time covered by the phylogeny used in this analysis. In all cases a decrease in absolute brain mass is accompanied by a decrease in absolute body mass. Body mass decreases much more frequently: 46% of branches show a decrease, accounting for 47% of the total evolutionary time covered. Decreases in relative brain mass occur less frequently, with only 4% (3/70) of branches showing a decrease in relative brain mass, representing only 2.1% of evolutionary time. Decreases in relative brain mass mostly appear to be linked to body mass increasing to a greater extent than brain mass. This provides support for the hypothesis that small relative brain size in gorillas reflects increased "somatisation" rather than decreased encephalization (Byrne, 1995; but see Deaner & Nunn, 1999).

To assess whether the proposed evolution of *Homo floresiensis* is consistent with observed decreases in brain mass which have occurred elsewhere in the primate phylogeny, I calculated the ratio change in brain and body mass [(brain descendant – brain ancestor)/(body descendant-body ancestor)] for branches showing a decrease in order to facilitate comparisons with the literature (see methods). I used log values to take variation in body mass into account; decreases here are therefore proportional decreases in absolute mass. The aim in this analysis is not to estimate the probability or likelihood of the evolution of a hominin with reduced brain and body mass but rather to test whether or not decreases seen during the proposed evolution of *Homo floresiensis* fall within the range of other observed decreases in other primates. First I consider the evolution of the *H. floresiensis* brain assuming descent from a known hominin by insular dwarfism, a widely cited hypothesis (Martin *et al.*, 2006, Niven, 2007; Weston & Lister, 2009). For the 10 branches which showed a decrease the average ratio was 0.253 and the range was 0.006 to 0.743. I calculated the same ratio using *H. floresiensis* and three possible ancestral

forms of *Homo erectus*, following Martin *et al.* (2006): *Homo erectus* broadly defined, Ngandong *H. erectus*, and Dmanisi hominins. I also include *Homo habilis* which has not been ruled out as a possible ancestor (Gordon *et al.*, 2008). The change in brain size and the ratio of the change in brain and body mass were calculated for the two extreme values of body mass estimated for *H. floresiensis* (16 & 32kg, Brown *et al.*, 2004) and their midpoint.

Under a number of scenarios the evolution of *H. floresiensis* lies within the range of decreases in brain mass estimated here (Table 3.5). For any ancestor, except Ngandong hominoids, and a *H. floresiensis* body mass of 16kg the decreases in brain and body mass always fall within the range of the decrease that I found in other primate branches. For a *H. floresiensis* body mass of 32kg the decrease in relative brain mass is not consistent with changes estimated in other branches, but assuming a body mass estimate of 24kg and descent from a Dmanisi hominin population, the decrease in relative brain size falls within the range of decreases observed elsewhere in the primate phylogeny. It is notable that for both body mass estimates the proportional change in absolute brain mass from either a Dmanisi hominin (-0.216) or *H. habilis* (-0.137) ancestor is actually smaller than the decrease in the terminal *Microcebus* branch (-0.273). The calculated change in relative brain mass from any of the four ancestors is compatible with the results obtained here only for a *H. floresiensis* body mass close to 16kg, or descent from either a Dmanisi hominin or *H. habilis* if *H. floresiensis* had a body mass towards 24kg.

In addition I used the brain/body mass scaling relationships [(brain descendant – brain ancestor)/(body descendant-body ancestor)] during the 10 decreases in brain mass to estimate the decrease in brain mass expected for the observed decrease in body mass for each ancestor and body mass. The results of this analysis are shown in Table 3.6 and invoke similar conclusions to those discussed above.

Table 3.5 Evolution of brain size during the evolution of *H. floresiensis* from four possible ancestors by insular dwarfism

Ancestor	*H. floresiensis* body mass (kg)	Ratio of change in log(absolute brain mass) & log(body mass)	Change in log(brain mass)	Change in log(relative brain mass)
H. erectus	16	0.720*	-0.398	-0.020*
	24	1.058	-0.398	-0.141
	32	1.586	-0.398	-0.226
Ngandong	16	0.784	-0.450	-0.058
	24	1.131	-0.450	-0.178
	32	1.649	-0.450	-0.264
Dmanisi	16	0.437*	-0.216*	0.122*
	24	0.678*	-0.216*	0.002*
	32	1.116	-0.216*	-0.084
H. habilis	16	0.420*	-0.137*	0.059*
	24	0.908	-0.137*	-0.034
	32	5.219	-0.137*	-0.147

* indicates a result which falls within the range of decreases in brain size across primates.

Table 3.6 Range of estimated decreases in brain mass during the evolution of *H. floresiensis* given scaling relationships during episodes of brain mass reduction

		estimated range of decreases in brain mass given observed decrease in body mass		
Ancestor	***H. floresiensis* body mass (kg)**	**minimum**	**maximum**	**actual calculated decrease in brain mass**
H. erectus	**16***	-0.003	-0.410	-0.398
	24	-0.002	-0.279	-0.398
	32	-0.001	-0.186	-0.398
Ngandong	16	-0.003	-0.426	-0.450
	24	-0.002	-0.296	-0.450
	32	-0.002	-0.203	-0.450
Dmanisi	**16***	-0.003	-0.368	-0.216
	24*	-0.002	-0.237	-0.216
	32	-0.001	-0.144	-0.216
H. habilis	**16***	-0.002	-0.243	-0.137
	24	-0.001	-0.112	-0.137
	32	0.000	-0.020	-0.137

* Where the actual calculated decrease is within the range of estimated decreases the *H. floresiensis* body mass is highlighted in bold with an asterisk.

Thus under the insular dwarfism model, if *H. floresiensis* descended Ngandong *H. erectus* the decrease in brain size is beyond the range found across primates. If it descended from an 'average' *H. erectus* populations, the decrease in brain mass is not compatible with my results unless *H. floresiensis* had a body mass near 16kg. The evolution of *H. floresiensis* also appears less likely if it had a body mass towards the upper estimate, as the decrease in relative brain mass falls outside my estimates on other branches. However, if *H. floresiensis* had a body mass of 16-24kg, descent from either a Dmanisi hominin or *H. habilis* ancestor is in line with decreases in brain and body mass along other primate lineages. I therefore conclude that further studies addressing the affinities of *H. floresiensis* with different possible ancestors and more accurate predictions of body mass are necessary to rule out the possibility of *H. floresiensis* being a true novel hominin using this kind of analysis. My analysis suggests it is possible that, under the insular dwarfism model, the only unexpected aspect of *H. floresiensis'* evolution is the rate at which brain mass decreased. However, some evidence suggests morphological evolution may accelerate on islands (Millen, 2006).

Next I performed several analyses to test whether the evolution of the *H. floresiensis* brain under the alternative phylogenetic scenario proposed by Argue *et al.* (2009), that *H. floresiensis* was not a dwarf but an earlier hominin species, by estimating the ancestral brain and body masses of the node at the base of the *H. floresiensis* lineage (Table 3.7) and subsequently analysing the evolution of brain size along that lineage. The analysis was run for each of the two most parsimonious trees separately and then for both trees together, taking advantage of BayesTraits' ability to take phylogenetic uncertainty into account. The results again suggest that if *H. floresiensis* body mass did not greatly exceed 24kg the decrease in brain size observed along the lineage leading to *H. floresiensis* falls within the range seen elsewhere in the primate phylogeny, scales with body mass in a way consistent with other episodes of brain mass reductions, and actually results in an increase in relative brain size (Table 3.8; Table 3.9). Conversely, a larger body size produces an allometric decrease in brain size beyond the range observed in the primate tree. To conclude, for a body mass toward the lower end of the range of estimates all the phylogenetic hypotheses on the ancestry of *H. floresiensis* so far proposed are consistent with the observed decrease in brain size.

Table 3.7 Estimated Log(body) and Log(brain) masses for the node at the base of the *H. floresiensis* terminal branch using the topologies proposed by Argue *et al.* (2009)[1]

Phylogeny	*H. floresiensis* body mass (kg)	Estimates				
		Log(Body mass)		Log(Brain mass)		Relative brain size
Argue tree 1	16	4.633	(±0.001)	5.752	(±0.002)	0.404
	24	4.649	(±0.001)			0.394
	32	4.659	(±0.001)			0.387
Argue tree 2	16	4.611	(±0.001)	5.754	(±0.003)	0.422
	24	4.625	(±0.001)			0.412
	32	4.635	(±0.001)			0.405
Both trees	16	4.619	(±0.001)	5.754	(±0.003)	0.416
	24	4.636	(±0.001)			0.404
	32	4.647	(±0.001)			0.400

[1]Estimates are given as the mean with 95% confidence intervals.

Table 3.8 Evolution of brain size during the evolution of *H. floresiensis* under two phylogenetic scenarios

Phylogeny	*H. floresiensis* body mass (kg)	Ratio of change in log(absolute brain mass) & log(body mass)[2]	Change in log(brain mass)	Change in relative brain size
Argue Tree 1	16	0.400*	-0.171*	0.121*
	24	0.639*	-0.171*	0.012*
	32	1.116	-0.171*	-0.066
Argue Tree 2	16	0.428*	-0.173*	0.104*
	24	0.709*	-0.173*	-0.006*
	32	1.336	-0.173*	-0.084
Both trees	16	0.418*	-0.176*	0.110*
	24	0.679*	-0.176*	-0.001*
	32	1.225	-0.176*	-0.076

* indicates a result which falls within the range observed across primates.

Table 3.9 Range of estimated decreases in brain mass during the evolution of *H. floresiensis* using the topologies proposed by Argue *et al.* (2007) scaling relationships during primate brain reduction

Phylogeny	*H. floresiensis* body mass (kg)	estimated range of decreases in brain mass given observed decrease in body mass		calculated decrease in brain mass
		minimum	maximum	
Argue Tree 1	**16***	-0.003	-0.319	-0.171
	24*	-0.002	-0.199	-0.171
	32	-0.001	-0.114	-0.171
Argue Tree 2	**16***	-0.002	-0.302	-0.173
	24*	-0.001	-0.182	-0.173
	32	-0.001	-0.097	-0.173
Both trees	**16***	-0.002	-0.308	-0.173
	24*	-0.002	-0.190	-0.173
	32	-0.001	-0.105	-0.173

* indicates a result which falls within the range of decreases in brain size for primates estimated in this study.

Finally I used the best-fitting evolutionary model of brain evolution (directional) to estimate the expected brain size for *H. floresiensis* under a number of phylogenetic scenarios. This analysis attempts to predict the brain size of this species given the evolutionary model. This predicted brain size value can then be compared to the observed value. One significant problem with this approach is that it is currently not possible to analyse two correlated traits simultaneously (brain size and body size in this case) that evolved according to different evolutionary models (directional model for brain size and non-directional model for body size, in this case). It is therefore not possible to incorporate body mass information into this analysis. Hence, given the strong directional component to brain evolution it is unlikely that the model will estimate a decrease in brain mass along a terminal branch where the tip value is not known, because information on changes in encephalization caused by the evolution of body mass will be lost. For example when I performed this analysis for the three species (*Microcebus*, *Callithrix*, *Cercocebus*) where the terminal branch shows a decrease in brain mass, the brain mass was

overestimated by 3.8-7.4%. Across all primates (extant and extinct) the mean absolute percentage error between estimated and real brain mass was 4.97% (range 1.14%-20.28%) and 4.46% (range 0.81%-10.37%) excluding extinct species. To my knowledge no model has been developed which can incorporate co-evolution between traits which evolve under different modes; the ability to do so would no doubt be a useful advance in comparative methodology. However, comparing the predicted values under multiple scenarios may still indicate which fits most closely to the observed *H. floresiensis* brain mass. I estimated the Log(brain mass) for *H. floresiensis* setting *H. floresiensis* in turn as a sister taxon to *H. erectus*, Dmanisi, Ngandong hominoids and *H. habilis*, to test the insular dwarfism model, and under the topologies proposed by Argue *et al.* (2007). Under the insular dwarfism model the age of the split between *H. floresiensis* and the sister species was set as 190,000 years, the age of the oldest hominin artefacts found in Liang Bua (Roberts *et al*., 2009). The results are presented in Table 3.10. For comparison, the estimated values for other hominins in the phylogeny shown in Figure 3.1 were on average within 1.84% of the real value, with a range between 0.74-3.47%.

Table 3.10 Predicted Log(brain mass) of *H. floresiensis* under a number of phylogenetic scenarios[1]

a) Insular dwarfism	**Ancestor**	**Estimated *H. floresiensis* Log(brain mass)**	**% error**
	H. erectus	5.968 (±0.002)	6.943
	Ngandong	6.003 (±0.002)	7.576
	Dmanisi	5.846 (±0.002)	4.762
	H. habilis	5.764 (±0.002)	3.283

b) Argue *et al.* (2009)	**Phylogeny**	**Estimated *H. floresiensis* Log(brain mass)**	**% error**
	Tree 1	5.868 (±0.002)	4.890
	Tree 2	5.848 (±0.004)	4.567
	Both trees	5.859 (±0.004)	4.745

[1] Estimates are given as the mean with the 95% confidence intervals.

Estimates made under all scenarios are larger than the real log brain mass (mg) of 5.581 as expected. It is notable that the estimates for descent from a *H. habilis* or Dmanisi ancestor have the lowest percentage errors, which is consistent with the results of the analyses discussed above. The error for a shared ancestry with *H. habilis* also falls within the range seen when estimating other hominins, whilst the error associated with a descent from Dmanisi hominids or under Argue *et al.*'s proposed typologies are also reasonably low.

The errors associated with body mass estimates are higher. Across all primates (extant and extinct) the mean absolute percentage error is 10.75% (range 0.32%-70.29%) and across extant primates the mean is 10.62% (range 0.32%-70.29%) with the largest error found among species with long terminal branches (e.g. *Tarsier* 29.32%) or dwarfed species (e.g. *Microcebus* 70.29%). Among hominins the percentage error ranged from 0.33%-2.82%. Estimates of *H. floresiensis* are higher than the error for other hominins but around average for the full primate dataset (Table 3.11).

Table 3.11 Predicted log(body mass) of *H. floresiensis* under a number of phylogenetic scenarios[1]

a) Insular dwarfism	**Ancestor**	**Estimated *H. floresiensis* Log(brain mass)**		**% error from 16kg**	**% error from 24kg**	**% error from 32kg**
	H. erectus	4.752	(<0.001)	13.025	8.482	5.473
	Ngandong	4.698	(<0.001)	11.748	7.255	4.281
	Dmanisi	4.700	(0.001)	11.798	7.303	4.328
	H. habilis	4.551	(<0.001)	8.253	3.901	1.020
b) Argue *et al.*	**Phylogeny**	**Estimated *H. floresiensis* Log(brain mass)**		**% error from 16kg**	**% error from 24kg**	**% error from 32kg**
	Tree 1	4.675	(0.001)	4.380	6.723	3.764
	Tree 2	4.647	(0.001)	4.380	6.081	3.139
	Both trees	4.661	(0.001)	4.380	6.421	3.470

[1] Estimates are given as the mean with the 95% confidence intervals. Percentage error is given from the minimum and maximum body mass estimates for *H. floresiensis* (LB1) and the midpoint.

To further study the selective pressures and anatomical changes associated with decreases in brain mass *Microcebus*, *Callithrix* and *Miopithecus* or *Cercocebus* may be useful, independent models. For example, Falk *et al.* (2005, 2009) identified a number of potentially derived features in an endocast of *H. floresiensis*, and comparative analyses of the brain anatomies of these species might show if similar structures are modified in independent episodes of brain mass reduction. Likewise a comparative analysis of the ecologies of these smaller brained primates may reveal selective pressures associated with decreases in brain and body mass. For both decreases in absolute and relative brain mass there appears to be no relation with isolation on islands, nor is there any clear single ecological trait that can explain these decreases. As with evolutionary increases in brain mass, decreases in mass are likely to be influenced by a number of ecological factors. For example, Taylor and van Schaik (2007) show that brain size has decreased during the evolution of *Pongo p. morio,* particularly in females. The authors suggest this reduction is associated with an increase in periods of food scarcity resulting in selection to minimise brain tissue which is metabolically expensive (Aiello & Wheeler, 1995). Food scarcity is also believed to have played a role in the decrease in brain size in the island bovid *Myotragus* (Köhler & Moyá-Solá, 2004). Taylor and van Schaik (2007) therefore propose that *H. floresiensis* may have experienced similar selective pressures as *Myotragus* and *Pongo p. morio*. Future studies are needed to address the relative contributions of proposed social and ecological factors in both decreases and increases in brain mass across primates and other species.

3.4 Conclusions

By reconstructing ancestral states of brain and body mass in primates I have shown that Organ *et al.*'s (2007) method, implemented in BayesTraits using Bayesian analysis, is least affected by the inclusion of fossil data and is therefore more reliable for my dataset. In this respect Organ's *et al.*'s approach outperforms parsimony and ML methods which instead tend to produce lower estimates at deep nodes when using only data of extant species. This is likely to be because BayesTraits first identifies the best predictive model based on known tip data to then infer unknown ancestral states at each node of interest in the tree and can incorporate evolutionary trends. If Organ *et al.*'s (2007) method generally outperforms ML and parsimony methods, this may have important implications for future studies which attempt to estimate ancestral states in groups where little fossil information is available, or where evolutionary trends are suspected, especially when the reconstruction is performed on deep nodes within phylogenies which cover large time periods. Studies on datasets with known ancestral states are thus needed to fully assess if the method implemented in BayesTraits consistently produces more reliable ancestral state reconstructions.

The results provide robust confirmation for the suggestion that strong evolutionary trends have governed the evolution of the primate brain size. In contrast body size evolution has not tended to increase in primates, implying brain and body mass have been subject to separate selection pressures and supporting the findings of previous studies in other taxonomic groups that these two highly correlated traits can show differences in their patterns of evolution (Lande, 1979; Finarelli & Flynn, 2009; Gonzalez-Voyer *et al.*, 2009). Brain mass began to increase early in primate evolution and has independently expanded in both absolute and relative terms in all the major clades of the primate phylogeny. I have highlighted branches along which the change or rate of change in brain mass is particularly large. Surprisingly only in terms of change in absolute mass is the terminal human branch exceptional; once scaling effects are accounted for, humans rank only 7th.

Despite the presence of an overall trend to increase mass, I also provide evidence for independent decreases in brain mass in New and Old World Monkeys and in strepsirhines. By comparing the evolution of *H. floresiensis* brain size under different phylogenetic hypotheses to other episodes in brain size reduction during primate evolution, I conclude that the evolution of

H. floresiensis is consistent with the range of decreases in brain mass seen across the primate phylogeny if it either evolved from populations of *H. habilis* or Dmanisi hominin by insular dwarfism, or under Argue *et al.*'s (2009) proposed phylogenetic scenarios, and if *H. floresiensis* had a body mass towards the lower end of the range of estimates obtained from skeletal remains. In this respect I note that Brown *et al.* (2004) arugued the lower body mass estimates are probably most appropriate, assuming *H. floresiensis* shared the lean body shape typical of Old World tropical modern humans. If this were true the evolution of *H. floresiensis* involved a reasonable decrease in absolute brain mass, but an increase in relative brain size. My analysis, together with studies of brain size in island populations of living primates (Bromham & Cardillo, 2007; Welch, 2009), therefore suggests we should perhaps not be surprised by the evolution of a small brained, small bodied hominin, although further clarification of the relationships between *H. floresiensis* and other hominins is required to confirm this observation. Finally, my results add to the growing number of studies that conclude that the evolution of the human brain size has not been anomalous when compared to general primate brain evolution (Zilles *et al.*, 1989; Semendeferi *et al.*, 2002; Bush & Allman, 2004; Sherwood *et al.*, 2006; Marino, 2006; Herculano-Houzel *et al.*, 2007). The results demonstrate that ancestral state reconstruction can be an informative way to infer evolutionary processes using data from living species but highlight the need to assess the reliability of these estimates when doing so.

Chapter 4

A curious case of convergence:

Dwarfism, life history & brain size reductions in the callitrichids & cheirogaleids

"When small men begin to cast big shadows,

it means that the sun is about to set."

Lin Yutang, quoted in *Hard-to-Solve Cryptograms*, 2001

4. A curious case of convergence: Dwarfism, life history & brain size reductions in the callitrichids & cheirogaleids

4.0 Summary

The callitrichids are the smallest anthropoids, whilst the cheirogaleids include the smallest of all primates. The small brains and bodies of these species are shown here to be derived traits. Using species-level analyses I show that both traits decrease in a gradual manner in parallel across callitrichids, and across cheirogaleids. I identify lineages with particularly rapid decreases and highlight the pygmy marmoset, *Callithrix pygmaea*, as a phenotypic outlier. I explore the evolution of life history strategies in each clade and provide evidence that the convergent evolution of small body size may have been achieved by changes in different ontogenetic stages. Whereas body size reduction in callitrichids appears to be almost exclusively due to alterations in prenatal growth rate, body size reduction in cheirogaleids may be due to reduced postnatal growth rates and reduced gestation lengths. In both clades brain mass shows a complex history, with numerous decreases occurring in parallel with decreases in body size, but with some lineages showing increasing brain mass in spite of a decrease in body mass. I argue that this pattern is further evidence that brain and body mass can and do respond to contrasting selection pressures and must therefore have largely separate developmental bases. Finally, the evolution of *C. pygmaea* is shown to be as improbable as the evolution of *Homo floresiensis*.

4.1 Introduction

Across primates the general trend towards increasing brain size is rarely broken. The few clades where brain mass decreases are characterised by rapid and large decreases in body size, in particular in the callitrichids and cheirogaleids (see chapter 3). A number of features of brain evolution in these clades are notable when brain size is analysed at the genus level: the extent of decreases in brain mass does not keep pace with reductions in body size, meaning relative brain size continues to increase. In addition, along some lineages brain mass increases when body size decreases suggesting the two traits are responding to distinct selection pressures. Understanding the developmental changes that occur during episodes of body mass reduction, and how these affect brain evolution could offer new insights into the nature of brain:body allometry and the constraints acting on brain size evolution.

Large decreases in body size are also of interest in their own right. Based on paleontological studies it has historically been accepted that mammals tend to increase in size through time ("Cope's Rule"; Alroy, 1998; Polly, 1998), although the evidence for such a trend is disputed (Boucot, 1976; Monroe & Bokama, 2010) and it does not seem to apply to primates (see chapter 3). Evolutionary reductions in body mass, or episodes of "dwarfism" or "nanism" are considered rare but may be more frequent on islands ("The Island Rule"; van Valen, 1973) where resource limitation selects for smaller body size in large mammals (Marshalll & Corruccini, 1978). The proposition that dwarfism (and giantism) is common on islands is disputed (Lomolino, 2005; Meiri *et al*., 2008) but does seem to be true for primates (Bromham & Cardillo, 2007; Welch, 2009). Insular dwarfing has been invoked to explain the small body size of a recently described hominin *Homo floresiensis* (Brown *et al*., 2004; Niven, 2006). However, controversy surrounds the description of *H. floresiensis* as a new species, with some arguing it may be a pathological modern human (see chapter 3). A significant amount of this debate has focused on the scaling relationship between brain and body size during dwarfism and whether or not the *H. floresiensis* brain is an allometric oddity (see Niven, 2006 for review). Understanding the evolutionary scenarios which bring about dwarfism and how this affects brain evolution in independent clades may offer new perspectives on these problems.

Although much of the focus around dwarfing has concerned islands, continental dwarfing may be a more common phenomenon than previously thought (Prothero & Sereno, 1982). It has

occurred independently in several mammalian lineages (e.g. Kurtén, 1959; Marshalll & Corruccini, 1978; MacFadden, 1986). Notable examples among living mammals include the pygmy hippopotamus (Weston & Lister, 2009) and the human pygmy phenotype (Perry & Dominy, 2008). It has previously been argued that callitrichid primates are dwarfs (Ford, 1980) and that the evolution of the smallest callitrichid, the pygmy marmoset (*Callithrix pygmaea*), involved some sort of paedomorphic event (Groves, 1989). Callitrichids are small (120g-650g), neotropical primates nested within the Cebidae (including *Cebus*, *Saimiri* and *Aotus*; 700g-2000g; Wildman *et al*., 2009; Perelman *et al*., 2011). They share a number of distinguishing features in addition to small body size including higher rates of twinning, the absence of third molars and hypocones, and the presence of claws. These were historically viewed as the retention of primitive characteristics (Hershkovitz, 1977) but Ford (1980) argued they made up an "adaptive suite" (Moynihan, 1976) which was the product of an evolutionary reduction in body size. The status of callitrichids as evolutionary dwarfs has been complicated by uncertainty in the phylogenetic relationships of different extant genera, which has only recently been resolved (Wildman *et al*., 2009; Arnold *et al*., 2010; Perelman *et al*., 2011), and the paucity of the fossil record (Martin, 1992). Hence the status of *Callimico*, which neither twins nor has lost the third molar, and the relationships of *Saguinus*, *Callithrix* and the pygmy marmoset, which some raise to the genus level (*Cebuella pygmaea*; Ford *et al*., 2009), have raised questions over whether these traits evolved in synchrony during one evolutionary event or evolved during parallel episodes of body size reduction (Martin, 1992; Ah-King & Tullberg, 2000). Regardless of the extent of dwarfism during callitrichid evolution Marroig and Cheverud (2005, 2010) provide evidence that suggests morphological diversification in callitrichids resulted from strong positive selection on size, indicating body size is a key adaptive trait in this clade.

Fossil species classified as being monophyletic with extant callitrichids include *Micodon kiotensis*, *Patasola magdalena*, *Lagonimico conclutatus* and *Mohanamico hershkovitzi*; all are from the mid-late Miocene and had body masses estimated to range from 1000g-1300g, above the range of living callitrichids (Feagle, 1999). However, extant callitrichids do not have large molars relative to their body size, a common feature seen in dwarfed species which is caused by negative allometry between body size and tooth size, perhaps questioning their status as dwarfs (Gould, 1975; Martin, 1992; Ravosa, 1992; Plavcan & Gomez, 1993) although such negative

allometry may also be absent in other dwarf species (Marshalll & Corruccini, 1978) and callitrichids do show some overscaling of the eye (Martin, 1992). A possible explanation for why callitrichids do not show negative allometry in tooth size has been proposed by Marroig and Cheverud (2009). It was previously noted that the relationship between body size and gestation length in callitrichids is weak (Martin, 1992). Marroig and Cheverud (2009) suggested *Callithrix* and *Callimico* show paedomorphic traits and that the constant gestation length must be associated with a slowdown in prenatal growth rate which, given the lack of variation in postnatal growth rate, could explain how body size was reduced. They also note that such a change in ontogeny is rare, with the majority of episodes of dwarfism being explained by changes in postnatal growth rate or gestation length (Gould, 1975; Plavcan & Gomez, 1993, Webster *et al*., 2004).

Unlike the callitrichids, the evolution of body size in cheirogaleids is less well studied. They too are small bodied (30g-450g) species nested within a clade of larger bodied (600g-8,500g) species (Perelman *et al*., 2011). *Microcebus* has often been cited as a potential model of the ancestral primate (Gebo, 2004; Martin *et al*., 2007); however, recent analyses suggest the small body size of *Microcebus* may not be a retention of a primitive feature but the product of evolutionary convergence and dwarfism (chapter 3; Masters *et al.*, 2007). Both clades are characterised by a reduction in brain mass, but not relative brain size (chapter 3) suggesting dwarfism has had knock-on effects on other aspects of development.

Miniaturisation and dwarfism in other animal groups is known to affect numerous morphological and behavioural traits and is commonly associated with reduction and simplification in morphology (Hanken & Wake, 1993). Where dwarfism is due to changes in postnatal growth it is predicted that relative brain size will increase because brain growth primarily occurs in early ontogenetic stages and so early cessation or slow down in postnatal growth will not affect brain size (Shea, 1983). However in some cases, such as in extinct dwarf hippopotami and in some domesticated animals, dwarfism may be caused by developmental adjustments in periods of rapid, early brain growth resulting in a reduction in both brain and body mass (Weston & Lister, 2009). This scenario may also apply to callitrichids if dwarfism in this clade is due to changes in prenatal growth rates (Marriog & Cheverud, 2009). However it is unclear to what extent allometric scaling between brain and body size constrains brain size

(Shea, 1983; Niven, 2006; chapter 3) and it is conceivable that brain and body evolution could be decoupled during episodes of dwarfism. When brain size does decrease in dwarfed lineages selection may act to produce structural changes which compensate for the reduction in size. For example, in plethodontid salamanders brain mass has decreased in association with a reduction in body size (Roth *et al*., 1990). In these highly visually-orientated species both brain and eye size show negative allometry, being relatively larger in smaller brained species (Roth *et al*., 1990). Within the brain ventricular volume is small, the visual centres are relatively large, the volume of grey matter increases relative to white matter and the cell density within grey matter increases; these features seem to act to maintain the number of neurons involved in visual and visuomotor processing (Roth *et al.*, 1990). The two independent episodes of phyletic dwarfism in cheirogaleids and callitrichids offer an opportunity to examine the evolutionary trajectory of brain size during body size reduction and the nature of brain:body scaling.

To test hypotheses surrounding the evolution of brain and body size it is necessary to incorporate phylogenetic history in order to test for co-evolution between traits and to reconstruct the timing and distribution of evolutionary events (Hanken & Wake, 1993; Gould & MacFadden, 2004). Such a full phylogenetic, comparative analysis has only been made possible recently with a confirmation of genus level relationships and the production of species level phylogenies (Wildman *et al*., 2009; Arnold *et al*., 2010; Perelman *et al*., 2011). In this chapter I perform a species-level analysis of body size evolution in callitrichids and cheirogaleids, I test the hypothesis that body size reduction in callitrichids is driven by changes in prenatal growth rate, ask whether or not the convergent evolution of small body size in callitrichids and cheirogaleids share changes in the same stages of ontogeny, and finally explore what happens to brain size during episodes of body size reduction.

4.2 Methods Summary

This chapter utilises the consensus species-level, extant primate tree from the recently released 10k Trees Project (Arnold *et al*., 2010). The analysis was also run using the species phylogeny from Bininda-Emonds *et al*. (2007); the results are nearly identical so I only present the results obtained using the 10k Trees phylogeny. I obtained data on neonatal and adult body mass from the PanTHERIA database (Jones *et al*., 2009). Data were available for both traits for a total of 101 species represented in the 10k Tree of which 11 are callitrichids (1 *Leontopithecus*, 1 *Callimico*, 4 *Callithrix* and 5 *Saguinus*) and 5 are cheirogaleids (2 *Cheirogaleus*, 1 *Mirza* and 2 *Microcebus*). Life history data were taken from the same source. The traits considered were gestation length (in days), weaning age (in days), litter size, inter birth interval (in days), age at sexual maturity (in days) and maximum longevity (in days). 68 species had data for all variables of which 7 are callitrichids and 3 are cheirogaleids. Using these traits I also calculated:

- Prenatal growth rate:

= log(neonatal body mass [g])/log(gestation length[days])

- Postnatal growth rate:

= log(adult body mass [g] - neonatal body mass [g])/log(age at sexual maturity[days])

- Maximum female reproductive output:

= log((((max. longevity[days])-(age sexual maturity [days]))/(inter birth interval [days]))(litter size))*

In addition endocranial volumes were taken from Isler *et al*. (2008) and converted to brain mass as described in chapter 2. Data were available for 96 species of which 9 are callitrichids and 5 are cheirogaleids. Many of these traits correlate with body mass; when a trait relative to body mass is considered I performed a phylogenetically-controlled regression using PGLS in BayesTraits (Pagel *et al.*, 2004; Pagel & Meade, 2006) to calculate residuals as described in chapter 2. The rate parameter lambda was estimated for all PGLS regression (see chapter 2) and unless otherwise stated was not significantly different to one.

The phylogenies of the callitrichids and cheirogaleids included the neonatal/adult body mass dataset are shown in Figure 4.1, together with their respective outgroups. Lineages which

end in blue circles show species which appear in the life history dataset. Nodes in blue boxes are nodes which appear in the phylogeny when just the life history traits are considered.

The evolutionary history of body size in callitrichids and cheirogaleids was analysed in two ways. First, I used phylogenetically controlled t-tests (Organ *et al.*, 2007) to statistically test whether callitrichids and cheirogaleids have significantly smaller neonatal and adult body masses than other anthropoids and platyrrhines or other strepsirrhines and lemurs respectively, and whether or not there are significant differences in gestation length (a measure of the length of prenatal growth), prenatal growth rate, age at sexual maturity (a measure of the length of postnatal growth) or postnatal growth rate. Second, I performed phylogenetically-controlled regression using PGLS in BayesTraits (Pagel *et al.*, 2004; Pagel & Meade, 2006) between species traits to assess whether variation in body mass is associated with variation in gestation length, prenatal growth rate, age at sexual maturity and postnatal growth rate. Finally, I used ancestral state reconstruction, implemented in BayesTraits, as described in chapters 2 and 3, to estimate the ancestral state of adult and neonatal body mass, gestation length and age at sexual maturity at each node labelled in Figure 4.1.

These were then used to calculate ancestral states of prenatal and postnatal growth rates (see above). Briefly, this involved estimating whether the rate parameters kappa, delta and lambda were significantly different to 1 in a ML framework (Table 4.1) and when they were, estimating these parameters in conjunction with the rate parameter alpha to build a model of evolution for each trait in MCMC which was subsequently used to estimate ancestral states. The change in trait along each branch was calculated by taking the difference between consecutive nodes. These branch-specific changes, which are independent of each other, were then used in a non-parametric linear regression model, implemented in GenStat, to test for time-dependent associations between body mass (as the dependent variable) and other traits. Neonatal and adult body mass were initially analysed using the full dataset, but were subsequently re-analysed using only the species where life history traits were available. Comparisons of estimates of body mass and life history trait estimates are therefore not affected by differences in sampling.

In addition to investigating the changes in growth patterns associated with dwarfism I analysed the evolution of life history traits which have been proposed to evolve in concert with dwarfism. Specifically I consider the effects of dwarfism on reproductive strategies, analysing

the evolution of litter size, inter birth interval, weaning age and maximum reproductive output. Where trait values relative to body size were considered I estimated the ancestral states of the absolute value and then controlled for body mass (i.e. the 'residuals second' method in chapter 3).

Finally, I analysed the evolutionary history of absolute and relative brain size in these clades to assess the allometric effects of reducing body size on brain evolution. In order to implement the directional model fossil data were added to the 10K tree as described in chapter 2.

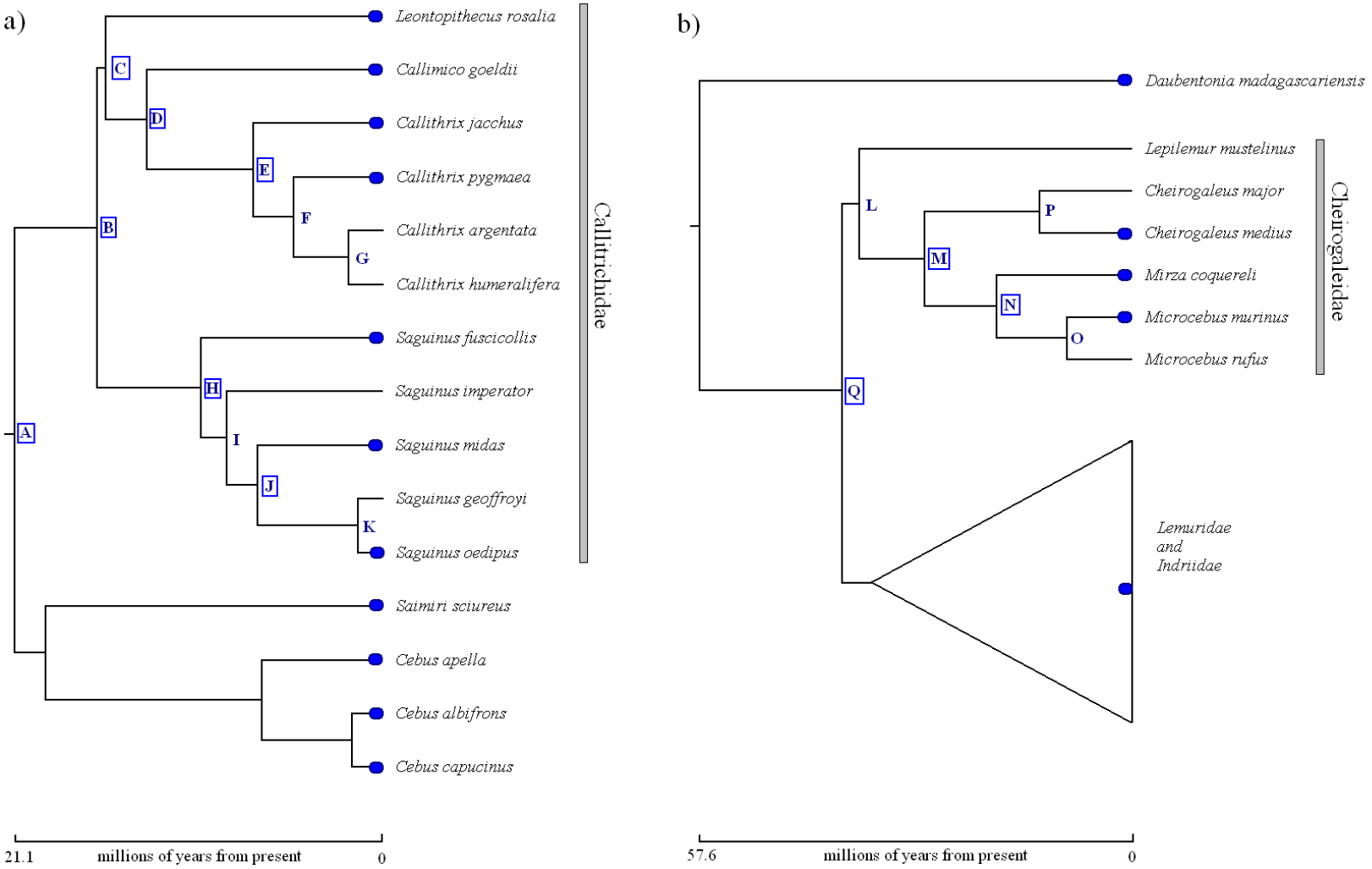

Figure 4.1 Phylogeny of a) Callitrichidae and b) Cheirogaleidae with outgroups
Branches are drawn proportional to time. All species shown have data for adult and neonatal body mass. Species with blue balls have data for life history variables. Node labels in blue boxes are therefore present in the phylogeny of species used to analyse life history traits.

Table 4.1 Estimation of rate parameters for traits under consideration

a) Full adult/neonatal body mass dataset

		Likelihoods				p-value			ML estimate*		
Trait	**n**	**Lh Null**	**Lh Lambda**	**Lh kappa**	**Lh delta**	**p lambda**	**p kappa**	**p delta**	**lambda**	**kappa**	**delta**
Adult body mass	101	-5.849	-5.850	-3.917	-4.389	0.964	0.049	0.087	-	1.442	-
Neonate body mass	101	17.946	17.972	18.026	19.340	0.820	0.743	0.098	-	-	-

b) Life history trait variables dataset

		Likelihoods				p-value			ML estimate*		
Trait	**n**	**Lh Null**	**Lh Lambda**	**Lh kappa**	**Lh delta**	**p lambda**	**p kappa**	**p delta**	**lambda**	**kappa**	**delta**
Adult body mass	68	-17.949	-17.949	-16.673	-17.383	0.973	0.110	0.287	-	-	-
Neonate body mass	68	-0.678	-0.678	-0.600	0.289	0.984	0.692	0.164	-	-	-
Sexual maturity age	68	25.942	32.985	33.784	33.450	0.000	0.206	0.335	0.953	-	-
Max. longevity	68	34.914	38.517	39.691	39.219	0.007	0.125	0.236	0.915	-	-
Gestation length	68	101.437	101.436	104.654	102.528	0.965	0.011	0.139	-	1.513	-
Inter birth interval	68	22.512	24.619	26.104	24.944	0.040	0.085	0.420	0.972	-	-
Litter size	68	82.848	82.848	83.417	83.233	0.970	0.286	0.380	-	-	-
Weaning age	68	-8.569	0.730	1.489	0.948	0.000	0.218	0.509	0.930	-	-

c) Brain mass

		Likelihoods				p-value			ML estimate*		
Trait	**n**	**Lh Null**	**Lh Lambda**	**Lh kappa**	**Lh delta**	**p lambda**	**p kappa**	**p delta**	**lambda**	**kappa**	**delta**
Brain mass	117	-1.752	-1.753	-1.375	2.785	1.000	0.385	0.003	-	-	0.270

* when significantly different to 1.

4.3 Results & Discussion

4.3.1 The evolution of body mass in callitrichids

Phylogenetically controlled t-tests confirm that callitrichids have significantly smaller adult body masses ($t_{69} = 2.658$, $p = 0.009$, $R^2 = 0.093$) and neonatal body masses ($t_{69} = 3.012$, $p = 0.004$, $R^2 = 0.116$) than other anthropoids and also when compared to just non-callitrichid New World monkeys (adult body mass: $t_{23} = 2.502$, $p = 0.019$, $R^2 = 0.214$; neonatal body mass: $t_{23} = 2.696$, $p = 0.012$, $R^2 = 0.240$). The estimated ancestral state of the last common ancestor of the Cebidae (Node A, Figure 4.2) suggests the callitrichids descended from a larger bodied ancestor with an adult body mass of 1198.10g and a neonatal body mass of 106.46g (95% confidence intervals, adult: 1193.77-1202.42g; neonate: 106.14-106.78g). Decreases in both adult and neonatal body mass appear to be widespread across callitrichids; however, the extremely small body size of *Callithrix pygmaea* appears to drag ancestral nodes towards it, with closely related lineages "rebounding" after diverging from the *C. pygmaea* lineage (Figure 4.2) suggesting this species is having a large influence on the estimated ancestral states. To test this I took advantage of the option in BayesTraits to estimate trait values for species tips (Organ *et al.*, 2007). I removed one species at a time, re-built the model and used this model to estimate the trait value of the missing species. In this way it is possible to compare an estimate for each species, which is independent of that species' trait, to the observed data to calculate how much each species estimate deviates from the observed value (Table 4.2).

The mean absolute percentage deviation between estimated and observed values is 4.26% and the median is 2.05% for adult body mass. For neonatal body mass the mean is 6.32% and the median is 3.93%. For both traits the error associated with *C. pygmaea* is substantially higher, and much higher than any other species; 24.70% for adult body mass and 34.96% for neonatal body mass (Figure 4.3; Table 4.2). This suggests body mass evolution along the terminal *C. pygmaea* lineage does not fit the general mode of evolution across callitrichids, and that dwarfism has been particularly rapid on this branch. This result is consistent with those of Eastman *et al*. (2011) who applied a novel method of estimating shifts in evolutionary rate to study primate body mass evolution. They show that the rate of body mass evolution along the *C. pygmaea* terminal branch is significantly accelerated compared to other primates (Eastman *et al*., 2011).

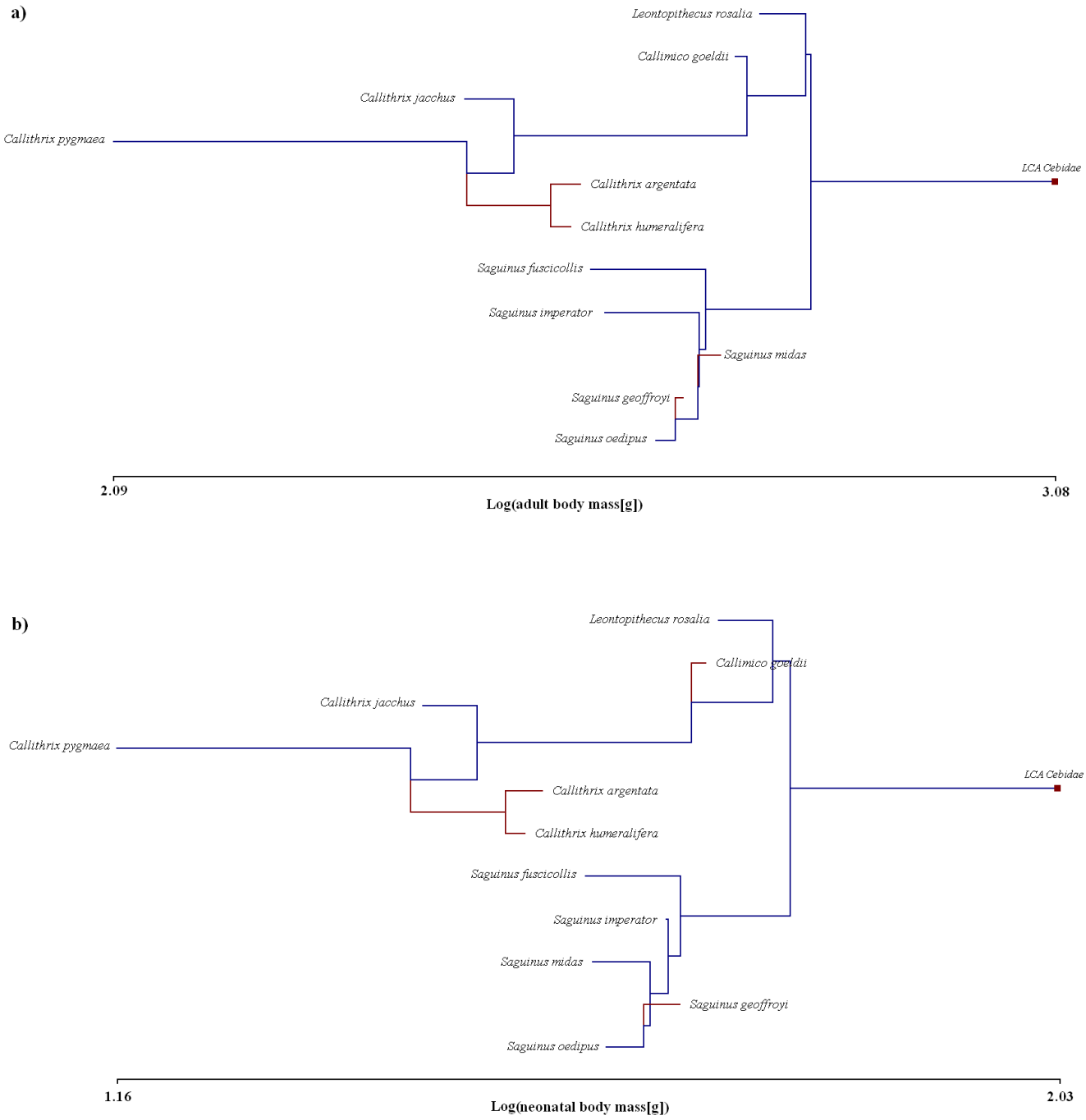

Figure 4.2 Phenograms for changes in a) adult body mass; **b) neonatal body mass in callitrichids** Including *C. pygmaea*. The topology of the tree is as shown in Figure 4.1 Branch lengths are drawn according to the difference in log(mass) between consecutive nodes such that at any point in the phenogram the phenotypic state can be read off the x-axis. Branches in red show increases in size, branches in blue show decreases.

Table 4.2 Observed and estimated adult and neonatal body mass for callitrichids

Species	True species values		Estimated species values					
			Adult			Neonate		
	Adult body mass	Neonate body mass	Mean	95% CI (±)	% error	Mean	95% CI (±)	% error
Callimico goeldii	2.747	1.703	2.762	0.005	-0.552	1.687	0.003	0.984
Callithrix argentata	2.583	1.554	2.524	0.002	2.291	1.494	0.001	3.845
Callithrix humeralifera	2.574	1.538	2.530	0.002	1.698	1.506	0.001	2.096
Callithrix jacchus	2.463	1.443	2.523	0.003	-2.448	1.513	0.003	-4.864
Callithrix pygmaea	2.093	1.161	2.610	0.002	-24.702	1.567	0.002	-34.916
Leontopithecus rosalia	2.773	1.715	2.823	0.005	-1.803	1.774	0.003	-3.425
Saguinus fuscicollis	2.595	1.593	2.742	0.004	-5.647	1.705	0.003	-7.008
Saguinus geoffroyi	2.692	1.680	2.671	0.001	0.789	1.620	0.001	3.582
Saguinus imperator	2.611	1.668	2.729	0.003	-4.524	1.669	0.003	-0.063
Saguinus midas	2.733	1.600	2.699	0.003	1.237	1.676	0.002	-4.764
Saguinus oedipus	2.665	1.613	2.695	0.001	-1.129	1.678	0.001	-4.018
Cheirogaleus major	2.649	1.257	2.399	0.005	9.447	1.220	0.003	2.964
Cheirogaleus medius	2.294	1.166	2.641	0.005	-15.116	1.278	0.003	-9.648
Lepilemur mustelinus	2.825	1.431	2.851	0.009	-0.895	1.533	0.005	-7.111
Microcebus murinus	1.839	0.679	1.988	0.002	-8.109	0.966	0.003	-42.243
Microcebus rufus	1.685	0.813	2.097	0.004	-24.488	0.875	0.003	-7.678
Mirza coquereli	2.514	1.111	2.214	0.006	11.939	1.065	0.004	4.145

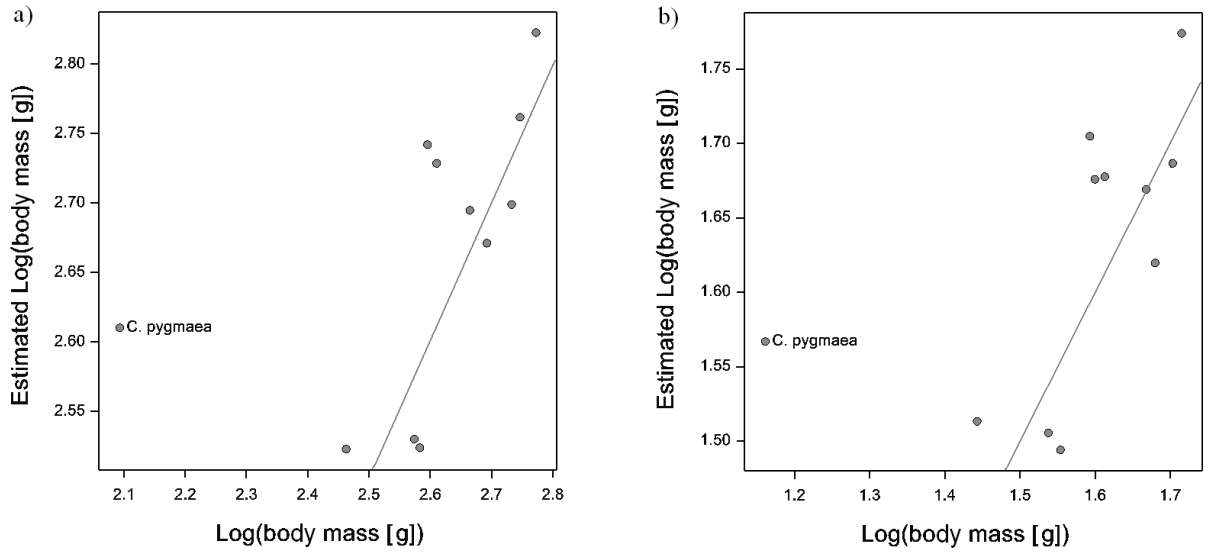

Figure 4.3 Estimated vs. observed values of a) adult body mass; b) neonatal body mass identify *C. pygmaea* as an outlier

Given the effect of *C. pygmaea* on the ancestral state estimates I repeated the ancestral state reconstructions for both adult and neonatal body mass excluding *C. pygmaea*. To incorporate change in body mass along the *C. pygmaea* lineage into the analyses I estimated the trait value at Node F (Figure 4.1) by setting the branch length of the *C. pygmaea* terminal branch to $1x10^{-6}$ and estimating the tip value. This data point is therefore effectively an estimate of the trait value at the point of divergence between *C. pygmaea* and *C. argentata/humeralifera* and was taken as such.

The removal of *C. pygmaea* leads to a slightly larger estimate for the cebid ancestor (Node A; Figure 4.1) with an adult body mass of 1246.88g and a neonatal body mass of 108.31g (95% confidence intervals, adult: 1121.89-1385.80g; neonate: 108.00-108.63g). The estimated adult body mass is consistent with the few mid-late Miocene primates assigned to the Callitrichidae (Fleagle, 1999). Estimated branch-specific changes in adult and neonatal body mass are strongly correlated (Spearman's correlation; $t_{19} = 4.26$, $p < 0.001$, $r_s = 0.699$). Decreases in both traits are widespread across the callitrichid phylogeny (Figure 4.4; Table 4.3). Adult body mass decreases along all but two branches and decreases account for 92.17% of evolutionary time. Neonatal body mass also decreases on all but two branches and decreases account for 96.95% of evolutionary time. The percentage reduction in neonatal/adult body mass is particularly high (>c.20%) along 6 lineages, including the stem branch of callitrichids, the stem of *Saguinus* and the stem of *Callithrix* suggesting small body size has evolved in parallel across callitrichids. The largest decrease is seen on the terminal *C. pygmaea* branch with a 60.0% reduction in neonatal body mass and a 69.5% reduction in adult body mass. The second largest decrease occurs along the stem callitrichid branch with a 41.7% decrease in neonatal body mass and a 42.0% decrease in adult body size.

I next controlled for branch length by dividing the difference in log body mass by branch length (in millions of years). The mean rate of change in neonatal body mass is -0.015 and lineages which fall in the lower quartile (<-0.024) include the stem callitrichid branch, the branches leading to the *Leontopithecus-Callimico-Callithrix,* the *Callimico-Callithrix* and the *Callithrix* clades, the terminal *C. pygmaea* lineage. For adult body mass the mean rate of change is -0.016; branches falling in the lower quartile (<-0.019) include the same branches as for neonatal body mass with the exception of the branch leading to the *Leontopithecus-Callimico-*

Callithrix clade and with the addition of the stem branch for *Saguinus*. The highest rate of change for both is the terminal *C. pygmaea* lineage, where the rate is 5.45 and 6.27 times faster than the mean for neonatal and adult body mass respectively. These rates are somewhat lower than rates of change in well studied episodes of dwarfism in Pleistocene mammals (Kurtén, 1959; Marshalll & Corruccini, 1978). However, the timescale considered in these cases is typically 1,000s of years, rather than millions and the percentage change is equal or greater than many other examples of insular dwarfing (Marshall & Corruccini, 1978). The range in rates of change in adult body mass overlaps with those seen in dwarfed lineages of fossil horses (MacFadden, 1986) which evolved over similar time periods (branch lengths 2-7 million years).

Table 4.3 Branch specific changes in adult and neonatal body mass in callitrichids

Branch	Change in Log(adult body mass)			Change in Log(neonatal body mass)			BL (my)	Rate of change	
	Mean	95% CI (±)	% change	Mean	95% CI (±)	% change		adult	neonate
A…B	-0.236	0.002	-41.980	-0.234	0.006	-41.660	4.765	-0.050	-0.049
B…C	-0.005	0.002	-1.080	-0.014	0.005	-3.116	0.469	-0.010	-0.029
C… *L. rosalia*	-0.085	0.002	-17.202	-0.072	0.004	-15.240	15.845	-0.005	-0.005
C...D	-0.045	0.002	-9.837	-0.060	0.006	-12.823	2.344	-0.019	-0.025
D…*C. goeldii*	-0.066	0.002	-13.519	-0.024	0.004	-5.377	13.501	-0.005	-0.002
D…E	-0.175	0.002	-33.118	-0.148	0.006	-28.807	6.109	-0.029	-0.024
E… *C. jacchus*	-0.175	0.002	-32.750	-0.137	0.004	-26.991	7.392	-0.024	-0.018
E…F	-0.027	0.003	-5.945	-0.012	0.005	-2.832	2.317	-0.011	-0.005
F…*C. pygmaea*	-0.518	0.002	-69.464	-0.406	0.004	-60.725	5.075	-0.102	-0.080
F…G	-0.023	0.002	-5.109	-0.016	0.004	-3.592	3.143	-0.007	-0.005
G…*C. argentata*	-0.006	0.001	-0.578	0.003	0.002	0.581	1.932	-0.003	0.001
G...*C. humeralifera*	-0.015	0.001	-2.637	-0.014	0.002	-3.071	1.932	-0.008	-0.007
B…H	-0.131	0.002	-26.065	-0.113	0.005	-22.878	5.937	-0.022	-0.019
H…*S. fusicollis*	-0.136	0.002	-26.339	-0.095	0.004	-19.603	10.378	-0.013	-0.009
H…I	-0.008	0.002	-1.899	-0.015	0.005	-3.485	1.475	-0.006	-0.010
I….*S. imperator*	-0.113	0.002	-22.261	-0.004	0.004	-1.031	8.903	-0.013	-0.001
I…J	-0.004	0.002	-0.966	-0.017	0.005	-3.743	1.772	-0.002	-0.009
J…*S. midas*	0.014	0.002	4.024	-0.056	0.004	-12.136	7.131	0.002	-0.008
J…K	-0.034	0.001	-7.621	-0.009	0.004	-1.956	5.734	-0.006	-0.001
K…*S. geoffroyi*	0.008	0.001	2.594	0.033	0.002	7.775	1.397	0.006	0.023
K…*S. oedipus*	-0.020	0.001	-3.751	-0.034	0.002	-7.634	1.397	-0.014	-0.025

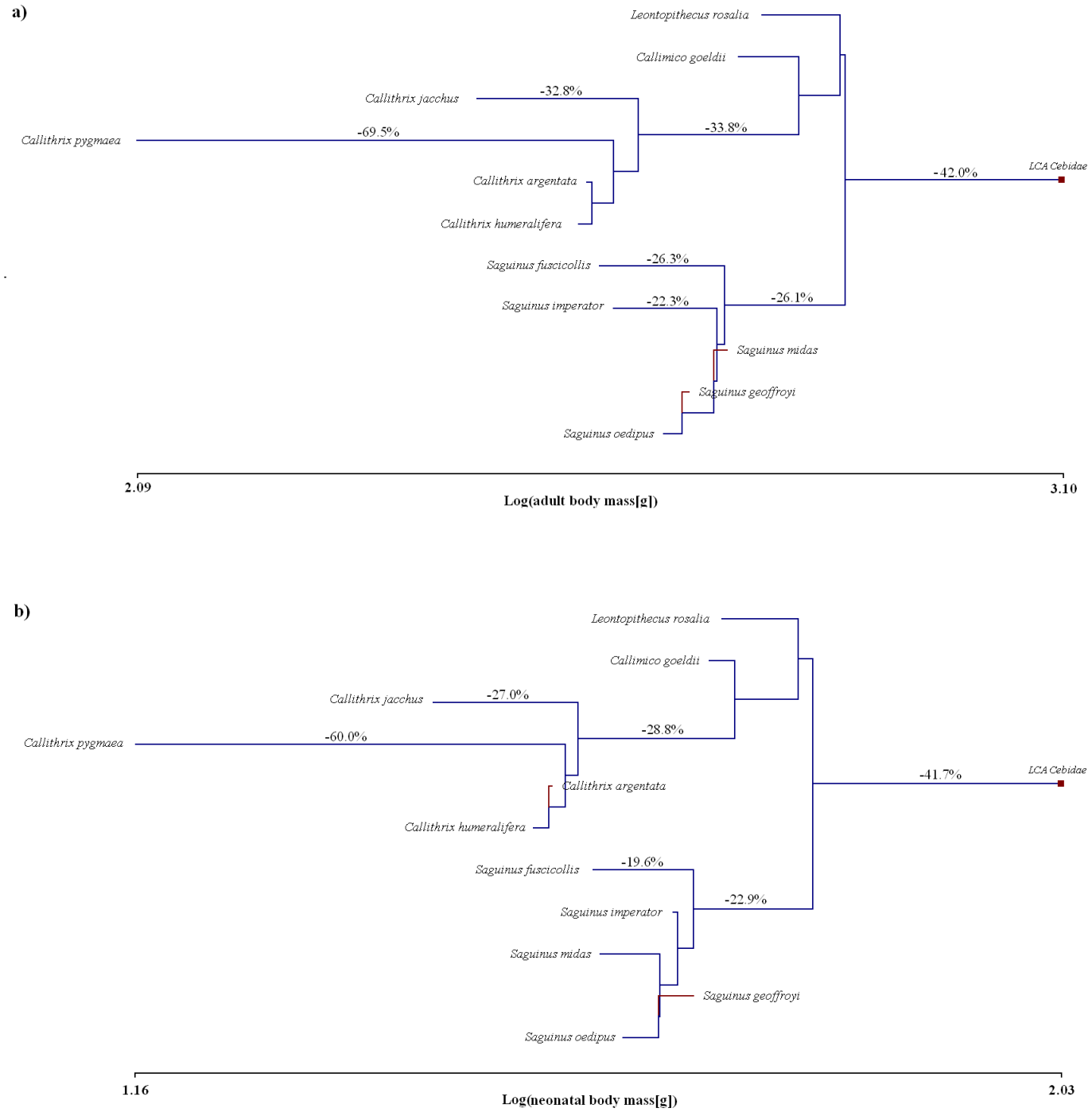

Figure 4.4 Phenograms for changes in a) adult body mass; **b) neonatal body mass, with *C. pygmaea* excluded from the reconstruction**

The topology of the tree is as shown in Figure 4.1 Branch lengths are drawn according to the difference in log(mass) between consecutive nodes such that at any point in the phenogram the phenotypic state can be read off the x-axis. Branches in red show increases in size, branches in blue show decreases. The percentage change is shown for branches with a percentage change greater/equal to 20%.

4.3.2 The evolution of gestation length in callitrichids

C. pygmaea falls within the range of other callitrichids for all traits considered below and does not have an overbearing affect on the results. Although gestation length and adult body size are significantly correlated across primates ($t_{66} = 5.695$, $p < 0.001$, $R^2 = 0.330$) and callitrichids are significantly smaller than other anthropoids, I confirmed statistically that gestation length is not significantly shorter in callitrichids than other anthropoids ($t_{49} = 1.794$, $p = 0.079$, $R^2 = 0.063$) or other New World monkeys ($t_{18} = 1.561$, $p = 0.136$ $R^2 = 0.119$) as previously suggested (Martin, 1992; Marroig & Cheverud, 2009). The ancestral cebid (Node A) is estimated to have had a gestation length of 161 days, and the ancestral callitrichid (Node B) 153 days (Table 4.5); both are slightly higher than the average gestation length across callitrichids (146 days). Although the majority of branches (10/13; Table 4.6, Figure 4.5) show decreases in gestation length these are relatively small (the mean change is -3.65 days) and regression analysis between branch-specific changes shows the reduction in gestation length does not explain the reduction in adult body mass ($t_{11} = 0.880$, $p = 0.396$). The largest decrease occurs along the *Leontopithecus* terminal branch (-18.87 days) followed by the terminal *S. midas* branch (-13.50 days), the terminal *C. pygmaea* branch (-9.96 days) and the stem callitrichid branch (-8.11 days). Increases occur on the terminal *S. oedipus* branch (+14.75 days) and the *Callimico* branch (+2.42 days).

In order to calculate pre and postnatal growth rates I reconstructed the evolution of age at sexual maturity, which is taken as the point when postnatal growth ceases. Sexual maturity decreases on 9/13 branches (Table 4.6) but the change in sexual maturity is not associated with changes in adult body size ($t_{11} = 0.080$, $p = 0.937$). Using data and ancestral state reconstructions for neonatal body mass, gestation length, adult body mass and age at sexual maturity I then estimated changes in pre and postnatal growth rates during callitrichid evolution as described in the methods section. Prenatal growth rate was found to be significantly slower in callitrichids compared to other anthropoids ($t_{51} = 4.052$, $p < 0.001$, $R^2 = 0.255$) or just other New World monkeys ($t_{18} = 3.886$, $p = 0.001$ $R^2 = 0.456$). In contrast, postnatal growth rate showed no significant difference for either comparison (anthropoids: $t_{51} = 4.052$, $p < 0.001$, $R^2 = 0.255$; New World monkeys: $t_{18} = 1.257$, $p = 0.225$, $R^2 = 0.081$). Prenatal growth rate is estimated to have decreased on all branches in the callitrichid tree, whilst postnatal growth rate decreased along 11/13 branches (Table 4.6; Figure 4.5).

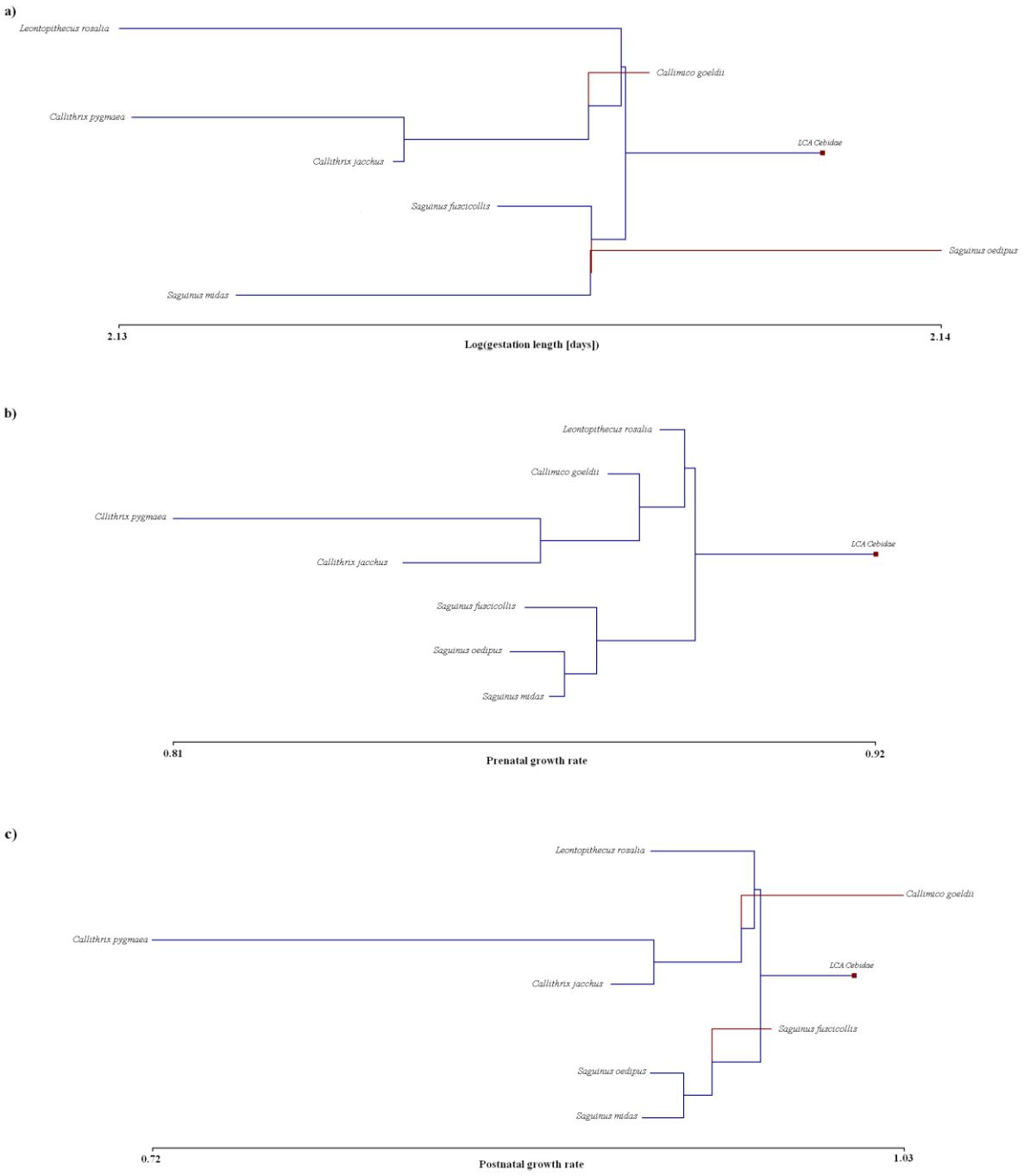

Figure 4.5 Phenograms for changes in a) gestation length; **b) prenatal growth rate; c) postnatal grown rate in callitrichids**

The topology of the tree is as shown in Figure 4.1 Branch lengths are drawn according to the difference between consecutive nodes such that at any point in the phenogram the phenotypic state can be read off the x-axis. Branches in red show increases in size, branches in blue show decreases.

Branches with estimated changes in prenatal growth which fall in the lower quartile (<-0.053) include the 5 branches highlighted as having large decreases in body size, whereas only three of these fall in the lower quartile (<-0.037) for postnatal body mass. Estimated changes in prenatal growth rate are significantly associated with changes in adult body mass (t_{11} = 20.420, $p < 0.001$, R^2 = 0.972). Changes in postnatal growth rate are also significantly associated with changes in adult body mass (t_{11} = 5.150 $p < 0.001$, R^2 = 0.681) but this association is strongly dependent on the change along the *C. pygmaea* branch, and when this is removed the association is no longer significant (t_{10} = 1.070, p = 0.308, R^2 = 0.014). Removal of *C. pygmaea* branch does not affect the significance for prenatal growth rate (t_{10} = 9.750, $p < 0.001$, R^2 = 0.892). In addition when both pre and postnatal growth rates are included as independent variables in a multiple regression with adult body mass only prenatal growth rate is significant (prenatal: t_{10} = 10.270, $p < 0.001$; postnatal: t_{10} = 0.360, p = 0.724). The distribution of rates of change for each trait is shown in Figure 4.6; note the predominance of decreases in all traits but gestation length, the greater skew in prenatal growth rates and the extremely high rates of change for *C. pygmaea*.

The same pattern of associations is also found if species values are used to test for associations using PGLS. Within callitrichids gestation length is not significantly associated with adult body size (t_5 = 0.573, p = 0.592, R^2 = 0.062), nor is age at sexual maturity (t_5 = 0.301, p = 0.775, R^2 = 0.022). Postnatal growth rate is significant (t_5 = 3.991, p = 0.010, R^2 = 0.761) but not if *C. pygmaea* is excluded (t_4 = 0.704, p = 0.508, R^2 = 0.110). In contrast, prenatal growth rate is significantly associated with adult body size with (t_5 = 11.600, $p < 0.001$, R^2 = 0.964) and without *C. pygmaea* (t_4 = 4.996, p = 0.002, R^2 = 0.862). When both pre and postnatal growth rate are included in a multiple regression using PGLS including *C. pygmaea*, prenatal growth rate is significantly associated with body size but postnatal growth rate is not (prenatal: t_3 = 4.785, p = 0.017; postnatal: t_3 = 0.184, p = 0.866).

These analyses provide robust support for the hypothesis that dwarfism across the callitrichids is associated with changes in prenatal growth rates and not in changes in the duration of prenatal or postnatal growth, or in postnatal growth rate (Martin, 1992; Marriog & Cheverud, 2009). However, the evolution of the extremely small body mass of *C. pygmaea* seemingly involved major decreases in both pre and postnatal growth rate (Figures 4.5 & 4.6). As discussed above dwarfism via changes in prenatal ontogeny is considered rare (Gould, 1975;

Plavcan & Gomez, 1993, Webster *et al*., 2004; Marriog & Cheverud, 2009). One notable example where change in prenatal growth rate is the major contributing factor to dwarfing comes from carnivores. Domestic breeds of dog vary greatly in body mass but, like the callitrichids (Martin, 1992), have almost invariant gestation lengths (Wayne, 1986a) and, also like callitrichids (Marriog & Cheverud, 2009), miniature breeds of dog show paedomorphic traits (Wayne, 1986b). Postnatal growth rates do not vary greatly between breeds and together these observations suggest dwarfism in the domestic dog is caused primarily by slowing foetal growth rate (Wyane, 1986a). Interestingly two wild carnivores which are thought to have undergone dwarfism in association with unpredictable food supply, the raccoon dog (*Nyctereutes procyonoides*) and the bush dog (*Speothos venaticus*), also have long gestation lengths relative to their body size and lower prenatal growth rates suggesting the slow prenatal growth rates of miniature breeds is not just an oddity caused by domestication (Wayne, 1986a). It is also notable that the small dog phenotype has a simple genetic basis (Sutter *et al*., 2007). Although it is unclear to what extent the genetic basis of phenotypic evolution under artificial selection is analogous to evolution under natural selection, it is possible that the rapid evolution of body size in the callitrichids may have been facilitated by having a simple genetic basis.

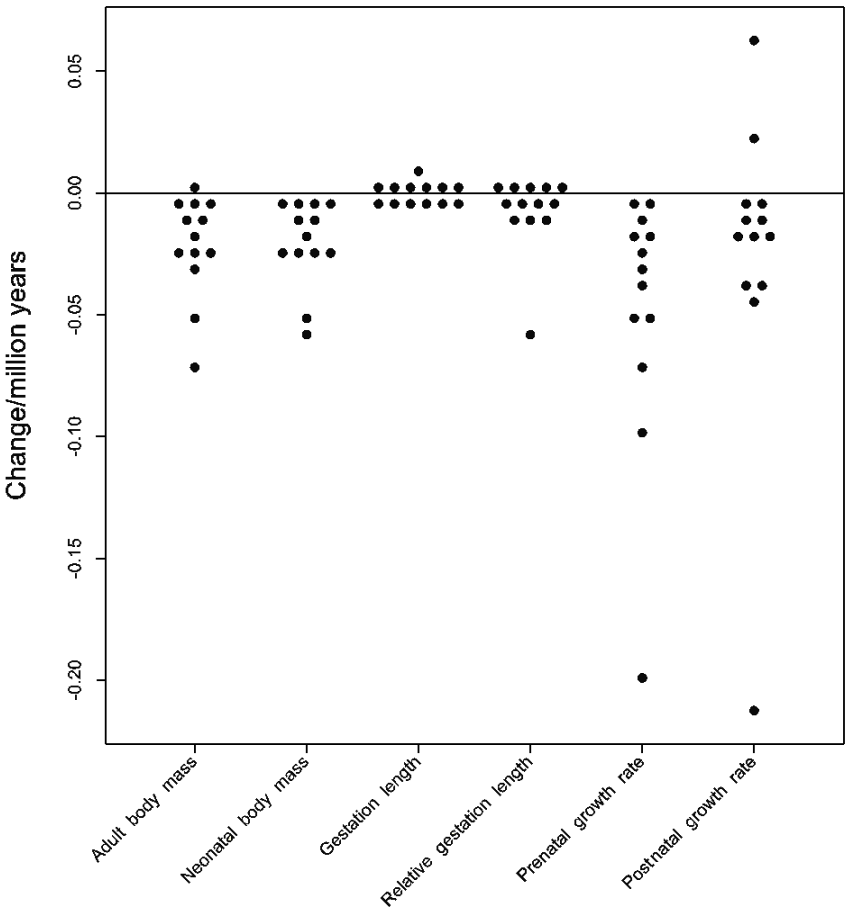

Figure 4.6 Dot-histograms for the rate of change in body mass and growth rate parameters along all branches in the callitrichid tree. The lowest values for pre and postnatal growth rate are for the *C. pygmaea* terminal branch.

Table 4.5 Ancestral state reconstructions of body mass and life history traits in callitrichids

a) Body mass & growth rate parameters

Node	Log(Adult body mass[g])		Log(Neonatal body mass[g])		Log(Gestation Length [days])			Log(Age at sexual maturity [days])			Prenatal growth rate	Postnatal growth rate
	Mean	95% CI (±)	Mean	95% CI (±)	Mean	95% CI (±)	relative to body mass	Mean	95% CI (±)	relative to body mass		
A	3.101	0.002	2.035	0.001	2.207	0.000	-0.041	3.023	0.001	0.030	0.922	1.013
B	2.858	0.002	1.803	0.001	2.185	0.000	-0.118	2.896	0.001	-0.140	0.825	0.973
C	2.843	0.002	1.790	0.001	2.184	0.000	-0.123	2.889	0.001	-0.151	0.819	0.970
D	2.784	0.002	1.734	0.001	2.181	0.000	-0.137	2.842	0.001	-0.184	0.795	0.965
E	2.639	0.002	1.603	0.002	2.160	0.000	-0.135	2.798	0.001	-0.304	0.742	0.928
H	2.740	0.002	1.684	0.001	2.181	0.000	-0.160	2.834	0.001	-0.224	0.772	0.952
J	2.720	0.002	1.647	0.001	2.181	0.000	-0.205	2.852	0.001	-0.253	0.755	0.940

b) Reproductive rate parameters

Node	Log(Litter size)		Log(Max. longevity [months])		Log(Inter birth interval [days])		Log(Weaning age [days])			Log(max reproductive output)	Log(max reproductive output) relative to body mass
	Mean	95% CI (±)	Mean	95% CI (±)	Mean	95% CI (±)	Mean	95% CI (±)	relative to body mass		
A	0.089	0.000	2.481	0.001	2.572	0.001	2.168	0.002	-0.041	1.429	0.130
B	0.178	0.000	2.428	0.001	2.429	0.001	2.011	0.002	-0.118	1.617	-0.044
C	0.182	0.000	2.425	0.001	2.417	0.001	2.001	0.002	-0.123	1.630	-0.054
D	0.186	0.000	2.398	0.001	2.373	0.001	1.968	0.002	-0.137	1.653	-0.105
E	0.272	0.000	2.349	0.001	2.300	0.001	1.923	0.002	-0.135	1.762	-0.210
H	0.239	0.000	2.415	0.001	2.410	0.001	1.930	0.002	-0.160	1.688	-0.136
J	0.264	0.000	2.397	0.001	2.384	0.001	1.879	0.002	-0.205	1.718	-0.144

Table 4.6 Branch specific changes in body mass and life history traits in callitrichids

a) Body mass & growth rate parameters

Branch		Log(Adult body mass[g])		Log(Neonatal body mass[g])		Log(Gestation Length [days])[1]			Log(Age at sexual maturity [days])[2]			Prenatal growth rate	Postnatal growth rate
	Branch length (my)	Mean	95% CI (±)	Mean	95% CI (±)	Mean	95% CI (±)	relative to body mass	Mean	95% CI (±)	relative to body mass		
A..B	4.765	-0.243	0.002	-0.232	0.002	-0.022	0.000	-0.048	-0.127	0.001	-0.170	-0.097	-0.040
B..C	0.469	-0.015	0.002	-0.013	0.002	-0.001	0.000	-0.027	-0.007	0.001	-0.011	-0.006	-0.003
C..D	2.344	-0.060	0.002	-0.056	0.002	-0.004	0.000	-0.024	-0.046	0.001	-0.034	-0.024	-0.005
C..*Leontopithecus*	15.845	-0.071	0.002	-0.075	0.001	-0.057	0.000	-0.004	0.061	0.001	-0.105	-0.013	-0.044
D…*Callimico*	13.501	-0.037	0.002	-0.031	0.001	0.007	0.000	-0.002	-0.226	0.001	0.092	-0.017	0.069
D…E	6.109	-0.146	0.003	-0.131	0.002	-0.021	0.000	-0.021	-0.044	0.001	-0.120	-0.053	-0.037
E…*C. jacchus*	7.392	-0.175	0.002	-0.160	0.002	-0.001	0.000	-0.022	-0.140	0.001	-0.096	-0.074	-0.018
E…*C. pygmea*	7.392	-0.544	0.002	-0.441	0.002	-0.031	0.000	-0.059	0.052	0.052	-0.575	-0.197	-0.212
B..H	5.937	-0.119	0.002	-0.119	0.002	-0.004	0.000	-0.020	-0.062	0.001	-0.083	-0.053	-0.021
H…*S. fusicolis*	10.378	-0.144	0.002	-0.091	0.001	-0.011	0.000	-0.009	-0.225	0.001	-0.015	-0.038	0.025
H..J	3.247	-0.019	0.002	-0.038	0.002	0.000	0.000	-0.012	0.018	0.001	-0.029	-0.017	-0.012
J…*S. midas*	7.131	0.012	0.002	-0.047	0.001	-0.040	0.000	-0.006	0.073	0.001	-0.029	-0.008	-0.018
J…*S. oedipus*	7.131	-0.056	0.002	-0.034	0.001	0.040	0.000	-0.006	-0.019	0.001	-0.045	-0.029	-0.014

[1] more negative values indicate a longer gestation length relative to neonatal body mass

[2] more positive values equate to earlier age of sexual maturity

Table 4.6 cont'd. Branch specific changes in body mass and life history traits in callitrichids

b) Reproductive rate parameters

Branch	Branch length (my)	Log(Litter size)		Log(Weaning age [days])[3]			Log(max reproductive output)	Log(max reproductive output) relative to body mass
		Mean	95% CI (±)	Mean	95% CI (±)	relative to body mass		
A...B	4.765	0.089	0.001	-0.157	0.002	-0.078	0.188	-0.174
B…C	0.469	0.004	0.001	-0.010	0.299	-0.005	0.013	-0.010
C…D	2.344	0.004	0.001	-0.033	0.002	-0.013	0.023	-0.051
C…*Leontopithecus*	15.845	0.106	0.000	-0.122	0.002	-0.099	0.309	0.044
D…*Callimico*	13.501	-0.165	0.000	-0.145	0.002	-0.133	-0.106	-0.076
D…E	6.109	0.086	0.001	-0.045	0.003	0.002	-0.074	0.074
E…*C. jacchus*	7.392	0.091	0.000	-0.143	0.002	-0.086	0.152	-0.120
E…*C. pygmea*	7.392	0.013	0.000	0.035	0.002	0.213	-0.056	-0.566
B…H	5.937	0.060	0.001	-0.081	0.002	-0.042	0.071	-0.092
H…*S. fusicolis*	10.378	0.024	0.000	0.024	0.002	0.071	0.039	-0.130
H…J	3.247	0.025	0.001	-0.051	0.003	-0.045	0.030	-0.008
J…*S. midas*	7.131	0.041	0.000	-0.037	0.002	-0.041	-0.048	-0.006
J…*S. oedipus*	7.131	0.015	0.000	-0.182	0.002	-0.163	0.083	-0.025

[3] more negative values indicate shorter weaning times relative to adult body mass

4.3.3 The evolution of life history and reproductive strategies in callitrichids

It has been suggested that dwarfism in the callitrichids was intimately associated with changes in reproductive strategy. It has been argued that the high rate of twinning in callitrichids is directly related to a reduction in body mass due to selection against single offspring which become relatively large with decreasing adult body mass and can therefore cause problems during parturition (Leutenegger, 1973). Ah-King and Tullberg (2000) however have suggested small size is not closely related to twinning but may be a prerequisite for the evolution of twinning. The absence of twinning in *Callimico* has caused some debate as to whether twinning evolved at the origin of callitrichids and was lost in *Callimico*, or whether the evolution of twinning occurred in parallel in *Callithrix*, *Leontopithecus* and *Saguinus* but not in *Callimico* (Martin, 1992; Porter & Garder, 2004). Martin (1992) noted *Callimico* begins breeding at an early age and suggested this may minimise the reduction in reproductive output associated with absence of twinning. This fast life history strategy may be related to changes in predation risk from aerial predators, which may also explain the cryptic pelage and behaviour, or due to increased, earlier reproductive opportunities in the natal group (Porter & Garber, 2004).

To test these hypotheses I reconstructed the evolutionary history of litter size, weaning age and maximum female reproductive output (see methods). I analysed litter size as a continuous trait rather than a discrete "present/absent" trait as in natural populations the frequency of multiple births can vary through time in a continuous manner. The ancestral litter size of the *Cebidae* (Node A) is estimated to be 1.23 increasing to 1.51 at the origin of the callitrichids (Node B) suggesting that an increase in the frequency of twinning occurred at the origin of callitrichids (Table 4.5). Viewed as a continuous trait the frequency of twinning increased in parallel in *Callithrix*, *Leontopithecus* and *Saguinus* but decreased in *Callimico* from 1.536 (Node D) to 1.05 (Table 4.6). There is no association between the estimated change in frequency of twinning and the change in adult body mass either including ($t_{11} = 0.627$, $p = 0.561$) or excluding *Callimico* ($t_{10} = 0.15$, $p = 0.883$). I subsequently analysed twinning as a discrete trait using Discrete in BayesTraits (Pagel *et al.*, 2004; Pagel & Meade, 2006). The results are in line with those obtained using continuous litter sizes: the probability that twinning was present at Node A is 0.108 increasing to <0.001 at the origin of callitrichids. The probability twinning was

present at the last common ancestory of *Callimico* and *Callithrix* is 0.071. Twinning is predicted to have been present at all other nodes within callitrichids ($p < 0.001$).

Relative to body size the branches which show the largest absolute changes in weaning time (upper quartile >0.099) include both positive and negative changes. The terminal *C. pygmaea* branch shows an increase towards longer weaning time, whilst the terminal *Callimico*, *S. oedipus* and *Leontopithecus* branches show decreases in weaning time (Table 4.6). The age at which sexual maturity is reached, relative to adult body size, tends to increase in callitrichids, with large decreases at the origin of callitrichids, *Callithrix*, *C. pygmaea* and *Leontopithecus* (Table 4.6). The only branch to show a decrease in relative age at sexual maturity is *Callimico* suggesting a more rapid life history strategy has indeed evolved in *Callimico* (Martin, 1992).

However, despite this increase in life history rate the maximum female reproductive rate still decreases with the reduction of twinning in *Callimico* (Table 4.6) from c. 45 offspring/female at node D to 35 offspring/female. This is the largest decrease seen in callitrichids. The largest increases occur along the stem callitrichid branch (27 to 41 offspring), the *Leontopithecus* terminal branch (43 to 87 offspring), and the *C. jacchus* terminal branch (58 to 82 offspring). The increase along the *C. jacchus* lineage may be inflated by an overestimation of the frequency of triplets from laboratory studies, however the increase along the *Leontopithecus* branch seems to be explained by an increase in the frequency of twinning and an increase in maximum longevity. Whilst these estimates are likely to be much greater than reproductive output in the wild, they suggest that alterations in life history alone may not explain how *Callimico* offsets the loss of twinning.

Branch specific changes in body size and life history traits are summarised in Figure 4.7.

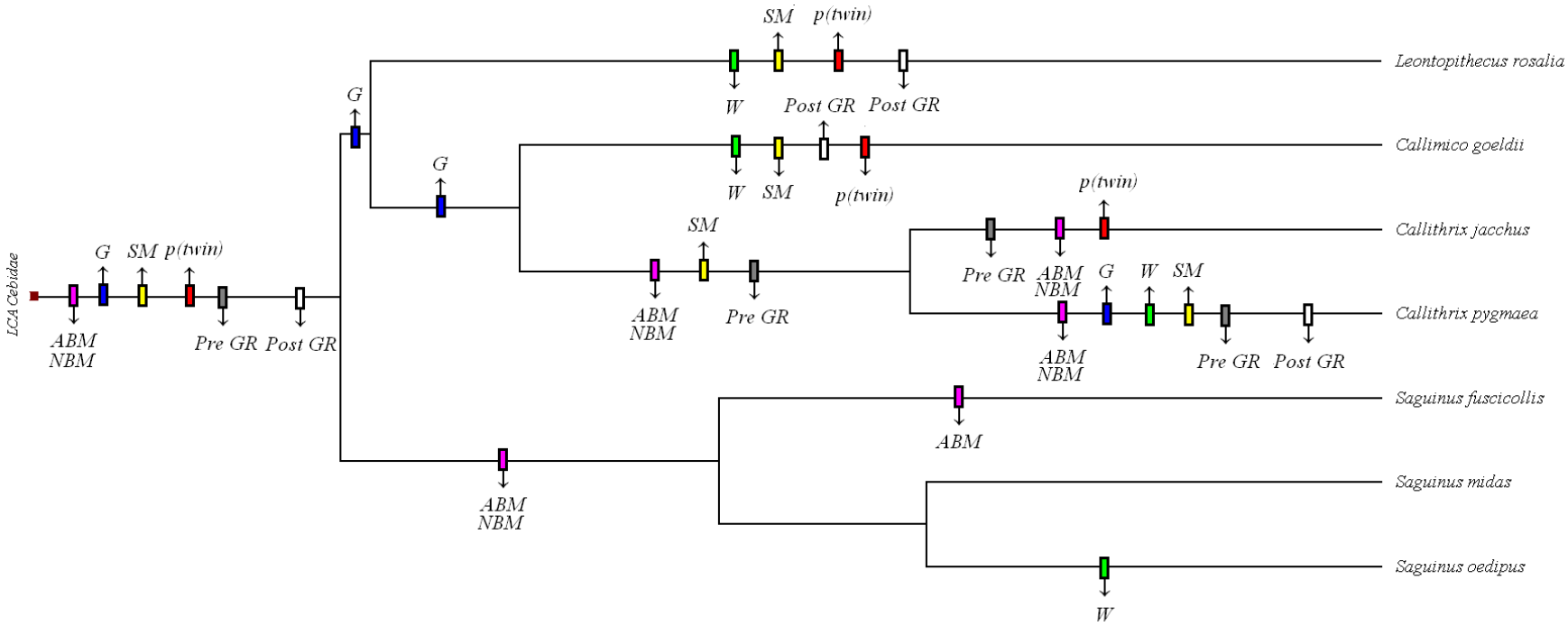

Figure 4.7 Distribution of major episodes of changes in body mass and life history traits in the callitrichids
Coloured boxes represent different traits, arrows indicate the direction of change (↑ = increase/shorter, ↓ = decrease/longer). Traits are labelled if they fall in the upper quartile of absolute change, or for body mass if the change is >20%. The label at the tip of the arrow head indicates the phenotype: ABM = adult body mass, NBM = neonatal body mass, G = gestation time relative to body mass, SM = age at sexual maturity relative to body mass, p(twin) = probability of twinning, Pre GR = prenatal growth rate, Post GR = postnatal growth rate, W = length of weaning relative to adult body mass.

4.3.4 The evolution of body mass in cheirogaleids

Cheirogaleids have significantly smaller adult body masses than other strepsirrhines (t_{28} = 2.809, p = 0.009, R^2 = 0.233) and other lemurs (t_{19} = 3.106, p = 0.006, R^2 = 0.362). They also have significantly smaller neonatal body masses than other strepsirrhines (t_{28} = 2.844, p = 0.009, R^2 = 0.237) and other lemurs (t_{19} = 3.843, p = 0.001, R^2 = 0.465). I repeated the analysis which aims to identify if any particular species has an over bearing effect on the ancestral state reconstructions as described above for callitrichids. Although the percentage error between real and estimated species values is larger for cheirogaleids than callitrichids, most likely due to the longer branch lengths, no single species appears to be more poorly estimated than others (Table 4.7, Figure 4.8).

Table 4.7 Observed and estimated adult and neonatal body mass for cheirogaleids

Species	True species value		Estimated species values					
			Adult			Neonate		
	Adult body mass	Neonate body mass	Mean	95% CI (±)	% error	Mean	95% CI (±)	% error
Cheirogaleus major	2.649	1.257	2.399	0.005	9.447	1.220	0.003	2.964
Cheirogaleus medius	2.294	1.166	2.641	0.005	-15.116	1.278	0.003	-9.648
Lepilemur mustelinus	2.825	1.431	2.851	0.009	-0.895	1.533	0.005	-7.111
Microcebus murinus	1.839	0.679	1.988	0.002	-8.109	0.966	0.003	-42.243
Microcebus rufus	1.685	0.813	2.097	0.004	-24.488	0.875	0.003	-7.678
Mirza coquereli	2.514	1.111	2.214	0.006	11.939	1.065	0.004	4.145

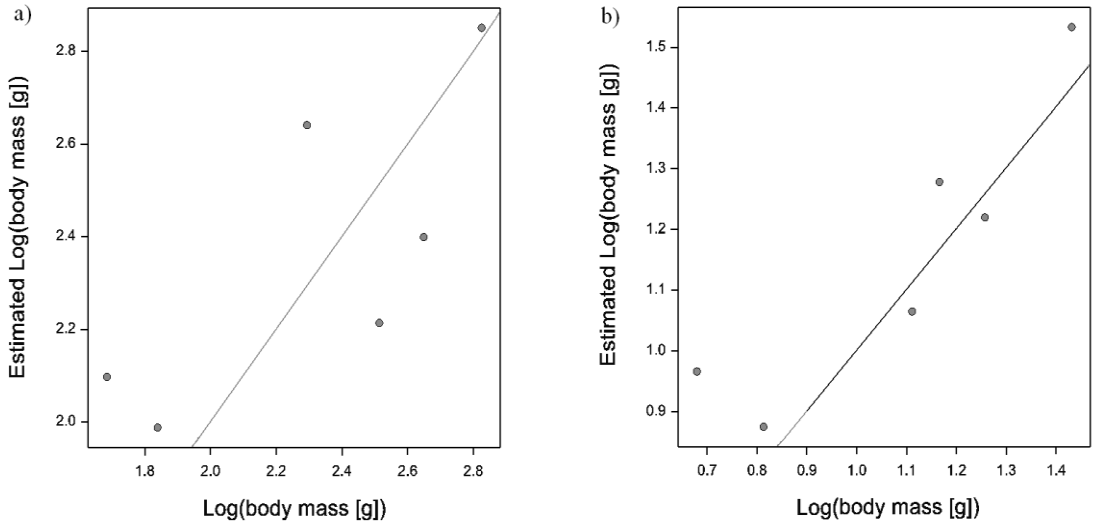

Figure 4.8 Estimated vs. observed values of a) adult body mass; **b) neonatal body mass in cheirogaleids**

The last common ancestor of *Lepilemur* and the cheirogaleids (Node L) is estimated to have had an adult body mass of 700.84g (95% CI: 697.00-704.70g) and a neonatal body mass of 32.81g (95% CI: 32.67-32.95g) both of which are larger than the maximum size seen within cheirogaleids (Table 4.8). As for callitrichids, decreases in both adult and neonatal body mass are widespread in cheirogaleids (Figure 4.9; Table 4.9) and strongly correlated (Spearman's correlation; $t_9 = 3.65$, $p = 0.005$, $r_s = 0.773$). The largest decreases in adult body mass occur along the stem cheirogaleid branch (-46.81%), the terminal *C. medius* branch (-37.55%), the branch leading to the *Mirza-Microcebus* clade (-47.99%), the branch leading to *Microcebus* (-56.33%) and the terminal *M. rufus* branch (-42.85%). The same branches are highlighted when change in mass is controlled for branch length. Large decreases in neonatal body mass (>14%) are also observed on all these branches with the exception of the *M. rufus* branch which shows a more modest decrease of 8.22% (Table 4.9). Interestingly when body size has increased, it is primarily restricted to adult body size. Increases in neonatal body size of 5.67% and 7.84% occurred on the *C. major* and *Mirza* terminal branches respectively, whilst adult body mass increased by 41.57% and 68.40% respectively. These results suggest decreases in neonatal body mass do play a major role in body size evolution but postnatal body growth also plays a role in both decreases (*M. rufus*) and increases (*C. major* and *Mirza*) in cheirogaleids body size.

Life history data is somewhat limited in cheirogaleids, with data only available for *C. medius*, *Mirza coquereli* and *M. murinus*. Based on these data cheirogaleids have significantly shorter gestation periods than other strepsirrhines ($t_{16} = 3.976$, $p = 0.014$, $R^2 = 0.530$) and other lemurs ($t_{10} = 3.507$, $p = 0.008$, $R^2 = 0.606$) unlike callitrichids. They have significantly slower prenatal growth rates (strepsirrhines: $t_{16} = 2.257$, $p = 0.040$, $R^2 = 0.267$; other lemurs: $t_{10} = 3.118$, $p = 0.014$, $R^2 = 0.549$) but also have (near) significantly slower postnatal growth rates (strepsirrhines: $t_{16} = 2.328$, $p = 0.035$, $R^2 = 0.279$; other lemurs: $t_{10} = 2.209$, $p = 0.058$, $R^2 = 0.379$).

Table 4.8 Ancestral state reconstructions of body mass and life history traits in cheirogaleids

a) Body mass & growth rate parameters

Node	Log(Adult body mass[g])		Log(Neonatal body mass[g])		Log(Adult body mass[g])		Log(Neonatal body mass[g])		Log(Gestation Length [days])			Log(Age at sexual maturity [days])			Prenatal growth rate	Postnatal growth rate
	Mean	95% CI (±)	Mean	95% CI (±)	Mean	95% CI (±)	Mean	95% CI (±)	Mean	95% CI (±)	relative to body mass	Mean	95% CI (±)	relative to body mass		
Q	2.889	0.002	1.582	0.002	2.951	0.003	1.590	0.002	2.036	0.000	-0.107	2.794	0.001	0.011	0.781	1.049
L	2.846	0.002	1.516	0.002	-	-	-	-	-	-	-	-	-	-	-	-
M	2.571	0.002	1.292	0.002	2.592	0.003	1.297	0.002	1.956	0.001	-0.086	2.693	0.001	-0.290	0.663	0.954
N	2.288	0.002	1.078	0.002	2.377	0.002	1.090	0.002	1.920	0.000	-0.052	2.626	0.001	-0.467	0.568	0.896
O	1.928	0.002	0.850	0.001	-	-	-	-	-	-	-	-	-	-	-	-
P	2.498	0.002	1.233	0.002	-	-	-	-	-	-	-	-	-	-	-	-

b) Reproductive rate parameters

Node	Log(Litter size)		Log(Max. longevity [months])		Log(Inter birth interval [days])		Log(Weaning age [days])			Log(max reproductive output)	Log(max reproductive output) relative to body mass
	Mean	95% CI (±)	Mean	95% CI (±)	Mean	95% CI (±)	Mean	95% CI (±)	relative to body mass		
Q	0.157	0.001	2.413	0.001	2.586	0.001	2.053	0.002	-0.107	1.431	-0.020
L	-	-	-	-	-	-	-	-	-	-	-
M	0.220	0.001	2.366	0.001	2.575	0.001	1.957	0.002	-0.086	1.463	-0.367
N	0.245	0.001	2.327	0.001	2.568	0.001	1.920	0.002	-0.052	1.458	-0.584
O	-	-	-	-	-	-	-	-	-	-	-
P	-	-	-	-	-	-	-	-	-	-	-

Table 4.9 Branch specific changes in adult and neonatal body mass in the cheirogaleids

Branch		Change in Log(adult body mass [g])			Change in Log(neonatal body mass [g])			Rate of change	
	BL (my)	Mean	95% CI (±)	% change	Mean	95% CI (±)	% change	adult	neonate
Q…L	32.519	-0.044	0.003	-9.580	-0.066	0.008	-14.173	-0.001	-0.002
L… *L. mustelinus*	32.519	-0.024	0.003	-4.539	-0.085	0.006	-17.706	-0.001	-0.003
L…M	7.722	-0.274	0.003	-46.811	-0.224	0.008	-40.270	-0.036	-0.029
M….P	13.782	-0.073	0.003	-15.484	-0.059	0.008	-12.692	-0.005	-0.004
P…. *C. major*	11.015	0.148	0.002	41.570	0.024	0.005	5.670	0.013	0.002
P…*C. medius*	11.015	-0.207	0.002	-37.547	-0.067	0.005	-14.377	-0.019	-0.006
M…N	8.623	-0.284	0.003	-47.990	-0.214	0.008	-38.867	-0.033	-0.025
N…*Mirza*	16.175	0.223	0.002	68.404	0.033	0.006	7.844	0.014	0.002
N…O	8.434	-0.360	0.003	-56.326	-0.228	0.007	-40.884	-0.043	-0.027
O…*M. murinus*	7.741	-0.091	0.002	-18.511	-0.171	0.004	-32.508	-0.012	-0.022
O…*M. rufus*	7.741	-0.245	0.002	-42.852	-0.037	0.004	-8.222	-0.032	-0.005

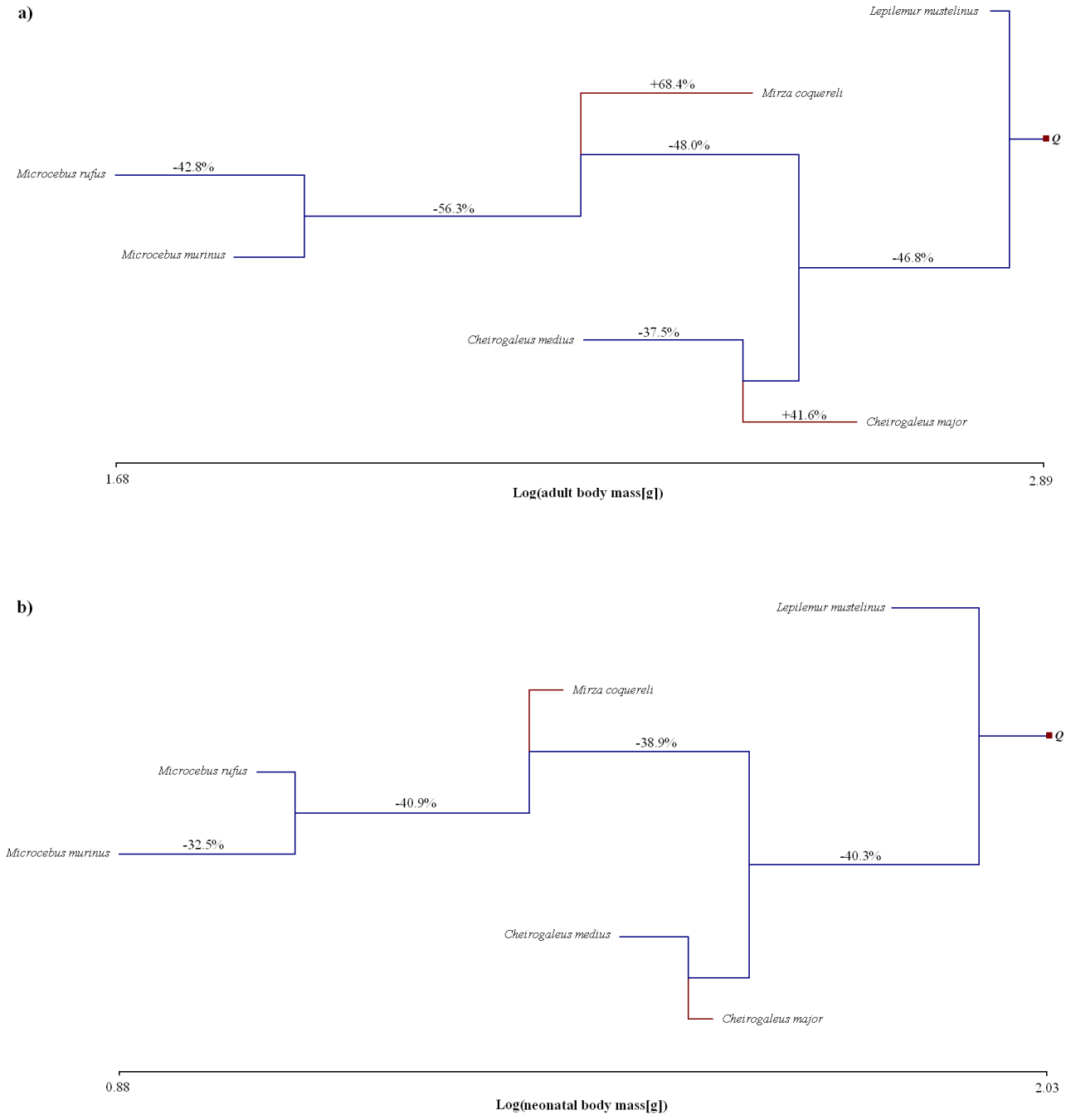

Figure 4.9 Phenograms for changes in a) adult body mass; **b) neonatal body mass in cheirogaleids**
The topology of the tree is as shown in Figure 4.1 Branch lengths are drawn according to the difference in log(mass) between consecutive nodes such that at any point in the phenogram the phenotypic state can be read off the x-axis. Branches in red show increases in size, branches in blue show decreases. The percentage change is shown for branches with a percentage change greater/equal to 20%.

There is insufficient data to test for associations between life history traits and body size using PGLS, but some insights can be gleaned from branch specific changes. Gestation length decreases more in cheirogaleids than callitrichids, with an average change of -14 days (Table 4.10). Age at sexual maturity also decreases across cheirogaleids. Estimated changes in gestation length are marginally non-significantly associated with changes in body mass ($t_3 = 2.580$, $p = 0.082$, $R^2 = 0.586$) and age at sexual maturity is not significantly associated with changes in body mass ($t_3 = 0.350$, $p = 0.747$). Estimated changes in prenatal growth rate are marginally non-significantly associated with changes in body size ($t_3 = 2.380$, $p = 0.098$, $R^2 = 0.538$) whereas changes in postnatal growth rate are significantly associated ($t_3 = 19.650$, $p < 0.001$, $R^2 = 0.990$). Although based on limited data this suggests that, in contrast to callitrichids, dwarfism in cheirogaleids is primarily driven by slowing postnatal growth, but possibly with some contribution by reducing the rate and duration of prenatal growth (Figure 4.10). Hence the convergent evolution of small body size in these two clades has been driven by changes in different ontogenetic stages.

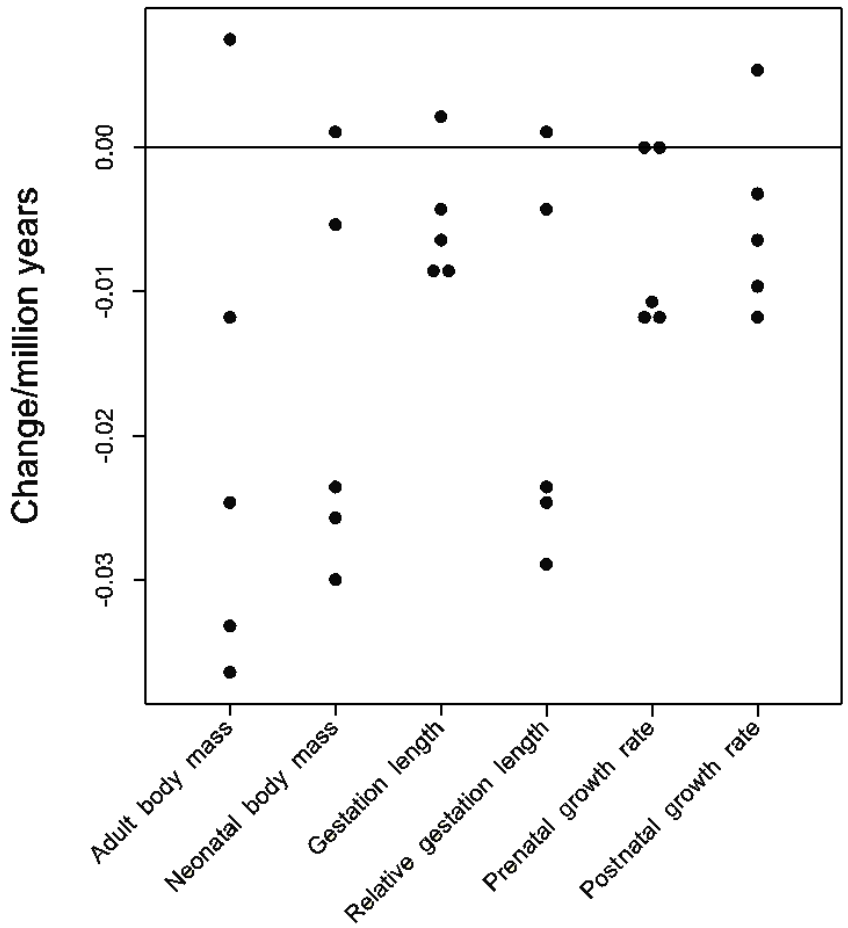

Figure 4.10 Dot-histograms for the rate of change in body mass and growth rate parameters along all branches in the cheirogalid tree. Note the range of each variable is smaller than in callitrichids (Figure 4.6).

The evolutionary history of reproductive traits also differs in cheirogaleids (Tables 4.8, 4.10). Twinning is predicted to have been relatively frequent in the last common ancestor of lemurs (Node Q, litter size = 1.436) but does increase by the origin of cheirogaleids (Node M, litter size = 1.659). However, this is not associated with a particularly large increase in maximum reproductive output (Node Q: 27 offspring/female, Node M: 29 offspring/female) and again there is no clear association between the frequency of twinning and changes in body size. Other reproductive traits show a mosaic pattern of change across cheirogaleids (Figure 4.11).

Table 4.10 Branch specific changes in body mass and life history traits in cheirogaleids

a) Body mass & growth rate parameters

Branch	BL (my)	Log(Adult body mass[g])		Log(Neonatal body mass[g])	
		Mean	95% CI (±)	Mean	95% CI (±)
Q…M	9.835	-0.358	0.004	-0.293	0.003
M…*C. medius*	24.797	-0.298	0.003	-0.131	0.002
M…N	8.623	-0.216	0.003	-0.207	0.003
N…*Microcebus*	16.175	-0.538	0.002	-0.410	0.002
N…*Mirza*	16.175	0.137	0.002	0.021	0.002

Branch	Log(Gestation length [days])			Log(Age at sexual maturity [days])			Prenatal growth rate	Postnatal growth rate
	Mean	95% CI (±)	relative to body mass	Mean	95% CI (±)	relative to body mass		
Q…M	-0.080	0.001	-0.029	-0.101	0.002	-0.300	-0.118	-0.095
M…*C. medius*	-0.165	0.001	-0.004	-0.076	0.001	-0.255	-0.012	-0.091
M…N	-0.037	0.001	-0.024	-0.067	0.002	-0.177	-0.095	-0.058
N…*Microcebus*	-0.139	0.000	-0.024	-0.075	0.001	-0.495	-0.186	-0.188
N…*Mirza*	0.028	0.000	0.001	-0.089	0.001	0.188	0.003	0.088

b) Reproductive rate parameters

Branch	BL (my)	Log(Litter size)		Log(Weaning age [days])			Log(max reproductive output)	Log(max reproductive output) relative to body mass
		Mean	95% CI (±)	Mean	95% CI (±)	relative to body mass		
Q…M	9.835	0.063	0.001	-0.096	0.003	0.021	0.031	-0.347
M…*C. medius*	24.797	0.090	0.001	-0.174	0.002	-0.077	0.107	-0.259
M…N	8.623	0.025	0.001	-0.037	0.003	0.034	-0.004	-0.217
N…*Microcebus*	16.175	0.056	0.001	-0.313	0.002	-0.137	0.005	-0.536
N…*Mirza*	16.175	-0.012	0.001	0.214	0.002	0.169	-0.068	0.112

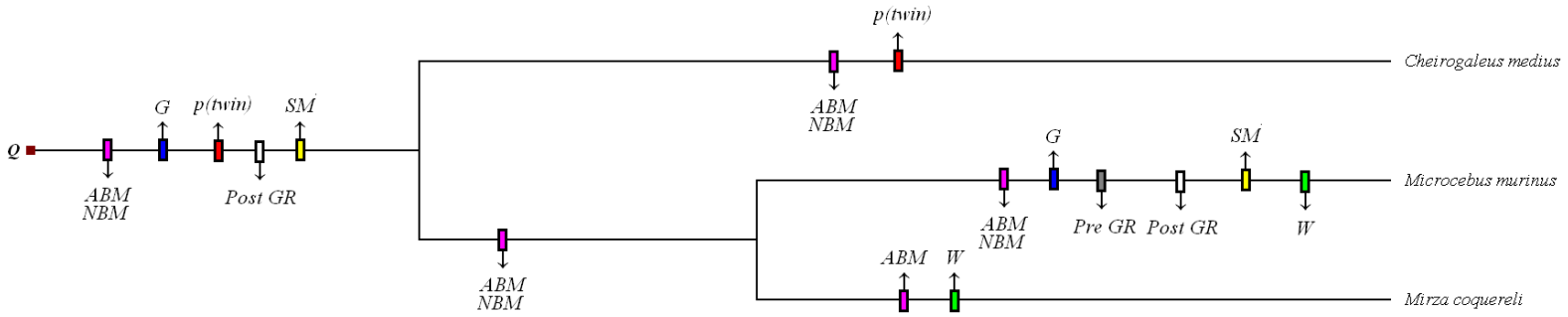

Figure 4.11 Distribution of major episodes of changes in body mass and life history traits in the cheirogaleids
Coloured boxes represent different traits, arrows indicate the direction of change (↑ = increase/shorter, ↓ = decrease/longer). The label at the tip of the arrow head indicates the phenotype: ABM = adult body mass, NBM = neonatal body mass, G = gestation time relative to body mass, SM = age at sexual maturity relative to body mass, p(twin) = probability of twinning, Pre GR = prenatal growth rate, Post GR = postnatal growth rate, W = length of weaning relative to adult body mass. Traits are labelled if they fall in the upper quartile of absolute change, or for body mass if the change is >20%.

4.3.5 Effects of body mass reduction on brain size evolution

I next sought to explore the patterns of brain size evolution during episodes of dwarfism. Brain mass is significantly smaller in both dwarfed clades compared to other members of their respective sub-orders and families (callitrichids vs. anthropoids: $t_{63} = 3.932$, $p < 0.001$, $R^2 = 0.197$; callitrichids vs. New World monkeys: $t_{23} = 3.779$, $p = 0.001$, $R^2 = 0.405$; cheirogaleids vs. strepsirrhines: $t_{26} = 3.277$, $p = 0.003$, $R^2 = 0.300$; cheirogaleids vs. lemurs: $t_{18} = 3.572$, $p = 0.002$, $R^2 = 0.444$). In contrast, there is no difference in relative brain size (callitrichids vs. anthropoids: $t_{63} = 0.692$, $p = 0.492$, $R^2 = 0.007$; callitrichids vs. New World monkeys: $t_{23} = 1.093$, $p = 0.287$, $R^2 = 0.054$; cheirogaleids vs. strepsirrhines: $t_{26} = 0.990$, $p = 0.332$, $R^2 = 0.039$; cheirogaleids vs. lemurs: $t_{18} = 1.054$, $p = 0.308$, $R^2 = 0.065$).

Like neonatal and adult body mass *C. pygmaea* appears to be an outlier for brain mass compared to the general pattern across callitrichids. The analysis which estimates each species tip in turn produces an error of -8.06% for *C. pygmaea* compared to a mean error of 1.96% and median error of 0.86%. *C. argentata* also has a relatively high error (3.66%) but this is due to *C. argentata* being the sister species to *C. pygmaea* in this analysis as no data is available for *C. humeralifera*. When both *C. argentata* and *C. pygmaea* are removed from the tree and each species trait is estimated in the absence of any influence from the other, the error remains high for *C. pygmaea* (-8.67%) but not for *C. argentata* (-0.99%; Figure 4.12). This suggests that, like body mass, the reduction in brain mass along the *C. pygmaea* lineage was unusually fast.

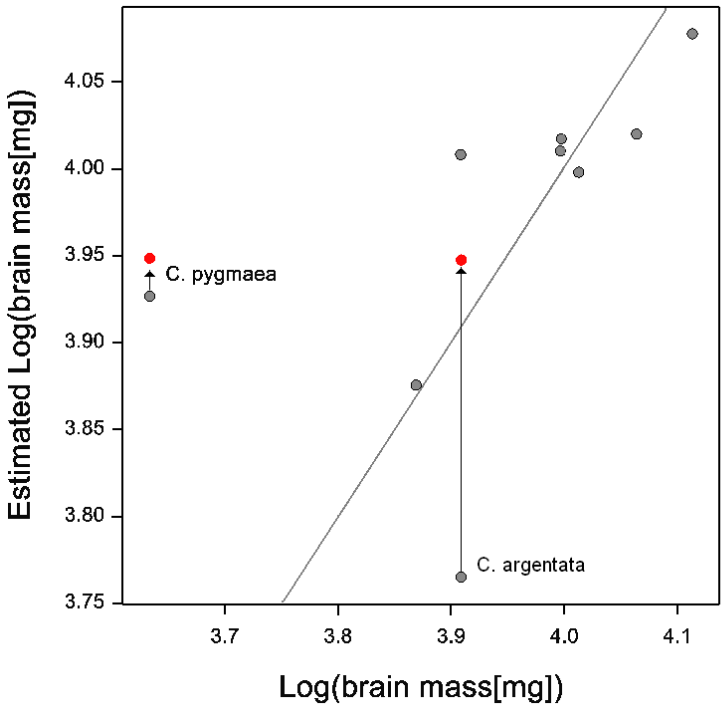

Figure 4.12 Estimated vs. observed values of brain mass mass identify *C. pygmaea* as an outlier. The two data points with arrows are *C. pygmaea* and *C. argentata* and show that the error associated with the latter decreases when the former is removed from the analysis (red dots), but the reverse is not true.

I encountered a methodological problem when trying to reconstruct ancestral brain mass within the callitrichids. Brain mass shows a directional trend to increase through time across primates, and if this trend is not accounted for ancestral states of brain mass are over estimated (chapter 3). However, applying this primate wide trend to clades where brain mass decreases may not be appropriate. Currently it is not possible to test for and implement different trends in different parts of the phylogeny. When the primate wide model of brain evolution, which includes a strong directional component, is used to reconstruct brain mass within the callitrichids I obtain estimates for the ancestral Cebidae (Node A) of 11.110g (95% CI: 11.076g – 11.144g) similar to that obtained previously (chapter 3). The estimate for the ancestral callitrichid is 8.040g (95% CI: 8.016-8.644g) which is lower than all extant callitrichids with the exception of *C. pygmaea*. Hence the model predicts a large decrease in brain mass at the origin of callitrichids followed by a "rebound" in all lineages except one (the *C. pygmaea* terminal branch). The same result is found if *C. pygmaea* is excluded. In a clade where body mass is decreasing in almost all lineages, this result seems biologically questionable and may be an artefact of applying a directional model of evolution to a clade where the trait has decreased.

I therefore sought an alternative method of analysing brain mass. Unfortunately the lack of fossil data for endocranial volumes for callitrichids means it is not possible to explicitly test for trends within the clade. I also found that the small size of the callitrichid phylogeny meant that it was not possible to get the MCMC chain in BayesTraits to converge analysing the callitrichids in isolation from the rest of the primates. I therefore turned to ANCML (Schluter *et al.*, 1997). I have previously showed that ANCML overestimated ancestral states of brain mass as it does not test for or implement directional models of evolution (chapter 3), but this may not be such a significant issue within the callitrichids. Furthermore it has been suggested that constraining the root of a tree may improve ancestral state reconstructions even when directional trends persist (Oakley & Cunningham, 2000; Webster & Purvis, 2002). To test if this is the case I first analysed adult body mass using ANCML using just the callitrichid clade and stem lineage, constraining the root or the stem lineage (Node A) to take the value estimated for this node using BayesTraits (see above); although this is not the "known" ancestral state it is the best estimate available. When this is done the ancestral state reconstructions in ANCML closely match those from BayesTraits such that the branch specific changes in adult body mass predicted by the two

methods are strongly correlated (Spearman's correlation; $t_{14} = 4.400$, $p < 0.001$, $r_s = 0.762$). The correlation is further improved by the removal of *C. pygmaea* from the ANCML analysis such that the estimated changes are almost identical (Spearman's correlation; $t_{14} = 15.94$, $p < 0.001$, $r_s = 0.974$; Figure 4.13).

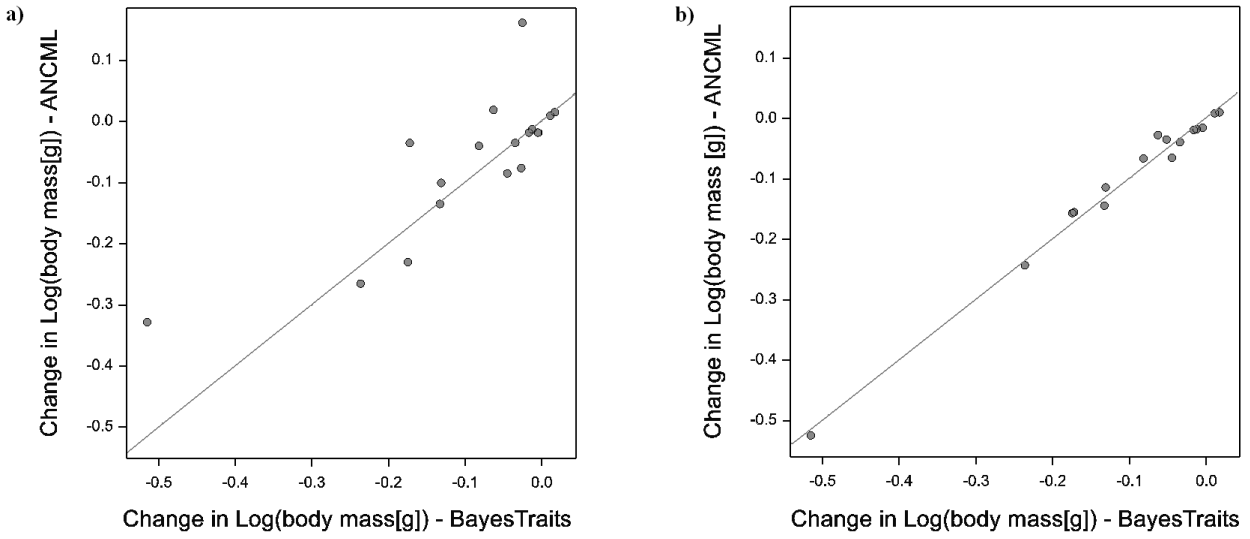

Figure 4.13 Correlations between estimated branch-specific changes in adult body mass using the constrained ANCML analysis and BayesTraits: a) including *C. pygmaea* in the ANCML analysis and b) excluding *C. pygmaea* in the ANCML analysis. The grey line shows the 1:1 expectation.

Hence by constraining the root of the stem lineage ANCML produces similar results to BayesTraits. I therefore applied this method to the analysis of brain mass constraining the root to take the trait estimate for Node A estimated by BayesTraits and excluding *C. pygmaea*. Unfortunately it is not possible to estimate a trait at a time point between nodes/species tips in the same way as can be done for BayesTraits, so the change in brain mass along the *C. pygmaea* lineage is incorporated by taking the change in mass from the nearest node (Node E) which creates a 3-way polytomy at the origin of *Callithrix*. All subsequent brain/body comparisons were performed using the ANCML results.

The ancestral state reconstruction for the last common ancestor of extant callitrichids is 10.41g (Table 4.11), suggesting a modest decrease (6.32%; Table 4.12) in brain mass at the origin of callitrichids followed by further parallel decreases in brain mass in *Callithrix* and *Saguinus* (Figure 4.14). A regression analysis between change in brain mass and change in body

mass shows the two are significantly correlated with (t_{14} = 6.780, $p < 0.001$, R^2 = 0.750) and without the inclusion of the *C. pygmaea* branch, although the amount of variance explained decreases markedly (t_{13} = 2.42, p = 0.031, R^2 = 0.258). The largest estimated decreases in brain mass occur along the *C. pygmaea* terminal branch (-49.57%), the terminal *S. fusicollis* branch (-19.64%), the *Callithrix* stem branch (-14.85%) and the terminal *C. jacchus* branch (-13.34%). Large increases are predicted to have occurred on the *Leontopithecus* (+24.79%) and *Callimico* (+15.56%) terminal branches. In terms of rate of absolute change the mean rate is 0.0073 and the branches falling in the upper quartile (>0.007) are both decreases; the stem *Callithrix* (0.011) branch and the terminal *C. pygmaea* branch (0.040). The rate of change in brain mass along the *C. pygmaea* branch is 5.54 times the mean for callitrichids. Brain mass decreased over 53.35% of the evolutionary time considered compared to 91.51% for body mass.

I next analysed relative brain size using the ANCML estimates for both brain and body mass and the allometric relationship described in chapter 3. Relative brain size is estimated to have increased on all branches except the terminal *S. midas* branch where a modest decrease occurs (Table 4.12). Hence relative brain mass only decreases over 7.10% of evolutionary time. Increases in relative brain size are associated with branches which show both decreases in brain mass (*C. pygmaea* terminal branch: +0.061, 4th highest increase; stem callitrichid branch: +0.138, 2nd highest increase) and increases in brain mass (*Callimico* terminal branch: +0.081, 2nd highest increase; *Leontopithecus* terminal branch: +0.141, highest increase). In the case of the latter the large increases are due to the combination of increasing brain mass, but decreasing body mass suggesting selection has acted to increase brain size, whereas the former show increasing relative brain size in association with decreases in both brain and body mass. Whether the increase in relative brain size in these cases is due to selection on increased encephalization (Jerison, 1973) or is an allometric effect (Shea, 1983) is therefore difficult to disentangle.

I performed the same analysis on brain and body mass in the cheirogaleids. As in callitrichids the ancestral cheirogaleid is estimated to have a smaller brain mass than extant species (Table 4.11) and decreases in brain mass occur in parallel along several lineages (Table 4.12; Figure 4.15). The largest estimated percentage decreases in mass occur along the terminal *C. medius* branch (-31.03%), the lineage leading to *Microcebus* (-34.84%) and the two terminal *Microcebus* branches (*M. murinus*: -19.88%; *M. rufus*: -15.65%). Large increases occurred along

the terminal *C. major* (+52.04%), *Mirza* (+81.44%) and *Lepilemur* (+144.15%) terminal branches. In terms of rate of absolute change the mean rate is 0.011 and the branches falling in the upper quartile (>0.015) include two increases; the terminal *C. major* (0.017) and *Mirza* (0.016) branches, and one decrease, the stem *Microcebus* branch (0.022). As in callitrichids, relative brain size tends to increase in cheirogaleids through time with decreases in relative brain size being observed on only the *M. murinus* and *C. medius* terminal branches both of which show decreases in brain mass. Brain mass decreases over 32.60% of evolutionary time considered, body mass over 62.04% and relative brain size over 11.93%.

If the ANCML results are viewed as representative of brain evolution in callitrichids and cheirogaleids it is apparent that although dwarfism in body mass is accompanied by a reduction in brain mass in some cases, this is not always the case with several lineages showing increases in brain mass in spite of a decrease in body mass. In other lineages both brain and body mass decrease, but brain mass tends to decrease less than body mass leading to an increase in relative brain size.

Table 4.12 Ancestral state reconstructions for brain and body mass in ANCML

a) Callitrichids

Node	Log(brain mass [mg])	Log(body mass [g])
A	4.046	3.096
B	4.017	2.853
C	4.017	2.838
D	4.001	2.774
E	3.931	2.617
H	3.986	2.739
J	3.994	2.722
K	4.003	2.683

b) Cheirogaleids

Node	Log(brain mass [mg])	Log(body mass [g])
Q	3.584	2.889
L	3.600	2.818
M	3.568	2.554
N	3.515	2.296
O	3.329	1.930
P	3.594	2.495

Table 4.13 Branch specific changes in body mass, brain mass and relative brain size using ANCML

a) Body mass

Branch	BL(my)	Change in log(mass [g])	Rate of change	% change	Branch	BL(my)	Change in log(mass [g])	Rate of change	% change
A…B	4.765	-0.243	-0.051	-42.794	Q…L	32.519	-0.072	-0.002	-15.221
B…C	0.469	-0.015	-0.032	-3.369	L… *L. mustelinus*	32.519	0.008	0.000	1.812
C… *L. rosalia*	15.845	-0.066	-0.004	-14.036	L…M	7.722	-0.264	-0.034	-45.534
C…D	2.344	-0.065	-0.028	-16.055	M….P	13.782	-0.059	-0.004	-12.638
D…*C. goeldii*	13.501	-0.027	-0.002	-6.046	P…. *C. major*	11.015	0.154	0.014	42.646
D…E	6.109	-0.156	-0.026	-30.220	P…*C. medius*	11.015	-0.201	-0.018	-37.072
E… *C. jacchus*	7.392	-0.155	-0.021	-29.974	M…N	8.623	-0.258	-0.030	-44.787
E…*C. argentata*	7.392	-0.034	-0.005	-7.604	N…*Mirza*	16.175	0.218	0.013	65.225
E… *C .pygmea*	7.392	-0.524	-0.071	-70.094	N…O	8.434	-0.366	-0.043	-56.950
B…H	5.937	-0.114	-0.019	-23.056	O…*M. murinus*	7.741	-0.091	-0.012	-18.890
H…*S. fusicollis*	10.378	-0.144	-0.014	-28.213	O…*M. rufus*	7.741	-0.245	-0.032	-43.117
H…J	3.247	-0.017	-0.005	-3.887					
J…*S. midas*	7.131	0.011	0.001	2.475					
J…K	5.734	-0.039	-0.007	-8.576					
K…*S. geoffroyi*	1.397	0.009	0.007	2.122					
K… *S. oedipus*	1.397	-0.019	-0.013	-4.193					

a) Brain mass

Branch	BL(my)	Change in log(mass [g])	Rate of change	% change	Branch	BL(my)	Change in log(mass [g])	Rate of change	% change
A…B	4.765	-0.028	-0.006	-6.320	Q…L	32.519	0.016	0.001	3.836
B…C	0.469	-0.000	-0.001	-0.076	L… *L. mustelinus*	32.519	0.388	0.012	144.154
C… *L. rosalia*	15.845	0.096	0.006	24.787	L…M	7.722	-0.032	-0.004	-7.171
C…D	2.344	-0.016	-0.007	-3.725	M….P	13.782	0.026	0.002	6.125
D…*C. goeldii*	13.501	0.063	0.005	15.558	P…. *C .major*	11.015	0.182	0.017	52.039
D…E	6.109	-0.070	-0.011	-14.849	P…*C. medius*	11.015	-0.161	-0.015	-31.027
E… *C. jacchus*	7.392	-0.062	-0.008	-13.341	M…N	8.623	-0.052	-0.006	-11.333
E…*C. argentata*	7.392	-0.022	-0.003	-5.003	N…*Mirza*	16.175	0.259	0.016	81.436
E… *C. pygmea*	7.392	-0.297	-0.040	-49.566	N…O	8.434	-0.186	-0.022	-34.837
B…H	5.937	-0.031	-0.005	-6.917	O…*M. murinus*	7.741	-0.096	-0.012	-19.883
H…*S. fusicollis*	10.378	-0.078	-0.008	-19.635	O…*M. rufus*	7.741	-0.074	-0.010	-15.751
H…J	3.247	0.007	0.002	1.704					
J…*S. midas*	7.131	0.004	0.001	0.919					
J…K	5.734	0.010	0.002	2.273					
K…*S. geoffroyi*	1.397	0.009	0.007	2.165					
K… *S. oedipus*	1.397	-0.007	-0.005	-1.582					

Table 4.13 cont'd Branch specific changes in body mass, brain mass and relative brain size using ANCML

c) Relative brain size

Branch	BL(my)	Change in log(mass [g])	Rate of change	Branch	BL(my)	Change in log(mass [g])	Rate of change
A…B	4.765	0.138	0.029	Q…L	32.519	0.065	0.002
B…C	0.469	0.010	0.021	L… *L. mustelinus*	32.519	0.382	0.012
C… *L. rosalia*	15.845	0.141	0.009	L…M	7.722	0.148	0.019
C..D	2.344	0.028	0.012	M….P	13.782	0.066	0.005
D…*C. goeldii*	13.501	0.081	0.006	P…. *C. major*	11.015	0.077	0.007
D…E	6.109	0.037	0.006	P…*C. medius*	11.015	-0.024	-0.002
E… *C. jacchus*	7.392	0.044	0.006	M…N	8.623	0.124	0.014
E…*C.argentata*	7.392	0.001	0.000	N…*Mirza*	16.175	0.110	0.007
E… *C. pygmea*	7.392	0.061	0.008	N…O	8.434	0.064	0.008
B…H	5.937	0.047	0.008	O…*M. murinus*	7.741	-0.034	-0.004
H…*S. fusicollis*	10.378	0.021	0.002	O…*M. rufus*	7.741	0.093	0.012
H…J	3.247	0.019	0.006				
J…*S. midas*	7.131	-0.003	0.000				
J…K	5.734	0.036	0.006				
K…*S. geoffroyi*	1.397	0.003	0.002				
K… *S. oedipus*	1.397	0.006	0.004				

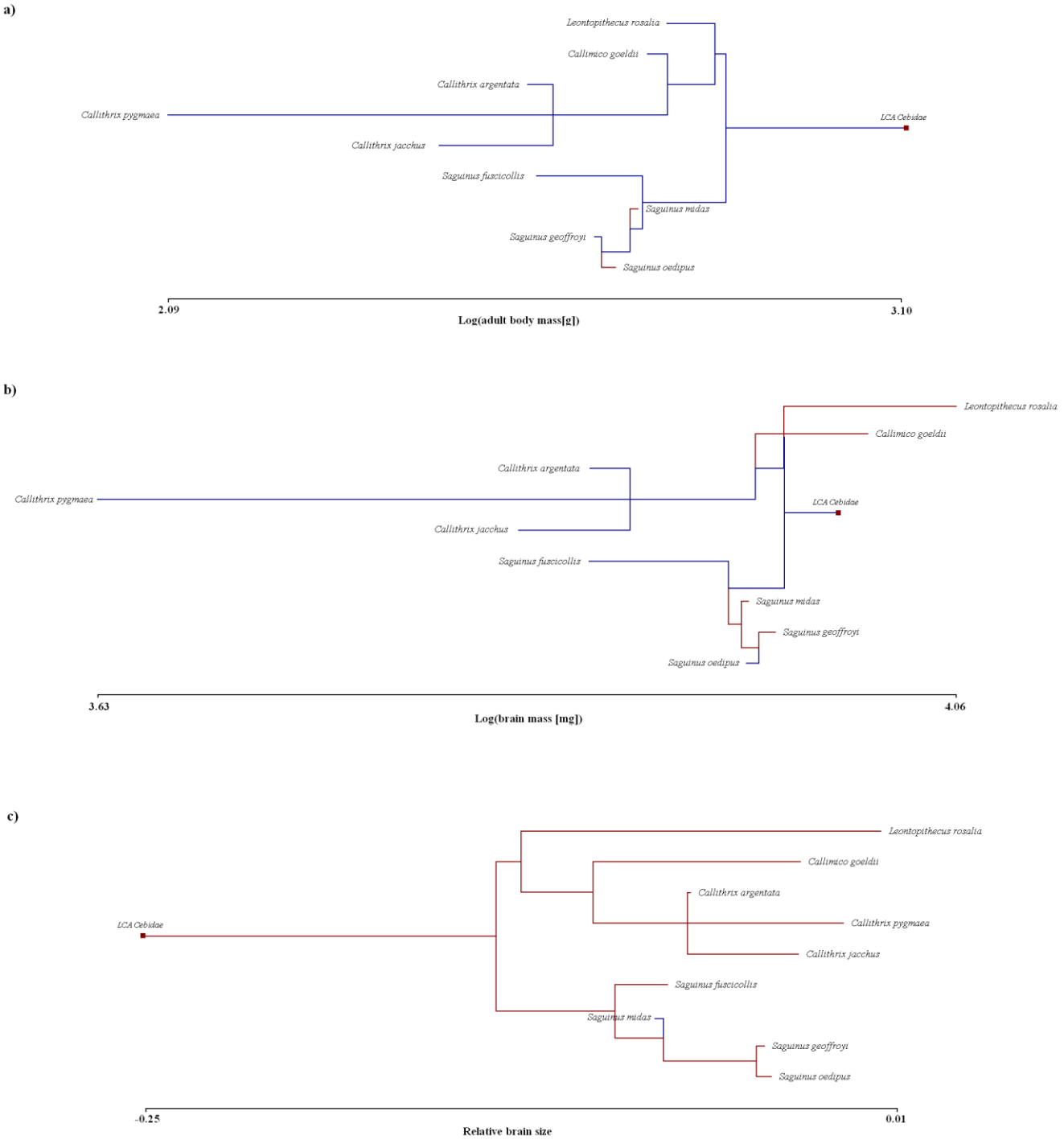

Figure 4.14 Phenograms for changes in a) body mass; **b) brain mass; c) relative brain size in callitrichids**

The topology of the tree is as shown in Figure 4.1 Branch lengths are drawn according to the difference between consecutive nodes such that at any point in the phenogram the phenotypic state can be read off the x-axis. Branches in red show increases in size, branches in blue show decreases.

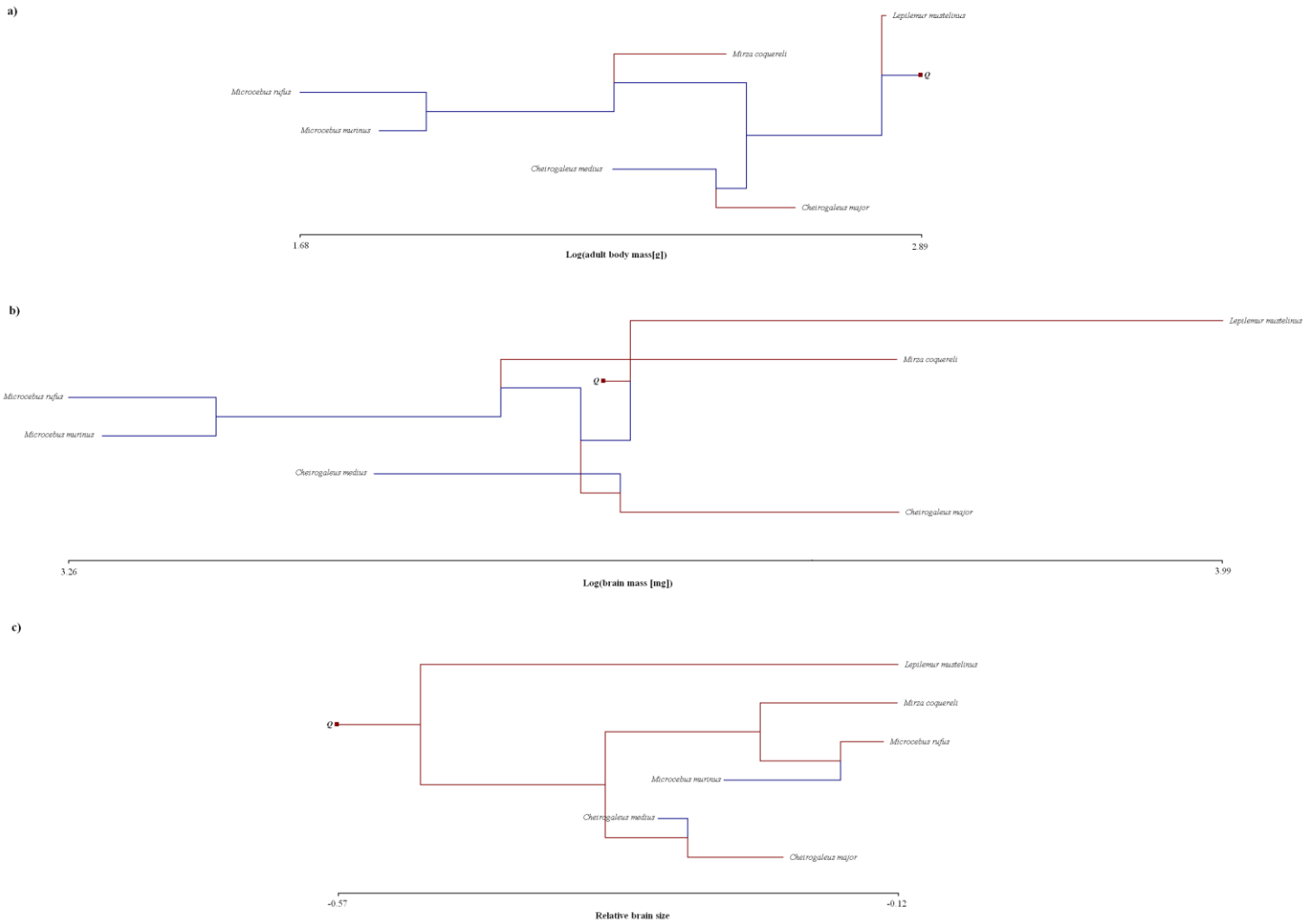

Figure 4.15 Phenograms for changes in a) body mass; **b) brain mass; c) relative brain size in cheirogaleids**

The topology of the tree is as shown in Figure 4.1 Branch lengths are drawn according to the difference between consecutive nodes such that at any point in the phenogram the phenotypic state can be read off the x-axis. Branches in red show increases in size, branches in blue show decreases.

4.3.6 *Homo floresiensis* revisited & the impossibility of the pygmy marmoset

Much of the debate surrounding the hominin remains found on the Island of Flores (Brown *et al.*, 2004) surround the small size of the brain of LB1 (Falk *et al*., 2005) which, it has been argued, is too small to be explained by insular dwarfism (Martin *et al*., 2006; see chapter 3). Martin *et al*. (2006) used a series of scaling models to show that for the degree of brain volume decrease predicted if *H. floresiensis* descended from *Homo erectus*, Ngandong *H. erectus* or the Dmanisi hominids the body mass estimated for *H. floresiensis* would range from <1g to 11.8kg, which is below the range of body size estimates for LB1. I applied the same scaling models to *C. pygmaea* to predict the expected body mass of this species given the decrease observed in brain mass from Node E. The estimates range from <1g to 58.626g (Model A, *Elephas* dwarfing: 48.805-58.626g; Model B, mammalian intraspecific scaling: 26.813g; Model C intraspecific scaling for *H. sapiens*: <1g-7.392g) which are all substantially lower than the real body mass of 124g. Using Martin *et al*.'s arguments against the possibility of *H. floresiensis* being a genuine species would therefore suggest that *C. pygmaea* is an impossible species. Of course, few would argue against *C. pygmaea* being a genuine species, as opposed to a microcephalic *C. argentata* for example. This result demonstrates the evolutionary malleability of brain:body allometry (Lande, 1979; Niven, 2006). It is also notable that the proportional change in both brain and body mass is greater than the predicted change in brain mass for *H. floresiensis* under a number of evolutionary scenarios (see chapter 3).

If the scaling relationship of brain and body mass along the *C. pygmaea* lineage is used to estimate body mass for *H. floresiensis* for the same three ancestors Martin *et al*. considered I obtain substantially larger estimates (*H. erectus*: 11.205kg; Ngandong: 8.523kg; Dmanisi: 19.583kg) which overlap with the range of body mass estimates for *H. floresiensis* (see chapter 3). Using the 16 callitrichid branches to estimate whether or not the pattern of allometry during the evolution of *H. floresiensis* is within the range of other episodes of primate dwarfism (see chapter 3) yields larger numbers of plausible scenarios (Table 4.14). The cheirogaleid lineages provide much higher support, but given that these changes occur over a much greater time period they are perhaps less relevant.

Table 4.14 Using callitrichid branches to model brain:body allometry in *H. floresiensis*

Scenario	*H. floresiensis* body mass	% of branches which support *H. floresiensis*
a) Phyletic change from:		
Argue *et al.* Tree 1	16	18.75
	24	12.5
	31	0
Argue *et al.* Tree 2	16	18.75
	24	12.5
	31	0
b) Insular dwarfism of		
H. erectus	16	6.25
	24	0
	31	0
Ngandong hominin	16	6.25
	24	0
	31	0
Dmanisi hominin	16	31.25
	24	6.25
	31	0
H. habilis	16	31.25
	24	6.25
	31	0

4.4 Conclusions

The results support the proposal that callitrichids are phyletic dwarfs, quantify the degree and pace of change, and suggest dwarfism occurred in parallel across callitrichids. The evolutionary reduction of body size in callitrichids is due to changes in prenatal growth rate rather than changes in the duration of prenatal growth or postnatal growth, with the exception of *C. pygmaea* which appears to have evolved its extremely small size by reducing both pre and postnatal growth. These results are therefore consistent with the suggestions of Marroig & Cheverud (2009). Martin (1992) discussed evidence that in *C. jacchus* the lag phase of slow growth at the beginning of *in utero* development is extended in order to delay the costs of pregnancy until weaning of the previous litter is completed. There is no comparative data for this observation, but if it is a general characteristic of callitrichids it may have relevance for the evolution of dwarfism and provide a link between life history strategy and the evolution of small body size. The analysis presented here does not include the recently described species assigned by taxonomic splitters to its own genus; *Callibella humilis* (van Roosmalen & van Roosmalen, 2003). *C. humilis* is of particular interest as it is intermediate in weight (c. 120-180g) between *C. pygmaea* and other members of the Argentata/Mico clade. Unfortunately little is known about the phylogenetic position of *C. humilis*. It appears to be closely related to *C. pygmaea* and the Argentata/Mico clade but the precise relationships between these three lineages are unresolved (van Roosmalen & van Roosmalen, 2003; Cortés-Ortiz, 2009). If *C. humilis* is not the sister species to *C. pygmaea* one must assume there was an additional episode of dwarfism. If *C. humilis* and *C. pygmaea* are sister taxa this additional data could help resolve how rapid the rate of body size reduction in *C. pygmaea* really was.

Dwarfism does not seem to be directly related to the evolution of twinning (Ah-King & Tullberg, 2000) with *Callimico* continuing to reduce in size despite the loss of twinning. I have explored whether alternative reproductive strategies compensate for the lack of twinning in *Callimico* (Martin, 1992) and found no theoretical evidence to suggest it does. I also find evidence for dwarfism in cheirogaleids suggesting their small body size is a derived trait rather than an ancestral retention. Dwarfism in cheirogaleids appears to be mainly driven by changes in postnatal growth rate with some contribution from prenatal growth duration and rate.

In both clades a reduction in body size is associated with a complex pattern of brain evolution. Brain mass is estimated to have decreased in parallel across both clades, although the amount of change in brain mass is less than the change in body mass. I suggest the fact that both clades, in particular callitrichids, have changes in their prenatal ontogeny means that brain development, which is predominantly a prenatal and early postnatal affair, is also either directly affected or targeted by selection to reduce brain mass. Despite this the amount of variance in changes in brain mass explained by changes in body mass is relatively low, indeed some lineages also show increases in brain mass despite having decreased body masses. This further suggests brain and body evolution are under and able to respond to contrasting selection pressures. The evolutionary history of relative brain size in both clades is complex; increases dominate but these are produced both by smaller decreases in brain mass than body mass and increases in brain mass whilst body mass decreases. These different routes to increased relative brain size must have a different developmental basis, raising further doubts over the meaning of relative brain size (Shea, 1983). It would be interesting to know if dwarfed lineages have structural changes in the brain which offset their reduction in size. Based on available data ventricular volume does not appear to be particularly small in callitrichids (Stephan *et al*., 1981) and although callitrichids do appear to have high neuron density in grey matter this trait is shared with other Cebidae (Herculano-Houzel *et al.*, 2008). Finally dwarfism and brain mass reduction in callitrichids and cheirogaleids further support the conclusion that there is nothing unsurprising about the brain of *H. floresiensis.*

Chapter 5

Evolutionary genetics of neural progenitor proliferation

& the expansion of radial units: Microcephaly genes as candidates

"The simple brain of a microcephalous idiot,
in as far as it resembles that of an ape, may in
this sense be said to offer a case of reversion."

Charles Darwin, *The Descent of Man*, 1873

5. Evolutionary genetics of neural progenitor proliferation & the expansion of radial units: Microcephaly genes as candidates

5.0 Summary

The anatomical basis and adaptive function of the expansion in primate brain size have long been studied; however, we are only beginning to understand the genetic basis of these evolutionary changes. Genes linked to human primary microcephaly have received much attention as they have accelerated evolutionary rates along lineages leading to humans. However these studies focus narrowly on apes and the link between microcephaly gene evolution and brain evolution is disputed. I analyzed the molecular evolution of five genes associated with microcephaly (*ASPM*, *CDK5RAP2*, *CENPJ*, *MCPH1*, *STIL*) across 21 species representing all major clades of anthropoid primates. Contrary to prevailing assumptions positive selection was not limited to or intensified along the lineage leading to humans. In fact all five loci were subject to positive selection across the anthropoid primate phylogeny. I develop clearly defined hypotheses to explicitly test if selection on these loci was associated with the evolution of brain size. Positive relationships were found between both *CDK5RAP2* and *ASPM* and neonatal brain mass and somewhat weaker relationships between these genes and adult brain size. In contrast, there is no evidence linking *CENPJ*, *MCPH1*or *STIL* to gross brain size evolution. The stronger association of *ASPM* and *CDK5RAP2* evolution with neonatal brain size than with adult brain size is consistent with these loci having a direct effect on prenatal neuronal proliferation. I next use data from twelve species of callitrichids to show that positive selection has acted on *ASPM* within this clade and the rate of *ASPM* evolution is significantly negatively correlated with callitrichid brain size, whereas the evolution of *CDK5RAP2* is not. Finally I provide evidence which suggests *CENPJ* and *MCPH1* may have roles in the evolution of sexual dimorphism in brain mass. Combined, these results suggest that primate brain size may have at least a partially conserved genetic basis and strongly suggest that *ASPM* in particular is intimately linked to both evolutionary increases and decreases in brain size in anthropoids.

5.1 Introduction

The expansion of the brain, and in particular the neocortex, is a major hallmark of primate evolution (Jerison, 1973; Martin, 1990). After correcting for allometric scaling with body mass, primates have larger brains than most other mammals (Martin, 1990; Barton, 2006a) and both absolute and relative brain size have increased along multiple, independent primate lineages (chapter 3). The adaptive significance and anatomical basis of the diversity of primate brains has long been studied using comparative methods (for review see Falk & Gibson, 2001; Finlay *et al.*, 2001; Barton, 2006a) but investigations into the genetic basis of primate brain expansion has only begun relatively recently and is currently a topic of intense interest.

The convergent evolution of increased brain size in different lineages (chapter 3) provides an opportunity to study whether the independent evolution of complex traits involves convergence at the molecular level (Arendt & Reznick, 2007) and may provide insights into lineage specific evolution, for example on the human lineage. Both scans of brain-expressed genes in published primate genomes (Dorus *et al.*, 2004a; Shi *et al.*, 2006; Yu *et al.*, 2006; Wang *et al.*, 2007) and studies of candidate genes (e.g. Enard *et al.*, 2002; Burki & Kaessmann, 2004; Wang *et al.*, 2005) have mostly focused on identifying changes along the lineage leading to humans and have largely ignored convergent or parallel increases in brain size in multiple primate lineages.

One group of genes of particular interest in relation to the evolution of gross brain size is the microcephaly genes. Autosomal recessive primary microcephaly is a congenital disorder characterised by reduced growth of the cerebral cortex in the absence of environmental, metabolic or cytogenetic aetiologies (Bond & Woods, 2006; Cox *et al*., 2006). In humans it is inherited as a recessive Mendelian trait involving at least eight loci, of which six have now been identified at the molecular level: *ASPM*, *MCPH1*, *CDK5RAP2*, *CENPJ* (Jackson *et al.*, 1998; Bond *et al.*, 2002; Bond *et al.*, 2005; Thornton & Woods, 2009) and the more recently identified *STIL* (Kumar *et al.*, 2009) and *WDR62* (Nicholas *et al*., 2010).

The six genes are expressed in the foetal brain during neurogenesis (Bond *et al*., 2002, 2005; Jackson *et al*., 2002; Kouprina *et al.*, 2005; Kumar *et al*., 2009). *ASPM, CDK5RAP2* and *CENPJ* all have roles in centrosome or microtubule formation (Bond *et al*., 2006; Cox *et al*., 2006; Fish *et al.*, 2006; Buchman *et al*., 2010) and can affect neurogenic mitosis by influencing

the spindle pole and astral microtubule network (Fish *et al*., 2006; Fong *et al.*, 2008; Cormier *et al*., 2009; Buchman *et al*., 2010). *MCPH1* functions in the DNA damage response pathway and apoptosis (Wood *et al*., 2007; Rickmyre *et al*., 2007; Wood *et al*. 2008) and may also affect the timing of cell cycle progression (Brunk *et al.*, 2007). Both apoptosis and cell cycle length are known to have significant roles in brain development (Roth & D'sa, 2001; Calegari & Huttner, 2003). The function of *STIL* and *WDR62* are less well studied, but *STIL* localises to the centrosome and has some functional similarities to *ASPM* (Kumar *et al*., 2009; Thornton & Woods, 2009) whilst *WDR62* also localises at the spindle poles of neural precursor cells (Nicholas *et al*., 2010).

The main hypotheses for how the number of neurons could increase during brain expansion (Rakic, 1988; Caviness *et al*., 1995; Rakic, 1995; Kriegstein *et al*., 2006) rely on switches between symmetric and asymmetric cell divisions, via changes in spindle pole orientation, at a particular stage of neurogenesis. The Radial Unit Hypothesis (Rakic, 1988) places particular emphasis on the proliferative division of progenitor cells which each go on to produce a column of neurons (or radial unit) during neurogenesis.The functions of microcephaly genes are therefore consistent with the developmental mechanisms proposed to have facilitated brain expansion (Cox *et al*., 2006; Kriegstein *et al*., 2006; Götz & Huttner, 2005). Notably, the phenotypes exhibited by individuals with microcephaly show that these loci affect cortical surface area, not thickness, consistent with a role in regulating the size of the neural progenitor pool (Desir *et al*., 2008). Recent studies in humans identified single nucleotide polymorphisms (SNPs) in *ASPM*, *CDK5RAP2* and *MCPH1* associated with total brain size or cortical surface area (Wang *et al*., 2008; Rimol *et al.*, 2010) but not cortical thickness, an observation that again is consistent with a role in controlling the size of the neural progenitor pool (Rimol *et al*., 2010; Montgomery & Mundy, 2010) and therefore the number of radial units produced (Rakic, 1988). Interestingly however these associations are sex-dependent (Wang *et al*., 2008; Rimol *et al.*, 2010).

Previous studies of the molecular evolution of the first four microcephaly loci to be identified supported the hypothesis that they have been subject to positive selection in primates (Zhang, 2003; Evans *et al.*, 2004a; Evans *et al.*, 2004b; Wang & Su, 2004; Kouprina *et al*., 2004; Evans *et al.*, 2006) but provided no direct evidence that the loci were involved in brain evolution

as brain size was not incorporated into the analyses and they did not include a diverse phylogenetic sample of species. However one recent study analyzed *ASPM* evolution in relation to brain size in primates and concluded that branches along which relative telencephalon volume (reported as cerebral cortex) increased greatly were associated with positive selection on *ASPM* (Ali & Meier, 2008) invoking an episodic view of brain evolution.

For a comprehensive understanding of the role of genes in primate brain evolution, broad comparisons across the primate phylogeny incorporating relevant phenotypes are needed (Carroll, 2003; Goodman *et al.*, 2005; Barton, 2006c; Pollen & Hoffman, 2008; Vallender, 2008). An important issue is which aspects of brain phenotype are most salient. Measures of brain size corrected for body size (i.e. relative brain size) are frequently used in studies investigating brain evolution as these take into account the strong correlation between brain and body mass (Barton, 2006a). However, given the implied functions of the four microcephaly genes in regulating the proliferation and survival of neurons, absolute brain mass may be a more relevant phenotypic measure as in primates it increases linearly with the total number of neurons (Herculano-Houzel *et al.*, 2007). In agreement with quantitative genetic analysis of brain and body size allometry (Lande, 1979), I have shown that primate brain and body size differ in their evolutionary trajectories (see chapter 3) suggesting that these two traits must be developmentally and genetically decoupled to some extent despite their closely correlated evolution (Lande, 1979; Shea, 1983). Crucially, because primate neocortical neurogenesis is largely restricted to prenatal development (Rakic, 1988; Rakic, 2002; Bhardwaj *et al.*, 2006) and microcephaly is primarily a disorder of foetal brain growth (Cox *et al*., 2006), microcephaly gene evolution should also be more closely related to neonatal brain size than to adult brain size. Postnatal brain growth is largely driven by gliagenesis (Low & Cheng, 2006), axon growth (Sauvageot & Stiles, 2002) and myelination (Sowell *et al.*, 2001), rather than by production of new neurons. There are only two known sites in the primate brain, which are small and non-cortical, in which substantial postnatal neurogenesis occurs (Jabes *et al.*, 2010). Apoptosis also eliminates large numbers of neurons pre and postnatally (Buss *et al*., 2006). Variation in these and other non-neurogenic processes will reduce the relationship between brain size and neuron number as development progresses, weakening any association with the molecular evolution of genes under selection in relation to pre-natal neurogenesis. Indeed patterns of postnatal brain growth vary considerably across

primates (Leigh, 2004). Finally, if there is an association with adult brain size, given the specific effect of microcephaly on the development of the cerebral cortex and their functions in cortical neurogenesis (Cox *et al.*, 2006; Thornton & Woods, 2009) we might expect to see a stronger association with neocortex volume than other regions of the brain.

Alternative hypotheses to explain the high evolutionary rates of microcephaly genes also exist. Four of the loci are known to widely expressed throughout the body and *ASPM*, *CDK5RAP2* and *CENPJ* are particularly highly expressed in the testes (Bond *et al.*, 2005; Kouprina *et al.*, 2005), where many genes have been shown to be under sexual selection in primates (Dorus *et al.*, 2004b; Clark & Swanson, 2005; Ramm *et al.*, 2008). However, the precise function of these genes in testes development and function is still unknown. For *ASPM*, a possible ciliary function led to the suggestion of a role in sperm flagellar movement which may affect sperm locomotion and hence be targeted by sexual selection (Ponting, 2006). If the microcephaly genes do have important roles in the testes or sperm their high rates of evolution may be associated with levels of sexual selection and be unrelated to changes in brain size. Hence explicit tests are required before the molecular evolution of microcephaly loci can be linked to brain evolution.

Here I investigate the molecular evolution of *ASPM*, *CDK5RAP2*, *CENPJ*, *MCPH1* and *STIL* in relation to brain size in anthropoid primates. First, I test whether these loci are under positive selection across anthropoids and whether or not different anthropoid clades have experienced different selective regimes. Second, I explore the association between the rate of molecular evolution of microcephaly genes and measures of brain size and investigate the relationship between microcephaly genes and relative testes size, a commonly used phenotypic correlate for sperm competition and sexual selection on males (Harcourt *et al.*, 1995; Ramm & Stockley, 2010). I then explore whether the sex specific effects of variation at these loci in humans suggests they have a role in the evolution of sexual dimorphism in brain size.

5.2 Methods summary

Details of phenotypic data and laboratory methods are given in chapter two. I sequenced exons which had previously been shown to have accelerated rates of evolution or contained a large proportion of the coding sequence. For *ASPM* I sequenced exons 3 and 18, totalling 6235bp (60% of the coding sequence (CDS)). For *MCPH1* three exons were sequenced: 8, 11 and 13, totalling 1556bp (62% of CDS). Exons 2 and 7 were sequenced for *CENPJ*, totalling 1556bp (52% of CDS). I sequenced 7 out of 38 exons of *CDK5RAP2*: exons 12, 20, 21, 24, 25, 32 and 33, (total 2120bp; 37% of CDS). Finally I sequenced 5 of the 16 coding exons of *STIL*: exons 7, 13, 15, 17 and 18 (total 2451bp; 63% of the CDS). See Appendix two for primer sequences. Exons of each locus were concatenated and analysed together. Sequences were obtained for 5 apes, 5 Old World monkeys and 10 New World monkeys representing all major clades of anthropoids (Figure 5.1). Where phenotypic data were not available for the species sequenced data from closely related congeneric species were used. The strepsirhines *Microcebus murinus* and *Otolemur garnettii* where used as outgroups when calculating the root-to-tip *dN/dS*; Ensembl IDs are shown in Appendix 3.

Estimation of *dN/dS* ratios (ω) was carried out using a codon-based maximum likelihood method (PAML version 4, Yang, 2007; see chapter 2). Several analyses were performed to test the hypothesis that the five loci have experienced positive selection across primates, in particular, in relation to brain size evolution. To detect positive selection across primates I implemented the site models. In addition I used the branch models to test whether the *dN/dS* of lineages leading to humans was significantly higher than non-human lineages and whether *dN/dS* significantly differed between Apes, Old World Monkeys and New World Monkeys. The branch models were also used to estimate the average *dN/dS* ratio from the ancestral anthropoid to each terminal species tip. These values were then set as species data and used in a PGLS regression with measures of brain size in BayesTraits to test for gene-phenotype associations (see chapter 2). One assumption of regression analysis is that the residuals of the model are normally distributed. As the residuals of the regression using *dN/dS* ratios were not normally distributed, I used Log_{10}(*dN/dS*) to improve normality. Residuals of regression analysis with log-transformed *dN/dS* did not violate assumptions of normality and constant variance.

First I examined the relationship between microcephaly gene molecular evolution and the evolution of absolute and relative neonatal brain size. As I specifically hypothesised a positive association between brain size and the selection pressure on these loci the significance of the regression coefficient was determined using a one-tailed t-test (see chapter 2). To minimise the influence of Type I errors, I restrict the analyses to a small number of critical tests, and I determined the specificity of relationships for microcephaly genes by testing for associations with other genes with no known role in neurogenesis and with alternative phenotypes. A Jack-knife approach was taken to test the robustness of the associations found and to identify any outliers which have a dominant effect on the slope of the regression. In addition to the standard *dN/dS* ratios, I used multiple regressions to investigate the association between phenotype and *dN* while controlling for *dS*. Here I predict a negative association between brain size and *dS* given known relationships between *dS* and life history traits such as body size (Nikolaev *et al*., 2007). I subsequently explored the relationship with volume of adult whole brain and neocortex. This analysis was performed to test my hypothesis that genes involved in neurogenesis should be more strongly associated with neonatal than adult brain mass, and that if there is an association with adult brain size it may be stronger for neocortex size than whole brain size. Comparisons of non-nested models were performed using Akaike Information Criterion. In addition, I explored the use of branch-site models to test for associations between positive selection and brain evolution, following Ali and Meier (2008) by setting branches with particularly large changes in brain size as the foreground branches (see chapter 2).

Finally, I tested for associations with relative testes size, calculated as described above for brain size, and with sexual dimorphism in brain mass. Sex specific data was taken from Isler *et al.* (2008) and residuals from a PGLS regression were used as a measure of sexual dimorphism in brain mass. I tested for an association with these raw residuals, where positive values indicate a larger than expected male brain, and also for absolute residuals such that deviation from the expected male:female relationship in either direction is treated in the same way.

5.3 Results & discussion

5.3.1 Sequence dataset

The full dataset comprises sequence data from 21 species for each gene including representative species from all major anthropoid clades and 11-17 newly sequenced species for each locus (Figure 5.1). This is the first analysis of the evolution of *STIL*. Previous datasets for *CDK5RAP2* and *CENPJ* have included only 4 species (Evans *et al*., 2006). With the exception of Ali and Meier's recent *ASPM* study (2008) which was published after the completion of my dataset, analyses of this gene have considered 3 (Zhang, 2003), 7 (Evans *et al*., 2004) and 8 species (Kouprina *et al*., 2004) whilst studies of *MCPH1* have included 7 (Evans *et al*., 2004b) and 13 species (Wang & Su, 2004). These studies were particularly lacking in a diverse range of New World Monkeys. Although I have sequenced only partial coding sequences, in the most part I have focused on regions of the gene which contain functionally important domains or which have previously been shown to have accelerated rates of evolution. The dataset therefore allows us to examine how widespread selection on these regions has been across anthropoids and to explore the relationship between this selection and phenotypic evolution.

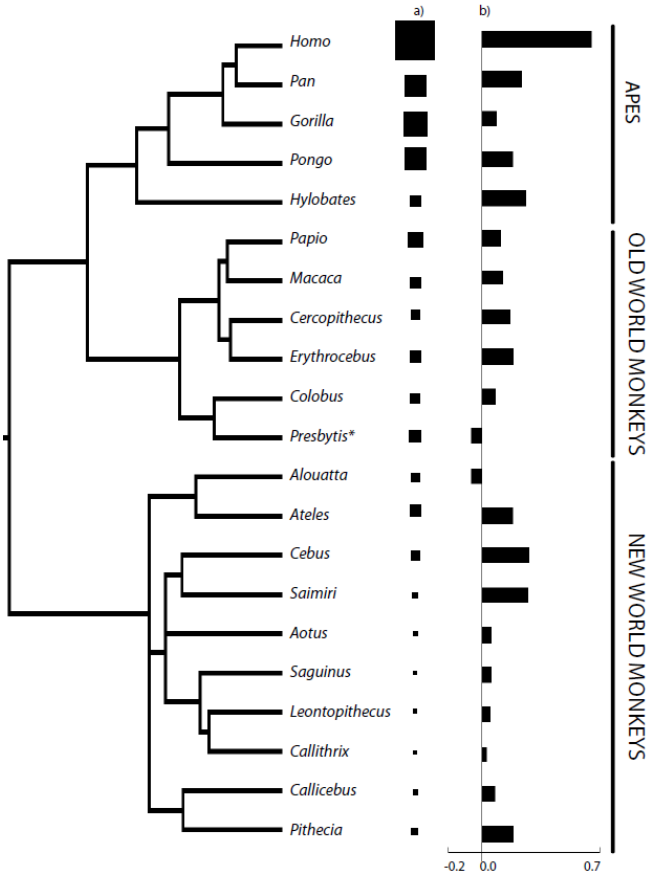

Figure 5.1 Phylogeny of anthropoid primates with an indication of (**a) Absolute brain mass** – the area of the square shows the mass of the brain as a percentage of the human brain and **(b) Relative brain mass** (on body mass), taken from chapter 2. The second species of *Colobinae* varied between loci (see Table 5.4).

5.3.2 Pervasive adaptive evolution of microcephaly genes in anthropoid primates

I first examined whether a signal of positive selection is present in five microcephaly loci by performing site model tests using a codon-based maximum likelihood method (Yang, 2007; Table 5.1). All five genes showed evidence for positive selection across anthropoids, with estimated omega of 2.18-5.39 at 2.28-7.68% of sites across the loci. The most significant results are for *ASPM* and *CDK5RAP2* which have 2.3% and 6.5% of sites having an omega of 5.39 and 4.42 respectively, with the weakest support found for *STIL*. In *CDK5RAP2*, a notable feature is the clustering of sites identified as being under positive selection using Bayes Empirical Bayes (p >95%) (Positions 929 - 977 and 1683 - 1690); these mostly fall within an SMC domain (Evans *et al.*, 2006) which is thought to play a role in chromosome segregation, regulation and repair (Hirano, 2006) but the functional significance of these particular sites are unknown.

Previous authors have proposed that *ASPM* and *MCPH1* have evolved at a higher rate along lineages leading from the last common ancestor of apes to modern humans than on other lineages (Evans *et al.*, 2004a & b). I tested this explicitly using a branch model and found that the evolutionary rate of change in lineages leading to humans does not significantly differ from that in other lineages (Table 5.2a). This is congruent with the fact that the proportional change in brain mass along this lineage is also not exceptional compared to the rest of primate brain size evolution (chapter 3). In addition I tested whether the evolutionary rate of the five loci differed between apes, Old World Monkeys and New World Monkeys and found no significant differences (Table 5.2b). Finally I performed site models to test for positive selection on each of the three clades separately. Although the results are influenced by differences in the number of sequences and the time depth for each clade, I found no instance where positive selection was found in Apes and not in Old or New World Monkeys (Table 5.3).

Table 5.1 Site models detecting positively selected sites for anthropoid primates*

Gene	N	lnL(null/M1a)	lnL(positive selection/M2a)	LRT statistic	p-value	Proportion of sites ω >1	Ω	Positively selected sites
ASPM	21	-20522.7	-20487.0	71.4	***<0.001***	0.0228	5.394	**195,** 1407, 1437, **1558,** 2016**, 2185**
CDK5RAP2	21	-7858.2	-7818.7	79.0	***<0.001***	0.0650	4.418	853, 881, **929**, **930**, **948**, 964, 977, **1581**, **1683**, 1687, 1688, **1690**
CENPJ	21	-7695.8	-7684.1	23.4	***<0.001***	0.0255	3.897	527, 813
MCPH1	21	-6375.3	-6369.0	12.6	***0.002***	0.0558	2.574	-
STIL	21	-6783.9	-6780.4	7.0	***0.030***	0.0768	2.184	-

***** Positively selected sites identified using Bayes Empirical Bayes are shown in the right hand column, numbered according to the full human coding sequence. Only sites with p>95% are presented; sites in bold have p>99%.

Table 5.2 Branch and Site model tests on separate anthropoid clades

a)	Model 2		Model 0			
Gene	***dN/dS* lineages leading to *Homo***	***dN/dS* 'non-human' lineages**	**lnL(M2)**	**lnL(M0)**	**LRT statistic**	**p-value**
ASPM	0.489	0.466	-21351.4	-21351.5	0.042	0.838
CDK5RAP2	0.729	0.676	-8718.4	-8718.4	0.054	0.816
CENPJ	0.623	0.503	-8664.8	-8665.0	0.373	0.542
MCPH1	0.793	0.579	-7301.2	-7301.5	0.704	0.401
STIL	0.400	0.437	-8680.9	-8681.0	0.045	0.831

b)	Model 2			Model 0			
Gene	***dN/dS* Apes**	***dN/dS* OWM**	***dN/dS* NWM**	**lnL(M2)**	**lnL(M0)**	**LRT statistic**	**p-value**
ASPM	0.473	0.415	0.479	-21350.9	-21351.5	1.122	0.571
CDK5RAP2	0.781	0.627	0.687	-8717.9	-8718.4	1.018	0.601
CENPJ	0.582	0.549	0.522	-8663.4	-8665.0	3.081	0.214
MCPH1	0.606	0.724	0.538	-7300.3	-7301.5	2.401	0.301
STIL	0.463	0.3891	0.445	-8680.7	-8681.0	0.462	0.793

Table 5.3 Site model tests on separate anthropoid clades

			Model 2a			Model 1a		
Gene	**Clade**	**n**	**lnL(M2a)**	**p, ω > 1**	**Ω**	**lnL(M1a)**	**LRT statistic**	**p-value**
ASPM	APES	5	-10068.8	0.002	31.076	-10071.1	4.591	0.101
	OWM	6	-9631.4	0.003	42.917	-9642.1	21.402	***<0.001***
	NWM	10	-15341.6	0.017	6.139	-15353.4	23.576	***<0.001***
CDK5RAP2	APES	5	-3641.2	0.247	3.783	-3646.8	11.131	***0.004***
	OWM	6	-3666.8	0.045	9.099	-3678.4	23.332	***<0.001***
	NWM	10	-5555.2	0.028	7.519	-5579.7	48.997	***<0.001***
CENPJ	APES	5	-3336.6	0.089	4.201	-3339.5	5.903	0.052
	OWM	6	-4016.1	0.022	7.330	-4020.0	7.859	***0.020***
	NWM	10	-3336.6	0.089	4.201	-3339.5	5.903	0.052
MCPH1	APES	5	-2675.9	0.510	1.117	-2675.9	0.043	0.979
	OWM	6	-2829.0	0.364	2.037	-2830.8	3.518	0.172
	NWM	10	-4533.2	0.115	2.029	-4535.9	5.381	0.068
STIL	APES	5	-3846.9	0.151	1.000	-3846.9	0.000	1.000
	OWM	6	-3782.9	0.001	27.124	-3783.1	0.426	0.808
	NWM	10	-5038.9	0.017	4.492	-5047.6	17.289	***<0.001***

Table 5.4 Root-to-tip *dN/dS* ratios

ASPM		***CDK5RAP2***		***CENPJ***		***MCPH1***		***STIL***	
Genus	***dN/dS***	**Genus**	***dN/dS***	**Genus**	***dN/dS***	**Genus**	***dN/dS***	**Genus**	***dN/dS***
Homo	0.5331	*Homo*	0.8852	*Homo*	0.8869	*Homo*	0.5605	*Homo*	0.4462
Pan	0.4755	*Pan*	0.8627	*Pan*	1.3910	*Pan*	0.5532	*Pan*	0.4138
Gorilla	0.4918	*Gorilla*	0.7344	*Gorilla*	0.6466	*Gorilla*	0.5571	*Gorilla*	0.4664
Pongo	0.4338	*Pongo*	0.9642	*Pongo*	1.2189	*Pongo*	0.7157	*Pongo*	0.2997
Hylobates	0.4683	*Hylobates*	0.9216	*Hylobates*	0.9421	*Hylobates*	0.4201	*Hylobates*	0.6374
Macaca	0.4076	*Macaca*	0.7051	*Macaca*	0.8290	*Macaca*	0.5390	*Macaca*	0.5048
Papio	0.3713	*Papio*	0.5539	*Papio*	0.7225	*Papio*	0.5752	*Papio*	0.4862
Cercopithecus	0.4301	*Cercopithecus*	0.7091	*Cercopithecus*	1.0951	*Cercopithecus*	0.5742	*Cercopithecus*	0.5176
Erythrocebus	0.4502	*Erythrocebus*	0.7586	*Erythrocebus*	0.8360	*Erythrocebus*	0.4474	*Erythrocebus*	0.6001
Presbytis	0.4326	*Trachypithecus*	0.8205	*Presbytis*	0.5856	*Presbytis*	0.4955	*Presbytis*	0.4634
Colobus	0.4130	*Colobus*	0.7326	*Colobus*	0.8648	*Colobus*	0.4589	*Colobus*	0.4954
Alouatta	0.4313	*Alouatta*	0.8095	*Alouatta*	0.6083	*Alouatta*	0.539	*Alouatta*	0.3583
Ateles	0.5104	*Ateles*	0.8015	*Ateles*	0.7805	*Ateles*	0.4502	*Ateles*	0.4113
Callicebus	0.5144	*Callicebus*	0.5883	*Callicebus*	0.5052	*Callicebus*	0.4338	*Callicebus*	0.2770
Pithecia	0.4737	*Pithecia*	0.7189	*Pithecia*	0.6465	*Pithecia*	0.4083	*Pithecia*	0.3671
Aotus	0.4468	*Aotus*	0.6594	*Aotus*	0.6061	*Aotus*	0.7704	*Aotus*	0.3189
Cebus	0.4639	*Cebus*	0.6172	*Cebus*	0.4797	*Cebus*	0.5542	*Cebus*	0.3516
Saimiri	0.4471	*Saimiri*	0.6098	*Saimiri*	0.5869	*Saimiri*	0.4613	*Saimiri*	0.2635
Saguinus	0.5634	*Saguinus*	0.5146	*Saguinus*	0.6471	*Saguinus*	0.5026	*Saguinus*	0.4252
Leontopithecus	0.4749	*Leontopithecus*	0.5154	*Leontopithecus*	0.6247	*Leontopithecus*	0.5702	*Leontopithecus*	0.4134
Callithrix	0.5432	*Callithrix*	0.5372	*Callithrix*	0.7063	*Callithrix*	0.4998	*Callithrix*	0.3263

5.3.3 Associations between gene evolution and anthropoid brain size expansion

To explicitly test the link between the molecular evolution of microcephaly genes and brain size I performed several tests. I first performed a phylogenetically controlled regression analysis in BayesTraits (Pagel, 1999; Pagel *et al*., 2004) between the root-to-tip *dN/dS* (Table 5.4), estimated using the branch models, and neonatal brain mass.

A significant association between the molecular evolution of *CDK5RAP2* and absolute neonatal brain mass was found (t_{11} = 2.07, p = 0.031, R^2 = 0.280) but there is no significant association between *ASPM*, *CENPJ* or *MCPH1* and this trait (Table 5.5). For *ASPM* however, *Callithrix* represented a strong outlier (Figure 5.2) and when this species was removed the association between the *dN/dS* of *ASPM* and neonatal brain mass is significant (t_{10} = 2.42, p = 0.018, R^2 = 0.369). *Callithrix*, and the other callitrichids, show high rates of evolution of *ASPM* (Table 5.4) but have the smallest brain masses among the anthropoid primates (Stephan *et al*., 1981); however, this is due to a secondary reduction in brain mass in this taxon (Ford, 1980; chapter 3 & 4). The significance of the regression between *ASPM* and neonatal brain mass was not affected by the removal of any other species. From here on, unless otherwise stated, regressions for *ASPM* were performed without the callitrichids. Removing *Callithrix* does not reveal a significant association with neonatal brain mass for *CENPJ* (t_{10} = 0.81, p = 0.218, R^2 = 0.061), *MCPH1* (t_{10} = -0.55, p = 1.000, R^2 = 0.029) or *STIL* (t_{10} = 0.283, p = 0.391, R^2 = 0.008). The high root-to-tip *MCPH1 dN/dS* ratio of *Pan* (1.39) appeared to be heavily influenced by a small number of synonymous substitutions on the terminal *Pan* branch (1 synonymous change, compared to 6 synonymous changes on the *Homo* branch), and I note previous studies have found a much lower *dN/dS* ratio on the terminal *Pan* lineage using the full coding sequence (Evans *et al*., 2004a; Wang & Su, 2004). I therefore repeated the regressions excluding the *Pan* data point but still found no significant result (t_{10} = -0.300, p = 1.000, R^2 = 0.006). No locus showed any association with relative neonatal brain size (Table 5.5).

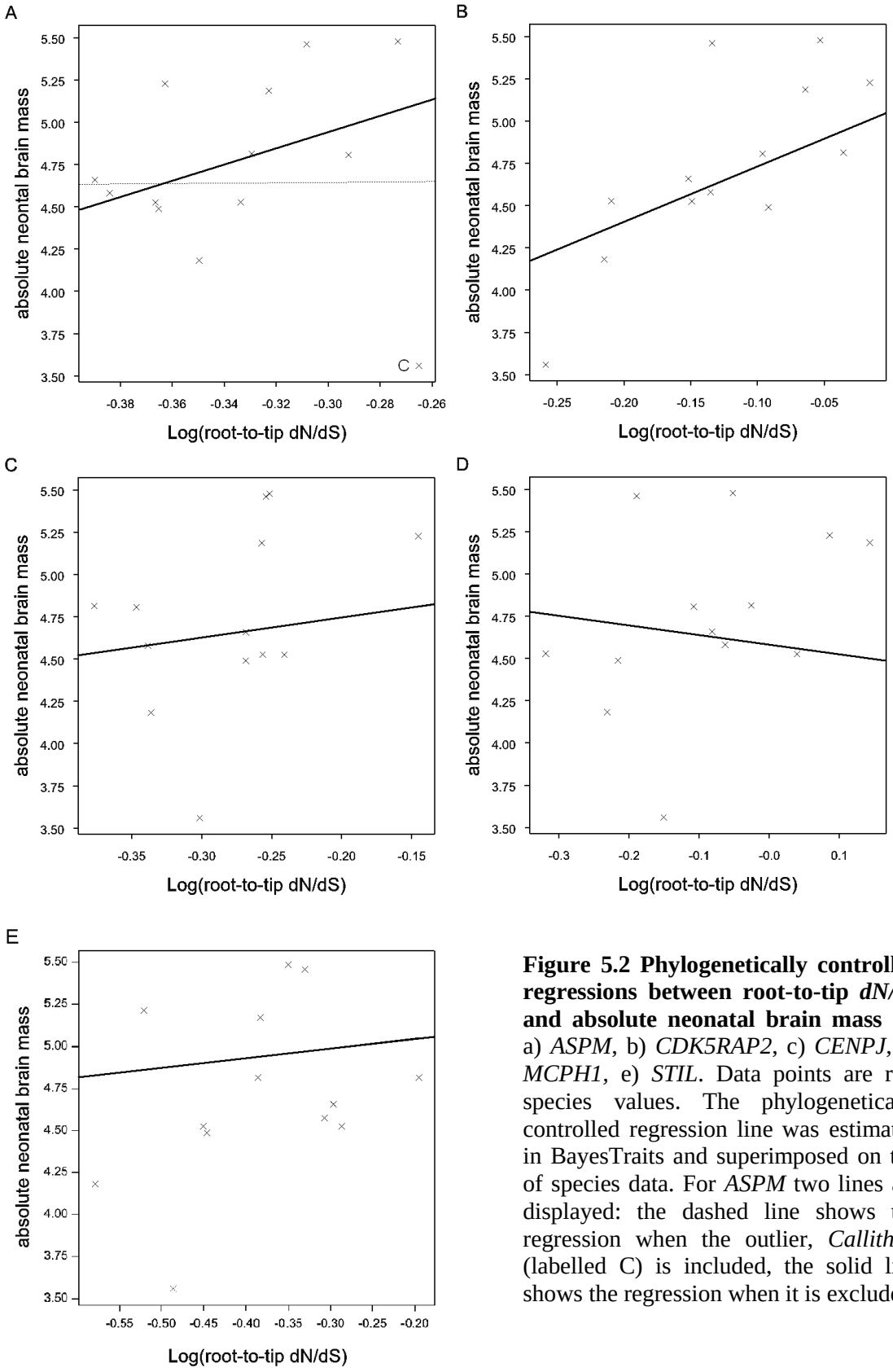

Figure 5.2 Phylogenetically controlled regressions between root-to-tip *dN/dS* and absolute neonatal brain mass for a) *ASPM*, b) *CDK5RAP2*, c) *CENPJ*, d) *MCPH1*, e) *STIL*. Data points are raw species values. The phylogenetically controlled regression line was estimated in BayesTraits and superimposed on top of species data. For *ASPM* two lines are displayed: the dashed line shows the regression when the outlier, *Callithrix* (labelled C) is included, the solid line shows the regression when it is excluded.

Table 5.5 Phylogenetically controlled regression analysis between root-to-tip *dN/dS* and brain size in anthropoid primates

		Absolute neonatal brain mass			Relative neonatal brain mass		
Gene	**n**	**t-statistic**	**p-value**	**R^2**	**t-statistic**	**p-value**	**R^2**
ASPM	13	0.040	0.484	0.000	0.797	0.221	0.055
ASPM (without Callitrichids)	12	2.420	***0.018***	0.369	0.967	0.178	0.086
CDK5RAP2	13	1.955	***0.039***	0.255	-0.500	1.000	0.022
CENPJ	13	0.631	0.270	0.035	-1.204	1.000	0.116
MCPH1	13	-0.697	1.000	0.042	-1.126	1.000	0.103
STIL	13	0.390	0.352	0.014	0.174	0.432	0.002

Table 5.6 Phylogenetically controlled regression analysis between root-to-tip *dN/dS* and adult brain size in anthropoid primates

	Adult whole brain						Adult neocortex						
		Absolute mass			Relative mass			Absolute volume			Relative volume		
Gene	**n**	**t-stat**	**p**	**R^2**	**t-stat**	**p**	**R^2**	**n**	**t-stat**	**p**	**R^2**	**t-stat**	**p**	**R^2**
ASPM	21	-0.264	1.000	0.003	1.770	***0.046***	0.142	19	-0.233	1.000	0.003	1.248	0.114	0.084
ASPM (without Callitrichids)	18	0.881	0.196	0.046	2.241	***0.020***	0.239	17	0.922	0.186	0.054	1.486	0.079	0.128
CDK5RAP2	21	0.946	0.178	0.045	0.949	0.177	0.045	19	0.853	0.203	0.039	0.441	0.332	0.011
CENPJ	21	0.452	0.328	0.010	-0.900	1.000	0.041	19	0.260	0.399	0.004	-1.037	1.000	0.004
MCPH1	21	-0.674	1.000	0.023	0.663	0.257	0.022	19	-0.646	1.000	0.024	1.012	0.163	0.103

I next explored whether the association with brain mass can be observed for adult phenotypes by performing regressions of root-to-tip *dN/dS* with absolute and relative neocortex and whole brain size. I found no significant association with any measure of absolute brain size for any locus (Table 5.6). To confirm this result I performed the same regressions but using only the species used in the neonatal regressions. Using this reduced dataset I subsequently found a significant association between both absolute neocortex and whole brain mass with *ASPM* (whole brain: $t_{10} = 2.732$, $p = 0.010$, $R^2 = 0.427$; neocortex $t_{10} = 2.980$, $p = 0.007$, $R^2 = 0.470$) and *CDK5RAP2* (whole brain: $t_{11} = 2.224$, $p = 0.024$, $R^2 = 0.310$; neocortex $t_{11} = 2.09$, $p = 0.030$, $R^2 = 0.285$) but not *CENPJ*, *MCPH1* or *STIL*. To identify the cause of this discrepancy I performed a reverse jack-knife, repeating the regressions with the full dataset of adult phenotypes and removing each species, one at a time (Table 5.7). I found that for both *ASPM* and *CDK5RAP2* the removal of *Papio* results in a significant association with absolute neocortex and whole brain mass (*ASPM*: whole brain: $t_{15} = 2.063$, $p = 0.028$, $R^2 = 0.221$: neocortex: $t_{14} = 2.128$, $p = 0.0257$ $R^2 = 0.244$; *CDK5RAP2*: whole brain: $t_{18} = 2.825$, $p = 0.005$, $R^2 = 0.307$, neocortex: $t_{17} = 2.124$ $p = 0.025$, $R^2 = 0.209$), whereas removing any other species does not have this affect, suggesting *Papio* is an outlier to a general trend.

I subsequently added the callitrichids back into the regressions with *ASPM* and found that the addition of any one callitrichid or all three together substantially reduces or negates the association (addition of *Saguinus* alone: $t_{16} = 0.612$, $p = 0.274$, *Leontopithecus* alone: $t_{16} = 1.842$, $p = 0.042$, *Callithrix* alone: $t_{16} = 0.612$, $p = 0.265$, all three: $t_{18} = 0.302$, $p = 0.2383$). In contrast, after removal of all three callitrichids the association with *CDK5RAP2* is still significant ($t_{15} = 1.803$, $p = 0.046$) and removal of any single species (removal of *Saguinus*: $t_{17} = 2.600$, $p = 0.009$, *Leontopithecus*: $t_{17} = 2.806$, $p = 0.005$, *Callithrix*: $t_{17} = 2.700$, $p = 0.007$) or any pair of callitrichids (retention of *Saguinus*: $t_{16} = 2.510$, $p = 0.011$, *Leontopithecus*: $t_{16} = 2.538$, $p = 0.011$, *Callithrix*: $t_{16} = 2.336$, $p = 0.016$) does not significantly affect the association. This confirms callitrichids are outliers to the general trend for *ASPM* but not for *CDK5RAP2*.

In addition I repeated the analysis using relative measures of adult brain and neocortex size. For *ASPM* there was a significant association with relative adult brain size on both the full dataset ($t_{19} = 1.77$, $p = 0.046$, $R^2 = 0.142$; without callitrichids $t_{15} = 2.241$, $p = 0.020$, $R^2 = 0.239$) and the reduced dataset used for regressions with neonatal data ($t_{10} = 2.59$, $p = 0.013$, $R^2 =$

0.402). However in both cases the result was dependent on the human data point and when this was removed the association is no longer significant (adult: $t_{18} = 0.574$, $p = 0.287$, $R^2 = 0.018$; without callitrichids: $t_{15} = 0.923$, $p = 0.185$, $R^2 = 0.054$; neonate $t_{18} = 0.880$, $p = 0.200$, $R^2 = 0.079$). No other significant relationship was detected (Table 5.6).

Table 5.7 Reverse Jack-knife to identify the cause of discrepancy between adult brain & *dN/dS* regressions on adult and neonate datasets

	ASPM				***CDK5RAP2***		
Genus excluded	**t_{15}**	**p-value**	**R^2**	**Genus excluded**	**t_{19}**	**p-value**	**R^2**
Alouatta	0.847	0.205	0.046	*Alouatta*	1.287	0.107	0.084
Aotus	0.745	0.234	0.036	*Aotus*	1.340	0.099	0.091
Ateles	0.454	0.328	0.014	*Ateles*	1.042	0.156	0.057
Callicebus	1.273	0.111	0.097	*Callicebus*	1.137	0.135	0.067
Callithrix	-	-	-	*Callithrix*	1.192	0.124	0.073
Cebus	0.856	0.203	0.047	*Cebus*	1.373	0.093	0.095
Cercopithecus	0.944	0.180	0.056	*Cercopithecus*	1.295	0.106	0.085
Colobus	0.785	0.222	0.040	*Colobus*	1.247	0.114	0.080
Erythrocebus	0.869	0.199	0.048	*Erythrocebus*	1.260	0.112	0.081
Gorilla	0.855	0.203	0.046	*Gorilla*	1.327	0.101	0.089
Homo	-0.174	1.000	0.002	*Homo*	1.074	0.149	0.060
Hylobates	0.937	0.182	0.055	*Hylobates*	1.479	0.078	0.108
Leontopithecus	-	-	-	*Leontopithecus*	1.261	0.112	0.081
Macaca	0.843	0.206	0.045	*Macaca*	1.339	0.099	0.091
Pan	0.66	0.260	0.028	*Pan*	1.371	0.094	0.095
Papio	**2.064**	***0.028***	**0.221**	***Papio***	**2.825**	***0.006***	**0.307**
Pithecia	0.854	0.203	0.046	*Pithecia*	1.234	0.117	0.078
Pongo	1.027	0.160	0.066	*Pongo*	1.173	0.128	0.071
Presbytis	0.828	0.210	0.044	*Presbytis*	1.372	0.094	0.095
Saguinus	-	-	-	*Saguinus*	1.126	0.137	0.066
Saimiri	0.777	0.225	0.039	*Saimiri*	1.251	0.113	0.080

I next used AIC to determine the best supported model for the associations between *ASPM* and *CDK5RAP2* and neonatal and adult brain mass using only the species for which data are available for both phenotypes. For both loci the regression with neonatal brain mass has a substantially lower AIC than whole brain mass (*ASPM*: neonate AIC = 2.44, adult AIC = 7.39; *CDK5RAP2*: neonate AIC = 11.76, adult AIC = 14.33) suggesting a closer association with neonatal brain mass. Comparing adult neocortex and whole adult brain size I found no substantial difference (*ASPM*: neocortex AIC = 7.43, whole AIC = 7.40; *CDK5RAP2*: neocortex AIC = 15.96, whole AIC = 14.33). However, when compared to the volume of the whole brain minus neocortical volume the relationship for *ASPM* is not significant (t_{14} = 1.579, p = 0.068, R^2 = 0.151) suggesting that *ASPM* may be specifically contributing to the expansion of the cortex. I also found that the association is stronger for neocortical grey matter than neocortical white matter (grey: t_9 = 1.866, p = 0.047, R^2 = 0.279, AIC: 13.28; white: t_9 = 1.627, p = 0.069, R^2 = 0.227, AIC: 18.233). However for *CDK5RAP2* the association with non-neocortex mass is significant (t_{16} = 3.235, p = 0.003, R^2 = 0.368) and indeed the AIC values are lower for non-neocortex (11.63) than neocortex (17.17) suggesting the evolutionary role of *CDK5RAP2* may not be as closely linked to the cortex as for *ASPM*. Consistent with this the support for an association with neocortical grey over neocortical white matter is weaker for *CDK5RAP2* (grey: t_9 = 2.312, p = 0.023, R^2 = 0.373 AIC: 11.75; white: t_9 = 2.585, p = 0.014, R^2 = 0.426, AIC: 14.96). Finally when both *ASPM* and *CDK5RAP2* root-to-tip *dN/dS* values are included in a multiple regression with whole brain size both loci remain significantly associated (*ASPM*: t_{13} = 2.207, p = 0.023; *CDK5RAP2*: t_{13} = 2.137, p = 0.026; R^2 = 0.421) suggesting both loci contribute to brain size evolution independently.

To further explore the relationship between brain evolution and the molecular evolution of the microcephaly genes I performed multiple regressions with neonatal brain size and root-to-tip *dN* and *dS* (log transformed) as independent variables. Significant negative partial regression coefficients were found for the three cytoskeletal genes and *dS* (1-tailed *ASPM*: t_8 = -2.958, p = 0.007; *CDK5RAP2*: t_9 = -2.077, p = 0.032; *CENPJ*: t_9 = -1.859, p = 0.046) but interestingly not for *MCPH1* or *STIL* (*MCPH1*: t_9 = -1.294, p = 0.114; *STIL*: t_9 = -1.209, p = 0.129). Neither *CENPJ*, *MCPH1* or *STIL*, which show no association between brain size and *dN/dS*, show a significant association with *dN* (*CENPJ*: t_9 = 0.049, p = 0.481; *MCPH1*: t_9 = -2.322, p = 1.000;

STIL: $t_9 = -0.368$, $p = 1.000$). For *ASPM* an association between *dN* and neonatal brain size was found ($t_8 = 2.032$, $p = 0.035$) but no significant association was obtained for *CDK5RAP2* ($t_9 = 1.060$, $p = 0.156$). This suggests the association between *ASPM* and *dN/dS* may be driven predominantly by an accelerated *dN* whilst the association for *CDK5RAP2* may have a more complex basis.

5.3.4 Controls for specificity of gene-phenotype associations

To exclude the possibility that the gene-phenotype correlations reported above are non-specific, I investigated eight loci (see Appendix 3 for sequence IDs) with no known function in neurogenesis, for which data were already available for a reasonably large number of species (n = 10-20) across the anthropoid phylogeny. This control set includes both genes which have previously been shown to have experienced positive selection across anthropoids and genes which appear to be under purifying selection (Table 5.8). I tested for an association between the root-to-tip *dN/dS* of these loci and absolute adult and neonatal brain mass in the same way as described above. No locus was found to have a significant association with either phenotype (Table 5.9); the removal of any one species does not result in a significant change in the regression slope and a positive association with brain size. This suggests that the significant results presented above are unlikely to be Type I errors.

Given the strong allometric relationship between brain and body mass I also checked whether molecular evolution of *ASPM* and *CDK5RAP2* could be more strongly associated with adult body mass than brain mass, due for example to differences in effective population size (Nikolaev *et al*., 2007) or general scaling effects, using the neonate dataset to allow comparisons using AIC. For *ASPM* there was no significant association with adult body mass with ($t_{13} = -0.368$, $p = 1.000$, $R^2 = 0.012$) or without inclusion of *Callithrix* ($t_{12} = 0.846$, $p = 0.210$, $R^2 = 0.067$). For *CDK5RAP2* there is a marginally significant association with body mass ($t_{13} = 1.910$, $p = 0.041$, $R^2 = 0.249$) but the AIC score for an association with absolute neonatal brain mass is substantially lower (Body mass AIC = 20.22; Neonatal brain mass AIC = 12.19) indicating that the association with brain mass has much more support, and that the weak association with body mass is likely to be due to correlated evolution between brain and body mass.

I next tested whether the adaptive evolution of the five loci could be better explained by sexual selection in relation to their expression in the testes. I performed phylogenetically controlled regressions between root-to-tip *dN/dS* and relative testes size, a commonly used correlate of sexual selection (see methods). No significant association was observed for *ASPM*, *CDK5RAP2*, *CENPJ* or *STIL*. A significant association was found for *MCPH1* (t_{18} = 1.959, p = 0.033, R^2 = 0.176; Table 5.10) but when *Pan* (which has an unexpectedly high *dN/dS*; see above) is removed, this association is no longer significant (t_{17} = 0.530, p = 0.301, R^2 = 0.016), suggesting more data will be required to confirm this result.

Table 5.8 Site model tests on control genes

Gene	N	Ln(L) M1a	Ln(L) M2a	LRS	p-value	proportion of sites, ω >1	ω > 1	Previous reports of selection
ASIP	15	-949.261	-949.261	0.000	1.000	-	-	Purifying selection (Mundy & Kelly, 2006)
CATSPER1	13	-4726.134	-4711.330	29.609	0.000	0.109	4.261	Positive selection (Podlaha & Zhang, 2003)
ENAM	12	-8479.060	-8453.730	50.659	0.000	0.050	5.658	Positive selection (Kelly & Swanson, 2008)
GRIN2A	17	-2525.452	-2521.426	8.052	***0.018***	0.003	14.094	Episodic positive selection (Ali & Meier, 2009)
MC1R	21	-3672.725	-3672.539	0.371	0.831	-	-	Purifying selection (Mundy & Kelly, 2003)
SEMG2	13	-6650.761	-6606.315	88.891	***0.000***	0.147	4.847	Positive selection (Dorus *et al.*, 2004a)
SRY	18	-3072.065	-3071.828	0.474	0.789	-	-	Neutral evolution/positive selection (Wang *et al.*, 2002)
ZAN	12	-14848.953	-14847.505	2.896	0.235	-	-	Positive selection (Gasper & Swanson, 2006)

Table 5.9 Phylogenetically controlled regression analysis of control genes

	Adult brain mass				Neonatal brain mass			
Locus	**n**	**$t_{(n-2)}$**	**p-value**	**R^2**	**n**	**$t_{(n-2)}$**	**p-value**	**R^2**
ASIP	14	0.183	0.429	0.003	8	0.567	0.296	0.051
CATSPER1	13	-0.234	1.000	0.005	9	-0.509	1.000	0.036
ENAM	10	1.690	0.065	0.263	7	1.441	0.105	0.294
GRIN2A	16	1.267	0.113	0.103	12	1.681	0.062	0.220
MC1R	20	0.379	0.355	0.008	13	0.663	0.260	0.038
SEMG2	13	-0.223	1.000	0.005	9	-0.330	1.000	0.015
SRY	17	-1.461	1.000	0.125	10	-2.717	1.000	0.480
ZAN	11	-0.294	1.000	0.009	7	-0.655	1.000	0.079

Table 5.10 Phylogenetically controlled regression analysis between root-to-tip *dN/dS* and relative testes mass

		Relative testis mass		
Gene	**n**	**t-statistic**	**p-value**	**R^2**
ASPM	20	0.097	1.000	0.097
CDK5RAP2	20	0.021	1.000	0.021
CENPJ	20	0.036	0.210	0.036
MCPH1	20	0.176	***0.032***	0.176
STIL	20	-0.988	1.000	0.051

5.3.5 Branch-site models to detect gene-phenotype associations

An additional method of investigating associations between genes and phenotypes is to test for an association between large phenotypic changes (e.g. in brain size) and high *dN/dS* ratios of relevant genes (e.g. microcephaly genes). This can be done by reconstructing ancestral states, selecting branches along which brain mass has increased greatly and setting these as fore-ground branches in branch-site models (Yang, 2005; Anisimova & Yang, 2007). This method therefore relies on obtaining reliable ancestral state reconstructions and a punctuated pattern of positive selection. Ali and Meier (2008) used branch-site models to investigate *ASPM* evolution in relation to brain size over a 15 primate phylogeny. They report that branches with large changes in relative telencephalon volume (reported as cerebral cortex, and reconstructed using parsimony methods) were associated with positive selection on *ASPM* which contradicts the results presented above.

To identify the sourse of this contradiction I performed an analysis based on choosing the most reliable ancestral state reconstructions, following chapter 3, for use in a branch-site model to test for associations between brain evolution and positive selection on *ASPM* and *CDK5RAP2*. I used the results from chapter 3 to assess the ability of estimates made under a constant variance model to highlight branches with large increases in brain mass identified using the better supported directional model. This comparison can only be conducted for whole brain mass as the directional model can only be fitted to trees that vary in total path length from root to species

tips. In an otherwise ultrametric tree, this variation is provided by inclusion of fossil data for whole brain size. As no fossil data is available for separate regions of the brain, neonatal brain size or for testis size it is not possible implement this method. A large degree of congruence is therefore required between branches picked out by the constant variance and the directional model for the results of the constant variance model for the branch-site results to be reliable.

Estimates of change in brain size along each branch obtained using the constant variance model and the directional model were significantly correlated ($t_{36} = 8.699$, $p < 0.001$) but the R^2 was quite low (0.678). This improved when fossil data were included ($t_{36} = 13.104$, $R^2 = 0.827$, $p < 0.001$; Figure 5.3). For relative brain mass the agreement between methods was lower; for a comparison between the constant variance model and the directional model less than 50% of the variance was explained ($t_{36} = 5.380$, $R^2 = 0.446$, $p < 0.001$; Figure 5.3). Again, including fossil data improves the fit, but a large amount of variance remained unexplained ($t_{36} = 8.141$, $R^2 = 0.648$, $p < 0.001$).

When the results from the constant variance and directional models were ranked, there was poor agreement between the two methods in identifying branches with a large amount of phenotypic evolution. For absolute brain mass only 57.8% of branches (11/19) identified as showing large changes using the directional model were found in the top half of changes under the constant variance model, whilst for relative brain mass this was 52.5% (10/19). Branches which were identified by both methods as falling in the upper half of changes in brain mass include several which show large decreases in brain mass under the constant variance model but a large increase under the directional model.

Based on these results I conclude that unless fossil data are included and a test for a directional trend can be performed, identifying foreground branches in this way is unreliable. Error in selecting branches in this way is likely to have a significant influence on the results obtained from branch-site tests for positive selection.

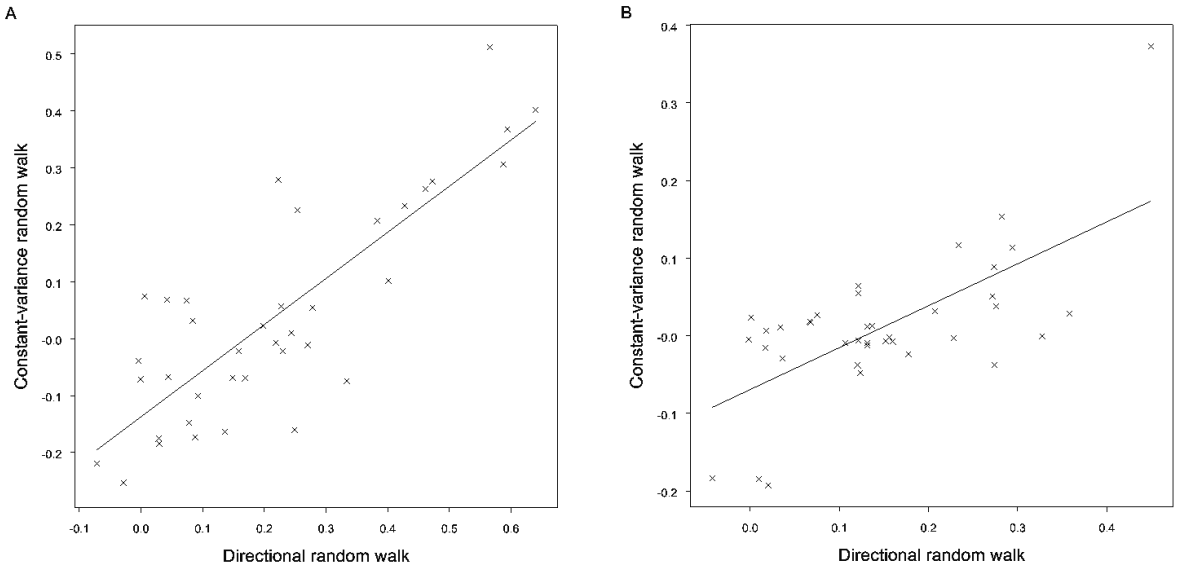

Figure 5.3 Comparison of estimated change along each branch using constant-variance and directional random walk models for a) change in absolute brain mass; b) change in relative brain mass

To implement the branch-site tests an experimental model, in which a proportion of sites in the foreground is allowed to have an $\omega > 1$, is compared to a null model, in which the ω of this class of sites is fixed to 1 (neutral evolution). For absolute and relative brain size, the absolute change along each branch of the phylogeny (Table 3.4) was ranked from highest to lowest, with the top half of branches in this distribution set as the foreground branches. Several tests were performed to investigate how robust significant results under the branch-site models are for a dataset which has been shown to be subject to positive selection across the phylogeny.

The results of the branch-site test where the top half of branches with the greatest increases in brain size were set as foreground are shown in Table 5.11. For *CDK5RAP2* tests for both relative and absolute whole brain mass were significant. The test was significant for *ASPM* and relative brain size. To test the robustness of these results, where a significant association was found, I swapped the branches set as foreground and background around and repeated the analysis. In each case a significant result was obtained (Table 5.12a). Furthermore, by randomly selecting foreground branches it was possible to obtain a significant result without segregating branches on the basis of brain mass evolution.

Table 5.11 Branch-site models for anthropoids: total change in brain mass*

Gene	Phenotype	N	lnL (model A, ω = 1)	lnL (model A, ω >1)	LRT statistic	p-value	Proportion of sites ω >1	ω	Positively selected sites[#]
ASPM	absolute brain	21	-22238.7	-22238.7	0.0	1.000	0.0000	-	-
	relative brain	21	-22238.6	-22234.2	8.8	***0.003***	0.0059	7.940	-
CDK5RAP2	absolute brain	21	-8645.5	-8632.3	26.4	***<0.001***	0.0231	7.940	**977**, 1699
	relative brain	21	-8644.8	-8637.8	14.0	***<0.001***	0.0552	3.836	881

***** The proportion of sites with ω >1 is the total of class 2a (purifying to positive selection) and 2b (neutral evolution to positive selection). Positively selected sites identified using Bayes Empirical Bayes are shown in the right hand column. Only sites with p>95% are presented, sites in bold have p>99%.

[#] sites numbered according to full human coding sequence**.**

Table 5.12 Branch-site control tests

a) Reversing branches set as foreground and background:

Gene	Phenotype	N	lnL (model A, ω = 1)	lnL (model A, ω >1)	LRT statistic	p-value	Proportion of sites ω >1	ω
ASPM	absolute brain	21	-22237.9	-22231.3	13.2	***<0.001***	0.0182	5.214
	relative brain	21	-22238.7	-22230.3	16.9	***<0.001***	0.0083	12.289
CDK5RAP2	absolute brain	21	-8645.7	-8638.4	14.6	***<0.001***	0.0420	4.924
	relative brain	21	-8645.7	-8617.9	55.6	***<0.001***	0.0271	11.316

b) Branch site test 2 using Ali and Meier's sequence data and branch classification*:

Gene	Phenotype	N	lnL (model A, ω = 1)	lnL (model A, ω >1)	LRT statistic	p-value	Proportion of sites ω >1	ω
ASPM	Relative telencephalon	15	-16372.5	-16363.4	18.2	***<0.001***	0.0167	14.204
	Random 1	15	-16371.8	-16371.8	0.0	1.000	0.0983	1.000
	Random 2	15	-16367.3	-16358.9	16.8	***<0.001***	0.0688	4.699
	Random 3	15	-16369.3	-16369.3	0.0	1.000	0.1730	1.000
	Random 4	15	-16372.4	-16366.6	11.6	***<0.001***	0.0081	12.254
	Random 5	15	-16372.4	-16367.3	10.2	***0.001***	0.0031	40.157
	Random 6	15	-16372.4	-16368.3	8.2	***0.004***	0.0054	23.413
	Random 7	15	-16372.5	-16370.8	3.4	0.065	0.0109	6.873
	Random 8	15	-16372.5	-16372.5	0.0	1.000	0.0000	1.000
	Random 9	15	-16371.5	-16368.3	6.4	***0.011***	0.0058	10.102
	Random 10	15	-16370.7	-16370.7	0.0	1.000	0.1345	1.000

* Nine branches were set as the foreground in each analysis, rows in bold show tests which found a significant result.

I repeated this analysis with branches one standard deviation above the mean change in brain mass in order to provide a direct comparison with a previous study (Ali & Meier, 2008). Once again, the results were not interpretable because they were not robust to branch-swapping as described above. Ali and Meier (2008) also report results of branch-randomisation tests but do not find a positive result by chance. However I note that they use model A (test 2) to test for positive selection on branches along which they estimated to show a large change in brain size, but used model B to test for selection on randomly selected branches. I downloaded Ali and Meier's sequence data (see Ali & Meier, 2008 for accession numbers) and repeated their analysis using test 2. I find the significant result reported for by Ali and Meier (2008) where 9 branches with large changes in relative telencephalon size show evidence for positive selection, but when I performed 10 tests where 9 branches were selected at random and set as the foreground I again found that it was possible to obtain a positive result by chance (Table 5.12b). As in my dataset a site-model test for positive selection having acted across the phylogeny is highly significant (LRT: 26.793, $p < 0.001$).

Theses results show that the branch-site models have limited use in demonstrating associations between positive selection and brain mass evolution as significant results can be obtained by chance. Presumably, this is because positive selection on *ASPM* and *CDKRAP2* is pervasive across the phylogeny in both my dataset and Ali and Meier's (2008), making it impossible to detect a change in relation to brain size with the current branch-sites models. Given the branch-site models are specifically constructed to test for episodic positive selection acting on a small number of branches (Anisimova & Yang, 2007), rejecting the hypothesis that positive selection has acted across the whole tree seems like a useful pre-requisite to their use. Furthermore I question the logic of using such a method, based as it is on the assumption of episodic positive selection, to detect associations with the evolution of a continuously distributed phenotype which is believed to evolve in a continuous, relatively gradual manner (see chapter 3). This analysis suggests the conclusion drawn by Ali and Meier (2008), that adaptive evolution of *ASPM* is specifically associated with changes in the relative size of the telencephalon, is not supported.

5.3.6 Gene-phenotype associations within the callitrichids and brain size reduction

Callitrichids have secondarily evolved smaller brain masses (chapter 3) associated with smaller bodies ("phyletic dwarfism") (Ford 1980) but follow the primate wide pattern of an increase in relative brain size. Phylogenetic analysis of brain and body mass suggest the reduction of both traits occurred along multiple lineages during callitrichid diversification (Ah-King & Tullberg 2000; chapter 3). The three callitrichid species (*Callithrix jacchus*, *Leontopithecus chrysomelas* and *Saguinus oedipus*) included in the anthropoid-wide analysis above were identified as strong outliers to the general association between *ASPM* and brain mass, with higher *dN/dS* values than would be predicted, but were not outliers for *CDK5RAP2*. I hypothesised that this may be related to the reduction of brain mass in this clade and further explore the evolution of these two genes within the Callitrichidae using a larger dataset to test the hypothesis that they contribute to the reduction of brain mass in this clade. In total I obtained sequence data for 11 species of callitrichids for both loci. Data was available for one additional tamarin species (*S. labiatus*) for *ASPM*; the results with and without *S. labiatus* do not vary so I present the results including it. The phylogenetic relationships between callitrichid species are taken from Bininda-Emonds *et al.* (2007) (Figure 5.4).

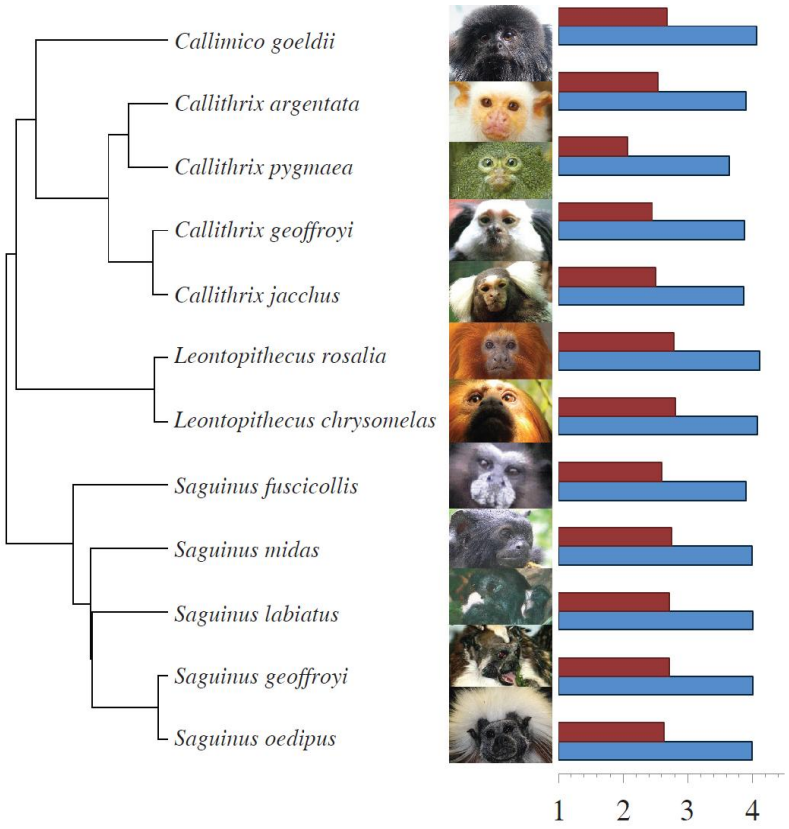

Figure 5.4 Phylogeny of callitrichids considered in this analysis with phenotypic information; log(brain mass[mg]) is shown by the blue bars, log(body mass[g]) by the red. Photographs are from Wikimedia Commons.

For *ASPM* the average *dN/dS* ratio across callitrichids is marginally, but significantly higher than across other anthropoid primates (callitrichid *dN/dS* = 0.558, other anthropoids *dN/dS* = 0.455; LRS = 4.05, p = 0.044). Within callitrichids the site-model test for positive selection is significant (LRS = 24.18, p < 0.001) and estimates that 3.93% of sites evolve adaptively with a *dN/dS* of 5.54, strongly suggesting that positive selection has acted on *ASPM* during callitrichid evolution. Next I tested for an association between the evolution of *ASPM* and callitrichid brain mass. When the pygmy marmoset (*C. pygmaea*) is excluded there is a strongly significant negative association between brain mass and root-to-tip *dN/dS* (t_9 = -2.885, p = 0.007, R^2 = 0.481). The inclusion of the pygmy marmoset, an obvious outlier (Figure 5.5), eliminates significance (t_{10} = -1.341, p = 0.102, R^2 = 0.153) but there is evidence suggesting that this species is a special case among the callitrichids. The pygmy marmoset is by far the smallest callitrichid, and indeed the smallest anthropoid, weighing only 120g, approximately a third of that of the closest relative included in this study, the silvery marmoset (*C. argentata*; Figure 5.4). The brain mass of the pygmy marmoset is almost half that of the silvery marmoset. The diminutive size of the pygmy marmoset is thought to have evolved by rapid and extreme paedomorphism driven by a slowdown in intrauterine growth rate which would affect most traits that are predominantly determined prenatally, such as brain size (Marroig and Cheverud, 2009; chapter 4). Hence, the pygmy marmoset departs from the developmental pathway taken by other callitrichids (chapter 4), which may explain why it is an outlier. I tested the strength of the general association using a Jack-knife approach; the removal of any other species before or after the removal of the pygmy marmoset does not affect the results indicating the pygmy marmoset is a sole outlier to a general trend (Table 5.13).

Consistent with the action of positive selection, the association between *dN/dS* of *ASPM* and callitrichid brain mass (minus the pygmy marmoset) is at least partly driven by changes in the nonsynonymous rate, since there is a significant negative association with *dN* in a partial regression controlling for *dS* (*dN*: t_7 = -2.127, p = 0.035; *dS*: t_7 = 2.857, p = 0.012; R^2 = 0.527). The association is specific to absolute brain mass (no relationship with relative brain size: with the pygmy marmoset: t_{10} = -1.173, p = 1.000, R^2 = 0.121; or without: t_9 = -1.257, p = 1.000, R^2 = 0.149) and cannot be explained by body mass which is unrelated to *dN/dS* (with the pygmy marmoset: t_{10} = -0.604, p = 0.279, R^2 = 0.035; or without: t_9 = -0.813, p = 0.217, R^2 = 0.068).

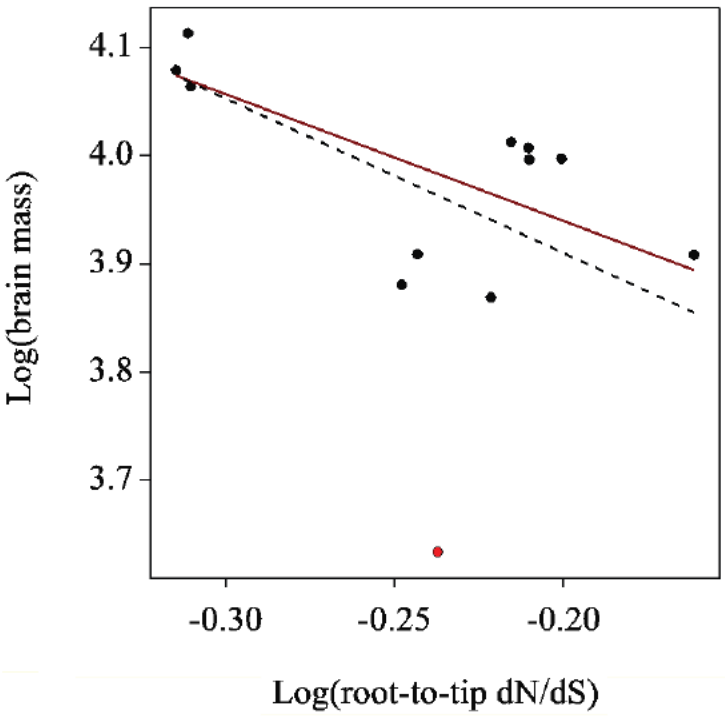

Figure 5.5 Phylogenetically controlled regression between root-to-tip *dN/dS* and brain mass for *ASPM*. The phylogenetically controlled regression line was superimposed on top of raw species values. The dashed line indicates the regression including the pygmy marmoset (*Callithrix pygmaea*, red data point) and the solid line indicates the regression excluding it.

In direct contrast to *ASPM*, the average *dN/dS* of *CDK5RAP2* across callitrichids is significantly lower than across other anthropoids (callitrichid *dN/dS* = 0.485, other anthropoids *dN/dS* = 0.721; LRS = 5.446, p = 0.020). Although there is evidence for positive selection on *CDK5RAP2* within callitrichids (LRS = 13.812, p = 0.001), regardless of whether or not the pygmy marmoset is included there is no significant association between *dN/dS* and either absolute brain mass (with the pygmy marmoset: t_{10} = -0.978, p = 0.175, R^2 = 0.096; without: t_9 = 0.393, p = 1.000, R^2 = 0.019) or relative brain size (with the pygmy marmoset: t_{10} = 1.667, p = 0.062, R^2 = 0.236; without: t_9 = 1.309, p = 0.110, R^2 = 0.176).

Together with the results presented above, this suggests that *ASPM* is intimately associated with both evolutionary increases and decreases in brain mass in anthropoids. These findings also reveal a novel disparity between *ASPM* and *CDK5RAP2*. Whilst both have experienced positive selection across anthropoids and within callitrichids, the phenotypic significance appears to differ, with *CDK5RAP2* being associated with brain mass expansion in anthropoids but not brain mass reduction.

Table 5.13 Jack-knife results to identify outliers and test the robustness of the association between brain size and molecular evolution of *ASPM*

a) before the removal of *C. pygmaea*

Species removed	n	t_n	R^2	p-value
Callimico goeldii	11	-1.007	0.101	0.168
Callithrix argentata	11	-1.444	0.188	0.088
Callithrix geoffroyi	11	-1.274	0.153	0.114
Callithrix jacchus	11	-1.433	0.186	0.090
Leontopithecus rosalia	11	-1.287	0.155	0.112
Leontopithecus chrysomelas	11	-1.365	0.171	0.100
Saguinus midas	11	-1.293	0.157	0.111
Saguinus geoffroyi	11	-1.244	0.147	0.120
Saguinus oedipus	11	-1.255	0.149	0.118
Saguinus labiatus	11	-1.272	0.152	0.115
Saguinus fuscicollis	11	-1.113	0.121	0.146
Callithrix pygmaea	11	-2.885	0.481	***0.007***

b) after the removal of *C. pygmaea*

Species removed	n	t_n	R^2	p-value
Callimico goeldii	10	-2.274	0.393	***0.023***
Callithrix argentata	10	-2.724	0.481	***0.010***
Callithrix geoffroyi	10	-3.239	0.567	***0.004***
Callithrix jacchus	10	-2.649	0.467	***0.012***
Leontopithecus rosalia	10	-3.313	0.578	***0.003***
Leontopithecus chrysomelas	10	-3.385	0.589	***0.003***
Saguinus midas	10	-2.795	0.494	***0.009***
Saguinus geoffroyi	10	-2.686	0.474	***0.011***
Saguinus oedipus	10	-2.694	0.476	***0.011***
Saguinus labiatus	10	-2.746	0.485	***0.010***
Saguinus fuscicollis	10	-2.154	0.367	***0.028***

An alternative explanation for positive selection on *ASPM* relates to its role in the proliferation of germ cells (Pulvers *et al.*, 2010). It has been proposed that *ASPM* could be under sexual selection acting on sperm development or function (Ponting, 2006; Pulvers *et al.*, 2010). However, there is no association between *ASPM* and relative testes size, a measure of sexual selection on males, across anthropoids (Table 5.10) and callitrichids generally do not have high levels of sperm competition (Dixson, 1993). *CDK5RAP2* may affect male fertility (Barrera *et al.*, 2010) but, as for *ASPM*, there is no association between the evolution of *CDK5RAP2* and relative testes mass in anthropoids (Table 5.10). Although it may not be formally possible to

reject this hypothesis there is currently no comparative evidence linking the molecular evolution of either gene to selection acting on testis development or sperm competition. In contrast, the intimate association between the molecular evolution of *ASPM* and both increases and decreases in brain mass evolution in anthropoids, and particularly with neonatal brain mass, strongly supports the hypothesis that *ASPM* had a significant role in primate brain evolution.

5.3.7 Do microcephaly genes contribute to sexual dimorphism in brain size?

Two recent studies have shown associations between brain size and variants of microcephaly genes, but in both of these studies the association is sex specific (Wang *et al*., 2008; Rimol *et al*., 2010) suggesting microcephaly genes may contribute to sexual dimorphism in brain size. Across primates, males and females are subject to differing selective pressures which have had a detectable influence on the evolution of the brain (Lindenfors *et al*., 2007). In humans, sexual dimorphism in whole brain size and the volume of gray and white matter is present at birth suggesting that sexual dimorphism is established during prenatal development (Gilmore *et al*., 2007). Sexual dimorphism in head circumference can also be observed at birth in non-human primates (Joffe *et al*., 2005) suggesting a conserved developmental origin. The production of dimorphism in specific brain regions is known to be related to the effects of testosterone on apoptotic pathways (see Morris *et al*., 2004 for review), hence the apoptotic function of *MCPH1* (Wood *et al*., 2007; Rickmyre *et al*., 2007) may be of relevance. Here I test whether or not the molecular evolution of five microcephaly genes is associated with levels sexual dimorphism in absolute brain size using the anthropoid-wide dataset.

Sex specific data on cranial capacities (Isler *et al*., 2008) were converted to brain mass following Martin (1990). To calculate a measure of sexual dimorphism for absolute brain size I regressed female brain size against male brain size, following Herlyn and Zischler's (2007) treatment of sexual dimorphism in body mass. As sexual dimorphism can result in larger brains in either sex, and because cellular processes such as sex-hormone regulated apoptosis can inhibit or promote cell death (Morris *et al*., 2004), I use both the raw and absolute values of residuals from the regression line as measures of sexual dimorphism. I perform the t-test for significance using a 1-tailed t-test for absolute scores of sexual dimorphism as one expects positive selection to act to bring about increased sexual dimorphism, and a 2-tailed t-test for raw scores as it is

assumed here that selection may act to bring about larger male or large female brains separately. The calculated measures of sexual dimorphism are given in Appendix 1.

Tests for an association with either measure of sexual dimorphism in absolute brain size were non-significant for *ASPM*, *CDK5RAP2* and *STIL* (Table 5.14). However for *CENPJ* I find a significant association with raw scores sexual dimorphism in absolute brain size ($t_{19} = 2.703$, $p = 0.014$, $R^2 = 0.278$; Figure 5.6a). I tested the robustness of this result using a Jack-Knife approach and found that the association is not dependent on the presence of any single data point (Table 5.15). The result is also not explained by an association with sexual dimorphism in body mass size ($t_{19} = 0.737$, $p = 0.470$, $R^2 = 0.028$).

For *MCPH1* I find no association with raw scores of sexual dimorphism (Table 5.14) or with absolute scores. However when *Pan*, which has a high *dN/dS* due in part to a low number of synonymous substitutions, is removed there is a significant positive association with absolute scores of sexual dimorphism (Table 5.14). Again, a Jack-Knife analysis suggests this association is relatively robust (Table 5.15) and the result is not explained by sexual dimorphism in body mass ($t_{19} = -0.435$, $p = 1.000$, $R^2 = 0.010$).

Table 5.14 Phylogenetically controlled regression analysis between root-to-tip *dN/dS* and sexual dimorphism in brain mass

		Absolute Sexual Dimorphism			Raw Sexual Dimorphism		
Gene	**n**	**t-statistic**	**p-value**	**R^2**	**t-statistic**	**p-value**	**R^2**
ASPM	21	0.690	0.250	0.031	-1.930	0.069	0.164
CDK5RAP2	21	0.315	0.378	0.005	-1.252	0.434	0.032
CENPJ	21	-0.374	1.000	0.007	2.703	***0.014***	0.278
MCPH1	21	1.015	0.161	0.051	-0.454	0.655	0.011
MCPH1 (no Pan)	20	1.922	***0.035***	0.170	-0.329	0.746	0.006
STIL	21	0.800	0.217	0.034	-0.643	0.528	0.022

These results suggest a link between the molecular evolution of *MCPH1*, *CENPJ* and the evolution of sexual dimorphism in brain mass in anthropoid primates. The finding that the evolution of these loci is potentially associated with sexual dimorphism in absolute brain mass across anthropoids is an interesting result. An important question therefore is if this relationship

is causative, and if so how could *MCPH1* and *CENPJ* control the development of sexual dimorphism?

Sexual dimorphism in whole brain size, gray matter and white matter develops during early prenatal development (Gilmore *et al.*, 2007) potentially before the second trimester (Joffe *et al*., 2005) meaning it seems likely to have a time of origin that overlaps with the onset of neurogenesis (Rakic, 1995). Combined with evidence linking sexual dimorphism to sex-specific apoptosis controlled by sex hormones (Morris *et al.*, 2004; Forger 2006) this suggests sexual dimorphism in whole brain size potentially results from differences in cell-survival of neural progenitor cells. Apoptosis amongst neural progenitors is thought to have a major influence on the development of brain size (Blaschke *et al.*, 1996; Haydar *et al*., 1999; Roth & D'sa, 2001) and hence sex dependent differences in cell survival at this early stage could result in sexual dimorphism in adult brain size.

MCPH1 is expressed in the foetal brain during neurogenesis and the pathology of *MCPH1*-linked microcephaly (head circumference 5-10 standard deviations below the mean controlled for age) suggests disruption of the gene's function has a major affect on prenatal neurogenesis (Jackson *et al*., 2002). Whilst there is some suggestion *MCPH1* may have an effect on the timing of cell cycle progression (Brunk *et al.*, 2007), there is strong evidence linking it to the DNA damage response pathway (Woods *et al*., 2007; Rickmyre *et al*., 2007; Wood *et al*. 2008). Wood *et al*. (2008) suggest *MCPH1* acts early on in the DNA damage response cascade, potentially promoting the amplification of the response by binding to H2AX, which marks DNA damage sites. It is also interesting to note that the region of the *MCPH1* gene that encodes the domain which interacts with H2AX, the C-terminal BRCT domain (Wood *et al*., 2007), contains the SNP (V761A) which is associated with variation in male but not female cranial capacity (Wang *et al*., 2008). Whilst it is not immediately apparent how *MCPH1* would affect sex-specific apoptosis, there is a strong suggestion that it is expressed at the right time and place, and that it interacts with the right cellular processes to potentially do so.

There are fewer clues as to how *CENPJ* may influence brain development in a sex specific manner. However, of potential interest is the finding that several genes involved in centrosome and spindle pole structure and function are differentially expressed in males and females in developing chick brains, suggesting genes involved in the centrosome may have a role

in the control of sexual differentiation and brain development (Lee *et al*., 2009). Until a clearer causative link can be established between these loci and sex differences in brain development, their role in sexual dimorphism must however remain a hypothesis. However, the combined results presented here, in Wang *et al*. (2008) and in Rimol *et al*. (2010) suggest understanding how microcephaly genes might have a sex-specific effect on brain development could be an interesting endeavour.

Table 5.15 Reverse Jack-knife to examine robustness of associations with scores of sexual dimorphism in brain mass

a) *CENPJ* and raw scores

Genus excluded	t_{19}	p-value	R^2
Alouatta	2.527	0.021	0.262
Aotus	2.300	0.034	0.227
Ateles	2.540	0.021	0.264
Callicebus	2.810	0.012	0.305
Callithrix	2.940	0.009	0.324
Cebus	2.593	0.018	0.272
Cercopithecus	2.645	0.016	0.280
Colobus	2.721	0.014	0.292
Erythrocebus	3.729	0.002	0.436
Gorilla	2.681	0.015	0.285
Homo	2.699	0.015	0.288
Hylobates	2.298	0.034	0.227
Leontopithecus	2.671	0.016	0.284
Macaca	2.827	0.011	0.308
Pan	2.628	0.017	0.277
Papio	2.519	0.021	0.261
Pithecia	2.431	0.026	0.247
Pongo	2.083	0.052	0.194
Presbytis	2.658	0.016	0.282
Saguinus	2.617	0.017	0.276
Saimiri	2.582	0.019	0.270

b) *MCPH1* and absolute scores after the removal of *Pan*

Genus excluded	t_{19}	p-value	R^2
Alouatta	1.796	0.045	0.159
Aotus	1.869	0.040	0.170
Ateles	1.429	0.085	0.107
Callicebus	1.673	0.056	0.141
Callithrix	1.975	0.032	0.187
Cebus	1.690	0.055	0.144
Cercopithecus	1.952	0.034	0.183
Colobus	1.931	0.035	0.180
Erythrocebus	2.056	0.028	0.199
Gorilla	2.335	0.016	0.243
Homo	2.439	0.013	0.259
Hylobates	1.932	0.035	0.180
Leontopithecus	1.860	0.040	0.169
Macaca	2.065	0.027	0.200
Pan	-	-	-
Papio	2.322	0.016	0.241
Pithecia	1.815	0.044	0.162
Pongo	1.339	0.099	0.095
Presbytis	1.730	0.051	0.150
Saguinus	1.889	0.038	0.173
Saimiri	1.868	0.040	0.170

5.4 Conclusions

5.4.1 Molecular evolution of microcephaly genes and brain evolution

Studying the molecular basis of convergent phenotypes has enhanced our understanding of the evolutionary genetics of adaptation and the constraints which act on phenotypic evolution (Arendt & Reznick, 2007). Here I have provided evidence that independent increases in brain mass across anthropoids may share a common genetic basis. This suggests the genetic basis of brain evolution may be strongly conserved and implies that strong developmental constraints may limit the way in which brain development can respond to selection.

By sampling a substantial number of phylogenetically diverse species I have demonstrated that positive selection acted on five microcephaly loci across the anthropoid phylogeny and was not, as previously reported, restricted to lineages leading to humans. To my knowledge this study is the first to implement robust codon based models to test for positive selection acting on these loci across anthropoids (a previous study reporting such a finding (Wang & Su, 2004) used Model 3 in PAML which is not a robust test for positive selection (Anisimova *et al*., 2002)). This is a striking result as pervasive positive selection is considered rare. However, as brain size has increased multiple times independently and is likely to have been under strong selection in all major groups of anthropoids (chapter 3), such widespread positive selection on genes involved in the evolution of brain size should perhaps be expected.

I explored whether this selection is relevant to gross brain size evolution using phylogenetically controlled regressions which show that the average *dN/dS* across *ASPM* and *CDK5RAP2* is significantly related to absolute neonatal brain mass and that in both cases a relatively large proportion of the variance is explained (R^2 = 0.369 and 0.255 respectively). Furthermore, two key predictions of a gene's involvement in prenatal neurogenesis were verified for *ASPM* and *CDK5RAP2*: (i) an association with absolute brain mass as this correlates closely with total neuron number (Herculano-Houzel *et al.*, 2007) and (ii) a stronger association with neonatal than adult brain mass as cortical neurogenesis is largely restricted to prenatal development (Rakic, 1988; Rakic, 2002; Bhardwaj *et al.*, 2006).

These results are not explained by a general association with body mass, nor can they be attributed to random or genome-wide effects, since no associations were found with three other

microcephaly genes (*CENPJ, MCPH1* and *STIL*) or eight control genes. Thus, although the results are only marginally significant, my control tests and the highly consistent pattern observed in the significant results strongly suggest the associations found are unlikely to be Type I errors. The results using multiple regressions suggest that while positive selection on *ASPM* has brought about an increase in *dN/dS* mainly through an acceleration in *dN* relative to *dS*, the pattern for *CDK5RAP2* may be more complex. This suggests that caution should be exercised in interpreting *dN/dS* ratios, and I recommend the use of supplementary analyses such as multiple regressions to disambiguate correlations involving this measure. Together with the demonstration of positive selection in the site analyses, these results imply that adaptive evolution on *ASPM* and *CDK5RAP2* has been involved in independent changes in brain size along multiple lineages during primate evolution through a role in prenatal neurogenesis.

Although I detect a general positive association for *ASPM* and *CDK5RAP2* there are notable outliers, which may suggest a more complex relationship between the evolution of these loci and brain size. For both loci *Papio* has a much lower *dN/dS* than would be predicted given the size of the brain in this species. Assuming the association between *ASPM, CDK5RAP2* and brain evolution has a genuine, functional basis, the *Papio* discrepancy may indicate brain expansion can occur independently of the evolution of these loci. However as *Papio* is not represented in my neonatal dataset I cannot say whether it is an outlier due to pre or postnatal developmental processes. The high rate of evolution of *ASPM* in callitrichids led me to explore the hypothesis that *ASPM* contributed to the evolution of reduced brain mass in this clade. I found a strong signal of positive selection and a negative association between *dN/dS* and brain mass within callitrichids suggesting this was the case. *ASPM* therefore appears to be intimately linked to both increases and decreases in brain mass. In contrast *CDK5RAP2* shows no association with brain mass in callitrichids suggesting some disparity in their evolutionary roles. This is supported by further differences in the association tests in anthropoids, whereas *ASPM* is particularly strongly associated with neocortex size, *CDK5RAP2* is not.

Despite demonstrating *CENPJ, MCPH1* and *STIL* have experienced pervasive positive selection during anthropoid evolution I found no significant relationship between either locus and any measure of absolute or relative brain mass. This potentially indicates a further dichotomy in evolutionary roles among microcephaly genes and raises the issue of whether these

loci are involved in the evolution of other traits or more specific aspects of brain phenotype that were not considered here. It is important to emphasize that the phenotype(s) on which selection for *CENPJ*, *MCPH1* and *STIL* is acting in primates has not been established and this study provides no evidence that they are involved in the evolution of gross measures of size of the whole brain or neocortex. Instead I provide evidence suggesting *CENPJ* and *MCPH1* may be involved in the evolution of sexual dimorphism, but functional links must be demonstrated to support this result.

It is often tempting to interpret studies of molecular evolution with reference to a particular phenotype, but this is clearly problematic. Genes with key developmental roles which evolve adaptively and which have major phenotypic effects when disrupted, such as the microcephaly loci, may have either no or only a subtle role in that phenotype's evolution. For example, as demonstrated here, *STIL* does not appear to be associated with any proposed phenotype whilst *MCPH1* and *CENPJ* may have a relatively subtle effect on brain evolution. These results suggest utilising the full diversity of primates and incorporating information about the evolutionary history of brain size in different lineages will prove a productive way of exploring the genetic basis of brain evolution.

5.4.2 Why do *ASPM* and *CDK5RAP2* differ?

The disparity between the roles of *ASPM* and *CDK5RAP2* in brain size reduction may ultimately be explained by differences in their cellular function. *ASPM* and *CDK5RAP2* appear to contribute to the proliferation of different progenitor cells, with *ASPM* influencing cell fate in neuroepithelial cells (Fish *et al.*, 2006) whilst *CDK5RAP2* has a proposed role in the proliferation of radial glial cells (Buchman *et al.*, 2010). The results suggest the significance of changes in the proliferation of neuroepithelial cells and radial glial cells may differ during brain size expansion and reduction in anthropoids. Of possible relevance is the reduction in gyrification (or folding) of the cortex in callitrichids (Zilles *et al.*, 1989). It has recently been shown that gyrencephalic brains are characterised by neural progenitor cell proliferation in the ventricular zone (VZ) and, unlike species with lissencephalic (smooth) brains, in the outer subventricular zone (OSZV). This additional region of proliferation in gyrencephalic species is hypothesised to make a significant contribution to cortical expansion (Fietz *et al.*, 2010; Hansen

et al., 2010). Proliferating cells in the OSVZ show characteristic features of radial glial cells (Fietz *et al.*, 2010) hence if *CDK5RAP2* has an evolutionary role contributing to the proliferation of radial glial (or radial glial-like) cells its capacity to influence brain evolution may be reduced in lissencephalic species with reduced levels of proliferation in the OSVZ. As *ASPM* contributes to regulating neuroepithelial cell fate in the VZ (Fish *et al.*, 2006) the ability of selection to shape brain size development through this locus would not be associated with changes in gyrification.

I also present evidence that *ASPM* is more closely linked to the evolution of cortical size, in particular cortical grey matter, than the size of the rest of the brain, whilst *CDK5RAP2* is not. It may be that the two loci contribute to the evolution of different brain components, a result that is not necessarily predicted by the phenotypes they present when disrupted in individuals with primary microcephaly (Thornton & Woods, 2009).

5.4.4 Summary

I have presented evidence implicating *ASPM* and *CDK5RAP2* in the evolution of brain size across anthropoid primates, a result which is consistent with an effect of the two loci on neurogenesis via mitotic spindle orientation. Despite showing that *CENPJ, MCPH1* and *STIL* have been subject to positive selection I find no evidence to link these loci to the evolution of gross brain size, the mechanism of selection acting on these loci is therefore unresolved but I provide evidence linking *CENPJ* and *MCPH1* to sexual dimorphism in brain mass. These results demonstrates the importance of including phenotypic data and a phylogenetically broad range of species when attempting to associate the evolution of genes with brain size evolution (Carroll, 2003; Goodman *et al*., 2005; Barton, 2006c; Pollen & Hoffmann, 2008; Vallender, 2008). This point is especially pertinent to the literature on human genetic evolution where claims are often based on differences between humans and chimpanzees or a small number of non-human primates. The results also clearly highlight the importance of including measures of neonatal brain size in studies of primate brain evolution. Finally my results suggest a conserved genetic basis for brain evolution in primates, providing an important example where genetic basis of a complex developmental phenotype has involved coding sequence evolution.

Chapter 6

Evolutionary genetics of neural progenitor proliferation

& the expansion of radial growth: *NIN* as a candidate

"There is nothing in this world constant, but inconstancy."

Jonathon Swift, *A Critical Essay upon the Faculties of the Mind*, 1707

6. Evolutionary genetics of neural progenitor proliferation & the expansion of radial growth: *NIN* as a candidate

6.0 Summary

Herculano-Houzel *et al*. recently provided convincing evidence that the number of neurons under a unit area of cortical surface is not constant, and therefore that the number of neurons per cortical mini-column is not constant, contradicting a long held dogma in comparative mammalian neuroanatomy. The Radial Unit Hypothesis predicts that increasing the duration of asymmetric, neurogenic division of radial glial cells would result in radial expansion through an increased number of neurons/column. Little is known about the genetics which contribute to the evolution of neuron number per radial unit but recently a centrosomal protein encoded by a gene called *NIN* has emerged as a candidate. *NIN* is necessary for centriole maturation and is critical for maintaining asymmetric, proliferative divisions of radial glial cells in the ventricular zone. Here I explore the molecular evolution of *NIN* across 22 species of anthropoids and demonstrate positive selection has acted on *NIN*. I present evidence linking the molecular evolution of *NIN* to variation in brain size and in particular variation in neuron number not explained by lateral expansion in surface area. These results are consistent with the Radial Unit Hypothesis and suggest cortical thickness and surface area have an independent genetic basis. However the results require confirmation in larger datasets.

6.1 Introduction

The expansion of the primate brain is largely due to an expansion in the surface area and concomitant folding of the cerebral cortex (Jerison, 1973; Prothero & Sundsten, 1984; Hofman, 1989). In contrast, it has historically been agreed that brain expansion in mammals is accompanied by a disproportionately small increase in cortical thickness (Hofman, 1989). Cortical surface area scales with brain volume in a log-log relationship with a slope of 0.8-0.9; in contrast, cortical thickness scales with a semi-log relationship, with a much lower slope of c. 0.2 and shows larger increases in smaller brained species with less gyrified brains than in species with large, highly folded brains (Hofman, 1989).

The Radial Unit Hypothesis (Rakic, 1988, 1995, 2007) provides a developmental explanation for this pattern of increasing surface area without major increases in thickness. The Radial Unit Hypothesis states that the cortex is constructed of stacks of radially arranged neurons, called ontogenetic columns, each of which has its origins from the same region of the ventricular zone (VZ), the area of the developing brain where cortical neurons originate (Rakic, 1988). The number of these ontogenetic columns determines the surface area of the cortex, whereas the number of neurons in each column determines the thickness (Rakic, 1988, 1995). The neurons in each column are derived from the same apical progenitor cell; these cells undergo a period of symmetric, proliferative division producing an exponentially increasing progenitor pool, before switching to asymmetric, neurogenic divisions (Götz & Huttner, 2005). Increasing the duration of the proliferative divisions of apical progenitor cells would therefore produce a lateral expansion of the cortex through increased numbers of ontogenetic columns, whereas increasing the duration of neurogenic division would result in radial expansion through increased numbers of neurons/column (Rakic, 1998, 1995; Cavines *et al*., 1995). A predominance of the role of the former would explain the dominant role of increases in surface area during brain expansion. The relative constancy in cortical thickness has been explained by invoking developmental constraints which either affect neuronal migration into ontogenetic columns along radial glial cells that may have an upper length limit, or affect the spacing of cortical columns, as increasing the number of neurons per column requires increasing distance between columns to allow axons and dendrites to pass down radially through the cortex (Streidter, 2005). Cortical thickness may therefore be an example of how brain evolution is intrinsically constrained, with

inherited developmental programs determining the paths brain evolution can take (Hofman, 1989).

Several extensions to the Radial Unit Hypothesis have been proposed. One criticism of the hypothesis that the expansion of the cortex is primarily due to a lateral expansion of radial units is that this would cause the observed increase in the surface area of the cortex but also an increase in the lateral ventrical, which is not seen (Kriegstein *et al.*, 2006). A role for the proliferation of neurogenic progenitor cells after the cessation of symmetric division of apical progenitors has therefore been invoked (Kriegstein *et al*., 2006; Pontious *et al.*, 2008; Fietz *et al*., 2010). At the onset of neurogenesis apical progenitors divide asymmetrically to produce a neuron and a radial glial cell. These radial glial cells undergo a number of asymmetrical divisions to produce another radial glial cell and either a neuron or a basal (or intermediate) progenitor cell which migrates to the sub-ventricular zone (SVZ) and divides symmetrically to produce two neurons (Götz & Huttner, 2005). A shift towards the production of basal progenitors over single neurons could therefore double the number of neurons produced (Kriegstein *et al*., 2006; Pontious *et al.*, 2008). The Radial Unit Hypothesis predicts these extra neurons would contribute to radial growth (i.e. an increase in radial unit thickness and the number of neurons per column). An alternative hypothesis, the Intermediate Progenitor Hypothesis, predicts these will contribute to two ontogenetic units and therefore to lateral expansion (Pontious *et al*., 2008).

It has recently been shown that gyrencephalic brains are characterised by neural progenitor cell proliferation in the VZ and, unlike species with lissencephalic (smooth) brains, in the outer subventricular zone (OSZV). This additional region of proliferation in gyrencephalic species is hypothesised to make a significant contribution to cortical expansion (Fietz *et al.*, 2010; Hansen *et al.*, 2010). Proliferating cells in the OSVZ show characteristic features of radial glial cells and repeatedly divide asymmetrically, self-renewing and producing a neuron with each division (Fietz *et al.*, 2010). The repeated division of these OSVZ progenitors could therefore affect neuron number, and could have a much larger effect than the apical-progenitor to basal-progenitor lineage (Fietz *et al.*, 2010). It is thought that increased neuronal production via OSVZ-progenitors would lead to cone-shaped radial units, with wider pial surfaces than ventrical surfaces, as OSVZ-progenitors maintain contact with the pial surface and may act as founder cells of radial subunits (Fietz & Huttner, 2010). Fietz and Huttner (2010) have therefore

suggested the increase in basal-over-apical ratio of radial units in gyrencephalic cortices reflects either an increase in the number of OSVZ-progenitors produced per apical progenitor and/or increase in the number of neurons produced per single OSVZ-progenitor. In both cases the mitotic division of the progenitor cells is asymmetric.

Rakic's (1988, 1995) ontogenetic columns, or radial units, are thought to be represented in the adult brain by cortical minicolumns (Mountcastle, 1997; Horton & Adams, 2005). Minicolumns are vertically orientated aggregations of cells which extend across cortical layers II-VI with vertical interconnections (Mountcastle, 1997). These minicolumns are preserved through pre and postnatal development and senescence (Casanova *et al*., 2007) and are thought to form functional units and the basic microcircuit in the cortex (Mountcastle, 1997; Casanova *et al.*, 2009).

A long held dogma in comparative neuroanatomy was that the number of neurons in each minicolumn was constant across mammals (Rockel *et al*., 1980; Cheung *et al*., 2007). This suggested that the number of asymmetric, neurogenic divisions per apical progenitor was highly conserved despite the expectation that variation in minicolumn configuration should emerge as species-specific adaptations (Buxhoeveden & Casanova, 2002). However, Herculano-Houzel *et al*. (2008) recently provided convincing evidence that the number of neurons under a unit area of cortical surface is not constant, and therefore that the number of neurons per mini-column is not constant. Across 9 species of primates and one treeshrew the number of neurons per $1mm^2$ of cortical surface area was shown to vary with neuron density, which did not covary with cortical mass (Herculano-Houzel *et al*., 2008). These results confirm previous reports that the number of neurons per minicolumn does vary across mammals (Haug, 1987; Stolzenburg *et al*., 1989; Poth *et al*., 2005; Casanova *et al*., 2009). In addition, variation in cortical thickness is associated with some neurodevelopmental disorders (Narr *et al.*, 2005; Hardan *et al*., 2006) and neurodegenerative disorders (Rosas *et al*., 2005; Lerch *et al*., 2005), suggesting a link between motor and cognitive performance and at least cortical thickness, if not the number of neurons per radial unit, suggesting there may be phenotypic consequences to these evolved differences. This variation in radial neuron number is presumably due to changes in the duration of asymmetric, neurogenic divisions of radial glial cells and/or OSVZ-progenitors suggesting these cell-fate switches play a role in the evolution of brain size in addition to evolved differences in the

proliferation and survival of apical progenitors. Whilst several candidate genes have been proposed to contribute to the expansion of the apical progenitor pool and hence the number of ontogenetic units and cortical surface area (see chapter 5) we know little about the genetics which might contribute to the evolution of increased numbers of neurons per radial unit.

Recently a possible candidate gene has emerged. *NIN* (or *ninein*) encodes a protein with a coiled-coil structure characteristic of centrosome-associated proteins (Bouckson-Castaing *et al*., 1996). It is thought to act in microtubule minus-end capping and stabilisation as an anchoring protein and centrosome maturation factor (Mogensen *et al.*, 2000; Chen *et al.*, 2003). NIN localises at the centrosome in most cells and primarily on the mother centrioles in post-mitotic cells (Piel *et al*., 2000). It is thought that mother and daughter centrioles make distinct contributions to centrosomal activity, related to differences in microtubule anchoring, and that this may contribute to asymmetric cell fate (Piel *et al*., 2000; Mogensen *et al*., 2000). In proliferating neuronal precursors localisation is specific to the centrosome but mother and daughter centrioles show differences in the concentration of NIN (Ohama & Hayashi, 2009). These differences have been proposed to contribute to variation in microtubule association of the centrosomes in dividing radial glial cells and may be responsible for the asymmetric fate of daughter cells (Ohama & Hayashi, 2009). The intrinsic asymmetry between mother and daughter centrioles has been shown to contribute to cell fate in asymmetrically dividing radial glial cells, with the differentiated neuron inheriting the daughter centrioles and the renewed radial glial cell inheriting the mother centrioles (Wang *et al*., 2009). Suppression of *NIN* is sufficient to disrupt this pattern of inheritance and results in premature depletion of radial glial cells and a temporal increase in neuron output (Wang *et al*., 2009). This suggests *NIN* is necessary for centriole maturation and is critical for maintaining asymmetric, proliferative divisions of radial glial cells in the VZ (Wang *et al*., 2009).

If *NIN* has a role in evolutionary changes to the duration of this type of division it could contribute to variation in the number of neurons per radial unit (Götz & Huttner, 2005) Alternatively if *NIN* has a similar role in the asymmetric division of radial glial-like OSVZ-progenitor cells (Fietz *et al*., 2010) it may contribute to the expansion of cortical surface area. However, *NIN* also has other non-neurogenic functions. As well as being localised at the centrosome it is found in cytoplasmic speckles (Moss *et al*., 2007). These speckles are

particularly prominent in neurons (Baird *et al*., 2004) and may have a role in the rapid reorganisation of microtubules in dendrites and epithelial cells and therefore to cell migration and morphology (Baird *et al*., 2004; Moss *et al*., 2007; Matsumoto *et al*., 2008).

In this chapter I describe an analysis of the molecular evolution of *NIN* across 22 species of anthropoid primates. I test the hypothesis that this locus has experienced positive selection during anthropoid evolution and explore how its rate of evolution relates to the evolution of brain size and the evolution of characteristics of radial units as inferred using data on cortical thickness, surface area and neuron number (Herculano-Houzel *et al*., 2008).

6.2 Materials summary

Laboratory methods are detailed in chapter two. I sequenced the two largest exons of *NIN*, exon 18 (503bp) and exon 19 (2141bp), which together account for 41.28% of the total coding sequence of the longest predicted transcript on Ensembl (ENST00000382041). This stretch includes the important functional coiled-coil domain. Sequences were obtained for 5 apes, 6 Old World monkeys and 11 New World monkeys representing all major clades of anthropoid primates. The phylogeny is as shown in Figure 5.1 with *Trachypithecus auratus* being the second species of Colobinae and with the addition of *Callimico goeldii*, which is the sister genus to *Callithrix* as shown in Figure 3.1. All phenotypic data are derived from sources discussed in chapter two; in this chapter whole brain size, cortical thickness, cortical surface area and cortical neuron number are used to test hypotheses relating to the role of *NIN* in brain evolution. Data for the cortical phenotypes are available for 8 anthropoids; *Callithrix jacchus*, *Aotus trivirgatus*, *Callimico goeldii*, *Saimiri sciureus*, *Cebus apella*, *Papio sp.* and two species of *Macaca* (*M. fasicularis* and *M. radiata*). As my genetic data comes from *Macaca mulatta* I took the average values of the two *Macaca* species. This dataset is therefore limited to only 7 species and therefore additional data may be needed to confirm the results obtained in this chapter; however the present analysis could provide some initial insights into the evolutionary role of *NIN*.

Estimation of *dN/dS* ratios (ω) was carried out using a codon-based maximum likelihood method (PAML version 4, Yang, 2007 see chapter 2). Several analyses were performed to test the hypothesis that *NIN* experienced positive selection across primates. To detect positive selection I implemented the site models. I used the branch models to test whether *dN/dS*

significantly differed between Apes, Old World Monkeys and New World Monkeys, between platyrrhine and catarrhines clades and stem branches. The branch models were also used to estimate the average *dN/dS* ratio from the ancestral anthropoid to each terminal species tip. These values were then set as species data and used in a PGLS regression with measures of brain size in BayesTraits to test for gene-phenotype associations (see chapter 2).

6.3 Results & discussion

6.3.1 *NIN* evolved under positive selection during anthropoid evolution

Site model tests using a codon-based maximum likelihood method (Yang, 2007) were performed to test for the signature of positive selection having acted on the concatenated sequences for exons 18 and 19 across 22 species of anthropoids. Strong evidence was found to support the hypotheses that *NIN* has evolved adaptively during anthropoid evolution (Table 6.1); 12.7% of sites evolved under a *dN/dS* of 2.274. Bayes Empirical Bayes identified 24 sites as evolving under positive selection but only two sites had significant posterior probabilities at $p < 0.05$: amino acid 644 ($p = 0.05$) and 740 ($p = 0.032$) both in exon 18 of the human transcript (ENST00000382041). I explored the distribution of positive selection between the three main anthropoid clades by performing site models on each clade separately (Table 6.1). In no case was the test significant, although for both New and Old World Monkeys the p-value approaches significance suggesting positive selection may be evenly distributed across the phylogeny and the loss of significance is due to a reduction in power with lower sample sizes or possibly due to particularly strong positive selection occurring on in the deeper branches. In support of this conclusion a branch model test comparing the evolutionary rate averages across sites between the three clades is not significant (Table 6.2a).

Table 6.1 Site model results: tests for positive selection

			Model 2a			Model 1a		
Gene	**Clade**	**n**	**lnL(M2a)**	**p, ω > 1**	**ω**	**lnL(M1a)**	**LRT statistic**	**p-value**
NIN	All anthropoids	22	-12762.9	0.127	2.274	-12771.9	18.014	***<0.001***
	Apes	5	-4047.5	-	-	-4048.0	0.938	0.626
	OWM	6	-4041.0	-	-	-4044.0	5.956	0.051
	NWM	11	-5694.2	-	-	-5694.2	5.349	0.069

Table 6.2 Branch model results: comparing rates between clades

a)	Model 2				Model 0		
Gene	***dN/dS* Apes**	***dN/dS* OWM**	***dN/dS* NWM**	**lnL(M2)**	**lnL(M0)**	**LRT statistic**	**p-value**
NIN	0.421	0.326	0.414	-10632.2	-10632.9	1.586	0.452

b)	Model 2			Model 0		
Gene	***dN/dS* Platyrrhine stem**	***dN/dS* Catarrhine stem**	**lnL(M2)**	**lnL(M0)**	**LRT statistic**	**p-value**
NIN	0.627	0.168	-10630.4	-10632.9	5.105	***0.024***

Gene	***dN/dS* Platyrrhine clade**	***dN/dS* Catarrhine clade**	**lnL(M2)**	**lnL(M0)**	**LRT statistic**	**p-value**
NIN	0.414	0.395	-10632.8	-10632.8	0.073	0.964

Branch models were also used to calculate the root-to-tip *dN/dS* for each species. These values were generally higher for platyrrhines than catarrhines (Table 6.3). To test if this was a significant difference I performed a phylogenetically-controlled t-test (Organ *et al*., 2007). This confirmed a significantly higher root-to-tip *dN/dS* for platyrrhines (t_{20} = 3.716, p = 0.013, R^2 = 0.269). To identify whether this was due to higher rates during the origin or diversification of platyrrhines I performed two branch model tests comparing the rates of evolution on the platyrrhine and catarrhine stem branches and the platyrrhine and catarrhine clades (excluding the stem branch). These show that the higher root-to-tip *dN/dS* values can be largely explained by a higher rate of evolution along the stem lineage leading to platyrrhines (*dN/dS* = 0.627) than on the stem lineage leading to catarrhines (*dN/dS* = 0.168). The average *dN/dS* in each clade excluding these branches was not significantly different. Whether this difference reflects positive selection or relaxed constraint, or whether it relates to some difference in phenotypic evolution at the origin of these two clades, is difficult to resolve.

Table 6.3 Root-to-tip *dN/dS* ratio for *NIN*

NIN	
Genus	***dN/dS***
Homo	0.287
Pan	0.268
Gorilla	0.298
Pongo	0.298
Hylobates	0.232
Macaca	0.213
Papio	0.220
Cercopithecus	0.214
Erythrocebus	0.261
Trachypithecus	0.275
Colobus	0.214
Alouatta	0.587
Ateles	0.607
Callicebus	0.455
Pithecia	0.540
Aotus	0.512
Cebus	0.377
Saimiri	0.405
Saguinus	0.409
Leontopithecus	0.386
Callithrix	0.370

6.3.2 Associations between evolutionary rate & brain mass

I next explored the relationship between the evolution of *NIN* and the evolution of whole brain size. Across anthropoids no significance association was found between adult brain mass and *NIN* root-to-tip *dN/dS* (Table 6.4). However, as there is a shift in *dN/dS* between platyrrhines and catarrhines this is not surprising. When analysed separately there is a trend between the two measures in both catarrhines and platyrrhines (Table 6.4; Figure 6.1). For each clade there is a single datapoint which appears to be an outlier; *Homo* for catarrhines and *Cebus* for platyrrhines. When these are removed the trend becomes significant and the effect is particularly strong for platyrrhines (Table 6.4; Figure 6.1). *Homo* and *Cebus* have the largest residuals from the regression equation in catarrhines and platyrrhines respectively (*Homo*: 0.623, non-*Homo* catarrhine range: -0.321 to 0.219; *Cebus*: 0.593, non-*Cebus* platyrrhines range -0.361 to 0.349).

Table 6.4 Phylogenetically controlled regression analysis between root-to-tip *dN/dS* and brain phenotypes

Clade	n	Adult whole brain		
		t-stat	p	R^2
All anthropoids	21	0.794	0.218	0.032
Catarrhines	10	1.799	0.055	0.288
Catarrhines without *Homo*	9	1.978	***0.044***	0.359
Platyrrhines	11	1.486	0.086	0.197
Platyrrhines without *Cebus*	10	3.368	***0.005***	0.586

Trends or significant associations are also found with neonatal brain mass for catarrhines (with *Homo*: $t_6 = 5.053$, $p = 0.001$, $R^2 = 0.810$; without *Homo*: $t_5 = 5.430$, $p = 0.001$, $R^2 = 0.855$) and platyrrhines (with *Cebus*: $t_3 = 1.369$, $p = 0.132$, $R^2 = 0.385$; without *Cebus*: $t_2 = 3.741$, $p = 0.056$, $R^2 = 0.790$) when considered separately. The sample sizes for the separated neonatal datasets are small precluding any definitive comparisons between associations with adult and neonatal brain mass. However AIC values are lower for the association with neonate brain size for catarrhines (with *Homo*: neonate AIC = -8.213, adult AIC = -7.893; without *Homo* neonate AIC = -8.632, adult AIC = -7.893) suggesting a better fit with neonatal brain size, although the difference is not substantial. Within the platyrrhines the AIC is marginally lower when *Cebus* is

included (neonate AIC = 7.618, adult AIC = 7.854) but when *Cebus* is excluded it is not (neonate AIC = 3.222, adult AIC = 1.773); again, in both cases the difference is less than the threshold for supporting one model over another. It is therefore not possible to say whether or not the evolution of *NIN* is more closely associated with prenatal brain growth than postnatal brain growth as would be predicted if it has a role in neurogenesis. It is notable however that *Homo*, and to lesser extent *Cebus*, have larger effects on the association with adult brain mass than neonatal brain mass (difference in p-values for catarrhines with/without *Homo* for neonatal brain mass = 0.000; for adult brain mass = 0.015; difference in p-values for platyrrhines with/without *Cebus* for neonatal brain mass = 0.077; for adult brain mass = 0.117) which perhaps suggests the deviation from the general trend is primarily due to postnatal changes in development.

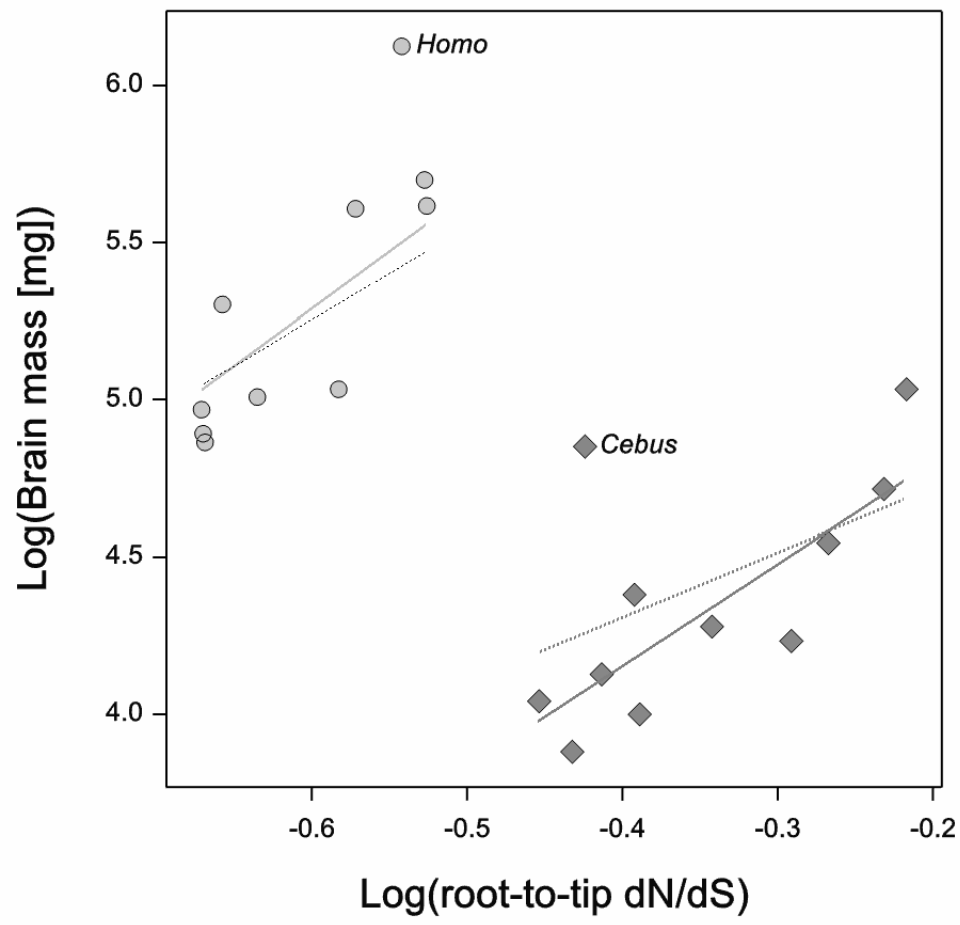

Figure 6.1 Phylogenetically controlled regressions between root-to-tip *dN/dS* and brain mass Catarrhines are shown in light grey circles, platyrrhines in dark grey diamonds. Solid lines are phylogenetically controlled regressions performed separately for the two clades without *Homo* or *Cebus*, apparent outliers, dashed lines are including them.

6.3.3 Associations between evolutionary rate & radial expansion

Although data on cortical phenotypes are limited, I used the available information to test the hypothesis that the observed trends between *NIN* and brain mass are explained by *NIN* having a role in the evolution of increased neural proliferation through asymmetric division bringing about changes in neuron number through radial growth rather than lateral expansion.

Of initial interest is the observation that platyrrhines and catarrhines may have differences in cortical cyto-architecture. Data from Herculano-Houzel *et al*. (2008) suggest that although the catarrhines sampled had larger cortical masses, surface areas and larger numbers of cortical neurons than the platyrrhines sampled, platyrrhines had higher neuron densities and larger numbers of neurons under 1mm^2 of cortical surface (Figure 6.2). This is of particular interest given the observed difference in evolutionary rates on the stem lineages leading to catarrhines and platyrrhines, if this phenotypic difference emerged at the origin of the two clades.

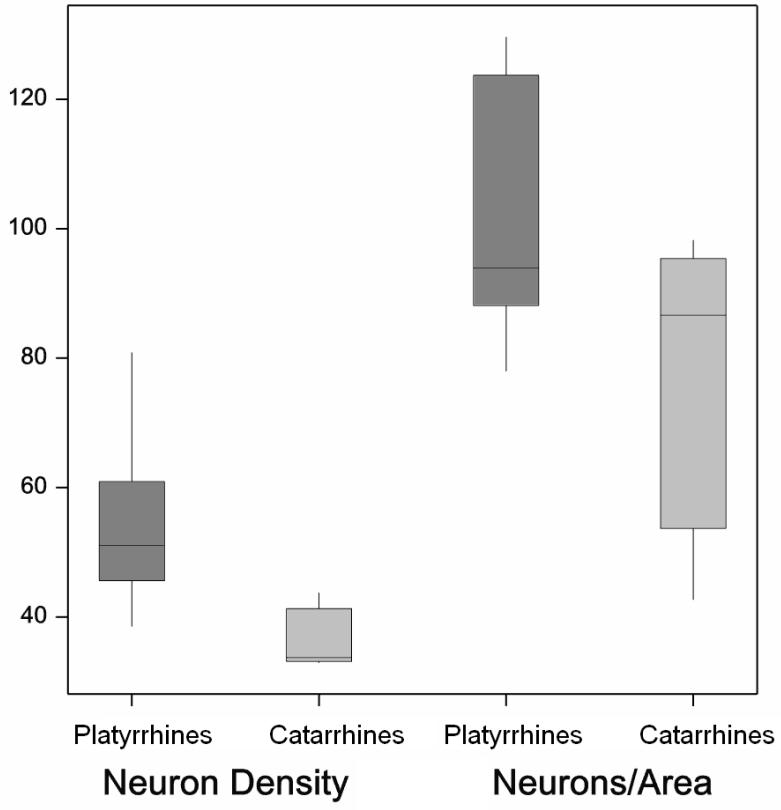

Figure 6.2 Boxplots showing neuron density and neurons per mm^2 of cortical surface in platyrrhines (dark grey) and catarrhines (light grey). The box that spans the interquartile range with a line indicating the median. Whiskers are drawn as far as the minimum and maximum values. The y-axis is neurons/mm^3 for neuron density and neurons/mm^2 for neurons/area.

However, phylogenetically-controlled t-tests (Organ *et al*., 2007) for differences in neuron density and neurons per mm^2 of cortical surface between the clades are not significant (neuron density: $t_6 = 0.700$, $p = 0.510$, $R^2 = 0.075$; neurons per mm^2 of cortical surface: $t_6 = 0.445$, $p = 0.672$, $R^2 = 0.032$) but given the small sample size (3 catarrhines, 5 platyrrhines) there may be little power in this test.

To test for associations between the evolution of *NIN* and radial expansion I first performed a regression analyses between neuron number and cortical surface area using PGLS (see chapter 2). The regression was significant ($t_6 = 12.716$, $p < 0.001$, $R^2 = 0.970$) as previously reported (Herculano-Houzel *et al*., 2008). The residuals from the regression equation:

*Log(cortical neuron number) = 1.196 * Log(cortical surface area) – 1.784*

were used as a measure of the variation in neuron number not explained by lateral expansion, which must therefore be explained by radial expansion. A phylogenetically controlled regression between these values (termed "radial neuron number") and root-to-tip *dN/dS* suggests a trend exists ($t_5 = 1.732$, $p = 0.072$, $R^2 = 0.373$; Figure 6.3). To test whether or not this trend exists due to variation in *dN* or *dS* I performed a multiple regression with *dN* and *dS* as separate variables. *dN* is found to show a positive trend with variation in radial neuron number but *dS* shows no association (*dN:* $t_3 = 1.957$, $p = 0.073$; *dS*: $t_3 = -0.376$, $p = 0.366$; $R^2 = 0.493$) consistent with the action of positive selection (see chapter 5).

I next sought to confirm that this trend was driven by an association with variation in neuron number, controlled for surface area, rather than vice versa. This was done using multiple regressions between root-to-tip *dN/dS*, neuron number and cortical surface area. The results are consistent with the trend being driven by neuron number (Table 6.5). I repeated this multiple regression replacing neuron number with cortical thickness to test the specificity of the association. The results suggest there is no underlying trend with cortical thickness (Table 6.5) and therefore implies specificity with variation in the number of neurons under a unit area of cortical surface. In addition there is no positive trend with total neuron number ($t_5 = -0.635$, $p = 1.000$, $R^2 = 0.075$) or surface area ($t_5 = -0.932$, $p = 1.000$, $R^2 = 0.148$) when considered alone suggesting *NIN* is not associated with lateral expansion of the primate cortex.

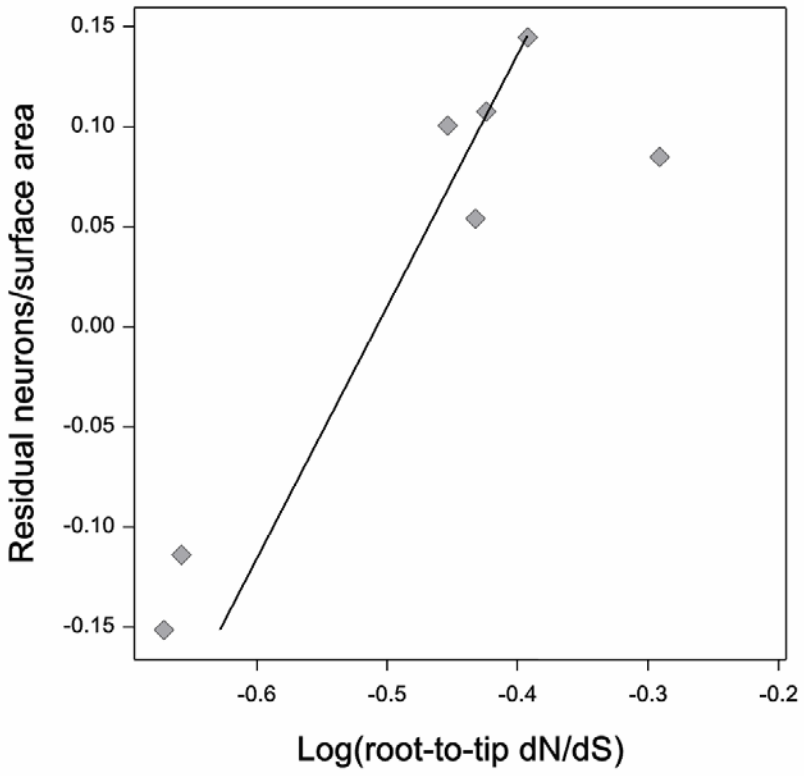

Figure 6.3 Phylogenetically controlled regressions between root-to-tip *dN/dS* and radial neuron number. Data points are raw species values. The phylogenetically controlled regression line was estimated in BayesTraits and superimposed on top of species data.

Table 6.5 Multiple regressions with cortical neuron number and thickness controlling for cortical surface area

Phenotype	**n**	**t-stat**	**p**	**t-stat**	**P**	**R^2**
Cortical neuron number	7	1.766	0.088	-	-	0.521
Cortical surface area		-	-	-1.412	1.000	
Cortical thickness	7	0.332	0.381	-	-	0.523
Cortical surface area		-	-	-0.840	1.000	

Although not significant at $p < 0.05$ and based on a limited dataset the trends may be indicative of a role for *NIN* in brain evolution. More phenotypic data are clearly needed to confirm this conclusion, but the combined results may indicate that the adaptive evolution of *NIN* may have phenotypic relevance to brain evolution, and I suggest this relevance could relate to its contribution to cell fate during asymmetric division of neural progenitors. Variation in the duration of asymmetric division of radial glial cells or radial glial-like OSVZ progenitors could make substantial contributions to the evolution of neuron number (Götz & Huttner, 2005; Fietz & Huttner, 2010). According to the Radial Unit Hypothesis (Rakic, 1988, 1995, 2007) extending the number of neurogenic divisions each radial glial cell undergoes would alter the number of neurons in each ontogenetic column, whereas extending the duration of neurogenic division of OSVZ-progenitors could affect the surface area of the cortex by producing cone-shaped radial units (Fietz & Huttner, 2010).

The results suggest that *NIN* may have a role in the evolution of asymmetric division of radial glial cells and therefore contribute to the evolution of neuron number per radial unit. This is supported by the trend between *NIN* molecular evolution and the variation in neuron number which is not explained by lateral expansion, as measured by cortical surface area. There is no trend with either raw neuron number or surface area suggesting no link with lateral cortical expansion through the addition of extra columns. The higher rate of *NIN* evolution at the origin of platyrrhines may be consistent with the suggestion that this clade has evolved higher neuron densities. An important question is how the evolution of amino acid sequence of *NIN* might bring about changes in the duration of asymmetric divisions in radial glial cells. One possibility is that changes in protein sequence of *NIN* result in altered biophysical properties and binding associations with other centrosomal proteins, which may in turn alter the rate or amount of divergence between mother and daughter centrioles (Bornens, 2002; Wang *et al*., 2009).

However, the results require confirmation in a larger dataset which can only be provided through the collection of data on cortical thickness, surface area and neuron number in a larger number of species and I cannot rule out the possibility that selection on *NIN* relates to other cell fate switches during neurogenesis or to its functions in other cells. One notable function is the contribution to neural cell morphology and growth (Baird *et al*., 2004; Moss *et al*., 2007;

Matsumoto *et al*., 2008). The possibility that selection on *NIN* relates to changes in neural morphology is also of potential interest.

6.3.4 Independent genetic mechanisms for different aspects of brain evolution

If the role of *NIN* in the evolution of radial expansion is confirmed, the results suggest cortical surface area and cortical thickness, which together contribute to cortical volume, are under the control of different genetic mechanisms. In chapter five I present evidence which suggests *ASPM* and *CDK5RAP2* may be involved in the lateral expansion of the cortex by influencing the duration of symmetric, proliferative divisions of neural progenitor cells therefore controlling the lateral expansion (or contraction) of primate brain evolution (see also Rimol *et al.*, 2010). I tested whether or not these loci show an association with radial neuron number and neither do (*ASPM*: $t_5 = 0.483$, $p = 0.483$, $R^2 = 0.001$; *CDK5RAP2*: $t_5 = -0.367$, $p = 1.000$, $R^2 = 0.043$). The conclusion that the evolution of cortical thickness and surface area has an independent genetic basis is consistent with the Radial Unit Hypothesis (Rakic, 1988; 1995) and associated hypotheses (Kriegstein *et al.*, 2006; Pontious *et al.*, 2008; Fish *et al*., 2008; Fietz & Huttner, 2010). It is also in agreement with recent studies in humans which show that variation in cortical thickness and surface area do not share a genetic basis; both being highly heritable but with distinctive patterns of heritabilities (Panizzon *et al.*, 2009; Winkler *et al*., 2010).

6.3.5 The effects of variation in minicolumn spacing

The test for an association between neuron number, controlling for variation in lateral expansion, does not highlight *Cebus* as an outlier despite its strong appearance as such when *dN/dS* is compared to brain mass. Together with the suggestion that *Cebus* is a stronger outlier for adult than neonatal brain mass may suggest that *Cebus* has post-natal developmental differences to other platyrrhines. Semendeferi *et al*. (2010) have shown that the spacing between cortical mini-columns is wider in the human prefrontal cortex than in other apes, which have relatively invariable spacing, and have suggested that this may be a general feature of the human frontal cortex. This wider spacing could explain the large residual for the human data point based on the expected *dN/dS*-brain mass regression. The human root-to-tip *dN/dS* is lower than would be expected for a catarrhine brain of its mass, as might be expected if cortical expansion was

associated with an increase in cortical column spacing and therefore a smaller increase in the number of these columns than expected. If this is the case, the large residual for *Cebus* may suggest similar changes in cortical structure. These changes would presumably occur postnatally as cortical spacing is determined by axon and dendrite growth, the number of interneurons and blood vessels (Buxhoeveden & Casanova, 2002). The apparent smaller effect on *Homo* and *Cebus* data points on neonatal than adult regression analyses and the observation that *Cebus* is not an outlier when neuron number is considered rather than brain mass would be consistent with this effect.

Platyrrhines are rarely considered in comparative studies of cortical cyto-architecture which generally seek to identify differences between humans and other apes so unfortunately no data exists to explore potential differences between *Cebus* and other platyrrhines. Such a comparison would be of great interest. The increased spacing between cortical minicolumns in the human prefrontal cortex (Schenker *et al*., 2008; Casanova *et al.*, 2009; Semendeferi *et al*., 2010) has been proposed to have some relevance to cognitive evolution in humans (Gustafsson, 1997, 2004; Elston, 2007; Semendeferi *et al*., 2010). Wider spacing between minicolumns is thought to be associated with greater connections between parts of the cortex (Douglas *et al.*, 1995) and variation in the amount of information convergence on a neuron (Williams & Jacobs., 1997) to produce more generalised processors (Gustafsson, 1997). Individuals with autism and Asperger's syndrome have been shown to have more closely packed minicolumns (Casanova *et al.*, 2002a, b) whilst people with dyslexia have more widely spaced minicolumns (Casanova *et al*., 2002c) further suggesting a link between cognition and the minicolumn. If the results presented here do indeed represent an evolutionary difference in cortical cyto-architecture between *Cebus* and other platyrrhines it is tempting to relate this to the evolution of increased general cognitive ability in this genus (Fragaszy *et al.*, 2005; Deaner *et al*., 2006; Reader *et al*., 2011). *Cebus* does at least have a lower cortical neuron density and approximately the same number of neurons per unit cortical surface area as *Saimiri*, its sister genus, despite having a cortical surface area approximately 50% larger (Herculano-Houzel *et al*., 2008) suggesting the expansion of the *Cebus* brain had a greater lateral than radial dimension in terms of neuron number.

6.4 Conclusion

I have presented evidence that demonstrates *NIN*, a gene encoding a centrosomal protein involved in the maintenance of asymmetric division of neural progenitors, has evolved under positive selection across anthropoids. The pattern of molecular evolution suggests *NIN* may have had a role in the evolution of brain size across anthropoids, and in particular in the evolution of the number of neurons in each ontogenetic column. Such a function would be consistent with the developmental role of *NIN* and the Radial Unit Hypothesis of cortex evolution. This association is supported by a trend between the rate of evolution of *NIN* and neuron number once variation in lateral expansion is accounted for. However, the dataset is small and further information on neuron number and surface area from a wider range of species is necessary to confirm that this trend is robust. *NIN* has other important functions in brain development, most notably in neural morphology, and I suggest understanding the phenotypic importance of positive selection on *NIN* through comparative developmental or functional studies could reveal further clarify the contribution of *NIN* to the evolution of brain morphology.

This page was intentionally left blank.

Chapter 7

Concluding thoughts

"Facts are simple and facts are straight
Facts are lazy and facts are late
Facts all come with points of view
Facts don't do what I want them to."

Talking Heads, *Crosseyed And Painless,* 1980

7. Concluding thoughts

7.1 Integrating comparative genetics and neurobiology

The results presented in chapters 5 and 6 are consistent with models of how neuron number might evolve. I have provided evidence that two microcephaly genes, *ASPM* and *CDK5RAP2*, have had a role in the evolution of brain size. The functions of these genes are consistent with developmental models of brain evolution. A single additional round of proliferative, symmetric divisions of neuroepithelial cells in the ventricular zone would double the number of neurons in the cortex (Rakic, 1988, 1995; Cavines *et al*., 1995). Neuroepithelial cells have apical-basal polarity and the switch from proliferative, symmetric to neurogenic, asymmetric divisions is controlled by the orientation of the spindle pole during mitotic division (Chenn & McConnell, 1995; Götz & Huttner, 2005). An alternative, but not mutually exclusive, model places greater emphasis on prolonged intermediate-progenitor cell division in the sub-ventricular zone, which may also occur by changes in spindle pole orientation (Kriegstein *et al*., 2006). *ASPM* and *CDK5RAP2* are both implicated in control of spindle pole orientation (Thornton & Woods, 2009). In addition, as brain size expands, neural progenitors become increasingly elongated (Smart *et al.*, 2002; Fish *et al*. 2008) and selection may be acting on cytoskeletal genes in response to the need to maintain the precision of spindle orientation during mitotic division of these highly elongated cells in larger brained species (Zhang, 2003; Kouprina *et al.*, 2004; Fish *et al*., 2008). In this way selection on these loci may be in response to the evolution of larger brains rather than causing the change in brain size. It is possible to envisage scenarios where the change in spindle orientation itself leads to the production of additional neurons and whether the role of these loci in brain size evolution is causative or responsive is yet to be determined. Both scenarios are consistent with the results presented here.

Notably, there is strong agreement between the results of studies investigating the expression of microcephaly genes (Bond *et al.*, 2002; Jackson *et al.*, 2002; Bond *et al.*, 2005; Kouprina *et al.*, 2005), their function (Bonds & Woods, 2006; Cox *et al.*, 2006; Fish *et al*., 2006; Brunk *et al.*, 2007; Wood *et al.*, 2007; Buchman *et al*., 2010), models of brain evolution (Rakic, 1988; Kriegstein *et al.*, 2006) and their molecular evolution which together implicate *ASPM* and *CDK5RAP2* as having significant roles in the evolution of neuron number and brain size. *ASPM*

is highlighted as a particularly strong candidate, being associated with brain size during episodes of brain mass expansion and reduction. In contrast, using a "humanised" mouse model Pulvers *et al*. (2010) found that disruption of *ASPM* causes both microcephaly and a reduction in testes mass by affecting proliferation in the germ line. Whether or not human individuals with microcephaly have such pleiotropic effects is not known. Pulvers *et al*. (2010) found that the human version of *ASPM* did not cause macrocephaly in mice and conclude that selection on *ASPM* may be linked to their function in testes development rather than brain development. However the human copy of *ASPM* also did not alter the development of testes mass and they therefore provide no evidence to support either hypothesis. It seems possible that ASPM may interact with several other proteins which may have evolved differences during the 90-100 million years since mice and humans last shared a common ancestor (Bininda-Emonds *et al*., 2007). Therefore the "humanised" mouse model may fail to find phenotypic effects because the genetic background in which *ASPM* has evolved has an important effect on the expression of functional differences. I have explored the hypothesis that selection on microcephaly genes is related to sexual selection and testes development and have found no robust support. The weight of comparative evidence therefore currently falls in favour of *ASPM* and *CDK5RAP2* having a role in brain evolution.

Three other microcephaly genes (*CENPJ*, *MCPH1* and *STIL*) also show signatures of positive selection but the link between selection and brain evolution is less clear. I found no evidence that the rate of evolution of these loci is associated with brain size. It is possible they have more subtle effects during brain evolution and I have presented some evidence that *CENPJ* and *MCPH1* are associated with measures of sexual dimorphism in brain size. This result is in line with previous reports that polymorphisms in *MCPH1* in human populations have sex-specific effects on brain size (Wang *et al*., 2008; Rimol *et al*., 2009) but the effect has not been reported for *CENPJ*. The developmental link between microcephaly genes and sexual dimorphism is poorly understood and whilst I have suggested some mechanisms which may be relevant, these results require further support from functional or developmental studies.

The motivation for studying these genes began after they were shown to be linked to a human disorder (Zhang, 2003; Evans *et al*., 2004a; Evans *et al*., 2004b; Wang & Su, 2004). After finding evidence of selection along some primate lineages attempts have been made to

understand the evolutionary function of microcephaly genes (Fish *et al.*, 2006; Ali & Meier, 2008; Pulvers *et al*., 2010; chapter 5). An alternative approach is to use developmental models of how brains evolve to derive hypotheses of what sorts of genes might be involved in particular aspects of brain evolution and to then use comparative analyses to test these hypotheses. This was the approach taken in chapter 6. I identified an additional potential source of variation in neuron number which relates to a cell fate switch occurring late in neurogenesis and I hypothesised that *NIN*, which maintains radial glial cell proliferation (Wang *et al*., 2009), may contribute to the evolution of radial growth and may therefore have been targeted by selection. Data from across anthropoid primates confirm that *NIN* did evolve adaptively and the results suggest a potential association with neuron number and brain size in a manner consistent with the hypothesised functional effect. Although the association with neuron number is based on a small dataset and is narrowly non-significant this chapter highlights the potential utility of using hypotheses derived from developmental biology to explore evolutionary mechanisms using a comparative approach.

The relationship between comparative genetics and developmental neurobiology can therefore be a two way street, providing complementary approaches to deriving and testing hypotheses. When these hypotheses relate to phenotypic evolution it is clearly necessary to incorporate both phenotypic information from extant species and information on the evolutionary history of that phenotype in order to make robust conclusions.

7.2 Evolution on many levels: Implications for the evolutionary genetics of adaptation

The primate brain is perhaps the most intensively studied trait of any large vertebrate group and has rapidly become an unlikely model system used to study the evolutionary genetics of adaptation. The inferred roles of *ASPM*, *CDK5RAP2* and *NIN* in the evolution of primate brain mass has implications for our understanding of the evolutionary genetics of adaptation. First, they provide evidence that a complex, polygenic quantitative phenotype evolved by convergence or parallelism at the molecular level (Cresko *et al.*, 2004; Mundy, 2005; Arendt & Reznick, 2007). A conserved genetic basis for evolutionary changes in brain size and structure suggests the developmental pathways involved are under strong constraints, limiting the potential ways in which brains can respond to selection. Second, my results provide a counter example to

a commonly asserted hypothesis that evolution of form occurs primarily through changes in *cis*-regulatory sequences (King & Wilson, 1975; Carroll, 2005; Wray, 20007; Carroll 2008).

Changes in *cis*-regulatory sequences are proposed to be more important for phenotypic evolution as their modular nature limits pleiotropic effects (Carroll, 2005; but see Hoekstra & Coyne, 2007; Lynch & Wagner, 2008; Stern & Orgogozo, 2008). In fact the evolution of brain mass has been singled out as an example where regulatory evolution is likely to be the predominant evolutionary mechanism: "the evolution of complex traits such as brain size… *must* have a highly polymorphic and largely regulatory basis" (Carroll, 2005; emphasis mine). It is therefore interesting that these genes are expressed throughout the body (Bond *et al.*, 2005; Kouprina *et al.*, 2005) but were subject to positive selection acting on their coding sequence. If *ASPM*, *CDK5RAP2* and *NIN* are in fact involved in brain evolution how are pleiotropic effects avoided?

The first point to note is that the pathology of primary microcephaly itself shows that pleiotropic effects of microcephaly gene disruption can be limited to the brain (Bond & Woods 2006). Both *ASPM* and *CDK5RAP2* are alternatively spliced (Kouprina *et al.*, 2005; Buchman *et al*., 2010), which may reduce pleiotropic effects (Hughes, 2006; Hoesktra & Coyne, 2007; Lynch & Wagner, 2008). Alternatively the evolution of *ASPM*¸ for example, may not affect non-neural cells either due to the elongated cell morphology of neuroepithelial cells (Fish *et al*., 2006) or cell-dependent recruitment factors (van der Voet *et al,*. 2009). These explanations are not mutually exclusive and provide plausible mechanisms to reduce the pleiotropic effects of protein evolution (Hoekstra & Coyne, 2007; Lynch & Wagner, 2008). However it would be interesting to explore the evolution of microcephaly gene expression to complement the analyses of coding sequence evolution.

Similar conclusions have been drawn from extensive studies of the phenotypic effects of *FOXP2*. *FOXP2* encodes a widely expressed transcription factor (Enard *et al*., 2009; Enard, 2011). In "humanised" mouse models however, variation in the amino acid sequence of FOXP2 between mice and humans is shown to affect very specific regions of the brain involved in cortico-basal ganglia circuits and has no effect on other regions examined including the amygdala and cerebellum (Enard *et al*., 2009; Reimers-Kipping *et al*., 2011). *FOXP2* is therefore

another example of a protein-coding gene involved in primate brain and behavioural evolution which manages to avoid pleiotropy (Reimers-Kipping *et al*., 2011).

More broadly, research is showing a diversity of mechanisms contribute to the genetic basis of aspects of primate brain evolution, including coding sequence evolution (e.g. this study; Enard *et al.*, 2002; Wang *et al.*, 2005; Vallender & Lahn, 2006; Uddin *et al.*, 2008) gene duplication (Burki & Kaessman, 2004; Marques-Bonet *et al.*, 2009), non-coding RNA evolution (Pollard *et al*., 2006; Zhang *et al.*, 2008), changes in regulatory sequences and gene expression (Khaitovich *et al.*, 2005; Rockman *et al.*, 2005; Gilad *et al.*, 2006; Khaitovich *et al.*, 2006; Prabhakar *et al.*, 2006; Haygood *et al.*, 2007; Somel *et al.*, 2009; McLean *et al*., 2011) and possibly changes in methylation, genomic imprinting and posttranscriptional modifications (Keverne *et al*., 1996; Vallender & Lahn, 2006; Wilkinson *et al*., 2007; Mattick & Mehler, 2008). Given the complexity and composite nature of brain evolution it is hardly surprising that so many sources of genetic variation have been implicated in having important roles. Asserting the primary importance of one particular mechanism of evolutionary change therefore seems premature.

7.3 Parallelism & brain evolution

Brain expansion is a quintessential feature of primate evolution (Jerison, 1973; Martin 1990). However, the fossil record of temporal changes in brain size in primates is incomplete and often difficult to interpret. As such, whether brain expansion was limited to a few lineages or was a ubiquitous trend across the primate phylogeny, and how frequently brain size has decreased, has not been clear. My results show that, from a small-bodied and small-brained ancestor, both absolute and relative brain size have shown strong temporal trends to increase and have done so multiple times independently across diverse primate lineages strongly rejecting the *scale naturae* that still permeates many branches of evolutionary neuroscience (Strediter, 2005; Barton, 2006a). The strong directionality suggests that brain mass was under persistent positive selection. The finding that brain expansion occurred across diverse primates may indicate that it is unlikely that one single factor can explain brain expansion and suggests that both ecological and social factors have been important (Barton *et al*., 1995; Barton, 1998; Dunbar & Schultz, 2007). Although treated as a unitary structure in chapter 3 the parallel expansion of the brain must have involved

the parallel evolution of multiple traits including neuron number and glial number in different brain regions, structures within particular regions such as cortical surface area, thickness and gyrification, and connections within and between brain regions, some of which are likely to have been genetically independent (Barton & Harvey, 2000; Fears *et al*., 2009; Panizzon *et al*., 2009; Rogers *et al*., 2010; Winkler *et al*., 2010; Barton & Capellini, 2011).

Despite a general trend to expand, brain size does decrease in some lineages. Major episodes of brain mass reduction occurred in the Callitrichidae and Cheirogaleidae and are associated with episodes of body size dwarfism. Relative brain size decreased less frequently and can be attributed to increased body mass rather than decreased brain mass. These results have implications for understanding a controversial member of our own genus, *H. floresiensis* (Brown, 2004; see chapter 3 & 4), but may also have a more general relevance for our understanding of the selection pressures and costs shaping brain evolution, the malleability of brain:body allometry and the frequency of evolutionary reversals.

7.4 Begging the question: The fallacy of human genetic uniqueness?

Understanding the genetic basis of the human brain and human uniqueness is a major goal of modern biology (King & Wilson, 1975; Carroll, 2003; Goodman *et al.*, 2005; Barton, 2006c; Pollen & Hoffman, 2008; Vallender, 2008). However, very few phenotypic traits have been identified in humans that do not conform to non-human primate brain architecture suggesting the human brain is primarily a 'scaled-up' primate brain (Sherwood *et al.*, 2008; Herculano-Houzel, 2009; Semendeferi *et al*., 2010). The search for human genetic uniqueness is therefore double-blind; we are looking for the genetic basis of a phenotype which itself is poorly defined. Most of the attention of evolutionary geneticists has focused on the human branch with the aim of identifying genetic changes or selective events that contribute to unique characteristics of humans. This approach makes the assumption that the genetic changes that contribute to human brain evolution and human uniqueness are themselves unique to the human lineage. This, it could be argued, may be an example of a form of logical fallacy called 'begging the question' where the answer is assumed implicitly in the question (i.e. human phenotypic uniqueness must have a unique genetic basis because it is the basis of unique phenotypes). Is this assumption justified? Or is it even useful?

As discussed above it is clear that parallelism in brain expansion across primates is extensive. It is also clear that the majority of phenotypic and developmental traits associated with the evolution of the human brain are conserved across primates (Zilles *et al.*, 1989; Semendeferi *et al.*, 2002; Bush & Allman, 2004; Sherwood *et al.*, 2006; Marino, 2006; Herculano-Houzel *et al*., 2007; Fietz *et al*., 2010). If primate brain evolution is viewed as a set of composite traits all evolving in parallel in association with brain expansion, coupled with the expectation that brain development is under strong constraint, it is not unreasonable to hypothesise that brain evolution may have a conserved genetic basis. The results presented in this thesis suggest the evolution of primate brain size does indeed have at least a partially conserved genetic basis.

Whether or not the same genes are generally involved in independent episodes of brain expansion is unclear but has major implications for looking for and interpreting human genetic uniqueness. For example, consider three independent episodes of brain expansion along the lineages leading to *Homo*, *Papio* and *Cebus* (Figure 7.1). If one were able to tally-up all the brain-expressed genes which were targeted by positive selection during the evolution of each species and examine the overlap between the three lists we can imagine a series of possible scenarios. Under one extreme a high level of overlap (Figure 7.2a) would imply a strongly conserved or parallel genetic basis to brain expansion with 'species-specific' selective events being rare. In this case there is a very low probability that any genetic change between humans and chimpanzees is actually 'unique' to human evolution. Under a second extreme, very low levels of overlap (Figure 7.2b) imply the genetic basis of primate brain size is not conserved, parallelism is rare and each species has high levels of unique selection events. In this case genetic changes along the human lineage have a high probability of being unique to humans, but whether or not, or how, these unique changes are more impressive than the unique changes on lineages leading to *Papio* or *Cebus*, for example, is unclear and identifying the most important functional changes becomes increasingly challenging. Under the final scenario (Figure 7.2c) parallelism is common across non-human primates but humans depart from the general primate pattern suggesting changes along the human lineage have a high probability of being unique to human evolution and may all contribute the unique aspects of human brains.

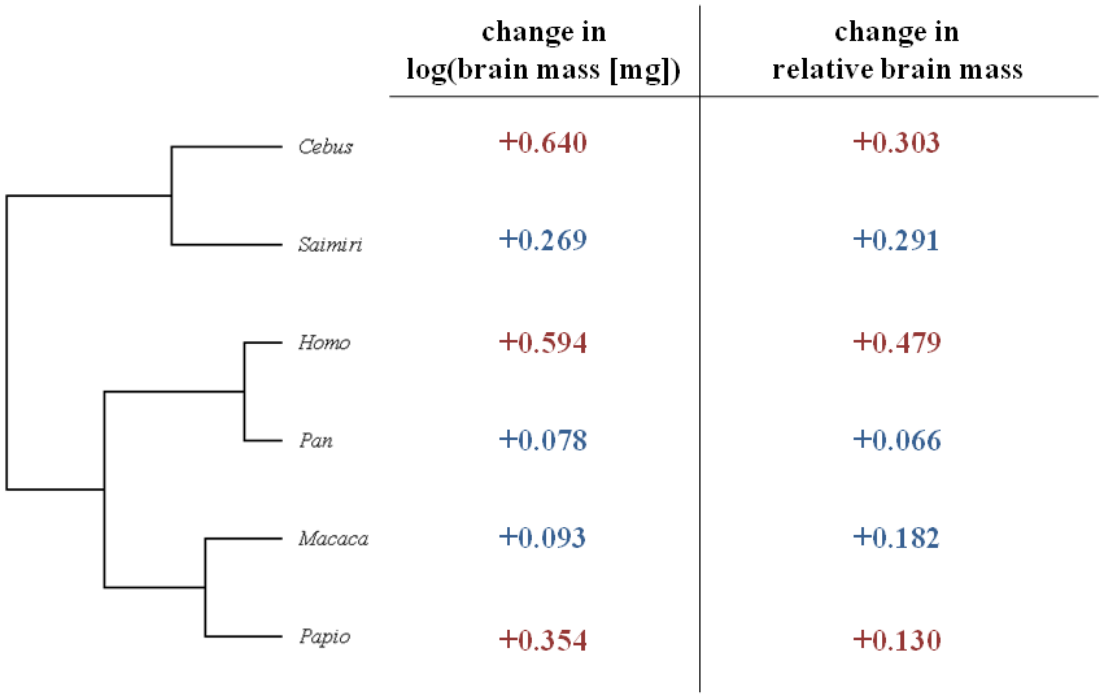

Figure 7.1 Three examples of pairs of genera which show a greater level of brain mass expansion in one linage (in red) than the other (in blue)

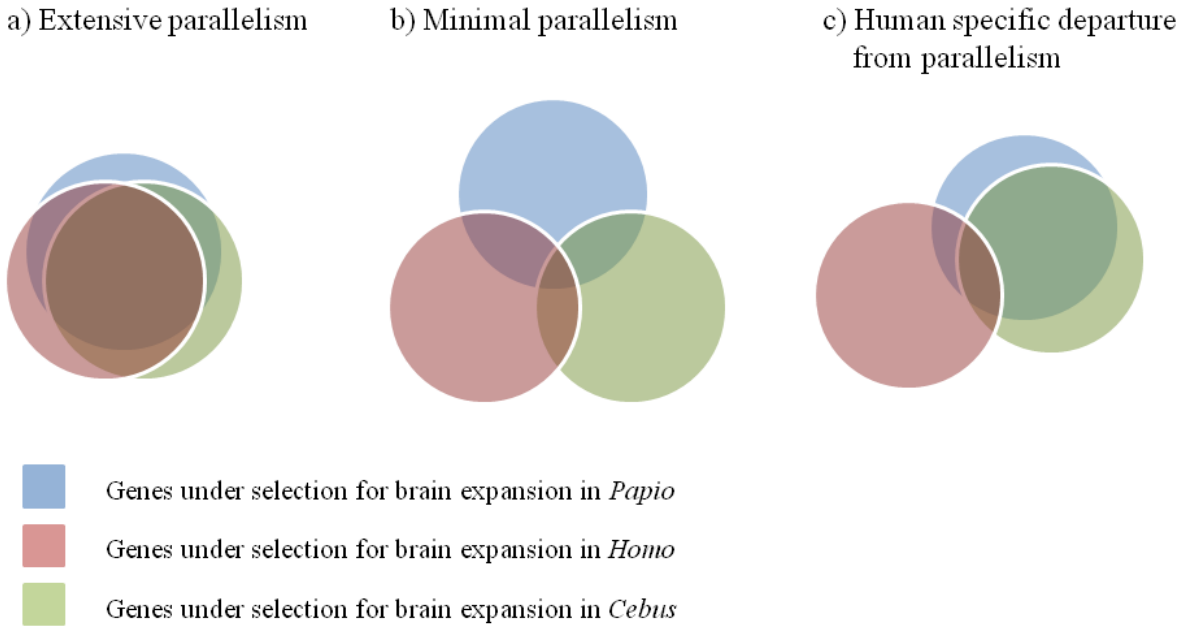

Figure 7.2 Three hypothetical scenarios exploring the overlap in genes targeted by selection during three independent episodes of brain expansion

This simple thought experiment demonstrates the inherent weakness of human-chimpanzee comparisons noted by previous authors (Carroll, 2003; Goodman *et al.*, 2005; Barton, 2006c; Pollen & Hoffman, 2008; Vallender, 2008). Is there evidence to support any one scenario over the other? The limited inclusion of non-human primates in genetic studies of primate evolution makes this question difficult to answer. It is certainly the case that when a diverse range of species are considered selection on many key candidate genes is not limited to the human lineage. For example, selection has acted on the microcephaly genes and *NIN* across anthropoid primates (chapters 5 & 6), high rates of evolution in non-human lineages are also detected for many genes involved in energy metabolism (Burki & Kaessmann, 2004; Grossman *et al*., 2004; Doan *et al*., 2005; Uddin *et al*., 2008).

Comparative genomic and transcriptomics studies have highlighted several categories of genes involved in neural development and function as having high rates of divergence along the human lineage (Preuss *et al*., 2004; Khaitovich *et al*., 2006b). However, genes with high rates of evolution or rapid changes in gene expression on the chimpanzee lineage also show enrichment for similar categories for genes including neuronal cell adhesion (Prabhakar *et al*., 2006), synapse and postsynaptic membrane function (McLean *et al*., 2011). These results are often discussed less than those for humans and often full details are lacking but one suspects that if these categories of genes were found for genes under selection on the human lineage they would be viewed with much more interest. Furthermore, recent studies suggest that some genes experienced positive selection on both the human and chimpanzee lineages, between other species pairs or experienced pervasive positive selection during great ape evolution (Bakewell *et al*., 2007; Locke *et al.*, 2011; Scally *et al*., in review). Enard *et al*. (2010) also performed a genome wide test for recent positive selection during the evolution of humans, chimpanzees orang-utans and macaques which showed that many genomic 'hot spots' of positive selection are shared across these four species; the authors suggest that if such extensive parallelism can be detected using just four species it must be a widespread phenomenon. Notably these hot spots of parallel positive selection are enriched for genes involved in forebrain development (Enard *et al*., 2010) which again hints at a conserved genetic basis to brain evolution.

This collective evidence suggests that there is some signature of parallel evolution between species of primates either at the level of genes or functional categories of genes.

Similarly some evidence also exists of convergence across greater taxonomic distances, for example similar categories of genes have been implicated in the evolution of large brain size in primates and elephants (Goodman *et al.*, 2009) and for sustained evolution of key brain development genes across long periods of time (Chapter 5,6; Locke *et al.*, 2011). Conversely, selection on some genes, such as *FOXP2* and *ADCYAP1*, does appear to be more human-specific (Enard *et al*., 2002; Wang *et al*., 2005; but see Enard *et al*., 2010 for evidence that selection on *FOXP2* is not so human-specific) and although there are some similarities between genes under selection in humans and chimpanzees both species have a large number of species-specific selective events (Bakewell *et al*., 2007). The release of the Neanderthal genome identified a number of genes with signatures of positive selection seemingly unique to modern humans (Green *et al*. 2010). A recent analysis of the molecular evolution of these candidates across apes found evidence for positive selection having acted on approximately 20% (Crisci *et al*., 2011). This again suggests a complex picture of pervasive selection, parallelism and lineage-specific adaptation.

It is therefore probably too early to tell which of the three scenarios discussed above is closest to reality. Clearly however knowing what genetic changes are shared between independent episodes of brain expansion could go a long way to uncovering what genetic changes are unique to particular species, including our own.

7.5 Reflections and critiques

The aim of this thesis was to integrate genetic studies of primate brain size with phenotypic information to test hypotheses regarding gene-phenotype associations. Although the dual approach has produced interesting results a number of limitations should be recognised. First, by taking a candidate gene approach I focus on a number of genes with known developmental functions. These are effectively treated in isolation from the rest of the genome meaning it is difficult to assess the relative contribution of these genes to brain evolution, which is expected to have a highly polygenic basis (Carroll, 2003). It is also likely that structural changes in the protein coding sequence of the genes studied would affect the way in which they interact with other proteins. We know little about what these interacting proteins are, but one potential approach to assessing how amino acid changes may affect protein function is to model protein folding across a range of species and reconstructed ancestral species. This approach was not considered in this thesis but could provide interesting and complementary results.

Although I have demonstrated that it is possible to detect gene-phenotype associations across species whether or not the approach taken is generally applicable to studying other phenotypic traits, or brain size in other orders, is an open question. For example, fluctuations in the direction of phenotypic evolution could introduce noise which overcomes a genuine association between root-to-tip *dN/dS* ratios and the phenotypes of extant species; as seen for *ASPM* and callitrichids. In clades where the phenotype under consideration evolves rapidly in a non-directional manner the tests used here may fail to detect gene-phenotype associations. In addition, if a locus makes an episodic contribution to the evolution of a trait which evolves in a continuous manner, perhaps because the trait has a polygenic basis or because constraints acting on a locus change over time, it may again be difficult to detect this association using the methods adopted here. It is possible, for example, that although I found no association between three of the microcephaly genes and gross measures of brain size that they still contribute to brain evolution but in a less regular manner than *ASPM* and *CDK5RAP2*. In addition, as I considered only partial coding sequence, for reasons explained in chapters 5 and 6, it is also possible that other regions of these genes show different patterns of gene-phenotype associations and that considering the full coding sequence could alter the results. However, when positive selection acts on restricted regions of a gene a case can be made for analyzing these regions in isolation

from the rest of the gene, when using root-to-tip *dN/dS* ratios and comparative methods, as regions evolving neutrally may add 'noise' which would diminish the strength of any genuine signal from regions under positive selection. The development of methods which can take into account variation in gene-phenotype associations across the length of a gene may be useful in this respect.

Detecting gene-phenotype associations using comparative methods provides evidence for co-evolution between a locus and a phenotype. However the direction of causality remains unanswered. It is possible, as discussed on p. 196, that selection on microcephaly genes is a response to brain expansion rather than a cause of it. Understanding which genes play a causative and responsive role in brain size evolution is necessary if we are to understand what sort of developmental constrains act on brain evolution and how selection negotiates these constraints. To fully resolve the direction of causality is a difficult task and may require a combination of comparative and functional analyses. These should also help illuminate the 'black box' between molecular and phenotypic evolution.

Finally comparative analyses of gene-phenotype associations and phenotypic evolution require relevant phenotypic data, collected in a controlled manner where possible, and models of evolution that accurately reflect phenotypic evolution. The model building approach of Bayes Traits is a major step in the right direction however it still has limitations, for example as seen in chapter 4, where different phenotypic trends occur in different parts of the phylogeny. The continuing development of more nuanced methods will greatly enhance our ability to analyse both phenotypic and molecular evolution. Of course, any analysis will be limited by the sort of data available. Datasets of brain volumes (e.g. Stephan *et al*., 1981) have long been a useful resource for comparative biologists. However, to continue developing our knowledge of how brains evolved different types of data, such as neural and non-neural cell numbers (see chapter 6), will be of considerable value but data is currently available for a relatively small number of species limiting statistical power of comparative studies. This lack of power and partial non-overlap between genetic and phenotypic datasets has been evident as a limiting factor in this thesis.

7.6 Future directions

The parallel evolution of brain expansion and the convergent reduction of brain mass in callitrichids and cheirogaleids provide an opportunity to utilise the diversity of primate brain sizes to uncover the general genetic and developmental mechanisms which bring about changes in brain size and structure, as well as identifying lineage-specific departures from the general primate pattern. An obvious strategy is to pursue the sort of thought experiment described above. The three genus pairs are statistically independent of one another so offer three 'natural experimental replicates'. A genome project is completed, planned or underway for a species of all of the six genera except *Cebus*, however coding sequence data could be rapidly collected using new sequencing techniques, with non-coding sequence filled in at a later date. These 6 genomes could then also permit studies on parallel evolution of non-coding sequence. Although the same set-up could be ideal for studying gene expression this is a much more daunting logistical task as age, sex and condition matched tissue would be required. *Papio*, *Cebus* and *Saimiri* are not routinely kept as laboratory animals so collecting such tissue would require co-ordinated opportunistic sampling from zoos, probably involving research groups from many countries in order to obtain sufficient samples. This is especially true for early, prenatal developmental stages which are likely to be of primary importance but are currently under studied.

A similar experiment could be performed using pairs of species where one lineage shows a greater *decrease* in brain size than the other, for example *C. jacchus/S. oedipus* and *M. murinus/M. coquerelli*. This would identify genes involved in the convergent reduction in brain mass. One could then combine the results from this experiment with the results from a convergent brain expansion experiment to identify key regulators in brain size (Figure 7.3). Genes involved in brain expansion but not brain reduction may highlight genes involved in behavioural complexity, if one considers whole brain mass as a good predictor of cognitive ability (Deaner *et al*., 2006). Genes involved in reductions but not expansions may suggest ways in which these species may counteract the costs of reduced brain size (see chapter 4).

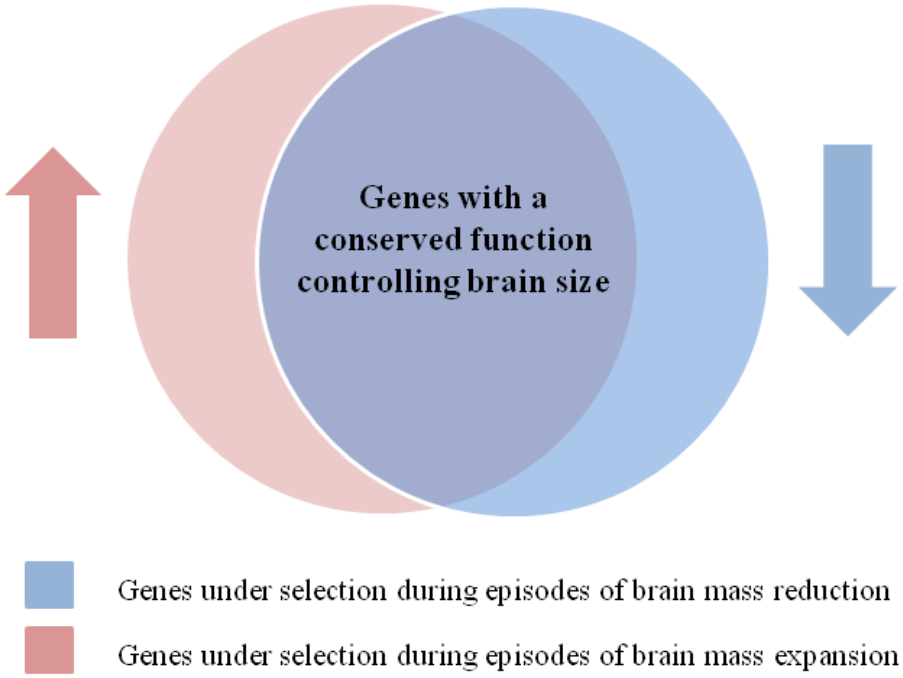

Figure 7.3 Overlap between genes involved in convergent episodes of brain expansion and reduction could identify key regulators of brain size

Genomic data from increased numbers of species will also provide greater power to detect loci under pervasive selection across primates. Although several studies suggest relatively few protein coding genes evolved under positive selection during human evolution (Nielsen *et al*., 2005; Shi *et al*., 2006; Wang *et al*., 2007) when larger number of taxa are considered the power to detect positive selection using site models will increase, potentially revealing more targets of persistent positive selection (e.g. Enard *et al.*, 2010). This is also potentially true for non-coding genes and promoter sequences. A major challenge will be to develop methods which allow us tomove beyond conserved non-coding genes with lineage specific shifts in selection to detecting non-coding sequences which have been targeted by selection for across longer periods of evolutionary time (see for example Hoffman & Birney, 2010). The ever growing availability of genomic information, with genome projects planned, underway or completed for 23 species of primate (Figure 7.4; Bradley & Lawler, 2011), should soon allow for this to be tested.

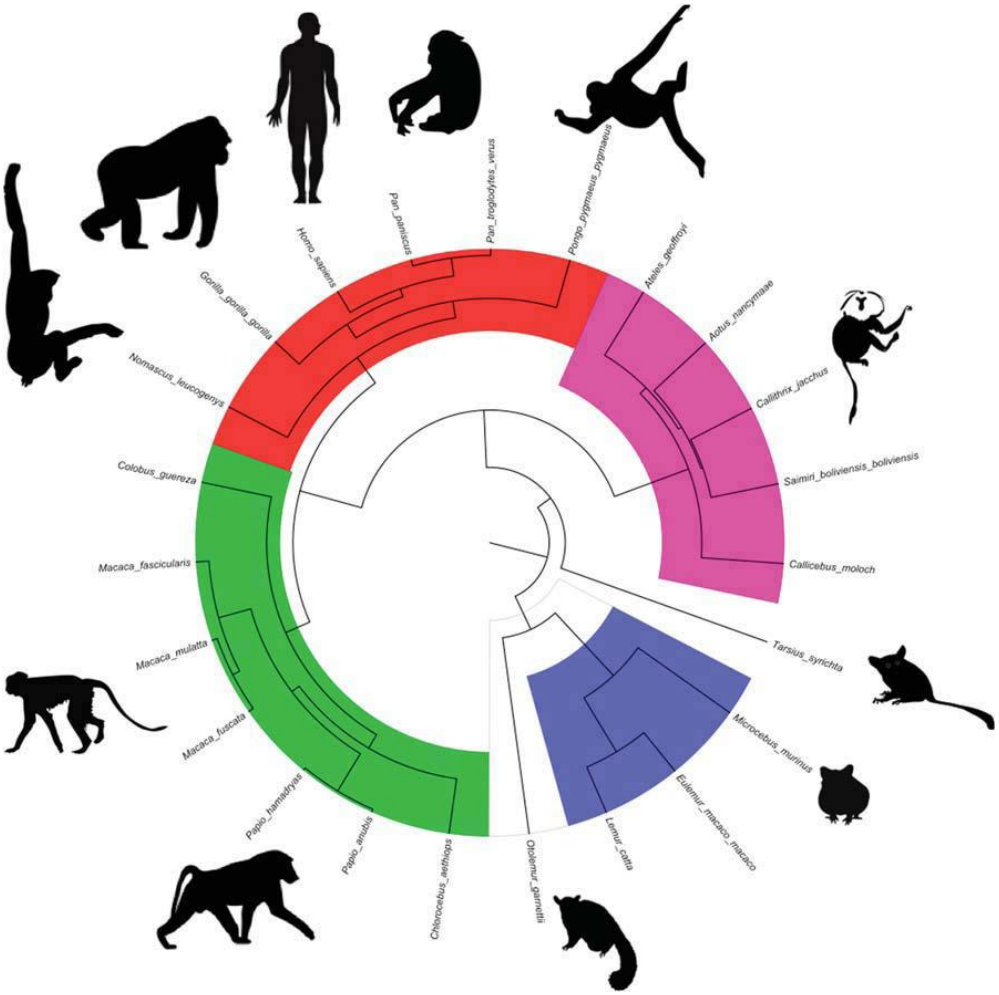

Figure 7.4 Primates with genome projects, species with silhouettes have completed draft genomes publically available. The red block are apes, the green block old world monkeys, the purple block new world monkey, the blue block are lemurs. Galagos and lemurs are represented by an *Otolemur*, tarsiers by *Tarsius syrichta*. Taken from Bradley and Lawler (2011) with permission.

These 23 species, together with additional data obtained using mass sequencing technologies such as exome capturing (Teer & Mullikin, 2010), will not only allow a full description of the targets of positive selection during the origin and radiation of primates but will also permit a move away from analysis of species pairs towards adopting full comparative methodology in a similar way to that used in this thesis but on a genome wide scale. This will allow genome scans to be conducted in a phenotypic context in order to identify genes will rates of evolution that correlate with variation in phenotypes such as brain size, body size or neuron number. Methods allowing such a test are in their infancy but several new models which attempt to directly integrate phenotypic and molecular information provide reasons for optimism

(O'Connor & Mundy, 2009; Lanfear *et al.*, 2010; Lartillot & Poujol, 2011; Mayrose & Otto, 2011) and the prospect of identifying genes with conserved roles in phenotypic evolution.

Of course, comparative analyses such as those described above require functional or developmental studies to fully understand the role of a highlighted gene in brain evolution. Comparative genetics must therefore work hand in hand with developmental approaches such as 'neuro-evo-devo' (Rakic, 2009) and transgenic mice (Enard *et al*., 2009). Although the relationship between these fields can be a two way street comparative genetics offers a way of generating and testing hypotheses in a non-invasive way and may therefore be a useful first step before turning to animal models. In addition, given the conserved nature of many developmental pathways across mammals insights into the evolutionary genetics of brain size and structure may be gleamed from more tractable systems. For example, different species of mice and other rodents show extensive variation in brain size and structure (e.g. Mace & Eisenber, 1982; Hafner & Hafner, 1984; Herculano-Houzel *et al*., 2006) as do different populations of the same species (Mace & Eisenber, 1982). Understanding the genetic basis of variation in brain size and structure in rodents where functional analyses may be more feasible and tissue is easier to obtain may be a useful complementary approach to investigating brain evolution in primates.

7.7 To conclude

Understanding the evolutionary trajectories of brain size, the selection pressures involved and the genetic and developmental changes that underpin brain evolution is a major challenge. The challenge is only made greater in large, endangered and protected mammals such as primates. It is my hope that this thesis has contributed to addressing these problems. In particular I have emphasised that the diversity of primates can be used as a tool for investigating brain evolution at both a phenotypic and molecular level. By demonstrating brain size has experienced a strong directional trend to expand across primates I highlight the frequency of parallelism in primate brain evolution, the distinct nature of brain and body mass evolution, and have provided a phenotypic framework for interpreting and planning studies of brain size and structure. This framework has provided insights both phenotypic and molecular evolution; for example the plausibility of the controversial hominin *H. floresiensis* and an explanation for why the molecular evolution of some brain development genes in callitrichids may be outliers compared to their small brain size. I have argued that the hypothesis that brain evolution has a conserved genetic basis has not been properly tested, let alone rejected, and have demonstrated that the evolution of several genes, in particular *ASPM, CDK5RAP2* and *NIN* appear to be consistent with a conserved role in the proliferation of neural progenitor cells across anthropoid primates. This result clearly has implications for studying the evolutionary genetics of brain size and indeed for uncovering species-specific changes such as those that contribute to the seemingly unique cognitive attributes of our own species. I have suggested some ways of moving the field forward by firmly basing genetic studies in a phenotypic context. As primate genomics continues to come of age (Varki *et al*., 2008; Marques-Bonet *et al*., 2009; Bradley & Lawler, 2011) we can look forward to further progress being made in our understanding of how brains evolve by integrating molecular, developmental, phenotypic and ecological perspectives. Along the way, perhaps some further '*light will be thrown on the* (genetic) *origin*(s) *of man and his* (evolutionary) *history*' (Darwin, 1859).

References

1. Ah-King M, Tullberg BS. 2000. Phylogenetic analysis of twinning in Callitrichidae. *Am J Primatol.* **51**: 135–146
2. Aiello LC, Wheeler P. 1995. The expensive-tissue hypothesis: the brain and the digestive system in human and primate evolution. *Curr Anthropol.* **36**: 199-221
3. Ali F, Meier R. 2008. Positive selection in *ASPM* is correlated with cerebral cortex evolution across primates but not with whole-brain size. *Mol Biol Evol.* **25 (11)**: 2247-2250
4. Ali F, Meier R. 2009. Primate home range and *GRIN2A*, a receptor gene involved in neuronal plasticity: implications for the evolution of spatial memory. *Genes Brain & Behav.* **8 (4)**: 435 – 441
5. Alroy J. 1998. Cope's Rule and the dynamics of body mass evolution in North American fossil mammals. *Science* **280**:731-734
6. Andrés AM, Soldevila M, Navarro A *et al*. (6 authors). 2004. Positive selection in *MAOA* gene is human exclusive: determination of the putative amino acid change selected in the human lineage. *Hum Genet.* **115 (5)**: 377-386
7. Anisimova M, Bielawski JP, Yang Z. 2002. Accuracy and power of Bayes prediction of amino acid sites under positive selection. *Mol Biol Evol.* **19(6)**: 950–958
8. Anisimova M, Yang Z. 2007. Multiple hypothesis testing to detect lineages under positive selection that affects only a few sites. *Mol Biol Evol.* **24 (5)**: 1219-1228
9. Arendt J, Reznick D. 2007. Covergence and parallelism reconsidered: what have we learned about the genetics of adaptation? *Trends Ecol Evol.* **23 (1)**: 26-32
10. Argue D, Morwood M, Sutikna T, Jatmiko, Saptomo W. 2009. *Homo floresiensis*: A cladistic analysis. *J Hum Evol.* **57 (5)**: 623-639
11. Arnold C, Matthews L, Nunn CL. 2010. The 10kTrees website: A new online resource for primate phylogeny. *Evol Anthropol Issues News Rev.* **19**: 114–118
12. Ash J, Gallup GG. 2007. Paleoclimatic Variation and brain expansion during human evolution. *Hum Nat.* **18 (2)**: 109-124
13. Atchley WR, Riska B, Kohn LAP, Plummer AA, Rutledge JJ. 1984. A quantitative genetic analysis of brain and body size associations, their origin and ontogeny: data from mice. *Evolution* **38 (6)**: 1165-1179

14. Azevedo FAC, Carvalho LRB, Grinberg LT *et al*. (9 authors). 2009. Equal numbers of neuronal and nonneuronal cells make the human brain an isometrically scaled-up primate brain. *J Comp Neuro.* **513 (5)**: 532-541
15. Babbitt CC, Fedrigo O, Pfefferle AD *et al*. (7 authors). 2010. Both noncoding and protein-coding RNAs contribute to gene expression evolution in the Primate brain. *Genome Biol Evol.* **2**: 67–79
16. Baird DH, Myers KA, Mogensen M, Moss D, Baas PW. 2004. Distribution of the microtubule-related protein ninein in developing neurons. *Neuropharmacology* **47 (5)**: 677-683
17. Bakewell MA, Shi P, Zhang J. 2007. More genes underwent positive selection in chimpanzee evolution than in human evolution. *Proc Natl Acad Sci USA.* **104 (18)**: 7489-7494
18. Balter M. 2006. Are human brains still evolving? Brain genes show signs of selection. *Science* **309 (5741)**: 1662-1663
19. Barrera JA, Kao L, Hammer RE, Seemann J, Fuchs JL, Megraw TL. 2010. *CDK5RAP2* Regulates Centriole Engagement and Cohesion in Mice. *Dev Cell*. **18 (6)**: 913-926
20. Barrett L, Henzi P. 2005. The social nature of primate cognition. *Proc R Soc B.* 272 (1575): 1865-1875
21. Barton RA 2007. Evolutionary specialization of mammalian cortical structure. *J Evol Biol.* **20(4)**: 1504-1511
22. Barton RA, Aggleton J, Grenyer R. 2003. Evolutionary coherence of the mammalian amygdala. *Proc R Soc B.* **270 (1514)**: 539-543
23. Barton RA, Capellini I. 2011. Maternal investment, life histories, and the costs of brain growth in mammals. *Proc Natl Acad Sci USA.* **108 (15):** 6169-6174
24. Barton RA, Harvey PH. 2000. Mosaic evolution of brain structure in mammals. *Nature* **405**: 1055-1058
25. Barton RA, Purvis A, Harvey PH. 1995. Evolutionary radiation of visual and olfactory brain systems in primates, bats and insectivores. *Phil Trans R Soc Lond B.* **348**: 381-392
26. Barton RA. 1992 Allometry of food intake in free-ranging anthropoid primates. *Folia Primatol.* **58**: 56-59
27. Barton RA. 1996. Neocortex size and behavioural ecology in primates. *Proc Roy Soc B.* **263 (1367)**: 173-177

28. Barton RA. 1998. Visual specialization and brain evolution in primates. *Proc R Soc B.* **265**: 1933-1937
29. Barton RA. 2002. How did brains evolve? *Nature* **415**: 134-135
30. Barton RA. 2006a. Primate brain evolution: integrating comparative, neurophysiological and ethological data. *Evol Anthropol Issues News Rev.* **15 (5)**: 224-236
31. Barton RA. 2006b. Olfactory evolution and behavioral ecology in primates. *Am J Primatol*. **68 (6)**: 545-58
32. Barton RA. 2006c. Chimp comparisons won't explain human evolution. *Nature* **443**: 632
33. Bates TC, Luciano M, Lind PA *et al*. (6 authors). 2008. Recently-derived variants of brain-size genes *ASPM, MCPH1, CDK5RAP2* and *BRCA1* not associated with general cognition, reading or language. *Intelligence* **36**: 689–693
34. Bauchot R, Stephan H. 1969. Encéphalisation et niveau evolutif chez les Simiens. *Mammalia* **33**: 225-275
35. Belknap JK, Phillips TJ, O'toole LA. 1992. Quantitative trait loci associated with brain weight in the BXD/Ty recombinant inbred mouse strains. *Brain Res Bull*. **29 (3-4)**: 337-344
36. Benefit BR, McCrossin. 1997. Earliest known Old World monkey skull. *Nature*. **388**: 368-371
37. Berkman MB, Pacheco JS, Plutzer E. 2008. Evolution and creationism in america's classrooms: A national portrait. *PLoS Biol.* **6(5)**: e124
38. Bhardwaj RD, Curtis MA, Spalding KL *et al*. (11 authors). 2006. Neocortical neurogenesis in humans is restricted to development. *Proc Natl Acad Sci USA*. **103 (33)**: 12564-12568
39. Bininda-Emonds ORP, Cardillo M *et al*. (10 authors). The delayed rise of present-day mammals. *Nature* **446**: 507-512
40. Blaschke AJ, Staley K, Chun J. 1996.Widespread programmed cell death in proliferative and postmitotic regions of the fetal cerebral cortex. *Development* **122**: 1165-1174
41. Bloch JI, Boyer DM. 2002. Grasping Primate origins. *Science* **298 (5598)**: 1606-1610
42. Bloch JI, Silcox MT, Boyer DM, Sargis EJ. 2007. New paleocene skeletons and the relationship of plesiadapiforms to crown-clade primates. *Proc Natl Acad Sci USA*. **104**: 1159-1164
43. Boerner M, Krüger O. 2008. Why do parasitic cuckoos have small brains? Insights from evolutionary sequence analyses. *Evolution*. **62**: 3157-3169

44. Bond J, Roberts E, Mochida GH *et al*. (12 authors). 2002. *ASPM* is a major determinant of cerebral cortical size. *Nat Genet.* **32**: 316-320
45. Bond J, Roberts E, Springell K *et al*. (20 authors). 2005. A centrosomal mechanism involving *CDK5RAP2* and *CENPJ* controls brain size. *Nat Genet.* **37 (4)**: 353-355
46. Bond J, Woods CG. 2006. Cytoskeletal genes regulating brain size. *Curr Op Cell Biol*. **18**: 95-101
47. Bornens M. 2002. Centrosome composition and microtubule anchoring mechanisms. *Curr Op Cell Biol.* **14 (1)**: 25-34
48. Bouckson-Castaing V, Moudjou M, Ferguson DJ *et al*. (7 authors). 1996. Molecular characterisation of ninein, a new coiled-coil protein of the centrosome. *J Cell Sci.* **109:** 179-190
49. Boucot AJ. 1976. Rates of size increase and of phyletic evolution. *Nature* **261**: 694 - 696
50. Bradley BJ, Lawler RR. 2011. Linking genotypes, phenotypes, and fitness in wild primate populations. *Evol Anthropol Issues News Rev.* **20 (3)**: 104–119
51. Bradley BJ. 2008. Reconstructing phylogenies and phenotypes: a molecular view of human evolution. *J Anat*. **212 (4)**: 337-353
52. Bromham L, Cardillo M. 2007. Primates follow the 'island rule': implications for interpreting *Homo floresiensis*. *Biol Lett.* **3**: 398-400
53. Brown P, Sutikna, T, Morwood, MJ *et al*. (7 authors). 2004. A new small-bodied hominin from the Late Pleistocene of Flores, Indonesia. *Nature* **431**:1055-1061
54. Brown WM .2001. Natural selection of mammalian brain components. *Trends Ecol Evol.* **16**:471-473
55. Brunk K, Vernay B, Griffith E *et al*. (7 authors). 2007. Micocephalin coordinates mitosis in the syncytial Drosophila embryo. *J Cell Sci*. **120**: 3578-3588
56. Buchman JJ, Tseng HC, Zhou Y *et al*. (6 authors). 2010. *CDK5RAP2* interacts with Pericentrin to maintain the neural progenitor pool in the developing neocortex. *Neuron* **66**: 386-402
57. Burki F, Kaessmann H. 2004. Birth and adaptive evolution of a hominoid gene that supports high neurotransmitter flux. *Nat Genet.* **35**: 1061-1063
58. Burnham KP, Anderson DR. 2002. *Model selection and multimodel inference: A practical information-theoretic approach*. Springer, New York

59. Bush EC, Allman JC. 2003. The scaling of white matter to gray matter in cerebellum and neocortex. *Brain Behav Evol.* **61**: 1-5

60. Bush EC, Allman JC. 2004. The scaling of frontal cortex in primates and carnivores. *Proc Natl Acad Sci USA.* **101:** 3962-3966

61. Bush EC, Lahn BT. 2005. Selective constraint on noncoding regions of hominid genomes. *PLoS Comput Biol*. **1(7)**: e73

62. Bush EC, Lahn BT. 2008. A genome-wide screen for noncoding elements important in primate evolution. *BMC Evol Biol.* **8**:17

63. Buss RR, Sun W, Oppenheim RW. 2006. Adaptive roles of programmed cell death during nervous system development. *Annu Rev Neurosci*. **29**: 1–35

64. Butler MA, King AA. 2004. Phylogenetic Comparative Analysis: A Modeling Approach for Adaptive Evolution. *Am Nat.* **164 (6)**: 683-695

65. Buxhoeveden DP, Casanova MF. 2002. The minicolumn hypothesis in neuroscience. *Brain* **125 (5)**: 935-951

66. Byrne RW. 1995. *The Thinking Ape: Evolutionary Origins of Intelligence*. Oxford University Press, Oxford

67. Cáceres M, Lachuer J, Zapala MA *et al*. (9 authors). 2003. Elevated gene expression levels distinguish human from non-human primate brains. *Proc Natl Acad Sci USA.* **100 (22)**: 13030-13035

68. Calegari F, Huttner WB. 2003. An inhibition of cyclin-dependent kinases that lengthens, but does not arrest, neuroepithelial cell cycle induces premature neurogenesis. *J Cell Sci.* **116**: 4947-4955

69. Capellini I, Venditti C, Barton RA. 2011. Placentation and Maternal Investment in Mammals. *Am Nat.* **177 (1)**: 86-98

70. Carmod RN, Wrangham RW. 2009. The energetic significance of cooking. *J Hum Evol*. **57 (4)**: 379-391

71. Carroll SB. 2003. Genetics and the making of *Homo sapiens*. *Nature* **422**: 849–857

72. Carroll SB. 2005. Evolution at two levels: on genes and form. *PLoS Biol.* **3**: 1160-1166

73. Carroll SB. 2008. Evo-Devo and an expanding evolutionary synthesis: a genetic theory of morphological evolution. *Cell* **134**: 25-36

74. Cartmill M. 1972. *Arboreal adaptations and the origin of the order Primates*. In: *The functional and evolutionary biology of Primates* (Aldine-Athertone TR, Eds). University of Chicago Press, Chicago
75. Casanova MF, Buxhoeveden DP, Cohen M, Switala AE, Roy E. 2002c. Minicolumnar pathology in dyslexia. *Ann Neurol.* **52 (1)**: 108–110
76. Casanova MF, Buxhoeveden DP, Switala AE, Roy E. 2002a. Minicolumnar pathology in autism. *Neurology* **58 (3)**: 428-432
77. Casanova MF, Buxhoeveden DP, Switala AE, Roy E. 2002b. Asperger's syndrome and cortical neuropathology. *J Child Neurol.* **17(2)**: 142-145
78. Casanova MF, Trippe II J, Tillquist C, Switala AE. 2009. Morphometric variability of minicolumns in the striate cortex of *Homo sapiens*, *Macaca mulatta*, and *Pan troglodytes*. *J Anat.* **214 (2)**: 226–234
79. Caviness VS, Takahashi T, Nowakowski RS. 1995. Numbers, time and neocortical neurogenesis: a general developmental and evolutionary model. *Trends Neurosci*. **18 (9)**: 279-282
80. Chaix R, Somel M, Kreil DP, Khaitovich P, Lunter GA. 2008. Evolution of primate gene expression: Drift and corrective sweeps? *Genetics* **180 (3)**: 1379-1389
81. Charnov E, Berrigan, D. 1993. Why do primates have such long lifespans and so few babies? *Evol Anthropol Issues News Rev*. **1**:191-194
82. Cheney D, Seyfarth R, Smuts B. 1986. Social relationships and social cognition in nonhuman primates. *Science* **234 (4782)**: 1361-1366
83. Chenn A, McConnell SK. 1995. Cleavage orientation and the asymmetric inheritance of Notch 1 immunoreactivity in mammalian neurogenesis. *Cell* **82**: 631-641
84. Cheung AFP, Pollen AA, Tavare A, DeProto J, Molnár Z. 2007. Comparative aspects of cortical neurogenesis in vertebrates. *J Anat*. **211 (2)**:164–176
85. Cheverud JM, Falk D, Vannier M *et al*. (6 authors). 1990. Heritability of Brain Size and Surface Features in Rhesus Macaques (*Macaca mulatta*). *J Hered*. **81 (1)**: 51-57
86. Chimpanzee Sequencing and Analysis Consortium. 2005. Initial sequence of the chimpanzee genome and comparison with the human genome. *Nature* **437 (7055)**: 69-87
87. Chitka L, Niven J. 2009. Are bigger brains better? *Curr Biol*. **19 (21)**: R995-R1008

88. Clark NL, Swanson WJ. 2005. Pervasive adaptive evolution in primate seminal proteins. *PloS Genet.* **1 (2)**: e35

89. Clutton-Brock TH, Harvey PH. 1980. Primates, brains and ecology. *J Zool*. **190 (3)**: 309-323

90. Cormier A, Clémont MJ, Knossow M *et al*. (9 authors). 2009. The PN2-3 domain of CPAP implements a novel mechanism for tubulin sequestration. *J Biol Chem*. **284**: 6909-6917

91. Cortés-Ortiz L. 2009. Molecular Phylogenetics of the Callitrichidae with an Emphasis on the Marmosets and *Callimico*. In: *The smallest anthropoids: the marmoset/callimico radiation* (Developments in primatology: progress and prospects) (Ford SM, Porter LM, Davis LC. Eds.). Springer, New York

92. Cox J, Jackson AP, Bond J, Woods CG. 2006. What primary microcephaly can tell us about brain growth. *Trends Mol Med.* **12 (8)**: 358-366

93. Cresko WA, Amores A, Wilson C *et al*. (7 authors). 2004. Parallel genetic basis for repeated evolution of armour loss in Alaskan threespine stickleback populations. *Proc Natl Acad Sci USA.* **101 (16)**: 6050-6055

94. Crespi B, Summers K, Dorus S. 2007. Adaptive evolution of genes underlying schizophrenia. *Proc R Soc B.* **274**: 2801-2810

95. Crisci JL, Wong A, Good JM, Jensen HD. 2011. On characterizing adaptive events unique to modern humans. *Genome Biol Evol*. In press

96. Cunningham CW, Omland KE, Oakley TH. 1998. Reconstructing ancestral character states: a critical reappraisal. *Trends Ecol Evol.* **13**: 361-366

97. Currat M, Excoffier L, Maddison W *et al*. (7 authors). 2006. Comment on ‘‘Ongoing adaptive evolution of *ASPM*, a brain size determinant in *Homo sapiens*’’ and ‘‘*Microcephalin*, a gene regulating brain size, continues to evolve adaptively in humans’’. *Science* **313:** 172a

98. Darwin C. 1859. *On the origin of species by means of natural selection, or the preservation of favoured races in the struggle for life*. John Murray, London

99. Darwin C. 1871. *The Descent of Man, and Selection in Relation to Sex*. John Murray, London

100. Davies W, Isles AR, Wilkinson LS. 2005. Imprinted gene expression in the brain. *Neurosci Biobehav Rev*. **29**: 421–430

101. de Winter W, Oxnard CE. 2001. Evolutionary radiations and convergences in the structural organization of mammalian brains. *Nature* **409**: 710-714
102. Deacon TW. 1990. Rethinking mammalian brain evolution. *Amer Zool.* **30**: 629-705
103. Deacon TW. 1997. What makes the human brain different? *Annu Rev Anthropol.* **26**: 337-257
104. Deaner RO, Isler K, Burkart J, van Schaik C. 2007. Overall brain size, and not encephalization quotient, best predicts cognitive ability across non-human primates. *Brain Behav Evol*. **70**:115-124
105. Deaner RO, Nunn CL. 1999. How quickly do brains catch up with bodies? A comparative method for detecting evolutionary lag. *Proc R Soc Lond B.* **266**: 687-694
106. Deaner RO, van Schaik CP, Johnson V. 2006. Do some taxa have better domain-general cognition than others? A meta-analysis of nonhuman primate studies. *Evol Psych*. **4**: 149-196
107. Delaval B, Doxsey S. 2008. Dwarfism, where *Pericentrin* gains stature. *Science* **319**: 732-733
108. Depaepe V, Suarez-Gonzalez N, Dufour A *et al*. (9 authors). 2005. *Ephrin* signalling controls brain size by regulating apoptosis of neural progenitors. *Nature* **435**: 1244-1250
109. Desir J, Cassart M, David P, Van Bogaert P, Abramowicz M. 2008. Primary microcephaly with *ASPM* mutation shows simplified cortical gyration with antero-posterior gradient pre- and post-natally. *Am J Med Genet A.* **146A**: 1439–1443
110. Dial KP, Greene E, Irschick DJ. 2008. Allometry of behavior. *Trends Ecol Evol.* **23**: 394-401
111. Dixson AF. 1993. *Callitrichid mating systems: laboratory and field approaches to studies of monogamy and polyandry*. In *Marmosets and Tamarins: systematic, behaviour and ecology* (Rylands, AB. Ed). Oxford University Press, Oxford
112. Doan JW, Schmidt TR, Wildman DE *et al*. (6 authors). 2005. Rapid nonsynonymous evolution of the Iron-Sulfur Protein in anthropoid Primates. *J Bioenerg Biomembr*. **37 (1)**: 35-41
113. Dobson SD, Sherwood CC. 2011. Correlated evolution of brain regions involved in producing and processing facial expressions in anthropoid primates. *Biol Lett*. **7 (1)**: 86-88

114. Dobson-Stone C, Gatt JM, Kuan SA *et al*. (7 authors). 2007. Investigation of *MCPH1* G37995C and *ASPM* A44871G polymorphisms and brain size in a healthy cohort. *NeuroImage* **37 (2)**: 394-400
115. Dorus S, Anderson JR, Vallender EJ *et al*. (9 authors). 2006. Sonic Hedgehog, a key development gene, experienced intensified molecular evolution in primate. *Hum Mol Genet*. **15 (13)**: 2031-2037
116. Dorus S, Evans PD, Wyckoff GJ, Choi SS, Lahn BT 2004b. Rate of molecular evolution of the seminal protein gene *SEMG2* correlates with levels of female promiscuity. *Nat Genet*. **36**: 1326-1329
117. Dorus S, Vallender EJ, Evans PD *et al*. (9 authors). 2004a. Accelerated evolution of nervous system genes in the origin of *Homo sapiens*. *Cell* **119**: 1027-1040
118. Douglas RJ, Mahowald M, Martin KAC, Stratford KJ. 1995. The role of synapses in cortical computation. *J Neurocytol.* **25 (1)**: 893-911
119. Dunbar R, Schultz S. 2007. Evolution in the social brain. *Science* **7**: 1344 –1347
120. Dunbar R. 1992. Neocortex size as a constraint on group size in primates. *J Hum Evol.* **22 (6)**: 469-493
121. Dunbar R. 1998. The social brain hypothesis. *Evol Anthropol Issues News Rev*. **6**: 178-190
122. Eastman JM, Alfaro ME, Joyce P, Hipp AL, Harmon LJ. 2011. A novel comparative method for identifying shifts in the rate of character evolution on trees. *Evolution* in press
123. Elston GN. 2007. *Specialization of the neocortical pyramidal cell during primate evolution*. In: *Evolution of nervous systems: a comprehensive reference* (Kaas JH, Preuss TM, Eds). Vol. 4. *Primates*. Elsevier; Boston
124. Enard D, Depaulis F, Roest Crollius H. 2010. Human and non-human primate genomes share hotspots of positive selection. *PLoS Genet.* **6 (2)**: e1000840
125. Enard W, Hammerschmidt K, Brückner M *et al*. (56 authors). 2009. A humanized version of *FOXP2* affects cortico-basal ganglia circuits in mice. *Cell* **137**: 961-971
126. Enard W, Przeworski M, Fisher SE *et al*. (8 authors). 2002. Molecular evolution of *FOXP2*, a gene involved in speech and language. *Nature* **418**: 869-871
127. Enard W. 2011. *FOXP2* and the role of cortic-basal ganlia circuits in speech and language evolution. *Curr Op Neurobiol*. **21 (3)**: 415-424

128. Evans PD, Anderson JR, Vallender EJ *et al*. (7 authors). 2004a. Adaptive evolution of *ASPM*, a major determinant of cerebral cortical size in humans. *Hum Mol Genet*. **13 (5)**: 489-494
129. Evans PD, Anderson JR, Vallender EJ, Choi SS, Lahn BT. 2004b. Reconstructing the evolutionary history of *Microcephalin*, a gene controlling human brain size. *Hum Mol Genet.* **13 (5)**: 1139-1145
130. Evans PD, Gilbert SL, Mekel-Bobrov N *et al*. (9 authors). 2005. *Microcephalin*, a gene regulating brain size, continues to evolve adaptively in humans. *Science* 209 (5741), 1717-1720
131. Evans PD, Vallender EJ, Lahn BT. 2006. Molecular evolution of the brain size regulator genes *CDK5RAP2* and *CENPJ*. *Gene* **375**: 75-79
132. Falk D, Gibson KR, editors. 2001. *Evolutionary anatomy of the primate cerebral cortex*. Cambridge University Press, Cambridge
133. Falk D, Hildebolt C, Smith K *et al*. (10 authors). 2005. The brain of LB1, *Homo floresiensis*. *Science* **308**: 242-245
134. Falk D, Hildebolt C, Smith K *et al*. (10 authors). 2007. Brain shape in human microcephalics and *Homo floresiensis*. *Proc Natl Acad Sci USA*. **104**: 2513-1518
135. Falk D, Hildebolt C, Smith K *et al*. (8 authors). 2009. LB1's virtual endocast, microcephaly, and hominin brain evolution. *J Hum Evol.* **57 (5)**: 597-60
136. Falls JG, Pulford DJ, Wylie A, Jirtle RL. 1999. Genomic imprinting: implications for human disease. *Am J Pathol.* **154**: 636-647
137. Fears SC, Melega WP, Service SK *et al*. (11 authors). 2009. Identifying Heritable Brain Phenotypes in an Extended Pedigree of Vervet Monkeys. *J Neurosci.* **29 (9)**: 2867-2875
138. Felsenstein J. 1985. Phylogenies and the comparative method. *Am Nat.* **125**:1-15
139. Fietz SA, Huttner WB. 2010. Cortical progenitor expansion, self-renewal and neurogenesis—a polarized perspective. *Curr Op Neurobiol.* **21 (1)**: 23-35
140. Fietz SA, Kelava I,Vogt J *et al*. (11 authors). 2010. OSVZ progenitors of human and ferret neocortex are epithelial-like and expand by integrin signaling. *Nat Neurosci*. **13**: 690–699
141. Finarelli JA, Flynn JJ 2007. The evolution of encephalization in Caniform carnivores. *Evolution* **61**:1758-1772

142. Finarelli JA, Flynn JJ. 2006. Ancestral state reconstruction of body size in the Caniformia (Carnivora, Mammalia): The effects of incorporating data from the fossil record. *Syst Biol*. **55**: 301-313
143. Finarelli JA, Flynn JJ. 2009. Brain-size evolution and sociality in Carnivora. *Proc Natl Acad Sci USA.* **106 (23)**: 9345-9349
144. Finlay BL, Darlington RB. 1995. Linked regularities in the development and evolution of mammalian brains. *Science* **268 (5217)**: 1578-1584
145. Finlay BL, Darlington, RB, Nicastro N. 2001. Developmental structure in brain evolution. *Behav Brain Sci*. **24**: 298-304
146. Fish JL, Dehay C, Kennedy H, Huttner WB. 2008. Making bigger brains – the evolution of neural-progenitor-cell division. *J Cell Sci*. **121**: 2783-2793
147. Fish JL, Kosodo Y, Enard W, Pääbo S, Huttner WB. 2006. *ASPM* specifically maintains symmetric proliferative divisions of neuroepithelial cells. *Proc Natl Acad Sci USA*. **103 (27)**: 10438-10443
148. Fleagle JG. 1999. *Primate adaptation and evolution*. John Wiley & Sons, New York
149. Flint J. 1992. Implications of genomic imprinting for psychiatric genetics. *Psychol Med*. **22(1)**: 5-10
150. Fong KW, Choi YK, Rattner JB, Qi RZ. 2008. *CDK5RAP2* is a pericentriolar protein that functions in centrosomal attachment of the γ-tubulin ring complex. *Mol Biol Cell*. **19 (1)**: 115-125
151. Ford S. 1980 Callitrichids as phyletic dwarfs, and the place of the Callitrichidae in Platyrrhini. *Primates* **21 (1)**: 21-43
152. Ford SM, Porter LM, Davis LC. (Eds) 2009. *The smallest anthropoids the marmoset/callimico radiation.* Developments in primatology: progress and prospects. Springer, New York
153. Forger NG. 2006. Cell death and sexual differentiation of the nervous system. *Neuroscience* **138 (3)**: 929-928
154. Fragaszy DM, Visalberghi E, Fedigan L (Eds). 2004. *The complete capuchin*. Cambridge University Press, Cambridge
155. Freckleton RP, Harvey PH, Pagel M. 2002. Phylogenetic analysis and comparative data: a test and review of evidence. *Am Nat.* **160 (6)**: 712-726

156. Freckleton RP, Harvey PH. 2006. Detecting Non-Brownian Trait Evolution in Adaptive Radiations. *PLoS Biol.* **4(11)**: e373
157. Freckleton RP. 2009. The seven deadly sins of comparative analysis. *J Evol. Biol*. **22 (7)**: 1367–1375
158. Fu X, Giavalisco P, Liua X *et al*. (13 authors). 2011. Rapid metabolic evolution in human prefrontal cortex. *Proc Natl Acad Sci USA.* **108 (15)**: 6181-6186
159. Fuller JL, Geils HD. 1972. Brain growth in mice selected for high and low brain weight. *Dev Psych.* **5 (4)**: 307-318
160. Gabi M, Collins CE, Wong P *et al*. (6 authors). 2010. Cellular scaling rules for the brains of an extended number of Primate species. *Brain Behav Evol.* **76**:32-44
161. Galtier N, Duret L. 2007. Adaptation or biased gene conversion? Extending the null hypothesis of molecular evolution. *Trends Genet*. **23 (6)**: 273-277
162. Garland JRT, Midford PE, Ives AR. 1999. An introduction to phylogenetically based statistical methods, with a new method for confidence intervals on ancestral values. *Amer Zool*. **39 (2)**: 374-388
163. Garland T, Bennet AF, Rezende EL. 2005. Phylogenetic approaches in comparative physiology. *J Exp Biol*. **208**: 3015-3035
164. Gasper J, Swanson WJ. 2006. Molecular population genetics of the gene encoding the human fertilization protein zonadhesin reveals rapid adaptive evolution. *Am J Hum Genet*. **79 (5)**: 820-830
165. Gebo DL. 2004. A shrew-sized origin for primates. *Am J Phys Anthropol.* **125 (39)**: 40-62
166. Genome 10K Community of Scientists. 2009. Genome 10K: A proposal to obtain whole-genome sequence for 10,000 vertebrate species. *J Hered.* **100 (6)**: 659-674
167. Gibson KR, Rumbaugh D, Beran M. 2001. *Bigger is better: primate brain size in relationship to cognition*. In: *Evolutionary Anatomy of the Primate Cerebral Cortex* (Falk D Gibson, KR, eds) Cambridge University Press, Cambridge
168. Giger T, Khaitovich P, Somel M *et al*. (11 authors). 2010. Evolution of neuronal and endothelial transcriptomes in Primates. *Genome Biol Evol.* **2**: 284–292
169. Gilad Y, Oshlack A, Smyth GK, Speed TP, White KP. 2006. Expression profiling in primates reveals a rapid evolution of human transcription factors. *Nature* **440**: 242-245

170. Gilbert SL, Dobyns WB, Lahn BT. 2005. Genetic links between brain development and brain evolution. *Nat Rev Genet.* **6**: 581-590

171. Gilks WR, Richardson S, Spiegelhalter DJ. 1996. *Introducing Markov Chain Monte Carlo*. In: *Markov Chain Monte Carlo in practice* (Gilks WR, Richardson S, Spiegelhalter DJ, Eds). Chapman and Hall, London

172. Gilmore JH, Lin W, Prastawa MW *et al*. (12 authors). 2007. Regional Gray Matter Growth, Sexual Dimorphism, and Cerebral Asymmetry in the Neonatal Brain. J Neurosci 27(6): 1255-1260

173. Gingerich PD, Gunnell GF. 2005. Brain of *Plesiadapis Cookei* (Mammalia, Proprimates): Surface morphology and encephalization compared to those of primates and Dermoptera. *Contributions from the Museum of Paleontology, University of Michigan* **31 (8)**: 185-195

174. González-Lagos C, Sol D, Reader SM. 2010. Large-brained mammals live longer. J Evol Biol. **23 (5)**: 1064–1074

175. Gonzalez-Voyer A, Winberg S, Kolm N. 2009. Distinct evolutionary patterns of brain and body size during adaptive radiation. *Evolution* **63**: 2266-2274

176. Goodman M, Grossman LI, Wildman DE. 2005. Moving primate genomics beyond the chimpanzee genome. *Trends Genet.* **21 (9)**: 511-517

177. Goodman M, Sterner KN, Islam M *et al*. (11 authors). 2009. Phylogenomic analyses reveal convergent patterns of adaptive evolution in elephant and human ancestries. *Proc Natl Acad Sci USA.* **106(49)**: 20824-9

178. Goos L, Silverman I. 2001. The influence of genomic imprinting on brain development and behaviour. *Evol Hum Behav.* **22 (6)**: 385-407

179. Gordon AD, Nevell L, Wood B. 2008. The *Homo floresiensis* cranium (LB1): Size, scaling, and early *Homo* affinities. *Proc Natl Acad Sci USA*. **105**: 4650-4655

180. Götz M, Huttner WB. 2005. The cell biology of neurogenesis. *Nat Rev Mol Cell Biol*. **6**: 777-778

181. Gould GC, MacFadden BJ. 2004. Gigantism, Dwarfism, and Cope's Rule: "Nothing in Evolution Makes Sense without a Phylogeny*". Bulletin of the American Museum of Natural History* **285**: 219-237

182. Gould SJ. 1975. Allometry in Primates, with emphasis on scaling and the evolution of the brain. *Contrib Primatol.* **5:**244-92

183. Green RE, Krause J, Briggs AW *et al*. (55 authors). 2010. A draft sequence of the Neandertal genome. *Science* **328**: 710-722
184. Gregg C, Zhang J, Butler JE, Haig D, Dulac C. 2010. Sex-specific parent-of-origin allelic expression in the mouse brain. *Science* **329 (5992)**: 682-5
185. Grossman LI, Wildman DE, Schmidt TR, Goodman M. 2004. Accelerated evolution of the electron transport chain in anthropoid primates. *Trends Genet.* **20 (11)**: 578-85
186. Groves CP. 1989. *A theory of human and Primate evolution.* Oxford University Press, Oxford
187. Groves CP. 2001. *Primate taxonomy*. Smithsonian Institution Press, Washington
188. Gurche JA. 1982. *Early Primate brain evolution.* Plenum, New York
189. Gustafsson L. 1997. Inadequate cortical feature maps: A neural circuit theory of autism. *Bio Psych.* **42**: 1138-1147
190. Gustafsson L. 2004. Comment on "Disruption in the inhibitory architecture of the cell minicolumn: Implications for autism". *Neuroscientist* **10**:189-191
191. Hafner MS, Hafner JC. 1984. Brain size, adaptation and heterochrony in geomyoid rodents. *Evolution* **38 (5)**: 1088-1098
192. Hall JG. 1997. Genomic imprinting: nature and clinical relevance. *Annu Rev Med.* **48**: 35–44
193. Hansen DV, Lui JH, Parker PRL, Kriegstein AR. 2010. Neurogenic radial glia in the outer subventricular zone of human neocortex. *Nature* **464**: 554–561
194. Hansen TF, Pienaar J, Orzack SH. 2008. A comparative method for studying adaptation to a randomly evolving environment. *Evolution* **62 (8)**: 1965-1977
195. Hansen TF. 1997. Stabilizing selection and the comparative analysis of adaptation. *Evolution* **51 (5)**: 1341-1351
196. Hansken J, Wake DB. 1993. Miniaturization of body size: Organismal consequences an evolutionary significance. *Annu Rev Ecol Syst*. **24**: 501-519
197. Harcourt AH, Purvis A, Liles L. 1995. Sperm Competition: mating system, not breeding season, affects testes size of primates. *Funct Ecol*. **9 (3)**: 468-476
198. Hardan AY, Muddasani S, Vemulapalli M, Keshavan MS, Minshew NJ. 2006. An MRI study of increased cortical thickness in autism. *Am J Psychiatry* **163**:1290-1292
199. Harvey PH, Krebs JR. 1990. Comparing brains. *Science* **249 (4965)**: 140-146

200. Harvey PH, Pagel MD. 1991. *The comparative method in evolutionary biology*. Oxford University Press, Oxford
201. Haug H. 1987. Brain sizes, surfaces, and neuronal sizes of the cortex cerebri: A stereological investigation of man and his variability and a comparison with some mammals (primates, whales, marsupials, insectivores, and one elephant). *Am J Anat.* **180 (2)**: 126-142
202. Haydar TF, Kuan CY, Flavell RA, Rakic P. 1999. The role of cell death in regulating the size and shape of the mammalian forebrain. *Cereb Cortex*. **9 (6)**: 621-626
203. Haygood R, Babbitt CC, Fegrigo O, Wray GA. 2010. Contrasts between adaptive coding and noncoding changes during human evolution. *Proc Natl Acad Sci USA*. **107 (17)**: 7853–7857
204. Haygood R, Fedrigo O, Hanson B, Yokoyama KD, Wray GA. 2007. Promoter regions of many neural- and nutrition-related genes have experienced positive selection during human evolution. *Nat Genet*. **39**: 1140-1144
205. Healy SD, Rowe C. 2007. A critique of comparative studies of brain size. *Proc R Soc B.* **274**: 453-464
206. Heesy CP. 2009. Seeing in stereo: The ecology and evolution of primate binocular vision and stereopsis. *Evol Anthropol Issues News Rev.* **18 (1)**: 21-35
207. Heissig F, Krause J, Bryk J *et al*. (6 authors). 2005. Functional analysis of human and chimpanzee promoters. *Genome Biology*. **6**: R57
208. Henneberg M. 1998. Evolution of the human brain: is bigger better? *Clin Exp Pharmacol Physiol*. **25**:745-749
209. Herculano-Houzel S, Collins CE, Wong P, Kaas JH, Lent R. 2008. The basic nonuniformity of the cerebral cortex. *Proc Natl Acad Sci USA*. **105 (34)**:12593-8
210. Herculano-Houzel S, Collins CE, Wong P, Kaas JH. 2007. Cellular scaling rules for primate brains. *Proc Natl Acad Sci USA.* **204 (9)**: 3562-3567
211. Herculano-Houzel S, Kaas JH. 2011. Gorilla and orangutan brains conform to the primate cellular scaling rules: implications for human evolution. *Brain Behav Evol*. **77 (1)**: 33-44
212. Herculano-Houzel S, Mota B, Lent R. 2006. Cellular scaling rules for rodent brains. *Proc Natl Acad Sci USA.* **103 (32)**: 12138-43
213. Herculano-Houzel S. 2009. The human brain in numbers: a linearly scaled-up primate brain. *Front Hum Neurosci.* **3**: 31

214. Herculano-Houzel S. 2010. Coordinated scaling of cortical and cerebellar numbers of neurons. *Front Neuroanat.* 104: 12
215. Herculano-Houzel S. 2011a. Scaling of brain metabolism with a fixed energy budget per neuron: implications for neuronal activity, plasticity and evolution. *PLoS One*. **6(3)**: e17514
216. Herculano-Houzel S. 2011b. Not all brains are made the same: New views on brain scaling in evolution. *Brain Behav Evol*. In press
217. Herlyn H, Zischler H. 2007. Sequence evolution of the sperm ligand *zonadhesin* correlates negatively with body weight dimorphism in primates. *Evolution* **61 (2)**: 289-98
218. Hershkovitz I, Kornreich L, Laron Z. 2007. Comparative skeletal features between *Homo floresiensis* and patients with primary growth hormone insensitivity (Laron Syndrome). *Am J Phys Anthropol*. **134**: 198-208
219. Hershkovitz P. 1977. *Living New World monkeys (Platyrrhini): With an introduction to primates.* University of Chicago Press, Chicago
220. Hirano T. 2006. At the heart of the chromosome: SMC proteins in action. *Nature Rev Mol Cell Biol.* **7**: 311-322
221. Hoekstra HE, Coyne JA. 2007. The locus of evolution: evo devo and the genetics of adaptation. *Evolution* **61 (5)**: 995-1016
222. Hoffman MM, Birney E. 2010. An effective model for natural selection in promoters. *Genome Res*. **20**: 685-692
223. Hofman MA. 1989. On the evolution and geometry of the brain in mammals. *Prog Neurobiol*. **32 (2)**: 137-58
224. Horton JC, Adams DL. 2005. The cortical column: a structure without a function. *Phil Trans R Soc B.* **360 (1456)**: 837-862
225. Horvath JE, Weisrock DW, Embry SL, Fiorentino I, Balhoff JP, Kappeler P, Wray GA, Willard HF, Yoder AD. 2008. Development and application of a phylogenomic tookit: Resolving the evolutionary history of Madagascar's lemurs. *Genome Res.* **18**: 489-499
226. Hughes AL. 2007. Looking for Darwin in all the wrong places: the misguided quest for positive selection at the nucleotide sequence level. *Heredity* **99:** 364–373
227. Hughes TA. 2006. Regulation of gene expression by alternative untranslated regions. *Trends Genet*. **22 (3)**: 119-122
228. Huxley TH. 1863. *Evidence as to man's place in nature.* Willams & Norgate, London.

229. International Human Genome Sequencing Consortium. 2001. Initial sequencing and analysis of the human genome. *Nature* **409**: 860-921

230. Isler K, Kirk EC, Miller JMA *et al*. (6 authos). 2008. Endocranial volumes of primate species: scaling analyses using a comprehensive and reliable data set. *J Hum Evol.* **55 (6)**: 967-978

231. Isler K, Van Schaik CP. 2006. Metabolic costs of brain size evolution. *Biol Lett.* **2 (4)**: 557-560

232. Ives AR, Midford PE, Garland T, Jr. 2007. Within-species variation and measurement error in phylogenetic comparative methods. *Syst Biol.* **56 (2)**: 252-270

233. Jabes A, Lavenex PB, Amaral DG, Lavenex P. 2010. Quantitative analysis of postnatal neurogenesis and neuron number in the macaque monkey dentate gyrus. *Eur J Neurosci*. **31**: 273-285

234. Jackson AP, Eastwood H, Bell SM, *et al*. (16 co-authors). 2002. Identification of microcephalin, a protein implicated in determining the size of the human brain. *Am J Hum Genet*. **71 (1)**: 136-142

235. Jackson AP, McHale DP, Campbell DA, *et al*. (13 co-authors). 1998. Primary autosomal recessive microcephaly (*MCPH1*) maps to chromosome 8p22-pter. *Am J Hum Genet*. **63 (2)**: 541-546

236. Jacob T, Indriati E, Soejono RP *et al*. (9 authors). 2006. Pygmoid Australomelanesian *Homo sapiens* skeletal remains from Liang Bua, Flores: Population affinities and pathological abnormalities. *Proc Natl Acad Sci USA.* **103**: 13421-13426

237. Jerison HJ. 1973. *Evolution of the brain and intelligence*. Academic Press, New York

238. Jernigan T, Bellugi U, Sowell E, Doherty S, Hesselink J. 1993. Cerebral morphological distinctions between Williams and Down syndromes. *Arch Neuro*. **50**: 186–191

239. Joffe TH, Dunbar RIM. 1997. Visual and socio–cognitive information processing in primate brain evolution. *Proc R Soc Lond B.* **264 (1386)**: 1303-1307

240. Jones KE, MacLarnon AM. 2004. Affording larger brains: Testing hypotheses of mammalian brain evolution on bats. *Am Nat.* **164 (1)**: E20-E31

241. Jones, KE, Bielby J, Cardillo M *et al*. (25 authors). 2009. PanTHERIA: a species-level database of life history, ecology, and geography of extant and recently extinct mammals. *Ecology* **90**: 2648–2648

242. Jungers WL, Harcourt-Smith WEH, Wunderlich RE *et al*. (8 authors). 2009. The foot of *Homo floresiensis*. *Nature* **459**: 81-84

243. Jungers WL. 1985. *Body size and scaling of limb proportions in primates*. In: *Size and Scaling in Primate Biology* (Jungers WL Ed). Plenum Press, New York

244. Kass RE, Raftery AE. 1995. Bayes factors. *J Am Stat Assoc*. **90**:773-795

245. Kaufman JA, Ahrens ET, Laidlaw DH, Zhang S, Allman JM. 2005. Anatomical analysis of an aye-aye brain (*Daubentonia madagascariensis*, Primates: Prosimii) combining histology, structural magnetic resonance imaging, and diffusion-tensor imaging. *Anat Rec A Discov* **287A:**1026–1037

246. Kay RF. 1984. *On the use of anatomical features to infer foraging behaviour in extinct primates*. In: *Adaptations for foraging in nonhuman primates* (Rodman PS, Cant JGH. Eds). Columbia University Press, New York

247. Kelley JL, Swanson WJ. 2008. Positive selection in the human genome: From genome scans to biological significance. *Annu Rev Genom Hum Genet.* **9**: 143-160

248. Kelly JL, Swanson WJ. 2008. Dietary change and adaptive evolution of *enamelin* in humans and among Primates. *Genetics* **178**: 1595-1603

249. Kety SS. 1957. *The general metabolism of the brain in vivo*. In: *Metabolism of the nervous system* (Richter D, Ed). Pergamon, London

250. Keverne EB, Fundele R, Narasimha M, Barton SC, Surani MA. 1996. Genomic imprinting and the differential roles of parental genomes in brain development. *Brain Res Dev Brain Res*. **92**: 91-100

251. Keverne EB, Martel FL, Nevison CM. 1996. Primate brain evolution: Genetic and functional considerations. *Proc R Soc Lond B.* **262**: 689–696

252. Keverne EB. 1997. Genomic imprinting in the brain. *Curr Opinn Neurobiol*. 7: 463-468

253. Khaitovich P, Pääbo S, Weiss G. 2005a Toward a neutral evolutionary model of gene expression. *Genetics* **170 (2)**: 929-939

254. Khaitovich P, Enard W, Lachmann M, Paabo S. 2006a. Evolution of primate gene expression. *Nat Rev Genet*. **7**: 693-702

255. Khaitovich P, Hellmann I, Enard W *et al*. (9 authors). 2005b. Parallel patterns of evolution in the genomes and transcriptomes of humans and chimpanzees. *Science* **309 (5742)**: 1850-1854

256. Khaitovich P, Tang K, Franz H *et al* (8 authors). 2006b. Positive selection on gene expression in the human brain. *Curr Biol.* **16 (10)**: R356-8

257. Khaitovich P, Weiss G, Lachmann M *et al*. (9 authors). 2004 A neutral model of transcriptome evolution. *PLoS Biol.* **2 (5)**: e132

258. King MC, Wilson AC. 1975. Evolution at two levels in humans and chimpanzees. *Science* **188 (4184)**: 107-116

259. Klingenberg C. 2010. Evolution and development of shape: integrating quantitative approaches. *Nat Rev Genet.* **11**: 623-635

260. Kochunov P, Glahn DC, Fox PT *et al*. (12 authors). 2009. Genetics of primary cerebral gyrification: Heritability of length, depth and area of primary sulci in an extended pedigree of *Papio* baboons. *NeuroImage* **53 (3)**: 1126-1134

261. Köhler M, Moyá-Solá S. 2004. Reduction of brain and sense organs in the fossil insular bovid Myotragus. *Brain Behav Evol.* **63**: 125-140

262. Kohn LA, Atchley WR. 1988. How similar are genetic correlation structures? Data from mice and rats. *Evolution* **42 (3)**: 467-481

263. Konopka G, Bomar JM, Winden K *et al*. (10 authors). 2009. Human-specific transcriptional regulation of CNS development genes by *FOXP2*. *Nature* **462**: 213-217

264. Kouprina N, Pavlicek A, Collins NK, *et al*. (18 co-authors). 2005. The microcephaly *ASPM* gene is expressed in proliferating tissues and encodes for a mitotic spindle protein. *Hum Mol Genet*. **14 (15)**: 2155-2165

265. Kouprina N, Pavlicek P, Mochida GH, *et al*. (13 co-authors). 2004. Accelerated evolution of *ASPM* Gene controlling brain size begins prior to human brain expansion. *PLoS Biol.* **2 (5)**: 653-662

266. Kriegstein A, Noctor S, Martínez-Cerdeño V. 2006. Patterns of neural stem and progenitor cell division may underlie evolutionary cortical expansion. *Nat Rev Neurosci*. **7**: 883-890

267. Kudo H, Dunbar RIM. 2001. Neocortex size and social network size in primates. *Anim Behav*. **62 (4)**: 711-722

268. Kuida K, Haydar TF, Kuan CY (9 authors). 1998. Reduced apoptosis and cytochrome c–mediated caspase activation in mice lacking *Caspase 9*. *Cell* **94 (3)**: 325-337

269. Kuida K, Zheng TS, Na S *et al*. (8 authors). 1996. Decreased apoptosis in the brain and premature lethality in *CPP32*-deficient mice. *Nature* **384**: 368 – 372

270. Kumar A, Girimaji SC, Duvvari MR, Blanton SH. 2009. Mutations in *STIL*, encoding a pericentriolar and centrosomal protein cause primary microcephaly. *Am J Hum Genet*. **84 (2)**: 286-290
271. Kurtén B. 1959. Rates of evolution in fossil mammals. *Cold Spring Harb Symp Quant Biol*. **24**: 205-215
272. Lai CSL, Fisher SE, Hurst JA, Vargha-Khadem F, Monaco AP. 2001. A forkhead-domain gene is mutated in a severe speech and language disorder. *Nature* **413:** 519 - 523
273. Lambert N, Lambot M-A, Bilheu A *et al*. (12 authors). 2011. Genes expressed in specific areas of the human fetal cerebral cortex display distinct patterns of evolution. *PLoS ONE* **6 (3)**: e17753
274. Lande, R. 1979. Quantitative genetic analysis of multivariate evolution, applied to brain: body size allometry. *Evolution* **33 (1)**: 402-416
275. Lanfear R, Welch JJ, Bromhan L. 2010. Watching the clock: Studying variation in rates of molecular evolution between species. *Trends Ecol Evol.* **25 (9)**: 495-503
276. Larson SG, Jungers WL, Tocheri MW *et al*. (8 authors). 2008. Descriptions of the upper limb skeleton of *Homo floresiensis*. *J Hum Evol*. **57 (5)**: 555-570
277. Lartillot N, Poujol R. 2011. A phylogenetic model for investigating correlated evolution of substitution rates and continuous phenotypic characters. *Mol Biol Evol.* **28 (1)**: 729-744
278. Lee SI, Lee WK, Shin JH *et al*. (9 authors). 2009. Sexually dimorphic gene expression in the chick brain before gonadal differentiation. *Poultry Science* **88**: 1003–1015
279. Lefebvre L, Reader SM, Sol D. 2004. Brains, innovations and evolution in birds and Primates. *Brain Behav Evol.* **63**: 233-246
280. Leigh SR. 2004. Brain growth, life history, and cognition in primate and human evolution. *Am J Primatol*. **62 (3)**: 139–164
281. Lerch JP, Evans AC. 2005. Cortical thickness analysis examined through power analysis and a population simulation. *NeuroImage* **24 (1)**: 163-173
282. Leudi PP, Dietrich FS, Weidman JR *et al*. (6 authors). 2007. Computational and experimental identification of novel human imprinted genes. *Genome Res*. **17**: 1723-1730
283. Leutenegger W. 1973. Maternal-fetal weight relationships in primates. *Folia Primatol*. **20**: 280-293

284. Lindenfors P, Nunn CL, Barton RA. 2007. Primate brain architecture and selection in relation to sex. *BMC Biol.* **5 (20)**

285. Locke DP, LaDeana WH, Warren WC *et al*. (101 authors). 2011. Comparative and demographic analysis of orang-utan genomes. *Nature* **469**: 529–533

286. Lomolino MV. 2005. Body size evolution in insular vertebrates: generality of the island rule. *J Biogeog.* **32 (10)**: 1683-1699

287. Lopsvold D. 1986. Quantitative genetics of morphological differentiation in *Permoyscus*. I. Tests of the homogeneity of genetic covariance structure among species and subspecies. *Evolution* **40 (3)**: 559-573

288. Low LK, Cheng HJ. 2006. Axon pruning: an essential step underlying the developmental plasticity of neuronal connections. *Philos Trans R Soc Lond B Biol Sci*. **361**:1531–1544

289. Lynch VJ, Wagner GP. 2008. Resurrecting the role of transcription factor change in developmental evolution. *Evolution* **62 (9)**: 2131-2154

290. Lyons DM, Afarian H, Schatzberg AF, Sawyer-Glover A. Moseley ME. 2002. Experience-dependent asymmetric variation in primate prefrontal morphology. *Behav Brain Res.* **136 (1)**: 51-59

291. Mace GM, Eisenberg JF. 1982. Competition, niche specialization and the evolution of brain size in the genus *Peromyscus*. *Biol J Linnean Soc*. **17 (3)**: 243–257

292. MacFadden BJ. 1986. Fossil horses from "*Eohippus*" (Hyracotherium) to *Equus*: scaling, Cope's Law, and the evolution of body size. *Paleobiology* **12 (4)**: 355-369

293. MacLean E, Barrickman NL, Johnson EM, Wall CE. 2009. Sociality, ecology and relative brain size in lemurs. *J Hum Evol*. **56 (5)**: 471-478

294. Maddison WP, Maddison DR. 2008. Mesquite: A modular system for evolutionary analysis. Version 2.5, http://mesquiteproject.org

295. Maddison WP. 1991. Squared-change parsimony reconstructions of ancestral states for continuous-valued characters on a phylogenetic tree. *Syst Zool*. **40**: 304-314

296. Mahaney MC, Williams-Blangero S, Blangero J, Leland MM. 1993. Quantitative genetics of relative organ weight variation in captive baboons. *Hum Biol.* **65(6)**: 991-1003

297. Marino L. 2006. Absolute brain size: did we throw the baby out with the bathwater. *Proc Natl Acad Sci USA.* **103**:13563-13564

298. Marques-Bonet T, Kidd JM, Ventura M, *et al*. (23 co-authors). 2009. A burst of segmental duplications in the genome of the African great ape ancestor. *Nature* **457**: 877-881
299. Marroig G, Cheverud JM. 2005. Size as a line of least evolutionary resistance: Diet and adaptive morphological radiation in New World monkeys. *Evolution* **59 (5)**: 1128-1142
300. Marroig G, Cheverud JM. 2009. *Size and shape in Callimico and marmoset skulls: Allometry and heterochrony in the morphological evolution of small anthropoids.* In*: The smallest anthropoids: the marmoset/callimico radiation (Developments in primatology: progress and prospects)* (Ford SM, Porter LM, Davis LC. Eds.). Springer, New York
301. Marroig G, Cheverud JM. 2010. Size as a line of least evolutionary resistance II: Direct selection on size or correlated response due to constraints? *Evolution* **64 (5)**: 1470-1488
302. Marshall LG, Corruccini RS. 1978. Variability, evolutionary rates, and allometry in dwarfing lineages. *Paleobiology* **4 (2)**: 101-119
303. Martin RD, MacLarnon AM, Phillips JL *et al*. (6 authors). 2006a. Comment on "the brain of LB1 *Homo floresiensis*". *Science* **312**: 999b
304. Martin RD, MacLarnon AM, Phillips JL *et al*. (6 authors). 2006b.Flores Hominoid: new species or microcephalic dwarf? *Anat Rec.* **288A**: 1123–1145
305. Martin RD, MacLarnon AM. 1985. Gestation period, neonatal size and maternal investment in placental mammals. *Nature* **116**: 60–124
306. Martin RD, Soligo C, Tavaré S. 2007. Primate Origins: Implications of a Cretaceous Ancestry. *Folia Primatol.* **78**: 277-296
307. Martin RD. 1981. Relative brain size and basal metabolic rate in terrestrial vertebrate. *Nature* **293**: 57 - 60
308. Martin RD. 1990. *Primate origins and evolution*. Princeton University Press, Princeton
309. Martin RD. 1992. Goeldi and the dwarfs: the evolutionary biology of the small New World monkeys. *J Hum Evol.* **22 (4-5)**: 367-393
310. Martin RD. 1996. Scaling of the mammalian brain: the maternal energy hypothesis. *Physiology* **11 (4)**: 149-156
311. Martins EP. 2000. Adaptation and the comparative method. *Trends Ecol Evol*. **15 (7)**: 296-299
312. Masters JC, Lovegrove BG, de Wit MJ. 2007. Eyes wide shut: can hypometabolism really explain the primate colonization of Madagascar? *J Biogeogr*. **34**:21-37

313. Matsumoto T, Schiller P, Dieterich LC *et al*. (10 authors). 2008. *Ninein* is expressed in the cytoplasm of angiogenic tip-cells and regulates tubular morphogenesis of endothelial cells. *Arterioscler Thromb Vasc Biol*. **28**: 2123-2130

314. Mattick JS, Mehler MF. 2008. RNA editing, DNA recoding and the evolution of human cognition. Trends Neurosci. **31 (5)**: 227-233

315. Mayrose I, Otto SP. 2011. A likelihood method for detecting trait-dependent shifts in the rate of molecular evolution. *Mol Biol Evol.* **28 (1)**: 759-770

316. McLean CY, Reno PL, Pollen AA *et al*. (13 authors). 2011. Human-specific loss of regulatory DNA and the evolution of human-specific traits. *Nature* **471**: 216–219

317. Meiri S, Cooper N, Purvis A. 2008. The island rule: made to be broken? *Proc R Soc B.* **275 (1631)**: 141-148

318. Mekel-Bobrov N, Gilbert SL, Evans PD *et al*. (8 authors). 2005. Ongoing adaptive evolution of *ASPM*, abrain size determinant in *Homo sapiens*. *Science* **309 (5741)**: 1720-1722

319. Mekel-Bobrov N, Posthuma D, Gilbert SL *et al*. (22 authors). 2007. The ongoing adaptive evolution of *ASPM* and *Microcephalin* is not explained by increased intelligence. *Hum Mol Genet.* **16 (6)**: 600-608

320. Millien V. 2006. Morphological evolution is accelerated among island mammals. *PLoS Biol.* **4**: e321

321. Mink JW, Blumenschine RJ, Adams DB. 1981. Ratio of central nervous system to body metabolism in vertebrates: its constancy and functional basis. *AJP - Regu Physiol*. **241 (3)**: R203-R212

322. Mogensen MM, Malik A, Piel M, Bouckson-Castaing V, Bornens M. 2000. Microtubule minus-end anchorage at centrosomal and non-centrosomal sites: the role of ninein. *J Cell Sci.* **113**: 3013-3023

323. Monroe MJ, Bokma F. 2010. Short communication: Little evidence for Cope's rule from Bayesian phylogenetic analysis of extant mammals. *J Evol Biol*. **23 (9)**: 2017–2021

324. Montagu MFA. 1955. Time, morphology, and neoteny in the evolution of man. *Am Anthropol*. **57 (1)**: 13-27

325. Montgomery SH, Mundy NI. 2010. Brain evolution: microcephaly genes weigh in. *Curr Biol*. **20 (5)**: R244-R246

326. Morris JA, Jordan CL, Breedlove SM. 2004. Sexual differentiation of the vertebrate nervous system. *Nat Neurosci*. **7**: 1034 – 1039
327. Moss DK, Bellet G, Carter JM *et al*. (8 authors). 2007. Ninein is released from the centrosome and moves bi-directionally along microtubules. *J Cell Sci*. **120**: 3064-3074
328. Mountcastle VB. 1997. The columnar organization of the neocortex. *Brain* **120 (4)**: 701-722
329. Moynihan M . 1976. *The New World Primates*. Princeton University Press, Princeton
330. Mundy NI, Kelly J. 2003. Evolution of a pigmentation gene, the *Melanocortin-1 Receptor*, in Primates. *Am J Phys Anthropol.* **121**: 67–80
331. Mundy NI, Kelly J. 2006. Investigation of the role of the agouti signaling protein gene (*ASIP*) in coat color evolution in primates. *Mamm Genome*. **17 (12)**: 1205-1213
332. Mundy NI. 2005. A window on the genetics of evolution: *MC1R* and plumage colouration in birds. *Proc R Soc B.* **272**: 1633-1640
333. Nadeau NJ, Burke T, Mundy NI. 2007. Evolution of an avian pigmentation gene correlates with a measure of sexual selection. *Proc R Soc B.* **274**: 1807-1813
334. Napier JR, Napier PH. 1995. *The natural history of the Primates.* British Museum (Natural History)/Cambridge University Press, London
335. Nargolwalla MC, Begun DR, Dean MC, Reid DJ, Kordos L. 2005. Dental development and life history in *Anapithecus hernyaki*. *J Hum Evol*. **49**: 99-121
336. Narr KL, Bilder RM, Toga AW *et al*. (12 authors). 2005. Mapping cortical thickness and gray matter concentration in first episode schizophrenia. *Cereb Cortex*. **15 (6)**: 708-719
337. Nicholas AK, Khurshid M, Désir J *et al*. (18 authors). 2010. *WDR62* is associated with the spindle pole and is mutated in human microcephaly. *Nat Genet*. **42**: 1010–1014
338. Nielsen R, Bustamante C, Clarke AG *et al*. (13 authors). 2005. A scan for positively selected genes in the genomes of humans and chimpanzees. *PLoS Biol*. **3(6)**: e170
339. Nielsen R, Yang Z. 1998. Likelihood models for detecting positively selected amino acid sites and applications to the HIV-1 envelope gene. *Genetics* **148 (3)**: 929-936
340. Nielsen R. 2009. Adaptionism-30 years after Gould and Lewontin. *Evolution* **63 (10)**: 2487-2490
341. Nikolaev SI, Montoya-Burgos JI, Popadin K *et al*. (7 authors). 2007. Life-history traits drive the evolutionary rates of mammalian coding and noncoding genomic elements. *Proc Natl Acad Sci USA.* **104 (51)**: 20443-20448

342. Niven JE. 2005. Brain evolution: Getting better all the time? *Curr Biol.* **15**: R625-R626
343. Niven JE. 2007. Brains, islands and evolution: breaking all the rules. *Trends Ecol Evol.* **22**:57–59
344. Nozawa M, Suzuki Y, Nei M. 2010. Is positive selection responsible for the evolution of a duplicate UV-sensitive *opsin* gene in *Heliconius* butterflies? *Proc Natl Acad Sci USA.* **107 (23)**: E96
345. Nunn CL, Barton RA. 2001. Comparative methods for studying primate adaptation and allometry. *Evol Anthropol Issues News Rev*. **10**: 81-98
346. Oakley TH, Cunningham CW. 2000. Independent contrasts succeed where ancestor reconstruction fails in a known bacteriophage phylogeny. *Evolution* **54**:397–405
347. O'Connor TD, Mundy NI. 2009. Genotype–phenotype associations: substitution models to detect evolutionary associations between phenotypic variables and genotypic evolutionary rate. *Bioinformatics*. **25 (12)**: i94-i100
348. Ohama Y, Hayaski K. 2009. Relocalization of a microtubule-anchoring protein, ninein, from the centrosome to dendrites during differentiation of mouse neurons. *Histol. Cell Biol*. **132 (5)**: 515-524
349. Oldham MC, Horvarth S, Geschwind DH. 2006. Conservation and evolution of gene coexpression networks in human and chimpanzee brains. *Proc Natl Acad Sci USA.* **103 (47)**: 17973-17978
350. Opazo JC, Wildman DE, Prychitko T, Johnson RM, Goodman M. 2006. Phylogenetic relationships and divergence times among New World monkeys (Platyrrhini, Primates*). Mol Phylogenet Evol*. **40**: 274–280
351. Organ CL, Shedlock AM, Meade A, Pagel M, Edwards SV. 2007. Origin of avian genome size and structure in nonavian dinosaurs. *Nature* **446**: 180-184
352. Page SL, Goodman M. 2001. Catarrhine phylogeny: Noncoding DNA evidence for a diphyletic origin of the mangabeys and for a human-chimpanzee clade. *Mol Phylogenet Evol.* **18 (1)**: 14-25
353. Pagel M, Meade A, Barker D. 2004. Bayesian estimation of ancestral character states on phylogenies. *Syst Biol*. **53**: 673-684
354. Pagel M, Meade A. 2006. Bayesian analysis of correlated evolution of discrete characters by reversible-jump Markov Chain Monte Carlo. *Am Nat.* **167**: 808-825

355. Pagel M. 1997. Inferring evolutionary processes from phylogenies. *Zoo Scripta.* **26 (4)**: 331-348

356. Pagel M. 1999. Inferring the historical patterns of biological evolution. *Nature* **401**: 877-884

357. Pagel MD, Harvey PH. 1988. Recent developments in the analysis of comparative data. *Q Rev Biol*. **63 (4)**: 413-440

358. Panizzon MS, Fennema-Notestine C, Eyler LT *et al*. (16 authors). 2009. Distinct genetic influences on cortical surface area and cortical thickness. *Cereb Cortex.* **19 (11)**: 2728-2735

359. Parker-Katiraee L, Carson AR, Yamada T *et al*. (16 authors). 2007. Identification of the imprinted KLF14 transcription factor undergoing human-specific accelerated evolution. *PLoS Genet*. **3**: 65-65

360. Pavlicek A, Jurka J. 2006. Positive selection on the nonhomologous end-joining factor *Cernunnos-XLF* in the human lineage. *Biology Direct*. **1**:15

361. Pedersen N, Holyoak DT, Newton AE. 2007. Systematics and morphological evolution within the moss family Bryaceae: A comparsion between parsimony and Bayesian methods for reconstruction of ancestral character states. *Mol Phylogenet Evol*. **43**: 891-907

362. Peper JS, Brouwer RM, Boomsma DI, Kahn RS, Pol HE. 2007. Genetic influences on human brain structure: A review of brain imaging studies in twins. *Human Brain Mapping*. **28 (6)**: 464-473

363. Perelman P, Johnson WE, Roos C *et al*. (14 authors). 2011. A molecular phylogeny of living primates. *PLoS Genet.* **7(3)**: e1001342

364. Pérez-Barberia FJ, Shultz S, Dunbar RIM. 2007. Evidence for coevolution of sociality and relative brain size in three orders of mammals. *Evolution* **61**: 2811-2821

365. Perry GH, Dominy NJ. 2009. Evolution of the human pygmy phenotype. *Trends Ecol Evol*. **24 (4)**: 218-225

366. Peters RH. 1983. *The ecological implications of body size*. Cambridge University Press, Cambridge

367. Piel M, Meyer P, Khodjakov A, Rieder C, Bornens M. 2002. The respective contributions of the mother and daughter centrioles to centrosome activity and behavior in vertebrate cells. *J Cell Biol*. **149 (2)**: 317

368. Plavcan JM, Gomez AM. 1993. Dental scaling in the callitrichinae. *Int J of Primatol*. **14 (1)**: 1770192

369. Podlaha O, Zhang J. 2003. Positive selection on protein-length in the evolution of a primate sperm ion channel. *Proc Natl Acad Sci USA.* **100 (21)**: 12241-12246

370. Pollard KS, Salama SR, Lambert N *et al*. (16 authors). 2006. An RNA gene expressed during cortical development evolved rapidly in humans. *Nature* **443**: 167-172

371. Pollen AA, Hoffmann HA. 2008. Beyond neuroanatomy: novel approaches to studying brain evolution. *Brain Behav Evol*. **72**: 145-158

372. Polly PD. 1998. Cope's Rule. *Science* **282**: 50-51

373. Polly PD. 2001. Paleontology and the comparative method: Ancestral node reconstructions versus observed node values. *Am Nat.* **157:** 596-609

374. Ponting C, Jackson AP. 2005. Evolution of primary microcephaly genes and the enlargement of primate brains. *Curr Op Genet Dev.* **15 (3)**: 241-248

375. Ponting C. 2006. A novel domain suggests a ciliary function for *ASPM*, a brain size determining gene. *Bioinformatics* **22 (9)**: 1031-1035

376. Pontious A, Kowalczyk T, Englund C, Hevner RF. 2008. Role of intermediate progenitor cells in cerebral cortex development. *Dev Neurosci*. **30:** 24-32

377. Poter LM, Garber PA. 2004. Goeldi's monkeys: A primate paradox? *Evol Anthropol Issues News Rev.* **13 (3)**: 104-115

378. Poth C, Fung C, Güntürkün O, Ridgway SH, Oelschläger HHA. 2005. Neuron numbers in sensory cortices of five delphinids compared to a physeterid, the pygmy sperm whale. *Brain Res Bull.* **66 (4-6)**: 357-360

379. Poux C, Douzery EJP. 2003. Primate phylogeny, evolutionary rate variations, and divergence times: a contribution from the nuclear gene *IRBP*. *Am J Phys Anthropol*. **124 (1)**: 1-16

380. Prabhakar S, Noonan JP, Pääbo S, Rubin EM. 2006. Accelerated evolution of conserved noncoding sequences in humans. *Science* **314**: 786

381. Preuss TM, Caceres M, Oldham MC, Geschwind DH. 2004. Human brain evolution: Insights from microarrays. *Nat Rev Genet*. **5**: 850-860

382. Preuss, T.M., 2001. *The discovery of cerebral diversity: An unwelcome scientific revolution.* In: *Evolutionary anatomy of the primate cerebral cortex* (Falk D, Gibson K. Eds). Cambridge University Press, Cambridge
383. Prothero DR, Sereno PC. 1982. Allometry and paleoecology of medial Miocene dwarf rhinoceroses from the Texas Gulf Coastal Plain. *Paleobiology* **8 (1)**: 16-30
384. Prothero JA, Sundsten JW. 1984. Folding of the cerebral cortex in mammals: A scaling model. *Brain Behav Evol.* **24**:152-167
385. Ptak SE, Enard W, Wiebe V *et al*. (7 authors). 2009. Linkage disequilibrium extends across putative selected sites in *FOXP2*. *Mol Biol Evol.* **26 (10)**: 2181-2184
386. Pulvers JN, Bryk J, Fish JL *et al*. (15 authors). 2010. Mutations in mouse *ASPM* (abnormal spindle-like microcephaly associated) cause not only microcephaly but also major defects in the germline. *Proc Nat Acad Sci. USA* **107 (38)**: 16595-16600
387. Purvis A. 1995. A composite estimate of primate phylogeny. *Phil Trans Roy Soc B.* **348 (1326)**: 405-421
388. Rakic P. 1988. Specification of cerebral cortical areas. *Science* **241 (4862)**: 170-176
389. Rakic P. 1995. A small step for the cell, a giant leap for mankind: a hypothesis of neocortical expansion during evolution. *Trends Neurosci*. **18**: 383-388
390. Rakic P. 2002. Neurogenesis in adult primate neocortex: an evaluation the evidence. *Nat Rev Neurosci*. **3**: 65-71
391. Rakic P. 2005. Less is more: progenitor death and cortical size. *Nat Neurosci*. **8**: 981-982
392. Rakic P. 2007. The radial edifice of cortical architecture: From neuronal silhouettes to genetic engineering. *Brain Res Rev*. **55 (2)**: 204-219
393. Rakic P. 2009. Evolution of the neocortex: a perspective from developmental biology. *Nat Rev Neurosci.* **10**: 724-735
394. Ramm SA, Oliver PL, Ponting CP, Stockley P, Emes RD. 2008. Sexual selection and the adaptive evolution of mammalian ejaculate proteins. *Mol Biol Evol.* **25 (1)**: 207-219
395. Ramm SA, Stockley P. 2010. Sperm competition and sperm length influence the rate of mammalian spermatogenesis. *Biol Lett*. **6**: 219-221
396. Ravosa MJ. 1992. Allometry and heterochrony in extant and extinct Malagasy Primates. *J Hum Evol.* **23 (2)**: 197-217

397. Reader SM, Hager Y, Laland KN. 2011. The evolution of primate general and cultural intelligence. *Phil Trans R Soc B.* **366 (1567)**: 1017-1027

398. Reader SM, Laland KN. 2002. Social intelligence, innovation, and enhanced brain size in primates. *Proc Natl Acad Sci USA.* **99**: 4436-4441

399. Reimers-Kipping S, Hevers W, Pääbo S, Enard E. 2010. Humanized *FOXP2* specifically affects cortico-basal ganglia circuits. *Neuroscience* **175**: 75–84

400. Rhesus Macaque Genome Sequencing and Analysis Consortium. 2007. Evolutionary and biomedical insights from the rhesus macaque genome. *Science* **316 (5822)**: 222-234

401. Rickmyre JL, DasGupta S, Ooi DLY *et al*. (8 authors). 2007. The *Drosophila* homolog of *MCPH1*, a human microcephaly gene, is required for genomic stability in the early embryo. *J Cell Sci.* **120**: 3565-3577

402. Rimol LM, Agartz I, Djurovic S *et al*. (16 authors). 2010. Sex-dependent association of common variants of microcephaly genes with brain structure. *Proc Natl Acad Sci USA.* **107 (1)**, 384-388

403. Riska B, Atchley WR. 1985. Genetics of growth predict patterns of brain-size evolution. *Science*. **229 (4713)**: 668-671

404. Roberts RG, Westaway KE, Zhao J *et al*. (7 authors). 2009. Geochronology of cave deposits at Liang Bua and of adjacent river terraces in the Wae Racang valley, western Flores, Indonesia: a synthesis of age estimates for the type locality of *Homo floresiensis*. *J Hum Evol.* **57 (5)**: 484-502

405. Rocha EP, Smith JM, Hurst LD *et al*. (7 authors). 2006. Comparisons of *dN/dS* are time dependent for closely related bacterial genomes. *J Theor Biol.* **239 (2)**: 226-35

406. Rockel AJ, Hiorns RW, Powell TPS. 1980. The basic uniformity in structure of the neocortex. *Brain* **103 (2)**: 221-244

407. Rockman MV, Hahn MW, Soranzo N *et al*. (6 authors). 2005. Ancient and recent positive selection transformed opioid cis-regulation in humans. *PLoS Biol*. **3 (12)**: e387

408. Roderick TH, Wimer RE, Wimer CC, Schwartzkroin PA. 1973. Genetic and phenotypic variation in weight of brain and spinal cord between inbred strains of mice. *Brain Res*. **64**: 345–353

409. Rogers J, Kochunov P, Lancaster J *et al*. (7 authors). 2007. Heritability of brain volume, surface area and shape: An MRI study in an extended pedigree of baboons. *Human Brain Mapping* **28 (6)**: 576-583
410. Rogers J, Kochunov P, Zilles K *et al*. (9 authors). 2010. On the genetic architecture of cortical folding and brain volume in primates. *NeuroImage* **53 (3)**: 1103-1108
411. Rosas HD, Hevelone ND, Zaleta AK *et al*. (6 authors). 2005. Regional cortical thinning in preclinical Huntington disease and its relationship to cognition. *Neurology* **65 (5)**: 745-747
412. Ross C. 1997. Primate life histories. *Evol Anthropol Issues News Rev*. **6**: 54-63
413. Roth G, Dicke U. 2005. Evolution of the brain and intelligence. *Trends Cogn Sci*. **9**: 250-257
414. Roth G, Rottluff B, Grunwald W, Hanken J, Linke R. 1980. Miniaturization in plethodontid salamanders (Caudata: Plethodontidae) and its consequences for the brain and visual system. *Biol J Linnean Soc*. **40 (2)**: 165-190
415. Roth KA, D'Sa C. 2001. Apoptosis and brain development. *Ment Retard De Disabil Res Rev*. **7 (4)**: 261-266
416. Roth VL. 1992. Inferences from allometry and fossils: dwarfing of elephants on islands. *Oxford Surveys in Evolutionary Biology* **8**:259–288
417. Rushton JP, Vernon PA, Bons TA. 2007. No evidence that polymorphsims of brain regulator genes *Microcephalin* and *ASPM* are associated with general mental ability, head circumference or altruism. *Biol Lett.* **3 (2)**: 157-160
418. Ruxton GD, Neuhäuser M. 2010. When should we use one-tailed hypothesis testing? *Methods Eco. Evol.* **1 (2)**: 114-117
419. Safi K, Seid MA, Dechmann KN. 2005. Bigger is not always better: when brains get smaller. *Biol Lett.* **1**:2 83-286
420. Sauvageot CM, Stiles CD. 2002. Molecular mechanisms controlling cortical gliogenesis. *Curr Opin Neurobiol.* **12**: 244–249
421. Sawaguchi T. 1992. The size of the neocortex in relation to ecology and social structure in monkeys and apes. *Folia Primatol*. **58**: 131-145
422. Scally A, Dutheil JY, Hillier LD *et al*. (71 authors). 2011. Insights into hominid evolution from the gorilla genome sequence. In review

423. Schenker NM, Buxhoeveden DP, Blackmon WL *et al*. (6 authors). 2008. A comparative quantitative analysis of cytoarchitecture and minicolumnar organization in Broca's area in humans and great apes. *J Comp Neurol.* **510 (1)**: 117–128
424. Schluter D, Price T, Mooers AO, Ludwig D. 1997. Likelihood of ancestor states in adaptive radiation. *Evolution* **51**: 1699-1711
425. Schmidt-Nielsen K. 1984. *Scaling: why is animal size so important?* Cambridge University Press, Cambridge
426. Schultz S, Dunbar RIM. 2010. Encephalization is not a universal macroevolutionary phenomenon in mammals but is associated with sociality. *Proc Natl Acad Sci USA*. **107 (50)**: 21582-21586
427. Sears KE, Finarelli JA, Flynn JJ, Wyss AR. 2008. Estimating body mass in New World "monkeys" (Platyrrhini, Primates), with a consideration of the Miocene platyrrhine, *Chilecebus carrascoensis*. *American Museum Novitates* **3617:**1-29
428. Semendeferi K, Lu A, Damasio H. 2002. Humans and great apes share a large frontal cortex. *Nat Neurosci*. **5**:272-276
429. Semendeferi K, Teffefr K, Buxhoeveden DP *et al*. (8 authors). 2011. Spatial organization of neurons in the frontal pole sets humans apart from great apes. *Cereb Cortex.* **21 (7)**: 1485-1497
430. Shea BT. 1983. Phyletic size change and brain/body allometry: A consideration based on the African pongids and other primates. *Int J Primatol*. **4 (1)**: 33-62
431. Sherwood CC, Stimpson CD, Raghanti MA *et al*. (11 authors). 2006. Evolution of increased glia-neuron rations in the human frontal cortex. *Proc Natl Acad Sci USA*. **203**:13606-13611
432. Sherwood CC, Subiaul F, Zawidzki TW. 2008. A natural history of the human mind: tracing evolutionary changes in brain and cognition. *J Anat*. **212 (4)**: 426-545
433. Shi P, Bakewell MA, Zhang J. 2006. Did brain-specific genes evolve faster in humans than in chimpanzees? *Trends Genet.* **22 (11)**: 608-613
434. Sholits SJ, Noonan JP. 2010. Gene regulation and the origins of human biological uniqueness. *Trends Genet.* **26**: 110-8
435. Sholl D. 1948. The quantitative investigation of the vertebrate brain and the applicability of allometric formulae to its study. *Proc R Soc Lond B.* **135 (879)**: 243-258

436. Silcox MT, Benham AE, Bloch JI. 2010. Endocasts of *Microsyops* (Microsyopidae, Primates) and the evolution of the brain in primitive primates. *J Hum Evol*. **58(6)**: 505-21
437. Silcox MT, Dalmyn CK, Bloch JI. 2009. Virtual endocast of *Ignacius graybullianus* (Paromomyidae, Primates) and brain evolution in early primates. *Proc Natl Acad Sci USA*.**106 (27)**: 10987-10992
438. Simmons AH. 1999. *Faunal extinction in an island society: Pygmy hippopotamus hunters of cyprus.* Plenum Press, New York
439. Simons EL, Rasmussen DT. 1996. Skull of *Catopithecus browni*. *Am J phys Anthrop*. **100**: 261–292
440. Simons EL. 2001. The cranium of *Parapithecus grangeri*, an Eygptian Oligocene anthropoidean Primate. *Proc Natl Acad Sci USA*. **98**: 7892-7897
441. Smart IHM, Dehay C, Giroud P, Berland M, Kennedy H. 2002. Unique morphological features of the proliferative zones of postmitotic compartments of the neural epithelium giving rise to striate and extrastriate cortex in the monkey. *Neuron* **12**: 37-53
442. Smuts BB, Cheney DL, Seyfarth RM, Wrangham RW, Struhsaker TT. 1987. *Primate societies*. University of Chicago Press, Chicago
443. Sol D, Bacher S, Reader SM, Lefebvre L. 2008. Brain size predicts the success of mammal species introduced into novel environments. *Am Nat.* 172: S63-S71
444. Sol D. 2009. Revisiting the cognitive buffer hypothesis for the evolution of large brains. *Biol Lett.* **5 (1)**: 130-133
445. Soligo C, Martin RD. 2006. Adaptive origins of primates revisited. *J Hum Evol.* **50**: 414-430
446. Soligo, C. 2006. Correlates of body mass evolution in primates. *Am J Phys Anthropol.* **130**: 283-293
447. Solter D. 1988. Differential imprinting and expression of maternal and paternal genomes. *Annu Rev Genet*. **22**: 127-146
448. Somel M, Franz H, Yan Z, *et al*. (15 co-authors). 2009. Transcriptional neoteny in the human brain. *Proc Natl Acad Sci USA*. **106 (14)**: 5743-5748
449. Sowell ER, Delis D, *STIL*es J, Jernigan, TL. 2001. Improved memory functioning and frontal lobe maturation between childhood and adolescence: a structural MRI study. *J Int Neuropsychol Soc.* **7**: 312-322

450. Steiper ME, Young NM. 2006. Primate molecular divergence dates. *Mol Phylogenet Evol*. **41 (2)**: 384-394

451. Stephan H, Frahm H, Baron R. 1981. New and revised data on volume of brain structures in insectivores and primates. *Folia Primatol*. **35**: 1-29

452. Stern DL, Orgogozo V. 2008. The loci of evolution: how predictable is genetic evolution? *Evolution* **62 (9)**: 2155–2177

453. Stolzenburg JU, Reichenbach A, Neumann M. 1989. Size and density of glial and neuronal cells within the cerebral neocortex of various insectivorian species. *Glia*. **2 (2)**: 78-84

454. Strauss WL, Schön MA. 1960. Cranial capacity of *Oreopithecus bambolii*. *Science* **132**: 670-672

455. Striedter GF. 2005. *Principles of brain evolution*. Sinauer Associates, Sunderland, MA

456. Surani MAH, Barton SC, Norris ML. 1986. Nuclear transplantation in the mouse: heritable differences between parental genomes after activation of the embryonic genome. *Cell* **45 (1)**: 127-36

457. Sussman RW. 1991. Primate origins and the evolution of angiosperms. *Am J Primatol*. **23 (4)**: 209–223

458. Sutter NB, Bustamante CD, Chase K *et al*. (21 authors). 2007. A single *IGF1* allele is a major determinant of small size in dogs. *Science* **316 (5821)**: 112-115

459. Suwa G, Asfaw B, Kono RT *et al* (6 authors). 2009. The *Ardipithecus ramidus* skull and its implications for Hominid origins. *Science* **326:** 68e168e7

460. Swanson WJ, Nielsen R, Yang Q. 2003. Pervasive adaptive evolution in mammalian fertilization proteins. *Mol Biol Evol*. **20 (1)**: 18-20

461. Tamura K, Dudley J, Nei M, Kumar S. 2007. MEGA4: Molecular evolutionary genetics analysis (MEGA) software version 4.0. *Mol Biol Evol.* **24 (8)**: 1596-1599

462. Taylor AB, van Schaik CP. 2007. Variation in brain size and ecology in *Pongo*. *J Hum Evol.* **52**: 59-71

463. Taylor MS, Kai C, Kawai J *et al*. (6 authors). 2006. Heterotachy in mammalian promoter evolution. *PLoS Genet.* **2**: e30

464. Teer JK, Mullikin JC. 2010. Exome sequencing: the sweet spot before whole genomes. *Hum Mol Genet*. **19 (R2)**: R145-R151

465. Thornton GK, Woods CG. 2009. Primary microcephaly: do all roads lead to Rome? *Trends Genet* **25 (11)**: 501-510

466. Timpson N, Heron J, Smith GD, Enard W. 2007. Comment on papers by Evans *et al*. and Mekel-Bobrov *et al* on evidence for positive selection of *MCPH1* and *ASPM*. *Science* **317**: 1036a

467. Tocheri MW, Orr CM, Larson SG *et al*. (9 authors). 2007. The primitive wrist of *Homo floresiensis* and its implications for Hominin evolution. *Science* **317**: 1743-1745

468. Uddin M, Opazo JC, Wildman DE *et al*. (7 authors). 2008. Molecular evolution of the *cytochrome c oxidase subunit 5A* gene in primates. *BMC Evol Biol*. **8 (8)**

469. Uddin M, Wildman DE, Liu G *et al*. (9 authors). 2004. Sister grouping of chimpanzees and humans as revealed by genome-wide phylogenetic analysis of brain gene expression profiles. *Proc Natl Acad Sci USA.* **101 (9)**: 2957-2962

470. Untergasser A, Nijveen H, Rao X *et al*. (6 authors). 2007. Primer3Plus, an enhanced web interface to Primer3. *Nucleic Acids Res.* **35**: W71-W74

471. Vallender EJ, Lahn BT. 2006. A primate-specific acceleration in the evolution of the caspase-dependent apoptosis pathway. *Hum Mol Genet.* **15 (20)**: 3034-3040

472. Vallender EJ, Mekel-Bobrov N, Lahn BT. 2008. Genetic basis of human brain evolution. *Trends Neurosci*. **31 (12)**: 637-644

473. Vallender EJ. 2008. Exploring the origins of the human brain through molecular evolution. *Brain Behav Evol.* **72**: 168-177

474. van der Voet M, Berends CWH, Perreault A *et al*. (8 authors). 2009. NuMA-related LIN-5, ASPM-1, calmodulin and dynein promote meiotic spindle rotation independently of cortical LIN-5/GPR/G. *Nat Cell Biol*. **11**: 269-277

475. van Roosmalen MGM, van Roosmalen T. 2003. The description of a new marmoset genus, *Callibella* (Callitrichinae, Primates), including its molecular phylogenetic status. *Neotrop Primates.* **11 (1)**: 1-10

476. Van Valen L, Sloan RE. 1965. The earliest primate. *Science* **150 (3697)**: 743-745

477. van Woerden J, van Schaik CP, Isler K. 2010. Effects of seasonality on brain size evolution: Evidence from strepsirrhine Primates. *Am Nat.* **176 (6)**: 758-767

478. Varki A, Geschwind DH, Eichler EE. 2008. Explaining human uniqueness: genome interactions with environment, behaviour and culture. *Nat Rev Genet*. **9**: 749-63

479. Varki A, Nelson DL. 2007. Genomic comparisons of humans and chimpanzees. *Annu Rev Anthropol*. **36**: 191-209

480. Vekua A, Lordkipanidze D, Rightmire GP *et al*. (12 authors). 2002. A new skull of early *Homo* from Dmanisi, Georgia. *Science* **297**: 85-89

481. Venter JC, Adams MD, Mysers EW *et al* (274 authors). 2001. The sequence of the human genome. *Science* **291 (5507)**: 1304-1352

482. Voight BF, Kudaravalli S, Wen X, Pritchard JK. 2006. A map of recent positive selection in the human genome. *PLoS Biol.* **4(3)**: e72

483. Wallace AR. 1889. *Darwinism: An exposition of the theory of natural selection, with some of its applications*. Macmillan, London

484. Wang HY, Chien HC, Osada N *et al*. (10 authors). 2007. Rate of evolution in brain expressed genes in humans and other primates. *PLoS Biol*. **5 (2)**

485. Wang JK, Li Y, Su B. 2008. A common SNP of *MCPH1* is associated with cranial volume variation in Chinese population. *Hum Mol Genet.* **17 (9)**: 1329-1335

486. Wang X, Tsai JW, Imai JH *et al*. (6 authors). 2009. Asymmetric centrosome inheritance maintains neural progenitors in the neocortex. *Nature* **461**: 947-955

487. Wang X, Zhang J, Zhang Y. 2002. Erratic evolution of *SRY* in higher Primates. *Mol Biol Evol*. **19**:582-584

488. Wang Y, Su B. 2004. Molecular evolution of *Microcephalin*, a gene determining human brain size. *Hum Mol Genet*. **13 (11)**: 1131-1137

489. Wang YQ, Qian YP, Yang S, *et al*. (13 co-authors). 2005. Accelerated evolution of the *pituitary adenylate cyclase-activating polypeptide* precursor gene during human origin. *Genetics* **170**: 801- 806

490. Wayne RK. 1986a. Cranial morphology of domestic and wild canids: The influence of development on morphological change. *Evolution*. **40 (2)**: 243-261

491. Wayne RK. 1986b. Developmental constraints on limb growth in domestic and some wild canids. *J Zool*. **210 (3)**: 381-397

492. Weber J, Czarnetzki A, Pusch CM. 2005. Comment on "The brain of LB1, *Homo floresiensis*". *Science* **310**: 236

493. Webster AJ, Gittleman JL, Purvis A. 2004. The life history legacy of evolutionary body size change in carnivores. *J Evol Biol.* **17 (2)**: 396-407

494. Webster AJ, Purvis A. 2002. Testing the accuracy of methods for reconstructing ancestral states of continuous characters. *Proc Roy Soc B.* **269**: 143-149

495. Weisbecker V, Goswami A. 2010. Brain size, life history, and metabolism at the marsupial/placental dichotomy. *Proc Natl Acad Sci USA.* **107(37)**: 16216–16221

496. Weiss LA, Purcell S, Waggoner S *et al*. (8 authors). 2007. Identification of *EFHC2* as a quantitative trait locus for fear recognition in Turner syndrome. *Hum Mol Genet*. **16 (1)**: 107-113

497. Welch JJ. 2009. Testing the island rule: primates as a case study. *Proc Roy Soc B*. **276**: 675-682

498. Weston EM, Lister AM. 2009. Insular dwarfism in hippos and a model for brain size reduction in *Homo floresiensis*. *Nature* **459**: 85-88

499. Whiting BA, Barton RA. 2002. The evolution of the cortico-cerebellar complex in primates: anatomical connections predict patterns of correlated evolution. *J Hum Evol*. **44 (1)**: 3-10

500. Wildman DE, Jameson NM, Opazo JC, Yi SV. 2009. A fully resolved genus level phylogeny of neotropical primates (Platyrrhini). *Mol Phylogenet Evol*. **53 (3)**: 694-702

501. Wilkinson LS, Davies W, Isles AR. 2007. Genomic imprinting effects on brain development and function. *Nat Rev Neurosci.* **8**: 833-843

502. Williams LR, Jacobs DW. 1997. Local parallel computation of stochastic completion fields. *Neural Comput.* **9 (4)**: 850-991

503. Winkler AM, Kochunov P, Blangero J *et al*. (8 authors). 2010. Cortical thickness or grey matter volume? The importance of selecting the phenotype for imaging genetics studies. *NeuroImage* **53(3)**: 1135-1146

504. Wolf JBW, Künstner A, Nam K, Jakobsson M, Ellegren H. 2009 Non-linear dynamics of non-synonymous (*dN*) and synonymous (*dS*) substitution rates affects inference of selection. *Genome Biol Evol*. **1 (1)**: 308-319

505. Wong WSW, Yang Z, Goldman N, Nielsen R. 2004. Accuracy and power of statistical methods for detecting adaptive evolution in protein coding sequences and for identifying positively selected sites. *Genetics.* **168 (2)**: 1041-1051

506. Wood B, Collard M. 1999. The human genus. *Science* **284**: 65-71

507. Wood JL, Liang Y, Chen J. 2008. Microcephalin/MCPH1 associates with the condensin II complex to function in homologous recombination repair. *J Biol Chem***. 283 (43)**: 29586-29592

508. Wood JL, Singh N, Mer G, Chen J. 2007. *MCPH1* Functions in an H2AX-dependent but MDC1-independent Pathway in Response to DNA Damage. *J Biol Chem*. 282 (48): 35416-35423

509. Woods RP, Freimer NB, De Young JA *et al*. (9 authors). 2006. Normal variants of *Microcephalin* and *ASPM* do not account for brain size variability. *Hum Mol Genet*. **15 (12)**: 2025-2029

510. Wray GA. 2007. The evolutionary significance of cis-regulatory mutations. *Nat Rev Genet*. **8**: 206-216

511. XueBin Q, Su Y, HongKun Z *et al*. (13 authors). 2008. Detecting positive darwinian selection in brain-expressed genes during human evolution. *Chin Sci Bull.* **52 (3)**: 324-335

512. Yang Z, Nielsen R, Goldman N, Pedersen AMK. 2000. Codon-substitution models for heterogeneous selection pressure at amino acid sites. *Genetics* **155**: 431-449

513. Yang Z, Wong WSW, Nielsen R. 2005. Bayes empirical Bayes inference of amino acid sites under positive selection. *Mol Biol Evol.* **22**: 1107-1118

514. Yang Z, Bielawski JP. 2000. Statistical methods for detecting molecular adaptation. *Trends Ecol Evol.* **15 (12)**: 496-503

515. Yang Z, dos Reis M. 2011. Statistical properties of the branch-site test of positive selection. *Mol Biol Evol.* **28 (3)**: 1217-1228

516. Yang Z, Nielsen R, Hasegawa M. 1998. Models of amino acid substitution and applications to mitochondrial protein evolution. *Mol Biol Evol.* **15 (12)**: 1600-1611

517. Yang Z, Nielsen R. 2002. Codon-substitution models for detecting molecular adaptation at individual sites along specific lineages. *Mol Biol Evol.***19 (6)**: 908-917

518. Yang Z. 1998. Likelihood ratio tests for detecting positive selection and application to primate lysozyme evolution. *Mol Biol Evol.* **15 (5)**: 568-573

519. Yang Z. 2005. *Bayesian inference in molecular phylogenetics*. In: *Mathematics of Evolution and Phylogeny* (Gascuel O. Ed.). Oxford University Press, Oxford

520. Yang Z. 2006. *Computational Molecular Evolution*. Oxford University Press, Oxford

521. Yang Z. 2007. PAML 4: Phylogenetic Analysis by Maximum Likelihood. *Mol Biol Evol*. **24**: 1586-1591

522. Yu F, Hill RS, Schaffner SF *et al*. (10 authors). 2007. Comment on "Ongoing adaptive evolution of *ASPM*, a brain size determinant in *Homo sapiens*" *Science* **316 (5823)**: 370

523. Yu, XJ, Zheng HK, Wang J, Wang W, Su B. 2006. Detecting lineage-specific adaptive evolution of brain-expressed genes in human using rhesus macaque as outgroup. *Genomics* **88 (6)**: 745-751

524. Zhang J, Nielsen R, Yang Z. 2005. Evaluation of an improved branch-Site likelihood method for detecting positive selection at the molecular level. *Mol Biol Evol*. **22 (12)**: 2472-2479

525. Zhang J. 2003. Evolution of the human *ASPM* gene, a major determinant of brain size. *Genetics* **165**: 2063-2070

526. Zhang R, Wang YQ, Su B. 2008. Molecular evolution of a primate-specific microRNA family. *Mol Biol Evol*. **25 (7)**: 1493-1502

527. Zhou WX, Sornette D, Hill RA, Dunbar RIM. 2005. Discrete hierarchical organization of social group sizes. *Proc R Soc Lond B.* **272 (1561)**: 439-444

528. Zilles K, Armstrong E, Moser KH, Schleicher A, Stephan H. 1989. Gyrification in the cerebral cortex of primates. *Brain Behav Evol.* **34**: 143-150

529. Zilles K, Rehkemper G. 1988. *The brain with special reference to the telencephalon*. In *Orang-utan Biology*. J.H. Schwartz, editor. Oxford University Press, Oxford

530. Zollikofer CPE, Ponce de León MS *et al*. (9 authors). 2005. Virtual cranial reconstruction of *Sahelanthropus tchadensis*. *Science* **434**: 755-759

APPENDIX 1. Phenotypic and life history data

Table A1.1 Brain and body mass of primates used in phylogenetic analysis in chapters 3, 5 & 6*

Species	Adult						Neonate	
	Body mass (g)	Brain mass (mg)	Brain volume (mm^3)	Neocortex volume (mm^3)	Telencephalon volume (mm^3)	Testis mass (g)	Body mass (g)	Brain mass (mg)
Alouatta palliata	-	-	-	-	-	-	363.9	30800.0
Alouatta sp.	6400.0	52000.0	49009.0	31660.0	37388.0	23.0	-	-
Aotus trivirgatus	1020.0	-	-	-	-	1.2	-	-
Aotus sp.	830.0	17100.0	16195.0	9950.0	12128.0	-	-	-
Ateles geoffroyi	8000.0	108000.0	101034.0	70856.0	79946.0	13.4	512.0	63950.0
Callicebus moloch	900.0	19000.0	17994.0	11163.0	13465.0	-	-	-
Callimico goeldii	480.0	11000.0	10510.0	6476.0	7733.0	-	-	-
Callithrix jacchus	280.0	7600.0	7241.0	4371.0	5318.0	1.3	28.2	3630.0
Cebus albifrons	-	-	-	-	-	-	232.9	33650.0
Cebus apella	3000.0	-	-	-	-	4.6	-	-
Cebus sp.	3100.0	71000.0	66939.0	46429.0	52113.0	-	-	-
Cercocebus albigena	7900.0	104000.0	97603.0	68733.0	77049.0	25.1	474.7	57480.0
Ceropithecus aethiops	4819.0	73200.0	63505.0	45166.0	51279.0	13.0	356.7	33500.0
Cheirogaleus major	450.0	6800.0	6373.0	2938.0	4314.0	2.3	-	-
Colobus badius	7000.0	78000.0	73818.0	50906.0	57885.0	-	340.0	38000.0
Colobus polykomos	10250.0	-	-	-	-	10.7	-	-
Daubentonia madagasc.	2800.0	45150.0	42611.0	22127.0	30196.0	-	-	-
Erythrocebus patas	7800.0	108000.0	103167.0	77141.0	84770.0	7.2	-	-
Eulemur fulvus	1400.0	23300.0	22106.0	12207.0	15566.0	7.8	73.4	10700.0
Galago senegalensis	186.0	4800.0	4512.0	2139.0	2997.0	1.7	13.6	2300.0
Gorilla gorilla	105000.0	500000.0	470369.0	341444.0	369878.0	29.6	2072.0	289000.0

Homo sapiens	65000.0	1330000.0	1251847.0	1006525.0	1063399.0	40.5	3320.8	300000.0
Hylobates lar	5700.0	102000.0	97505.0	65800.0	76001.0	5.5	354.8	65000.0
Lagothrix lagotricha	5200.0	101000.0	95503.0	65873.0	74822.0	11.2	-	-
Leontopithecus rosalia	590.0	13400.0	-	-	-	1.5	-	-
Lepilemur ruficaudatus	915.0	7600.0	7175.0	3282.0	4708.0	-	27.0	2900.0
Loris tardigradus	322.0	6600.0	6269.0	3524.0	4552.0	1.8	10.8	2700.0
Macaca mulatta	7800.0	93000.0	87896.0	63482.0	71080.0	46.2	475.6	45500.0
Mandrillus sphinx	32000.0	179000.0	-	-	-	68.0	-	-
Microcebus murinus	54.0	1780.0	1680.0	740.0	1129.0	2.5	-	-
Nasalis larvatus	20640.0	-	-	-	-	11.8	-	-
Nycticebus coucang	800.0	12500.0	11755.0	6192.0	8495.0	-	49.7	4000.0
Pan troglodytes	46000.0	405000.0	382103.0	291592.0	313493.0	118.8	1528.3	153280.0
Papio anubis	25000.0	201000.0	190957.0	140142.0	154987.0	93.5	-	-
Pithecia monacha	1500.0	35000.0	32867.0	21028.0	24920.0	-	-	-
Pithecia pithecia	1600.0	-	-	-	-	0.9	-	-
Pongo pygmaeus	57021.5	413300.0	305555.0	219800.0	238300.0	35.5	1601.9	168750.0
Presbytis entellus	21319.0	119400.0	-	-	-	11.1	-	-
Propithecus verreauxi	3480.0	26700.0	25194.0	13170.0	17040.0	-	-	-
Pygathrix nemaeus	7500.0	77000.0	72530.0	48763.0	56189.0	-	-	-
Saguinus oedipus	380.0	10000.0	9537.0	5894.0	7052.0	3.4	-	-
Saimiri sciureus	660.0	24000.0	22572.0	15541.0	17635.0	3.2	153.5	15240.0
Semnopithecus maurus	-	-	-	-	-	-	389.5	32000.0
Tarsius bancanus	-	-	-	-	-	-	25.4	2100.0
Tarsius sp.	125.0	3600.0	3393.0	1768.0	2258.0	-	-	-
Varecia variegatus	3000.0	31500.0	29713.0	15293.0	20461.0	17.2	91.9	10600.0

Extant species		
Adapis parisiensis	2350.0	8961.0
Aegyptopithecus zeuxis	67100.0	34194.0
Anapithecus hernyati	13500.0	107116.0
Australopithecus Africa.	36000.0	433953.0
Catopithecus browni	900.0	3215.0
Chilecebus carrasoensis	582.6	7618.0
Homo erectus	57000.0	951228.0
Homo ergaster	58000.0	802015.0
Homo habilis	34000.0	522414.0
Homo heidelbergensis	62000.0	1118362.0
Homo rudolfensis	45000.0	707814.0
Mioeuoticus sp.	1280.0	7959.0
Necrolemur antiquus	233.0	3927.0
Notharctus tenebrosus	1990.0	10559.0
Oreopithecus bambolii	30000.0	383060.0
Paranthropus boisei	44000.0	486134.0
Parapithecus grangeri	1800.0	11555.0
Proconsul africanus	10500.0	161426.0
Pronycticebus gaudryi	1220.0	4940.0
Rooneyia viejaensis	782.0	7558.0
Smilodectes gracilis	1960.0	9660.0
Tetonius homunculus	74.0	1576.0
Victoriapithecus macin.	4500.0	53250.0

*Adult brain and body data from Bauchot & Stephan (1969); Stephan *et al.* (1981); Zilles & Rehkempe (1988). Testis data from Harcourt *et al.*, 1995; fossil data from Montgomery *et al.*, 2010; neonatal body and brain data from Capellini *et al*., 2011

Table A1.2. Phenotypic and life history data used in phylogenetic analysis in chapter 4

Unless otherwise indicated all data is from the PanTHERIA dataset (Jones *et al.*, 2009).

a) Adult body mass, neonatal body mass and adult endocranial volume/brain mass

Species	Adult Body Mass (g)	Neonate Body Mass (g)	Endocranial volume (cc)[1]	brain mass (mg)[2]
Allenopithecus nigroviridis	4749.960	240.710	58.021	57142.630
Alouatta caraya	5576.960	260.600	52.626	51918.582
Alouatta palliata	6576.990	318.290	49.876	49252.805
Alouatta pigra	7172.060	480.000	51.125	50463.769
Alouatta seniculus	6398.310	293.420	55.223	54434.379
Aotus lemurinus	865.960	97.470	16.298	16416.024
Arctocebus calabarensis	258.010	31.820	6.921	7077.753
Ateles fusciceps	9067.940	499.990	114.239	111169.711
Ateles geoffroyi	7582.400	425.850	105.087	102414.930
Ateles paniscus	8697.250	478.640	103.850	101230.389
Callicebus moloch	958.130	74.400	18.162	18258.597
Callimico goeldii	558.000	50.500	11.432	11586.744
Callithrix argentata	382.920	35.800	7.951	8110.664
Callithrix humeralifera	374.990	34.500	-	-
Callithrix jacchus	290.210	27.740	7.241	7398.824
Callithrix pygmaea	123.940	14.500	4.173	4305.966
Cebus albifrons	2509.680	231.920	65.453	64324.598
Cebus apella	2758.380	231.380	66.631	65462.242
Cebus capucinus	3005.990	238.360	72.926	71532.172
Cercopithecus ascanius	3540.240	371.000	59.575	58646.112

Cercopithecus cephus	3444.880	337.190	65.265	64143.310
Cercopithecus diana	4358.910	466.900	62.608	61577.569
Cercopithecus mitis	5041.290	402.000	71.334	69997.540
Cercopithecus mona	3980.170	280.490	61.839	60834.399
Cercopithecus neglectus	5324.520	259.950	65.973	64827.113
Cercopithecus nictitans	5256.910	403.830	71.125	69796.441
Cercopithecus wolfi	3255.180	435.000	61.450	60458.266
Cheirogaleus major	446.020	18.080	5.813	5963.039
Cheirogaleus medius	196.760	14.650	2.600	2705.166
Colobus guereza	9925.880	444.920	74.387	72939.638
Colobus polykomos	8797.290	489.890	73.828	72401.329
Daubentonia madagascariensis	2731.370	121.790	44.850	44372.173
Erythrocebus patas	7966.300	621.670	97.727	95364.472
Eulemur coronatus	1699.850	57.810	20.651	20713.231
Eulemur fulvus	2376.990	74.990	25.769	25746.038
Eulemur macaco	2470.430	60.500	24.515	24513.979
Eulemur mongoz	1771.130	59.480	20.172	20241.328
Eulemur rubriventer	2015.400	84.970	26.233	26200.760
Galago alleni	266.030	23.930	-	-
Galago moholi	191.960	11.730	3.705	3831.047
Galago senegalensis	215.200	11.500	3.965	4094.645
Gorilla gorilla	112588.990	2095.890	490.407	465094.040
Hapalemur griseus	916.000	45.200	14.093	14231.216
Homo sapiens	58540.630	3182.960	-	-
Hylobates lar	5578.610	398.860	103.323	100725.626
Lagothrix lagotricha	6263.690	437.090	96.500	94187.961

Lemur catta	2626.480	75.800	22.905	22931.711
Leontopithecus rosalia	592.520	51.890	12.831	12978.147
Lepilemur mustelinus	669.030	27.000	9.560	9720.210
Lophocebus albigena	7418.710	498.580	93.974	91765.036
Loris tardigradus	249.220	11.000	5.871	6021.205
Macaca arctoides	9358.040	488.990	100.700	98213.323
Macaca cyclopis	5748.940	399.860	82.000	80266.120
Macaca fascicularis	4569.320	328.760	63.977	62899.259
Macaca fuscata	10114.760	501.570	102.920	100339.806
Macaca maura	7290.300	388.460	-	-
Macaca nemestrina	7820.780	472.920	105.593	102899.057
Macaca nigra	7359.390	457.770	94.900	92653.682
Macaca radiata	4999.990	367.520	74.873	73408.215
Macaca silenus	5995.250	416.110	85.000	83149.840
Macaca sylvanus	11471.530	449.850	93.200	91023.010
Macaca thibetana	10593.060	499.990	-	-
Mandrillus leucophaeus	14253.300	718.150	148.000	143365.843
Mandrillus sphinx	16685.060	612.890	153.877	148955.791
Microcebus murinus	69.000	4.780	1.631	1710.738
Microcebus rufus	48.390	6.500	1.716	1798.989
Miopithecus talapoin	1248.860	179.040	37.351	37073.123
Mirza coquereli	326.500	12.920	5.796	5945.436
Nasalis larvatus	12265.650	450.000	92.304	90163.166
Nomascus leucogenys	7320.000	497.330	119.375	116077.467
Nycticebus coucang	924.550	50.470	10.130	10289.619
Nycticebus pygmaeus	342.320	19.890	7.229	7386.639

Otolemur garnettii	811.170	49.210	11.496	11650.469
Pan paniscus	35119.950	1399.530	341.292	325756.882
Pan troglodytes	45000.000	1745.020	368.349	351108.954
Papio anubis	17728.560	947.310	167.424	161828.308
Papio cynocephalus	15822.150	709.880	163.187	157804.417
Papio hamadryas	14007.080	890.000	146.167	141621.124
Papio papio	18026.050	600.380	142.500	138130.521
Papio ursinus	17729.440	599.990	178.000	171864.684
Perodicticus potto	1081.810	37.160	12.416	12565.514
Pongo pygmaeus	53408.290	1644.200	377.377	359560.003
Propithecus coquereli	4189.270	102.450	30.194	30082.399
Propithecus diadema	6568.990	134.990	39.799	39458.907
Propithecus tattersalli	3531.390	97.470	-	-
Propithecus verreauxi	3588.260	102.650	26.206	26174.417
Pygathrix nemaeus	9411.100	191.940	91.415	89309.980
Rhinopithecus bieti	11000.540	424.720	117.757	114531.785
Saguinus fuscicollis	393.990	39.180	7.939	8098.252
Saguinus geoffroyi	492.500	47.840	10.136	10295.511
Saguinus imperator	407.910	46.550	-	-
Saguinus midas	540.560	39.780	9.784	9943.883
Saguinus oedipus	462.040	41.000	9.758	9917.844
Saimiri sciureus	749.470	107.500	24.136	24142.589
Symphalangus syndactylus	10839.000	517.000	123.505	120020.990
Tarsius bancanus	114.390	23.930	3.165	3281.430
Tarsius syrichta	115.910	25.600	3.359	3478.791
Theropithecus gelada	15964.110	464.920	133.327	129391.007

Trachypithecus francoisi	8139.930	454.560	-	-
Trachypithecus obscurus	7247.880	339.180	62.117	61103.160
Varecia variegata	3849.990	93.690	32.123	31968.790

1 Data from Isler *et al*., 2008

[2] Brain size was estimated by conversion from ECV to mg using the equation given in Martin [23]: *Log(cranial capacity) =[1.018 x Log(brain mass)] – 0.025*

Table A1.2 cont'd. Phenotypic and life history data used in phylogenetic analysis in chapter 4

Unless otherwise indicated all data is from the PanTHERIA dataset (Jones *et al.*, 2009).

b) Life history traits

Species	Age at Sexual Maturity (days)	Max. Longevity (months)	Gestation Length (days)	Inter Birth Interval (days)	Litter Size	Weaning Age (days)
Alouatta caraya	1276.72	243.6	185.92	337.62	1.01	323.16
Alouatta palliata	1578.42	300	185.42	684.37	1.02	495.6
Alouatta seniculus	1690.22	300	189.9	507.35	1.42	370.04
Aotus lemurinus	755.15	216	132.23	365	1.01	74.57
Arctocebus calabarensis	298.91	156	133.74	144.47	1.01	109.26
Ateles fusciceps	1799.68	288	224.7	851.66	1.01	482.7
Ateles geoffroyi	2104.57	327.6	226.37	1048.15	1.01	816.35
Ateles paniscus	2104.57	453.6	228.18	1072.18	1	805.41
Callicebus moloch	1262.74	303.6	164	365	1.01	58.85
Callimico goeldii	413.84	214.8	153.99	182.5	1.05	66.53
Callithrix jacchus	455.99	201.6	144	159.8	2.31	60.24
Callithrix pygmaea	708.5	181.2	134.44	182.5	1.93	90.73
Cebus albifrons	1501.69	528	158.29	547.5	1.01	270.32
Cebus apella	1760.81	541.2	154.99	657	1.05	263.12
Cebus capucinus	2134.73	657.6	161.06	790.83	1.01	514.07
Cercopithecus ascanius	1718.73	339.6	148.5	1580.45	1.01	146.54
Cercopithecus mitis	2049.25	325.2	138.39	565.75	1	688.08
Cercopithecus neglectus	2076.39	315.6	172.07	584	1.02	417.62
Cheirogaleus medius	413.84	231.6	61.79	365	2.04	60.65

Colobus guereza	1929.19	294	169.02	486.66	1	387.79
Colobus polykomos	1629.84	366	172.69	442.41	1	213.78
Daubentonia madag.	834.72	291.6	166.48	760.41	1.01	197.7
Erythrocebus patas	1246.07	286.8	167.2	365	1.01	211.79
Eulemur fulvus	791.75	444	120.83	547.5	1.1	134.64
Eulemur macaco	660.75	360	127.49	365	1.04	143.28
Galago moholi	420.91	198	122.29	182.5	1.6	90.46
Galago senegalensis	330.37	204	126.98	219	1.5	93.93
Gorilla gorilla	3353.12	648	257	1430.8	1.05	920.35
Hapalemur griseus	1003.17	205.2	141.24	334.58	1.5	136.29
Homo sapiens	5582.93	1470	274.78	958.12	1	725.86
Hylobates lar	3852.57	480	212.91	983.67	1.01	725.86
Lagothrix lagotricha	1729.33	360	223.99	638.75	1.01	312.66
Lemur catta	831.62	360	134.74	468.41	1.18	126.51
Leontopithecus rosalia	890.34	297.6	134	182.5	1.94	75.69
Lophocebus albigena	2525.48	392.4	182.64	770.15	1.01	211.71
Loris tardigradus	350.76	196.8	165.99	182.5	1.44	167.49
Macaca arctoides	1570.01	360	176.6	544.6	1.01	377.66
Macaca fascicularis	1319.5	456	164.69	398.45	1	283.53
Macaca fuscata	1460.77	396	172.99	486.66	1.02	265.04
Macaca nemestrina	1427.17	411.6	171	405.07	1.01	292.6
Macaca nigra	1984.51	216	172.43	540.2	1.01	365
Macaca radiata	1785.78	360	161.56	365	1.01	332.25
Macaca silenus	1912.19	480	172	510.39	1.01	362.93
Macaca sylvanus	1542.25	264	164.84	431.71	1.02	210.25
Mandrillus leucophaeus	1745.96	400.8	179.22	513.43	1.01	486.66
Mandrillus sphinx	2122.11	555.96	173.99	521.64	1.02	348.01
Microcebus murinus	355.53	186	60.34	365	2	40.45
Miopithecus talapoin	1733.36	370.8	164.38	365	1.01	178.98
Mirza coquereli	343.74	183.6	88.58	365	1.71	136

Nasalis larvatus	1894.11	252	165.04	547.5	1.02	211.75
Nycticebus coucang	660.82	318	191.09	365	1.12	181.21
Otolemur garnettii	592.15	204	132.24	215.95	1.02	139.2
Pan paniscus	5465.72	576	235.24	1715.5	1.01	1081.31
Pan troglodytes	3897.96	720	231.49	1825	1.05	1260.81
Papio cynocephalus	2560.56	540	172.99	669.16	1.01	450.42
Papio hamadryas	1652.37	450	180	608.33	1.01	363.96
Papio ursinus	1543.35	540	185.92	882.08	1.01	877.09
Perodicticus potto	561.58	312	193	354.05	1.09	149.15
Pongo pygmaeus	3318.62	720	259.42	2007.5	1.07	1088.8
Propithecus verreauxi	943.94	247.2	149.77	365	1.02	177.83
Saguinus fuscicollis	406.61	294	148	293.5	1.83	90.1
Saguinus midas	841.82	184.8	138.24	206.83	2.02	69.6
Saguinus oedipus	680.38	277.2	166.49	233.06	1.9	49.85
Saimiri sciureus	1399.88	324	164.09	383.25	1	177.41
Symphalangus syndactylus	3788.23	456	230.66	1003.75	1.02	635.38
Tarsius bancanus	658.68	144	125.84	240.29	1	78.55
Theropithecus gelada	1894.11	336	178.64	766.5	1.01	494.95
Varecia variegata	701.52	384	102.5	365	2.16	90.73

Table A1.3 Sex specific estimates of brain mass and sexual dimorphism scores used in phylogenetic analysis in chapter 5

Species	**Log(male brain mass [mg])**	**Log(female brain mass [mg])**	**Residual (sexual dimorphism)[1]**
Homo sapiens	6.1339	6.0892	-0.0026
Pan troglodytes	5.5656	5.5243	0.0029
Gorilla gorilla	5.6966	5.6364	0.0200
Pongo pygmaeus	5.5984	5.5084	0.0519
Hylobates lar	5.0028	4.9913	-0.0185
Papio anubis	5.2456	5.1691	0.0437
Mandrillus sphinx	5.1927	5.1525	0.0076
Cercocebus albigena	5.0562	4.9672	0.0593
Macaca mulatta	4.9615	4.9161	0.0165
Ceropithecus aethiops	4.8005	4.7334	0.0411
Erythrocebus patas	5.0164	4.9388	0.0484
Colobus polykomos	4.8887	4.8356	0.0255
Presbytis entellus	4.8762	4.8318	0.0169
Pygathrix nemaeus	4.9471	4.8999	0.0186
Alouatta sp.	4.7078	4.6765	0.0063
Lagothrix lagotricha	4.9673	4.9806	-0.0431
Ateles geoffroyi	4.9917	5.0283	-0.0672
Cebus apella	4.8305	4.8009	0.0026
Saimiri sciureus	4.3849	4.3806	-0.0162
Aotus sp.	4.2475	4.2109	0.0188
Saguinus oedipus	3.9892	4.0036	-0.0290
Leontopithecus rosalia	4.1187	4.1077	-0.0052
Callimico goeldii	4.0459	4.0813	-0.0511
Callithrix jacchus	3.8803	3.8577	0.0103
Callicebus moloch	4.3022	4.2884	-0.0052

Pithecia pithecia	4.5531	4.5640	-0.0343
Tarsius bancanus	3.5123	3.4840	0.0219
Galago senegalensis	3.6170	3.6049	0.0038
Loris tardigradus	3.7797	3.7840	-0.0154
Nycticebus coucang	4.0480	3.9866	0.0471
Daubentonia madagasc.	4.6379	4.6688	-0.0559
Propithecus verreauxi	4.4112	4.3964	-0.0059
Lepilemur ruficaudatus	3.8510	3.8423	-0.0033
Cheirogaleus major	3.7886	3.7616	0.0162
Microcebus murinus	3.1900	3.2398	-0.0524
Varecia variegatus	4.5286	4.4918	0.0145
Eulemur fulvus	4.4144	4.4044	-0.0108

[1] negative values indicate a smaller male brain size given the female brain size

APPENDIX 2. Source of DNA and primer sequences

Table A2.1 Source of DNA for species for which new data was collected

Species	Lab ID	Donor*
Gorilla gorilla	Ggo2	ZSL
Hylobates lar	Hla1	ZSL
Cercopithecus aethiops	Cae1	NMS
Colobus guereza	Cgu1	ZSL
Erythrocebus patas	Epa1	ZSL
Papio anubis	Pan2	NMS
Presbytis entellus	Pen1	ZSL
Trachypithecus auratus	Tau9	NMS
Alouatta caraya	Acr1	NMS
Aotus sp.	Aot1	NMS
Ateles paniscus	Apa1	ZSL
Callicebus cupreus	Ccu	NMS
Callicebus moloch	Cmo/CIM	CRES
Cebus albifrons	Cal1	ZSL
Pithecia pithecia	Ppi1	CRES
Saimiri boliviensis	Sbo1	NMS
Callimico goeldii	Cag20	ZSL
Callithrix argentatata	Car2	ZSL
Callithrix geoffroyi	Cge32	NMS
Callithrix jacchus	Cja292	CRES
Callithrix pygmaea	Cep 592	CRES
Leontopithecus chrysomelas	Lch1	ZSL
Leontopithecus rosalia	LR 111	NMS
Saguinus geoffroyi	Sge1	NMS
Saguinus fusicollis	Sfi1	NMS
Saguinus midas	Smi3	NMS
Saguinus Oedipus	Soe296	CRES

*CRES: Center for Reproduction of Endangered Species, San Diego Zoo; NMS: National Museums Scotland; ZSL: Zoological Society London

Table A2.2 Primer sequences used for data collection in chapters 5 &6

Primer name	Locus/Exon	Use	PCR with	Annealing T°C	Taxon	Sequence (5'-3')
ASPM_3_F1	ASPM exon3	PCR/Seq	ASPM_3_F2	60°C	Anthropoids	TTCAGCCTCTACAAGTCACAACA
ASPM_3_R2	ASPM exon3	PCR/Seq	ASPM_3_F1	60°C	Anthropoids	GGCTCTGAGGGAGAAAAATG
ASPM_3_IntF2	ASPM exon3	Seq			Anthropoids	GTGCAACTTGCTTGCCACT
ASPM_3_IntF3	ASPM exon3	Seq			Anthropoids	AAATCAGGATCTAGAATCAGAGTCA
ASPM_3_IntF4	ASPM exon3	Seq			Anthropoids	CCAAAAGCAAAAAGATGTCTCA
ASPM_3_IntR2	ASPM exon3	Seq			Anthropoids	TGAAACATTGGCGCTGTCTA
ASPM_3_IntR3	ASPM exon3	Seq			Anthropoids	TTCCCCAATCTTGTAGAGACTGT
ASPM_3_IntR4	ASPM exon3	Seq			Anthropoids	ACTGGATCTATAATTGGAAGATAAGAA
ASPM_18long_F1	ASPM exon 18	PCR/Seq	ASPM_18long_R1	60°C	Most anthropoids	TCAATCGTCCTGCAATCTAGG
ASPM_18long_R1	ASPM exon 18	PCR/Seq	ASPM_18long_F1	60°C	Most anthropoids	GTTTTCTGGTTTGCCACGTC
ASPM_18bitsA_F1	ASPM exon 18	PCR/Seq	ASPM_18bitsA_R1	58°C	Anthropoids (used when long range PCR failed)	TATTATTCAATCGTCCTGCAATC
ASPM_18bitsA_R1	ASPM exon 18	PCR/Seq	ASPM_18bitsA_F1	58°C	Anthropoids (used when long range PCR failed)	CTGCCTTTTTGACCTGCAA
ASPM_18bitsB_F1	ASPM exon 18	PCR/Seq	ASPM_18bitsB_R1	58°C	Anthropoids (used when long range PCR failed)	ATACCTGGTCCGAAAGCAGA
ASPM_18bitsB_R1	ASPM exon 18	PCR/Seq	ASPM_18bitsB_F1	58°C	Anthropoids (used when long range PCR failed)	GCTGCATTTTCCCCTGATAA
ASPM_18bitsC_F1	ASPM exon 18	PCR/Seq	ASPM_18bitsC_R1	58°C	Anthropoids (used when long range PCR failed)	AAAATTACAAACCATCAGTATAAGGAG
ASPM_18bitsC_R1	ASPM exon 18	PCR/Seq	ASPM_18bitsC_F1	58°C	Anthropoids (used when long range PCR failed)	AGCAGAATGCCACTGTTTGG
ASPM_18bitsD_F1	ASPM exon 18	PCR/Seq	ASPM_18bitsD_R2	60°C	Anthropoids (used when long range PCR failed)	GGCTGCAGTTCTCATTCAGG
ASPM_18bitsD_R2	ASPM exon 18	PCR/Seq	ASPM_18bitsD_F1	60°C	Anthropoids (used when long range PCR failed)	CCGTTTCTGTATAAATCCTTTGG
ASPM_18bitsA_intF2	ASPM exon 18	Seq			Anthropoids	GAATGGCATCTAAGGAAACGA
ASPM_18bitsA_intF3	ASPM exon 18	Seq			Anthropoids	GAGCTGCTTGTGTTATTCAGTCA
ASPM_18bitsA_intF4	ASPM exon 18	Seq			Anthropoids	TTGCAGTCAATTGTTAGGATGAA
ASPM_18bitsA_intR2	ASPM exon 18	Seq			Anthropoids	GGAATGGTAGCATTGCTGGA
ASPM_18bitsA_intR3	ASPM exon 18	Seq			Anthropoids	TTTCTTACGTGTGCCTGCAA
ASPM_18bitsA_intR4	ASPM exon 18	Seq			Anthropoids	GCTTGAAAGCACCGAAATCT
ASPM_18bitsB_intF2	ASPM exon 18	Seq			Anthropoids	TCTGTAGCTGCTGTTAAAATTCA
ASPM_18bitsB_intF3	ASPM exon 18	Seq			Anthropoids	GACTGCAGGAAGGAAGCAAC
ASPM_18bitsB_intF4	ASPM exon 18	Seq			Anthropoids	GTGAGAAAAAGAATAAAGGATTGC
ASPM_18bitsB_intR2	ASPM exon 18	Seq			Anthropoids	TCTGTAGCTGCTGTTAAAATTCA
ASPM_18bitsB_intR3	ASPM exon 18	Seq			Anthropoids	TGGAGTATATTGAACTCCGTCA
ASPM_18bitsB_intR4	ASPM exon 18	Seq			Anthropoids	AAAGGATTGCAACAAAGCAG
ASPM_18bitsB_intF2	ASPM exon 18	Seq			Anthropoids	CCTTCAGGCAAACTTTAGAGGA
ASPM_18bitsB_intF3	ASPM exon 18	Seq			Anthropoids	CAACCCTCATTCAGAGGAGA
ASPM_18bitsB_intF4	ASPM exon 18	Seq			Anthropoids	GCAGAGGCAGCATTATCTCA
ASPM_18bitsB_intR2	ASPM exon 18	Seq			Anthropoids	CAAATGGTGGCTCGGTATTT
ASPM_18bitsB_intR3	ASPM exon 18	Seq			Anthropoids	CCCTATGCATCTCTCGCATC
ASPM_18bitsB_intR4	ASPM exon 18	Seq			Anthropoids	TGCCTCAGTTTGTTATACCTTTGA
ASPM_18bitsB_intF2	ASPM exon 18	Seq			Anthropoids	GCTGCTATCATAATACAAAGCACA
ASPM_18bitsB_intF3	ASPM exon 18	Seq			Anthropoids	CAGTGCATACCCAAGCAGTT
ASPM_18bitsB_intF4	ASPM exon 18	Seq			Anthropoids	GAAGCATGAAAGTTAGACAAAAATTG
ASPM_18bitsB_intR2	ASPM exon 18	Seq			Anthropoids	TCTTCTTCGATACACAGCCATC

ASPM_18bitsB_intR3	ASPM exon 18	Seq			Anthropoids	AAAAGCAGCCTGAATAGTTCGT
ASPM_18bitsB_intR4	ASPM exon 18	Seq			Anthropoids	AGGGAAGTCTGGTGCTGTTC
CDK5RAP2_12_F1	CDK5RAP2 exon 12	PCR/Seq	CDK5RAP2_12_R1	60°C	Anthropoids	TCTGAAAACTATGAGGCTGCTC
CDK5RAP2_12_R1	CDK5RAP2 exon 12	PCR/Seq	CDK5RAP2_12_F1	60°C	Anthropoids	ATGGTGCAATCTCCTCTGCT
CDK5RAP2_12_intF2	CDK5RAP2 exon 12	Seq			Anthropoids	TGAGGCTGCTCTATCAGGAAA
CDK5RAP2_12_intR2	CDK5RAP2 exon 12	Seq			Anthropoids	ATGGTGCAGTCTCCTTTGCT
CDK5RAP2_20_F1	CDK5RAP2 exon 20	PCR/Seq	CDK5RAP2_20_R1	60°C	Old world monkeys & Apes	GCCAGACCTTCTGAAAGTGG
CDK5RAP2_20_R1	CDK5RAP2 exon 20	PCR/Seq	CDK5RAP2_20_F1	60°C	Old world monkeys & Apes	AATACCAGGGAGGGAAAGGA
CDK5RAP2_20_F2	CDK5RAP2 exon 20	PCR/Seq	CDK5RAP2_20_R2	58°C	New world monkeys	AAGTGCTGCAGGAACTGCTT
CDK5RAP2_20_R2	CDK5RAP2 exon 20	PCR/Seq	CDK5RAP2_20_F2	58°C	New world monkeys	ACCAGGGAAAGAAGGGAGAG
CDK5RAP2_20_intF3	CDK5RAP2 exon 20	Seq			Anthropoids	CATTTTGTCCAAACCAACTCA
CDK5RAP2_20_intR3	CDK5RAP2 exon 20	Seq			Anthropoids	CCAAGCCTCTCTTGTTGCTT
CDK5RAP2_21_F1	CDK5RAP2 exon 21	PCR/Seq	CDK5RAP2_20_R1	56°C	Anthropoids	AGGCTAAGAAGTCCCGCTTG
CDK5RAP2_21_R1	CDK5RAP2 exon 21	PCR/Seq	CDK5RAP2_20_F1	56°C	Anthropoids	CATTCAGCAACGTTTTGTCG
CDK5RAP2_21_intF2	CDK5RAP2 exon 21	Seq			Anthropoids	GCAGCTGCAGAGCCAGAT
CDK5RAP2_21_intR2	CDK5RAP2 exon 21	Seq			Anthropoids	CATCACTGCTTCAGCCAGAAT
CDK5RAP2_24_F1	CDK5RAP2 exon 24	PCR/Seq	CDK5RAP2_20_R1	57°C	Anthropoids	CTCTGAGATTTGCCCACCTG
CDK5RAP2_24_R1	CDK5RAP2 exon 24	PCR/Seq	CDK5RAP2_20_F1	57°C	Anthropoids	ATTCTGCAGATTATGGATCTCAC
CDK5RAP2_24_intF2	CDK5RAP2 exon 24	Seq			Anthropoids	CCATGACTTGGAAACTGAGC
CDK5RAP2_24_intR2	CDK5RAP2 exon 24	Seq			Anthropoids	CTTCTGTCCCACACAAAACT
CDK5RAP2_25_F1	CDK5RAP2 exon 25	PCR/Seq	CDK5RAP2_25_R1	58°C	Anthropoids	CGATTCATTAGTTCAGTCCCAAG
CDK5RAP2_25_R1	CDK5RAP2 exon 25	PCR/Seq	CDK5RAP2_25_F1	58°C	Anthropoids	GAAATAGCTTTTCCAATTTCTCCA
CDK5RAP2_31_F1	CDK5RAP2 exon 32	PCR/Seq	CDK5RAP2_31_R1	58°C	Anthropoids	GTCGGGAGAAGGCTGGAAG
CDK5RAP2_31_R1	CDK5RAP2 exon 32	PCR/Seq	CDK5RAP2_31_F1	58°C	Anthropoids	CGTGTTTGTCAGGCTGAAGG
CDK5RAP2_31_intF2	CDK5RAP2 exon 32	Seq			Anthropoids	TCTGCGCTTGCAACTAGAAA
CDK5RAP2_31_intR2	CDK5RAP2 exon 32	Seq			Anthropoids	TCCTTCCTGTGCCTTCTCTG
CDK5RAP2_33_F1	CDK5RAP2 exon 33	PCR/Seq	CDK5RAP2_31_R2	58-60°C	Anthropoids	CCTCCACTCTCTGGGAATGA
CDK5RAP2_31_R2	CDK5RAP2 exon 33	PCR/Seq	CDK5RAP2_33_F1	58-60°C	Anthropoids	TGTTCCCAGCTCTTGACTTG
CDK5RAP2_33_intF2	CDK5RAP2 exon 33	Seq			Anthropoids	AGTTCGGCAACTAGCACTCC
CDK5RAP2_33_intR3	CDK5RAP2 exon 33	Seq			Anthropoids	CTGGCTGATCTGTTTGAGCA
CENPJ_2_L2	CENPJ exon 2	PCR/Seq	CENPJ_2_R2	59°C	Anthropoids	TGGTAGGACATCTAATGGCTTT
CENPJ_2_R2	CENPJ exon 2	PCR/Seq	CENPJ_2_L2	59°C	Anthropoids	TTGCTTCTCTGCCTTCTCTTCT
CENPJ_2_intL3	CENPJ exon 2	Seq			Anthropoids	TGGACATTTCTACCAGCTTTCC
CENPJ_2_intR3	CENPJ exon 2	Seq			Anthropoids	GGGCTGTTTGACTCCAACTT
CENPJ_7_L2	CENPJ exon 7	PCR/Seq	CENPJ_7_R2	58°C	Anthropoids	AGGACCATTGCCAATCAAAG
CENPJ_7_R2	CENPJ exon 7	PCR/Seq	CENPJ_7_L2	58°C	Anthropoids	CCAGGTGGTTGGTCTTGACT
CENPJ_7_intL4	CENPJ exon 7	Seq			Anthropoids	CTTTGCAGATCTGTTGATCCA
CENPJ_7_intL5	CENPJ exon 7	Seq			Anthropoids	CCCAAACAACTCCGTTCACT
CENPJ_7_intL6	CENPJ exon 7	Seq			Anthropoids	AAGATGACAGTAGCGATGAGTCTG
CENPJ_7_intR4	CENPJ exon 7	Seq			Anthropoids	ATCGTCACCTGCATTCCATT
CENPJ_7_intR5	CENPJ exon 7	Seq			Anthropoids	TGATATTTCATCAGCAGCTTGTT
CENPJ_7_intR6	CENPJ exon 7	Seq			Anthropoids	GGTCTCTACATTGCCCATC

MCPH1_8_L3	MCPH1 exon 8	PCR/Seq	MCPH1_8_R3	58-60°C	Anthropoids	GCTCTCCGTTAATGTTTTCCAG
MCPH1_8_R3	MCPH1 exon 8	PCR/Seq	MCPH1_8_L3	58-60°C	Anthropoids	TTTAGCGAAGGTGACTTGGA
MCPH1_8_intL4	MCPH1 exon 8	Seq			Anthropoids	AAAATAGTCACCCCTGACCAAA
MCPH1_8_intL5	MCPH1 exon 8	Seq			Anthropoids	CCGAAGGAAAAATGCAAGAG
MCPH1_8_intL6	MCPH1 exon 8	Seq			Anthropoids	CATTACCCGTTTCACAGCAA
MCPH1_8_intR4	MCPH1 exon 8	Seq			Anthropoids	AGGGTCCTCAGCAGGGTAAG
MCPH1_8_intR5	MCPH1 exon 8	Seq			Anthropoids	GGAAAAATCTGCCATTTCCA
MCPH1_8_intR6	MCPH1 exon 8	Seq			Anthropoids	TCCGCTTTCTCTTGCATTTT
MCPH1_11_L2	MCPH1 exon 11	PCR/Seq		56°C	Anthropoids	GGCATGTGCAACAAAGTCAT
MCPH1_11_R2	MCPH1 exon 11	PCR/Seq		56°C	Anthropoids	CCTCAGGGTGACCCACTCTA
MCPH1_11_intL3	MCPH1 exon 11	Seq			Anthropoids	TYGYRCCAGAMGTCTGTGAG
MCPH1_13_L2	MCPH1 exon 13	PCR/Seq	MCPH1_13_R2	58°C	Anthropoids	TCGCCTACGCTATGGAGACT
MCPH1_13_R2	MCPH1 exon 13	PCR/Seq	MCPH1_13_L2	58°C	Anthropoids	CAGATCTGGACCACACCACA
MCPH1_13_intL3	MCPH1 exon 13	Seq		58°C	Anthropoids	CGTACCGTGGAACCCTCTT
MCPH1_13_intR3	MCPH1 exon 13	Seq		58°C	Anthropoids	AGGGTCCGATGATGATGCTA
STIL _ex7L3	STIL exon 7	PCR/Seq	STIL_ex7R3	56-58°C	Anthropoids	GCAAAGATTCCTTGGACTGTG
STIL_ex7R3	STIL exon 7	PCR/Seq	STIL_ex7L3	56-58°C	Anthropoids	TTATAAGTCCCTTGAACTTGAGAAA
STIL_ex7SaiL1	STIL exon 7	PCR/Seq	STIL_ex7SaiR1	56-58°C	New world monkeys	GCAAAGATTCCTTGGACTGTG
STIL_ex7SaiR1	STIL exon 7	PCR/Seq	STIL_ex7SaiL1	56-58°C	New world monkeys	TCCCTTGAACTTGAGAAATATTCAG
STIL_ex7intL1	STIL exon 7	Seq			Anthropoids	GCAAAGATTCCTTGGACTGTG
STIL_ex7intR1	STIL exon 7	Seq			Anthropoids	TGTTGGAATAATGGGGATGG
STIL_ex13L1	STIL exon 13	PCR/Seq	STIL_ex13R1	56-58°C	Anthropoids	AGATCCAACCATCAGTTCCTG
STIL_ex13R1	STIL exon 13	PCR/Seq	STIL_ex13L1	56-58°C	Anthropoids	TGTGCCTGAAGTAGTCTTAGCTG
STIL_ex13missL1	STIL exon 13	PCR/Seq	STIL_ex13missR1	56-58°C	Anthropoids	TGTGTTRGATGGCAATTTCR
STIL_ex13missR1	STIL exon 13	PCR/Seq	STIL_ex13missL1	56-58°C	Anthropoids	TGYTCTGTGAGRAACCGATA
STIL_ex13intL1	STIL exon 13	Seq			Anthropoids	ATTGCAACCCCAGCTTTATG
STIL_ex13intL2	STIL exon 13	Seq			Anthropoids	AGTCCCAACCACMYRATTTT
STIL_ex13intL3	STIL exon 13	Seq			Anthropoids	RAGCYCTTCAAAAGCATTCW
STIL_ex13intR1	STIL exon 13	Seq			Anthropoids	ATTGCTGTGGGGAGAACAAC
STIL_ex13intR2	STIL exon 13	Seq			Anthropoids	GCTCCTTGCCAAGAATWTAGY
STIL_ex13intR3	STIL exon 13	Seq			Anthropoids	GGAGGGTCTTATAGGATACTCTTYR
STIL_ex15L1	STIL exon 15	PCR/Seq	STIL_ex15R1	56-58°C	Anthropoids	CTTGTTTTGGAATGCAGCWG
STIL_ex15R1	STIL exon 15	PCR/Seq	STIL_ex15L1	56-58°C	Anthropoids	TTTYTGCTGCATCTCACTGC
STIL_ex17L1	STIL exon 17	PCR/Seq	STIL_ex17R1	56-58°C	Anthropoids	TTCCTCCAAGGAAACTGAGC
STIL_ex17R1	STIL exon 17	PCR/Seq	STIL_ex17L1	56-58°C	Anthropoids	CTGGCGTGATCCACGTTRT
STIL_ex17EpaL1	STIL exon 17	PCR/Seq	STIL_ex17EpaR1	56°C	Colobines	GAGCAGCCATCTACCAAAGC
STIL_ex17EpaR1	STIL exon 17	PCR/Seq	STIL_ex17EpaL1	56°C	Colobines	TCCACGTTGTGTGCATTTTT
STIL_ex17PpiL1	STIL exon 17	PCR/Seq	STIL_ex17PpiR1	56°C	Pithecines	GAGCAGCCATCTACCAAAGC
STIL_ex17PpiR1	STIL exon 17	PCR/Seq	STIL_ex17PpiL1	56°C	Pithecines	CTGGCGTGATCCACGTTAT
STIL_ex17intL1	STIL exon 17	Seq			Anthropoids	AAACTGAGCAGCCRTCTACC
STIL_ex17intL2	STIL exon 17	Seq			Anthropoids	AATGCACCAGAACCCAAAAC
STIL_ex17intR1	STIL exon 17	Seq			Anthropoids	TCCAAGGCTTCTTAGTTGCTT

STIL_ex18L1	STIL exon 18	PCR/Seq	STIL_ex18R1	56-58°C	Anthropoids	GATCTCTGGATTAAACTGCATGTC
STIL_ex18R1	STIL exon 18	PCR/Seq	STIL_ex18L1	56-58°C	Anthropoids	TGAATTCATGCTATTCATCTGYTT
STIL_ex18CcuL1	STIL exon 18	PCR/Seq	STIL_ex17CcuR1	56°C	Pithecines	GATCTCTGGATTAAACTGCATGTC
STIL_ex17CcuR1	STIL exon 18	PCR/Seq	STIL_ex18CcuL1	56°C	Pithecines	TGAATTCATGCTATTCATCTGCTT
STIL_ex18intL1	STIL exon 18	Seq			Anthropoids	AAGCACAGTRGGGCTYAGTT
STIL_ex18intL2	STIL exon 18	Seq			Anthropoids	TTACAAATGAAGTTTTGCAGWCA
STIL_ex18intR1	STIL exon 18	Seq			Anthropoids	GCTGTTTKGCTTTTGWCTGC
STIL_ex18intR2	STIL exon 18	Seq			Anthropoids	TCTTCRCTATTGTCACTGCTTTG
NIN_ex18_L1	NIN exon 18	PCR/Seq	NIN_ex18_R1	56-60°C	Anthropoids	TRTGAAAAGCAGCTGGAYGA
NIN_ex18_R1	NIN exon 18	PCR/Seq	NIN_ex18_L1	56-60°C	Anthropoids	CYTTTGGTGCTTTTCCAAGA
NIN_ex18_intL1	NIN exon 18	Seq			Anthropoids	CAGGCATGAGGAGGAGAARA
NIN_ex18_intR1	NIN exon 18	Seq			Anthropoids	CCTGAGTCAAGCCTCTCACC
NIN_ex18_intL2	NIN exon 18	Seq			Anthropoids	CTTCAGAGTMGCGCCTGGAC
NIN_ex18_intR2	NIN exon 18	Seq			Anthropoids	CTCATGATRTGCCTCCTTRA
NIN_ex19_L2	NIN exon 19	PCR/Seq	NIN_ex19_R2	56-58°C	Anthropoids	GCCCAGTTTCAGTCTGATTGT
NIN_ex19_R2	NIN exon 19	PCR/Seq	NIN_ex19_L2	56-58°C	Anthropoids	TCCTGCAACCTGAAAACCTC
NIN_ex19_L3	NIN exon 19	PCR/Seq	NIN_ex19_R3	56-58°C	Anthropoids	CTGGGAAGTACAGGGACVAK
NIN_ex19_R3	NIN exon 19	PCR/Seq	NIN_ex19_L3	56-58°C	Anthropoids	TTTYTGCTGCATCTCACTGC
NIN_ex19_missNWML1	NIN exon 19	PCR/Seq	NIN_ex19_missNWMR1	56°C	NWM	AACAGAGCCGTTTTTACAGCA
NIN_ex19_missNWMR1	NIN exon 19	PCR/Seq	NIN_ex19_missNWML1	56°C	NWM	CTGAAGGCAGTCATTTTCTCG
NIN_ex19_missCguL1	NIN exon 19	PCR/Seq	NIN_ex19_missCguR1	56°C	Colobines	GACACGCTATGATGAGGCACT
NIN_ex19_missCguR1	NIN exon 19	PCR/Seq	NIN_ex19_missCguL1	56°C	Colobines	CATCATGGCCTTCAGCTCTT
NIN_ex19_L4	NIN exon 19	PCR/Seq	NIN_ex19_R4	56-60°C	Anthropoids	CAAAAYCRAAYGAAGCAAGT
NIN_ex19_R4	NIN exon 19	PCR/Seq	NIN_ex19_L4	56-60°C	Anthropoids	GCCTTCAGCTCTTCCTCCTT
NIN_ex19_L5	NIN exon 19	PCR/Seq	NIN_ex19_R3	56-58°C	Anthropoids	RGCAGTGAAGGAAAATGTGAA
NIN_ex19_Lint1	NIN exon 19	Seq			Anthropoids	AGCAAAGCCWGCTGTCYGA
NIN_ex19_Lint2	NIN exon 19	Seq			Anthropoids	GCAGGCMRCATCTCCTCTCT
NIN_ex19_Lint3	NIN exon 19	Seq			Anthropoids	CAAAAYCRAAYGAAGCAAGT
NIN_ex19_Lint4	NIN exon 19	Seq			Anthropoids	CGGACTGTGATCGAGCTTCT
NIN_ex19_Rint1	NIN exon 19	Seq			Anthropoids	MATTAGCTGTKCCTGAAGCTGA
NIN_ex19_Rint2	NIN exon 19	Seq			Anthropoids	TTTGYAGCCTCTGYTGCAATCT
NIN_ex19_Rint3	NIN exon 19	Seq			Anthropoids	CTCCATGGCYAGAAGCTTRG
NIN_ex19_Rint4	NIN exon 19	Seq			Anthropoids	CTCCAGCATCTCYCTCTCCTG
NIN_ex19_CguRint1	NIN exon 19	Seq			Colobines	CACCGCTGGACCATACTTTC
NIN_ex19_CguLint1	NIN exon 19	Seq			Colobines	GAGGTTTTCAGGTTGCAGGA
NIN_ex19_CguLint2	NIN exon 19	Seq			Colobines	TGCCCAGGGTTAGGAGTGTA
NIN_ex19_CguRint2	NIN exon 19	Seq			Colobines	CCTGACGCTGAAAATGTTTG

APPENDIX 3. Accession IDs of published sequences

a) Accession IDs of published microcephaly genes from chapter 5

ENS from ensembl.org, all others from GenBank. Newly obtained sequences are indicated in bold italics. Data for the additional *ASPM* for callitrichids, *STIL* and *NIN* are unpublished. These data will be deposited in Genbank when published in a peer reviewed journal.

	ASPM	
Species	exon 3	exon 18
Gorilla gorilla	AY497014	AY497014
Homo sapiens	ENST00000367409	ENST00000367409
Hylobates lar	AY488969	AY488984
Hylobates hoolock	-	-
Pan troglodytes	ENSPTRT00000003276	ENSPTRT00000003276
Pongo pygmaea	ENSPPYT00000000459	ENSPPYT00000000459
Cercopithecus aethiops	AY486114	AY486114
Colobus guereza	AY488997	AY489012
Erythrocebus patas	***HQ540089***	***HQ540100***
Macaca mulatta	ENSMMUT00000000360	ENSMMUT00000000360
Papio anubis	***HQ540090***	***HQ540101***
Presbytis entellus	***HQ540088***	***HQ540099***
Pygathrix nemaeus	-	-
Trachypithecus auratus	-	-
Alouatta caraya	***HQ540093***	***HQ540104***
Aotus sp.	AY485422	AY485422
Ateles geoffroyi	-	AY497018
Ateles paniscus	***HQ540094***	-
Callicebus cupreus	-	-
Callicebus moloch	***HQ540097***	***HQ540106***
Callithrix jacchus	***HQ540091***	***HQ540102***
Cebus albifrons	***HQ540092***	***HQ540103***
Leontopithecus chrysomelas	***HQ540096***	***HQ540105***
Pithecia pithecia	***HQ540098***	***HQ540107***
Saguinus labiatus	-	AY497015
Saguinus oedipus	***HQ540095***	-
Saimiri boliviensis	AY485419	AY485419
Microcebus murinus	ENSMICT00000002068	ENSMICT00000002068
Otolemur garnettii	-	-

				CDK5RAP2			
Species	exon 12	exon 21	exon 21	exon 24	exon 25	exon 32	exon 34
Gorilla gorilla	DQ430803	DQ430803	DQ430803	DQ430803	DQ430803	DQ430803	DQ430803
Homo sapiens	ENST00000359309	ENST00000359309	ENST00000359309	ENST00000359309	ENST00000359309	ENST00000359309	ENST00000359309
Hylobates lar	***HQ540178***	***HQ540194***	***HQ540210***	***HQ540226***	***HQ540242***	***HQ540258***	***HQ540274***
Hylobates hoolock	-	-	-	-	-	-	-
Pan troglodytes	ENSPTRT00000043882	ENSPTRT00000043882	ENSPTRT00000043882	ENSPTRT00000043882	ENSPTRT00000043882	ENSPTRT00000043882	ENSPTRT00000043882
Pongo pygmaea	ENSPPYT00000022810	ENSPPYT00000022810	ENSPPYT00000022810	ENSPPYT00000022810	ENSPPYT00000022810	ENSPPYT00000022810	ENSPPYT00000022810
Cercopithecus aethiops	***HQ540179***	***HQ540195***	***HQ540211***	***HQ540227***	***HQ540243***	***HQ540259***	***HQ540275***
Colobus guereza	***HQ540180***	***HQ540196***	***HQ540212***	***HQ540228***	***HQ540244***	***HQ540260***	***HQ540276***
Erythrocebus patas	***HQ540182***	***HQ540198***	***HQ540214***	***HQ540230***	***HQ540246***	***HQ540262***	***HQ540278***
Macaca mulatta	ENSMMUT00000032715	ENSMMUT00000032715	ENSMMUT00000032715	ENSMMUT00000032715	ENSMMUT00000032715	ENSMMUT00000032715	ENSMMUT00000032715
Papio anubis	***HQ540183***	***HQ540199***	***HQ540215***	***HQ540231***	***HQ540247***	***HQ540263***	***HQ540279***
Presbytis entellus	-	-	-	-	-	-	-
Pygathrix nemaeus	-	-	-	-	-	-	-
Trachypithecus auratus	***HQ540181***	***HQ540197***	***HQ540213***	***HQ540229***	***HQ540245***	***HQ540261***	***HQ540277***
Alouatta caraya	***HQ540187***	***HQ540203***	***HQ540219***	***HQ540235***	***HQ540251***	***HQ540267***	***HQ540282***
Aotus sp.	***HQ540193***	***HQ540209***	***HQ540225***	***HQ540241***	***HQ540257***	***HQ540273***	***HQ540289***
Ateles geoffroyi	-	-	-	-	-	-	-
Ateles paniscus	***HQ540188***	***HQ540204***	***HQ540220***	***HQ540236***	***HQ540252***	***HQ540268***	***HQ540283***
Callicebus cupreus	***HQ540191***	***HQ540191***	***HQ540223***	***HQ540239***	***HQ540255***	***HQ540271***	***HQ540287***
Callicebus moloch		-	-	-	-	-	-
Callithrix jacchus	***HQ540184***	***HQ540200***	***HQ540216***	***HQ540232***	***HQ540248***	***HQ540264***	***HQ540286***
Cebus albifrons	***HQ540185***	***HQ540201***	***HQ540217***	***HQ540233***	***HQ540249***	***HQ540265***	***HQ540280***
Leontopithecus chrysomelas	***HQ540190***	***HQ540206***	***HQ540222***	***HQ540238***	***HQ540254***	***HQ540270***	***HQ540285***
Pithecia pithecia	***HQ540192***	***HQ540208***	***HQ540224***	***HQ540240***	***HQ540256***	***HQ540272***	***HQ540288***
Saguinus labiatus	-	-	-	-	-	-	-
Saguinus oedipus	***HQ540189***	***HQ540205***	***HQ540221***	***HQ540237***	***HQ540253***	***HQ540269***	***HQ540284***
Saimiri boliviensis	***HQ540186***	***HQ540202***	***HQ540218***	***HQ540234***	***HQ540250***	***HQ540266***	***HQ540281***
Microcebus murinus	ENSMICT00000003275	ENSMICT00000003275	ENSMICT00000003275	ENSMICT00000003275	ENSMICT00000003275	ENSMICT00000003275	ENSMICT00000003275
Otolemur garnettii	ENSOGAT00000006307	ENSOGAT00000006307	ENSOGAT00000006307	ENSOGAT00000006307	ENSOGAT00000006307	ENSOGAT00000006307	ENSOGAT00000006307

	CENPJ	
Species	exon 2	exon 7
Gorilla gorilla	***HQ540108***	***HQ540125***
Homo sapiens	ENST00000381884	ENST00000381884
Hylobates lar	***HQ540109***	***HQ540126***
Hylobates hoolock	-	-
Pan troglodytes	ENSPTRT00000010527	ENSPTRT00000010527
Pongo pygmaea	ENSPPYT00000006175	ENSPPYT00000006175
Cercopithecus aethiops	***HQ540110***	***HQ540127***
Colobus guereza	***HQ540111***	***HQ540128***
Erythrocebus patas	***HQ540113***	***HQ540130***
Macaca mulatta	ENSMMUT00000043474	ENSMMUT00000043474
Papio anubis	***HQ540114***	***HQ540131***
Presbytis entellus	***HQ540112***	***HQ540129***
Pygathrix nemaeus	-	-
Trachypithecus auratus	-	-
Alouatta caraya	***HQ540118***	***HQ540135***
Aotus sp.	***HQ540124***	***HQ540141***
Ateles geoffroyi	-	-
Ateles paniscus	***HQ540119***	***HQ540136***
Callicebus cupreus	***HQ540122***	***HQ540139***
Callicebus moloch	-	-
Callithrix jacchus	***HQ540115***	***HQ540132***
Cebus albifrons	***HQ540116***	***HQ540133***
Leontopithecus chrysomelas	***HQ540121***	***HQ540138***
Pithecia pithecia	***HQ540123***	***HQ540140***
Saguinus labiatus	-	-
Saguinus oedipus	***HQ540120***	***HQ540137***
Saimiri boliviensis	***HQ540117***	***HQ540134***
Microcebus murinus	ENSMICT00000010399	ENSMICT00000010399
Otolemur garnettii	ENSOGAT00000014829	ENSOGAT00000014829

	MCPH1		
Species	exon 8	exon 11	exon 13
Gorilla gorilla	***HQ540142***	***HQ540154***	***HQ540166***
Homo sapiens	ENST00000344683	ENST00000344683	ENST00000344683
Hylobates lar	-	-	-
Hylobates hoolock	AY505993	AY506194	AY506287
Pan troglodytes	ENSPTRT00000036980	ENSPTRT00000036980	ENSPTRT00000036980
Pongo pygmaea	ENSPPYT00000021337	ENSPPYT00000021337	ENSPPYT00000021337
Cercopithecus aethiops	***HQ540143***	***HQ540155***	***HQ540167***
Colobus guereza	AY553045	AY553048	AY553050
Erythrocebus patas	AY505994	AY506187	AY506288
Macaca mulatta	XM_001097449	XM_001097449	XM_001097449
Papio anubis	***HQ540144***	***HQ540156***	***HQ540168***
Presbytis entellus	-	-	-
Pygathrix nemaeus	AY505995	AY506190	AY506290
Trachypithecus auratus	-	-	-
Alouatta caraya	***HQ540148***	***HQ540160***	***HQ540172***
Aotus sp.	***HQ540153***	***HQ540165***	***HQ540177***
Ateles geoffroyi	-	-	-
Ateles paniscus	***HQ540149***	***HQ540161***	***HQ540173***
Callicebus cupreus	***HQ540151***	***HQ540163***	***HQ540175***
Callicebus moloch	-	-	-
Callithrix jacchus	***HQ540145***	***HQ540157***	***HQ540169***
Cebus albifrons	***HQ540147***	***HQ540159***	***HQ540171***
Leontopithecus chrysomelas	***HQ540146***	***HQ540158***	***HQ540170***
Pithecia pithecia	***HQ540152***	***HQ540164***	***HQ540176***
Saguinus labiatus	-	-	-
Saguinus oedipus	***HQ540150***	***HQ540162***	***HQ540174***
Saimiri boliviensis	AY570949	AY570949	AY570949
Microcebus murinus	-	-	-
Otolemur garnettii	ENSOGAT00000015048	ENSOGAT00000015048	ENSOGAT00000015048

b) Accession IDs of control genes used in chapter 5

ASIP	
Aotus trivirgatus	AB236882.1
Callimico goeldii	EF094497.1
Callithrix jacchus	EF094494.1
Cercopithecus aethiops	AB236875.1
Colobus polykomos	AB236881.1
Erythrocebus patas	AB236876.1
Gorilla gorilla	AB236871.1
Homo sapiens	ENST00000374954
Leontopithecus rosalia	EF094499.1
Macaca mulatta	AB299207.1
Pan troglodytes	EF094481.1
Papio anubis	NM_001164331.1
Pongo pygmaeus	AB236872.1
Saguinus oedipus	AB236883.1
Trachypithecus obscurus	AB236879.1

CATSPER1 exon 1	
Aotus trivirgatus	AY382297.1
Ateles geoffroyi	AY382295.1
Cercopithecus aethiops	AY382301.1
Colobus guereza	AY382303.1
Gorilla gorilla	AY382307.1
Homo sapiens	NM_053054.3
Lagothrix lagotricha	AY382294.1
Macaca mulatta	XM_001118063.1
Macaca mulatta	AY382300.1
Pan troglodytes	XR_024041.1
Papio hamadryas	AY382302.1
Pongo pygmaeus	AY382308.1
Saguinus oedipus	AY382296.1
Saimiri sciureus	AY382298.1

ENAM	
Callithrix jacchus	ENSCJAT00000028463
Colobus a. palliatus	EU482100.1
Gorilla gorilla	EU482103.1
Homo sapiens	ENST00000396073
Lagothrix lagotricha	EU482106.1
Macaca mulatta	XR_013230.1
Nasalis larvatus	EU482105.1
Pan troglodytes	XM_526591.2
Papio anubis	EU482099.1
Pongo pygmaeus	ENSPPYG00000014808
Saguinus labiatus	EU482107.1
Symphalangus syndactylus	EU482104.1

GRIN2A	
Alouatta caraya	FJ455240.1
Ateles fusciceps	FJ455241.1
Callicebus moloch	FJ455242.1
Callithrix jacchus	ENSCJAT00000033386
Cercopithecus diana	FJ455245.1
Colobus angolensis	FJ455248.1
Homo sapiens	ENST00000396573
Hylobates muelleri	FJ455249.1
Lagothrix lagotricha	FJ455250.1
Macaca mulatta	XM_001105525.1

MC1R	
Alouatta palliata	AY205135.1
Aotus sp.	AY205129.1
Ateles geoffroyi	AB296241.1
Callimico goeldii	AY205121.1
Callithrix jacchus	AY205120.1
Cebus albifrons	AY205128.1
Cercopithecus aethiops	AY205095.1
Colobus guereza	AY205107.1
Erythrocebus patas	AB296228.1
Gorilla gorilla	AY205088.1

SEMG2	
Aotus nancymaae	gi|87295496:230946-231021
Ateles geoffroyi	AY781393.1
Callithrix jacchus	AY965734.2
Chlorocebus aethiops	gi|87295494:386999-387074
Colobus guereza	AY781392.1
Gorilla gorilla	ENSGGOT00000002565
Homo sapiens	ENST00000372769
Hylobates lar	AY781389.1
Macaca mulatta	XM_001109141.1
Pan troglodytes	NM_001009138.1

Pan troglodytes	NM_001034189.1	*Homo sapiens*	AB241546.1	*Papio anubis*	gi|87295517:261945-262020
Papio hamadryas	FJ455258.1	*Hylobates lar*	AY205089.1	*Pongo pygmaeus*	AY781388.1
Pongo pygmaeus	ENSPPYG00000007089	*Leontopithecus rosalia*	AY205114.1	*Saguinus oedipus*	AJ002153.2
Pygathrix nemaeus	FJ455260.1	*Macaca mulatta*	AY205103.1		
Saimiri boliviensis	AY665238.1	*Pan troglodytes*	AB296236.1		
Trachypithecus cristatus	FJ455261.1	*Papio anubis*	NM_001164589.1		
		Pongo pygmaeus	AY205087.1		
		Presbytis comata	AY205108.1		
		Saguinus oedipus	AB296240.1		
		Saimiri sciureus	AB296239.1		
		Trachypithecus obscurus	AY205112.1		
SRY		***ZAN***			
Alouatta pigra	DQ875677.1	*Ateles geoffroyi*	DQ383294.1		
Aotus infulatus	AF338376.1	*Callithrix jacchus*	AY428845.1		
Ateles geoffroyi	DQ976605.1	*Eyrthrocebus pata*	DQ383291.1		
Callimico goeldii	AF338383.1	*Homo sapiens*	NM_003386.1		
Callithrix jacchus	FJ527004.1	*Lagothrix lagotricha*	DQ383285.1		
Cebus apella	AF338387.1	*Macaca mulatta*	AY428851.1		
Cercocebus agilis	AY665631.1	*Pan troglodytes*	DQ383284.1		
Cercopithecus aethiops	AY450882.1	*Papio hamadryas*	AY428853.1		
Erythrocebus patas	AY048073.1	*Pongo pygmaeus*	DQ383286.1		
Gorilla gorilla	X86382.1	*Saguinus oedipus*	AY428857.1		
Homo sapiens	NG_011751.1	*Saimiri sciureus*	AY428855.1		
Hylobates lar	X86384.1				
Leontopithecus rosalia	AF338373.1				
Macaca mulatta	FJ527022.1				
Pan troglodytes	DQ977342.1				
Presbytis melalophos	AF284282.2				
Pygathrix nemaeus	AF454972.1				
Saimiri sciureus	AF151695.1				